University of Novi Sad
FACULTY OF TECHNICAL SCIENCES
DEPARTMENT OF PRODUCTION ENGINEERING
21000 NOVI SAD, Trg Dositeja Obradovica 6, SERBIA

UDK 621 ISSN 1821-4932

JOURNAL OF

PRODUCTION ENGINEERING

Volume 20 Number 1

Novi Sad, June 2017

Journal of Production Engineering, Vol.20 (2017), Number 1

Publisher: FACULTY OF TECHNICAL SCIENCES
DEPARTMENT OF PRODUCTION ENGINEERING
21000 NOVI SAD, Trg Dositeja Obradovica 6
SERBIA

Manuscript submitted for publication: June 30, 2017.
Printing: 1st
Circulation: 300 copies

CIP classification:

CIP – Катаголизација у публикацији
Библиотека Матице српске, Нови Сад

621

JOURNAL of Production Engineering / editor in chief Pavel Kovač. – Vol. 12, No. 1 (2009)- . – Novi Sad : Faculty of Technical Sciences, Department for Production Engineering, 2009-. – 30 cm

Dva puta godišnje (2012-). Je nastavak: Časopis proizvodno mašinstvo = ISSN
0354-6446
ISSN 1821-4932

Printing by: FTN, Graphic Center ***GRID,*** *Novi Sad*

ISSN: 1821-4932

http://doi.org/10.24867/JPE-2017-01

INTERNATIONAL EDITORIAL BOARD

Editorial

The ***Journal of Production Engineering*** *dates back to 1984, when the first issue of the* ***Proceedings of the Institute of Production Engineering*** *was published in order to present its accomplishments. In 1994, after a decade of successful publication, the Proceedings changed the name into Production Engineering, with a basic idea of becoming a Yugoslav journal which publishes original scientific papers in this area.*

In 2009 year, our Journal finally acquires its present title - ***Journal of Production Engineering****. To meet the Ministry requirements for becoming an international journal, a new international editorial board was formed of renowned domestic and foreign scientists, refereeing is now international, while the papers are published exclusively in English. From the year 2011 Journal is in the data base Google scholar, COBISS and KoBSON presented.*

The Journal is distributed to a large number of recipients home and abroad, and is also open to foreign authors. In this way we wanted to heighten the quality of papers and at the same time alleviate the lack of reputable international and domestic journals in this area.

Editor in Chief

Professor Pavel Kovač, PhD,

Journal of Production Engineering
Vol.20 No.1

Contents

http://doi.org/10.24867/JPE-2017-01-001

Journal of Production Engineering

Vol.20 No.1

JPE (2017) Vol.20 (1) Review Paper

Reddy, Y.R.M., Prasad, B.S.

ANALYSIS OF VIBRATION ASSISTED DRILLING –A BASE FOR TOOL PERFORMANCE EVALUATION

Received: 10 February 2017 / Accepted: 30 April 2017

Abstract: *The primary aim of present work is to evaluate the performance of tungsten carbide (uncoated), and HSS (high-speed steel) twist drill bits in vibration-assisted drilling. Another important objective of the present work is to investigate the effects of process parameters on vibration amplitude, (i.e., displacement) in the drilling of aerospace alloys like Ti-6Al-4V and Al7075. Effect of workpiece hardness, cutting speed, feed rate, and the number of holes drilled on tool wear is also examined in dry machining. As per the full factorial design technique, experimental tests conducted on a radial drilling machine. A Laser Doppler Vibrometer used for acquiring the vibration signals occurred during the drilling process. The vibration displacement determined by FFT (Fast Fourier Transform) algorithm. It observed that at all cutting conditions (tested), tungsten carbide drill clearly outperformed HSS (High-Speed Steel) Drill. Results of this work can use as a basis for the real-time capable tool condition monitoring system in vibration-assisted drilling.*

Key words: *Drilling, vibration, tool wear, drill tool, Ti-6Al-4V, Al7075, tool condition monitoring.*

Analiza bušenja potpomognuta vibracijama- osnova za ocenu rada alata. *Primarni cilj ovog rada je da procene performanse alata za izradu burgije potpomognute vibracijama od tvrdog metala (nepresvučen), i BČ (brzorezni čelik). Još jedan važan cilj ovog rada je da se ispita uticaj procesnih parametara na amplitudu vibracije (tj, pomeranje) pri bušenju legura za avio industriju kao sto su Ti-6Al-4V i Al7075. Ispitivan je uticaj tvrdoće obradka, brzine rezanja, kapaciteta punjenja, kao i broj izbušenih rupa na habanje alata pri suvoj obradi. Prema punom faktornom planu eksperimenta izvedeni su eksperimentalni testovi na radijalnoj bušilici. Laserski Dopler Vibrometer korišćen je za izazivanje vibracija tokom procesa bušenja. Analiza vibracija vršena je pomoću FFT (Fast Fourier Transform) algoritam. Primetno je da je u svim uslovima pri rezanju (testiranim), burgija od tvrdog metala nadmašila burgiju od BČ. Rezultati ovog rada se mogu koristiti kao osnova za monitoring stanja alata u realnom vremenu pri obradi bušenjem uz pomoć vibracija.*

Ključne reči: *Bušenje, vibracija, habanje alata, burgija, Ti-6Al-4V, Al7075, monitoring stanja alata.*

1. INTRODUCTION

The titanium alloy Ti–6Al–4V and aluminum alloy Al7075 used for a variety of applications in aerospace and chemical industries because of their properties such as high strength to weight ratio and excellent corrosion resistance [1]. In the present day scenario, the titanium alloys are extensively used in aerospace structure as they have the best combination of metallurgical and physical properties, in addition to its lightweight. However, due to the low thermal conductivity of titanium and its alloy, the temperature at the tool/workpiece interface increases, which results in poor machinability that can affect the tool life [2]. Nowadays, cutting processes play an enormous role in supporting the economies of developing countries. The process of drilling holes constituted one-third of machining work and applied as the finished operation in aerospace and automobile industries [3]. Ease of the application and economic aspects associated with drilling are the main reason behind the selection of drilling as part of machining methods for the manufacturing of various industrial products. Drilled holes come in different forms, in which through hole is drilled entirely throughout the workpiece as a blind hole is drilled only to a certain depth. The failure of a twist drill occurs by one of the two modes; fracture and excessive wear. Grzesik [4] presented a summarized picture of the fundamental causes, mechanisms, types and consequences of the different tool wear types in machining. Tool wear considered as a result of mechanical (thermo-dynamic wear, mostly abrasion) and chemical (thermo-chemical wear, diffusion) interactions between the tool and workpiece [5]. Most common wear mechanisms as part of machining presented in figure 1.

In drilling heat generation, excessive vibrations, pressure, friction and stress distribution are the main contributors of drill wear. The drill wear classified into [6]: flank wear (VB), crater wear (KM), outer corner (w), margin wear (Mw). Besides with two types of chisel edge wear (CT and CM) as well as chipping at the cutting lips (PT and PM). Classifications of drill wear presented in figure 2.

Drilling holes is an essential process in the structural frames of an aircraft and contribute to 30 to 60% of the total material removal operations [7]. Flank wear value is vigilantly monitored as one of the criteria to measure the performance of a drill. However, Kanai et al. [8] recommended that outer corner wear can serve as the primary criteria for to evaluate the tool performance of the comparative

simplicity of measurement and the close association of this kind of wear and the drill bit tool life. Crater wear is too evidently visible on the rake face of the drill and can exist apparently in the region of the outer corners of the cutting edges [9-10].

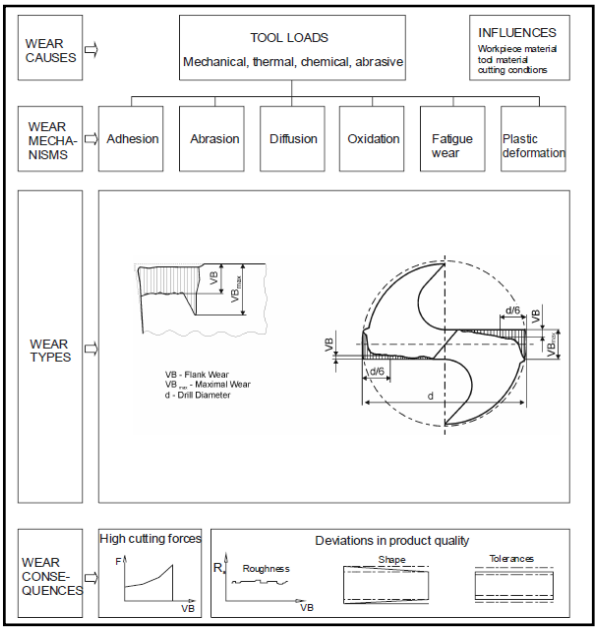

Fig. 1. Overview of the tool wear in machining [4]

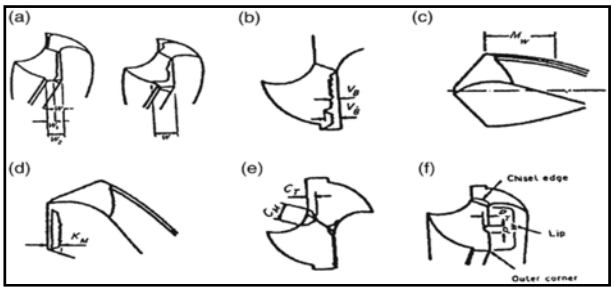

Fig. 2. Types of drill wear: (a) outer corners, (b) flank, (c) margin, (d) crater, (e) chisel edge and (f) chipping [6].

Harris et al. [11] considered the outer edge wear as their tool rejection criteria. Tetsutaro & Zhao [12] found that the tool rejected when the highest flank wear value is obtained, as 0.6 mm while drilling plain steel. Lin and Ting [13] dismissed the tool based on the tool rejection criteria when maximum flank wear land exceeded 0.8 mm, and surface roughness value exceeded 5.0 µm. Imran et al. [14] their study focuses on the surface integrity and wear mechanisms associated with mechanical micro- drilling of nickel-base superalloy (Inconel718) under dry and wet cutting conditions. Tarng et al. [15] demonstrated an in-process method for prediction of corner wear in drilling operations using a polynomial network. Thrust force and torque in drilling processes have interrelated with corner wear in this study. It reveals that the thrust force is better than the torque as the sensed signal parameter for the in-process prediction of corner wear. Under normal drilling conditions, [16] the letdown of the drill tool owing to breakage was witnessed with lesser size drills (diameter < 3 mm), whereas extreme wear was the first failure type with large size drills (diameter > 3 mm). When drilling compared with turning, and milling operations, the kinematic and dynamic structures were more or less similar, and the chip flow and the distribution of cutting temperatures were the same. In drilling, the chip formation occurs in a closed area, which is not visible and this is the major drawback associated with drilling. The unwanted vibrations created during machining results in lower workpiece surface quality, undesired sensitivity to the gauge integrity, early wear, breaking of cutting tools, damage to machine elements and high noise levels [17]. Studies have shown that the vibrations created during machining operations are of a complex structure. Vibration is an integral part of the manufacturing process and, also a crucial factor in high-speed machining for limiting the metal removal rates [18]. During machining, the formation of self-excited vibration is defined as chatter and is the basis of the vibration phenomenon. Chatter recognized as one of the most common issues related to all types of manufacturing operations. Chatter has adverse effects on the cutting process, reduces the tool life, accelerates tool wear, forms a rough surface and can damage some machine parts [19]. The modeling and the monitoring of vibrations in machining processes gained attention among the researchers over the last 10–15 years.

Quintana and Ciurana [20] still consider chatter in machining has been an important topic in manufacturing research. Adverse effects of chatter stimulate interest in solving the problem along with the complexity of the chattering phenomenon gives challenges to researchers. Prediction of chatter occurrence is still the subject of much research, even though the regenerative effect, the primary cause of chatter, was identified and studied very early on [21-22]. Ema and Marui [23] studied the chatter vibrations during the deep hole drilling operation. It found that chatter vibration tends to occur because of their low bending stiffness and viscous damping. Chatter vibration not only sources a decrease of tool life and machined hole accuracy but also averts quicker and more efficient drilling operations. Ema et al. [24] investigated the chatter vibration of long drills using various drill bits with different overhang lengths and special drill bits. The amplitude, frequency, initiation boundary and unstable range of chatter vibrations measured at various cutting parameters. The experimental results showed that the vibration is a regenerative chatter and its frequency is equal to the natural bending frequency of the drill when the drill point supported in a machined hole. Based on the experimental results, the stability of chatter vibration discussed. Mehrabadi et al. [25] presented the investigations on chatter vibration occurring in drills for deep hole machining. A finite element method is used to simulate the tool path at different spindle speeds. Moreover, chatter can occur in various metal removal including drilling [26-30] operations.

Fang Ning et al. [31] investigated the effects of built-up edge (BUE) on cutting vibrations at different cutting conditions in the turning of aluminum 2024-T351 alloy and observed that the vibration amplitude

was affected by the cutting speed, the feed rate, and their interaction. According to their findings, there exist three distinct BUE regions, characterized by different patterns of cutting vibrations. Abuthakeer et al. [32] investigated the effects of spindle vibrations on surface roughness by using an artificial neural network (ANN) in the dry turning of Al6063 aluminum workpiece material. Rahim et al. [33] investigated the performance of uncoated carbide tools in the high-speed drilling of the Ti6Al4V alloy. Machining responses of the drilling process such as vibration, thrust force, chip formation, and torque examined at different test conditions. It apparently found that cutting speed and feed rate significantly influenced machining responses. Dornfeld et al. [34] investigated the effects of tool geometry and process parameters on drilling burr formation of Ti-6Al-4Vusing carbide drills with and without coolant, and high-speed cobalt drills without coolant. Performance evaluation of high-speed steel (HSS) tools presented under different test conditions. The main wear mechanisms critically analyzed with scanning electron microscope and also identified adhesion, and abrasive wear on flank face, besides, BUE at chisel and cutting edges [35]. Sakurai et al. [36] have investigated the tool life, burr shape, and chips formation under different cutting strategies in drilling using coated drills. Machinability study of Ti–6Al4V using short length drills of high-speed steel discussed.

Khanna et al. [37] present the use of Taguchi approach for better tool wear rate in the drilling of Al-7075. The optimal combination of drilling process parameters and their levels of tool wear obtained. Erkki Jantunen [38] presented the summary of the monitoring methods, signal analysis and diagnostic techniques for tool wear and failure monitoring in drilling by using indirect monitoring methods such as force, vibration and current measurements. Rehorn et al. [39] presented a detailed review of various sensors and signal analysis methods used for tool condition monitoring systems in industrial machining applications. Loparo and Ertunc [40] showed several innovative monitoring methods for on-line tool wear condition monitoring in drilling operations. Monitoring and measurement techniques using of force signals (thrust and torque) and power signals (spindle and servo) also discussed. Jemielniak et al. [41] presented the structure of tool condition monitoring (TCM) system for drilling operation consisting of cutting forces, vibration, acoustic emission signals. These process variables measured by appropriate sensors producing analog signals. Downey et al. [42] demonstrated the automatic data acquisition system by employing multiple sensors deployed on a CNC turning center in a real-time production environment. The combination of sensors and data acquisition is novel in that it brings together all the popular sensing techniques in the field of tool condition monitoring and tests the validity of these technologies in a live production environment.

Independent operator response on the recital of the operation concerning together product dimensional steadiness and machined surface integrity used for assessment of the attained data applicability for tool condition monitoring. Erturk et al. [43] proposed a computer vision-based approach to drilling tool condition monitoring. Experimental results show that the proposed method detects the condition of all tested tools successfully.

Moreover, tool condition monitoring is used in modern manufacturing environments to reduce machine tool downtime and facilitate optimum utilization of unsupervised machining centers. Tool condition monitoring is required mainly to detect tool wear and avoid tool breakage to protect the product as well as machinery. A machining process, in general, was accomplished through a series of multiple changes of process dynamics. The number ranges of the occurrences involved with the process of metal cutting; they are mostly damaging for the cutting tool condition and workpiece surface roughness. The uncontrolled machining operation creates chatter, vibrates the system, and disturbs the machining stability, which eventually affects the state of the cutting tool and product quality. Hence, drilling process requires a tool condition monitoring system that is capable of observing the performance of a cutting tool during machining and quantifies vibration levels, and the damages occurred to it due to responsible process mechanics [44].

An efficient detecting technique required for evaluating the performance of drill bits based on the vibration signal analysis. For this purpose, several methods detecting the tool failure and monitoring the cutting force, vibration, acoustic emission (AE), Acousto optic emission (AOE) and current of tool machine have been investigated [45]. The important primary goal in the application of tool condition monitoring (TCM) is to find the possible correlation between tool flank wear and vibration displacement so as to identify the condition of the drill bit in the present study. As per the reason mentioned above, it necessary to measure vibration and determine displacement due to vibration to provide reliable data in understanding the performance of the drill bit based chatter phenomenon. An efficient detecting technique like this can prevent possible damage to the cutting tool, workpiece, and machine tool. Reports on the performance of HSS (high-speed steel) drill bit and carbide drill bit tools when drilling Ti-6Al-4V and Al7075 alloys and are still lacking. Present work is carried out with an objective to evaluate the performance of HSS (high-speed steel) and carbide twist drill bits at various cutting combinations. The effect of varying cutting speeds on tool wear, tool life and surface finish of the hole produced investigated.

2. EXPERIMENT DETAILS

The vibrations in turning, milling, and some researchers have examined drilling operations by using force sensors, microphones, and accelerometers. A Laser Doppler vibrometer (LDV) employed for acquiring vibration signal in real time.

These vibration causes high-frequency displacements in feed direction which leads to defects in the hole diameters, accelerates the wear, and decreases tool life. As per procedural steps are shown

in figure 3, drilling tests were carried out with drills of 10 mm diameter using a radial drilling machine under dry cutting conditions. Blind holes drilled with a constant 8 mm depth at different test conditions. A significant increase in tool wear observed when increasing cutting speed, feed rate and the number of holes drilled. The utmost wear type seen in the form of flank wear. The purpose of experiments is to evaluate the drill bit performance based on vibration levels and establish a relation with tool life at different drilling conditions as listed in Table 1.

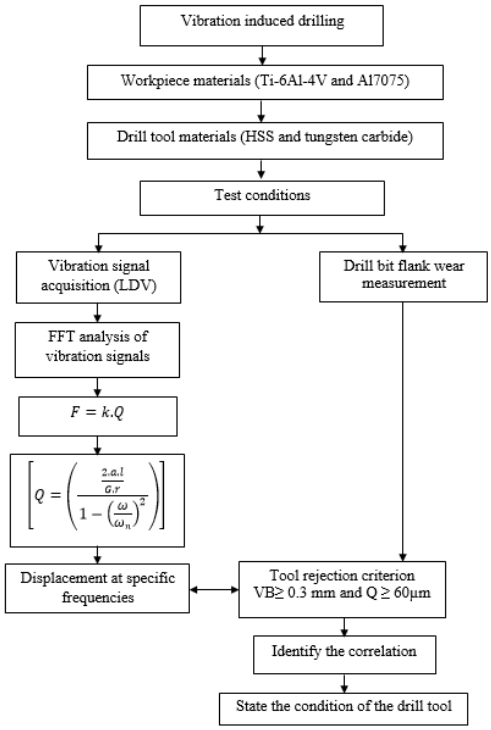

Fig. 3. Procedural steps in the proposed methodology

Levels	Factors		
	1	2	3
Cutting speed, Vc : m/min (Rpm)	19.6(625)	24.9(795)	39.2(1250)
Feed rate, f: mm/rev	0.02	0.04	0.06
Workpiece materials, H(Vickers's hardness)	Ti-6Al-4V(349 HV)		AL7075(175 HV)
Drill bit	HSS		Tungsten carbide

Table 1. Factors and levels used in the experiment

Most commonly used materials in aircraft and automobile industry such as titanium alloys (Ti-6Al-4V) and aluminum alloys (Al7075) of dimensions (150mmX150mm X10mm) are selected as specimens for experimental investigation. Table 2 gives the mechanical properties and chemical composition of workpiece materials.

Workpiece (Young's modulus)	Mechanical properties				
	Density	Hardness, HV	Yield strength	Tensile strength	Thermal conductivity
Ti-6Al-4V (120 Gpa)	4420 kg/m³	349	880 Mpa	950 Mpa	6.7 W/m-K
Al7075 (72 Gpa)	2800 kg/m³	175	503	572	130 W/m-K

Chemical composition of workpiece materials					
Ti-6Al-4V	Al	Fe	O	Ti	V
	6	Max.25	Max.25	90	4

	Al	Zn	Cu	Cr	Fe	Mg	Mn
AL7075	87.1 - 91.4%	5.1 - 6.1% max	1.2 - 2.0%	0.18 - 0.28%	0.5 max	2.1 - 2.9%	0.3% max

Table 2. Mechanical properties and chemical composition of workpiece materials Ti-6Al-4V alloy and AL7075 alloy

Both high-speed steel and tungsten carbide drill bit of Ø10mm diameter selected as cutting tool materials. Table 3 presents the properties of the drill bits whereas Table 4 gives the chemical composition of drill tools used the current study.

The tests are carried out on 38mm cap radial drilling machine, manufactured by Siddharupa machine tools, Gujarat, India. Principal specifications include; Drill Capacity: 38 mm drill head, Spindle nose: MT 4, Spindle Travel: 220, No. of Spindle Speed: 8, the range of Spindle Speed: 62-1980 rpm, Range of Power Feed (mm/Rev): 2, working table: 380mmx300mmx300mm. The cutting parameters selected according to the tool supplier's recommendation for tool and workpiece combinations. Cutting tests are planned to conduct at dry machining conditions. Cutting velocity and feed rates are chosen based on the tool manufacturer's (Sandvik) recommendations for workpiece material and drill bit combination. The schematic representation of experimental setup for the drilling operations presented in figure 4a. Real-time experimental setup and vision based drill bit tool wear measuring equipment shown in figure 4b. Figure 4c gives a particular tool wear measurement using Opto mech vision inspection system.

Properties	HSS drill	WC drill
Standard	DIN 338	DIN 338
Diameter, mm	10	10
Material	HSS	Tungsten carbide
Hardness,HV	918	1300
Type	2-flute Twist drill	2-flute Twist drill
Length, mm	133	133
Flute length, mm	87	87
Number cutting edges	2	2
Lip length, mm	4.5	4.5
Web thickness, mm	2	2
Margin, mm	1.25	1.25
Point angle, °	118	118
Helix angle, °	30	30
Relief angle, °	8-12	8-12
Lip angle, °	55	55
Coating	Uncoated	Uncoated
Cutting direction	Right	Right

Table 3. Properties of drill bits

HSS	Si	V	Cr	Mn	Ni	Nb	Mo	Co	Fe
	3.709	1.95	3.97	0.046	0.688	0.792	6.469	4.382	77.993
WC	W	Cu	Zn	Ni	Co	C			
	54	20	16	4	3	3			

Table 4. Chemical composition of the drill

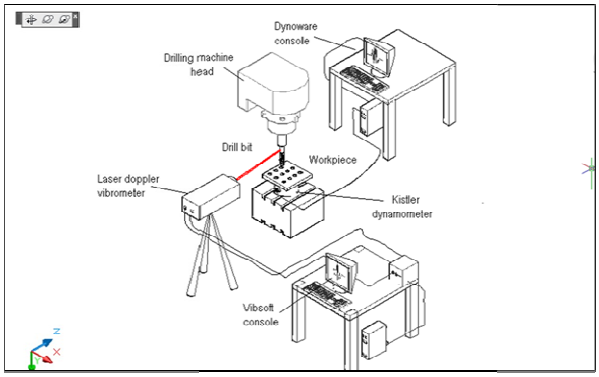

Fig. 4a. Schematic representation of experimental setup for drilling process

Fig. 4b. Physical experimental setup


Fig. 4c. Drill wear under vision inspection system

A constant 8 mm depth of cut maintained throughout the experiment. Both cutting speed and feed rate varied according to the design of the experiments for different workpiece - tool combination. A non-contact vibration transducer Laser Doppler Vibrometer (LDV) PolyTec 100V with a data acquisition scheme is kept at a constant distance (2m) from the rotating drill bit during machining to measure the shift during the drilling process.

Laser from the LDV is being focused [46-47] on the rotating cutting tool (drill bit), and the impact of the measured vibrations in the feed direction (cutting direction) is too high during the drilling operation. Variations in the vibration signals give an idea about the tool wear. A 10 mm diameter hole drilled in the workpiece material and corresponding displacement amplitude due to vibration recorded. The package program was used to collect the vibration data created during the tests into the computer environment. Lastly, the displacement values determined from vibration amplitude data with the aid of FFT algorithm by using MATLAB code. Tool wear values measured for each drilling condition under vision inspection systems. Cutting forces measured with Kistler® 9272 force dynamometer with a multi-channel analyzer, which placed below the workpiece.

2.1 Tool rejection criteria adopted in the present study

In the present work, the performance of the drill bit is evaluated based on both ISO 10816 and ISO 3685. According to ISO 3685 standard, three conditions of the tool considered: sharp tool (flank wear VB= 0 mm), the semi-dull tool (Flank wear VB≤ 0.3mm), and dull tool (flank wear VB ≥0.3 mm) in drilling [48]. ISO 10816 for vibration severity standard for rotating members is applied to evaluate the drill bit performance based on vibration displacement values. As per ISO 10816, displacement value for a rotating object (drill bit) up to 20 microns do not have any effect on drill bit flank wear. Tool flank wear is found to be affected by the displacement value between 20 microns to 60 microns. Any value of displacement parameter beyond 60 microns is not acceptable as per standard.

3. MODELLING OF AMPLITUDE OF VIBRATION IN DRILLING

Consider the drill bit as a straight round bar that fixed at one end, and it presented in figure 5and drill bit is rotating and drilling a hole into the workpiece. In this case, forced vibrations produced because of rotation of the spindle. These vibrations have a frequency of external excitation (ω) which is nothing but spindle speed in rad/sec.

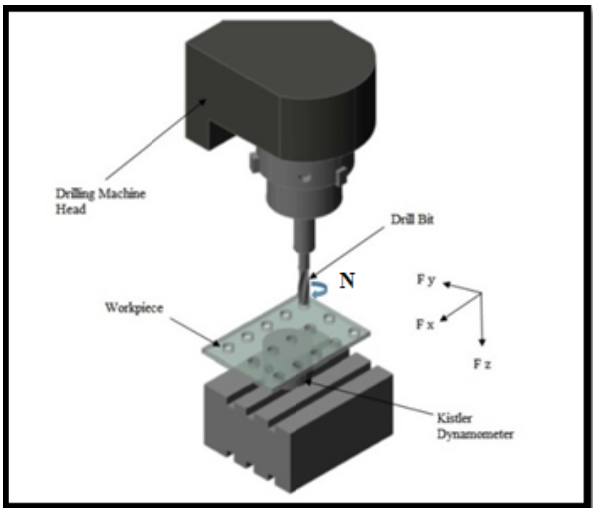

Fig. 5. Drill bit entered into the workpiece

In the drilling operation, the spindle rotates with speed N and N_z is the number of flutes in the drill bit. Vibration frequency (f) of the rotational speed of the spindle computed by the following expression. In drilling spindle rotates with speed N, then the vibration frequency (f) for the rotational speed of the spindle. The exciting frequency ω is related to the vibration frequency (f) in Hz is defined through the relation [49-51]:

$$f = \frac{\omega}{2\pi} \ [Hz] \qquad (1)$$

The cutting process generates forced vibrations through transient cutting forces, especially in the cutting process like drilling. The forcing frequency is usually the spindle rotational frequency and

harmonics, or the tooth impact frequency and harmonics. In drilling, the frequency of the forced vibration equals the product of the tool/spindle rotational frequency and the number of teeth on the tool (or tooth passing frequency,f_n). It also called as the fundamental forcing frequency (FFF), f_n and easily changed by adjusting the spindle rpm or some teeth on the tool. Tooth passing frequency of the drill bit computed by following relation [52] where l is the length of the drill bit. Tooth-passing frequency is a critical operational frequency and this defined as the inverse of the time between two subsequent tooth-passes. For a multi-tooth cutter with z teeth and uniform angular spacing between the individual cutting inserts, the tooth passing frequency (f_n) is defined as:

$$f_n = \left(\frac{N}{60}\right) * N_z \ [Hz] \quad (2)$$

In drilling, an amplitude of forced vibrations depends on the magnitude of the exciting force and on the dynamic stiffness of the machine tool, cutting tool, and the workpiece, which are often an order of an amount lower than the static values. Frequency response function (FRF) will exhibit compliance or flexibility of the part at every frequency. For a linear system the displacement of the part at each frequency can be determined from the FFF and FRF [53]:

Displacement, Q (μm) = FFF (N) x FRF (μm/N) (3)

Present work mainly focused on the transverse vibrations. It is due to the transverse vibrations produced during the drilling operation are the primary cause of the enlargement of the diameter of the hole produced beyond tolerance limit. It is important to note that a large part of the energy dissipation occurs at the tool holder–spindle interface. It is often convenient to characterize a linear system by its response to a specific sinusoidal input force $f(t)$ given by

$$f(t) = Fe^{\omega.t} \quad (4)$$

Where
F is the forcing amplitude
t is the time
ω is the exciting frequency in rad/sec

A modal Fourier transform analysis is performed using $Q(\omega)$for the displacement $q(t)$. Where the forcing function is $f(t)$and $F(\omega)$ is the Fourier transform of $f(t)$. The steady-state response of this system, which is present as long as the forcing function is active, is given by:

$$Q(\omega) = G(\omega).F(\omega) \quad (5)$$

$$G(\omega) = \frac{Q(\omega)}{F(\omega)} \quad (6)$$

$Q(\omega)$, the frequency response function (FRF) of the system is the ratio of the complex amplitude of the displacement (which is a harmonic motion with frequency ω) to the magnitude For the forcing function.

The amplitude of vibration produced by a unit force at the frequency 'ω.'
In the present work, both forces applied by the machine on the tool and resistive force applied by the workpiece during the drilling operation considered. When drill touches the workpiece and starts cutting the material to produce the hole, the upward resistive force acts on the drill because of the tensile stress of the workpiece material. When the material breaks during drilling the hole, its failure in the longitudinal direction considered as the compressive failure. The amplitude (Q) of the forced vibration computed with no damping condition using the formula given below [51]:

$$Q = \left[\frac{\frac{2.a.l}{G.r}}{1-\left(\frac{f}{f_n}\right)^2}\right] \quad (7)$$

Where f= frequency of vibration, f= tooth passing frequency, A = amplitude of excitation, G -shear modulus, a - acceleration of drill and r - radius of the drill.

The maximum displacement amplitude will found at the 1st harmonic of the forcing frequency. Displacement amplitude maximum because the dynamic flexibility is near the resonant frequency. To characterize the ability to resist this kind of vibration, an index of machine tool dynamic stiffness (k) is used [53]:

$$k = \frac{F}{Q_{max}} \quad (8)$$

4. VIBRATION SIGNAL PROCESSING USING FAST FOURIER TRANSFORM

The actual implantation of the real-time monitoring system typically starts with designing a proof-of-concept experiment. Acousto optic emission (AOE) based tool wear identification is primarily subject to the interpretation of the captured signals. However, the extraction of essential features useful for tool wears identification from the collected acousto optic emission signal. In this work, time-series analysis applied to the wave signals for detecting percent of the amplitude of displacement due to vibration during drilling. All the time domain signals in the present work are filtered using a 0-500Hz band pass filter, and signal processing involved signal blocks of 3200 data points collected over a sampling interval 500 milliseconds. In the present work, vibration raw signals are gathered using an LDV, and the vibration amplitude plotted against time domain. This form of representation is called waveform graph, and it showed in figure 6 which consists of time domain data while drilling holes at 5th, 10th, 15th and 20th.Wave graphs give the percentage of vibration amplitude only for a particular time domain data. Hence, it is tough or often impossible to quantify the vibration levels with the help of wave graph.

Moreover, direct time-series analysis is usually incapable of isolating defect-scattered information appropriately from noise in different frequency bands. Therefore, time domain signal must convert into converted to frequency domain as spectrum graphs by using a fast Fourier transform (FFT). Fast Fourier transform is utilized to determine the vibration parameter, i.e., displacement (microns) in the frequency domain for analysis of the vibration signal.

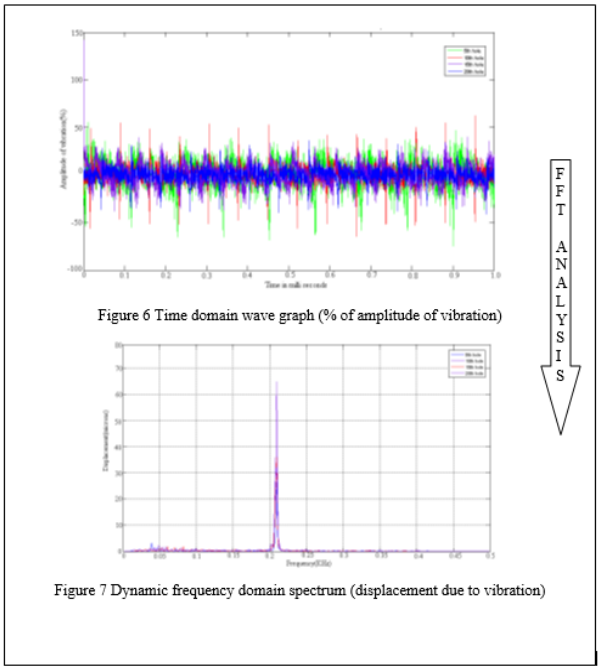

Figure 6 Time domain wave graph (% of amplitude of vibration)

Figure 7 Dynamic frequency domain spectrum (displacement due to vibration)

Fig. 7. Tthe spectrum graph for the corresponding time domain based wave graph corresponding to drilled holes at 5th, 10th, 15thand 20th.

Figure 7 gives the spectrum graph for the corresponding time domain based wave graph corresponding to drilled holes at 5th, 10th, 15thand 20th. The spectrum graph presented in figure 7 provides more information about machining process than the waveform graph.

Figure 7 presents the response of dynamic signal in the frequency domain by applying 2D-FFT to direct time signal in time domain. The displacement plotted for the frequency. The detailed results and discussion presented in the next section. Throughout the present work, vibration parameter considered for the experimental analysis is displacement in microns. The peak amplitude varies from 5 µm to 150 µm depending on the severity of the chatter and cutting speed as shown in Table 1.

4.1 Effects of process parameters on displacement and tool wear

A series of 10 mm diameter holes drilled on Ti-6Al-4V (349HV) and Al7075 (175HV) work pieces according to full factorial plan at the constant depth of cut as 8 mm. In each condition, 20 holes drilled, and readings gathered during 5th, 10th, 15thand 20th cut. The performance of high-speed steel and tungsten carbide drill bit is evaluated based on the amount of the displacement (Q) value and its correlation with tool wear (VB). The most important parameters affecting displacement parameter value are workpiece hardness (H), cutting speed (V_c), feed rate (f), and machining time (number of holes). The effect of drill length/tool overhang ignored by selecting a standard length drill bits based on the literature review as part the present paper. Results shown in figure 7 consists of the spectrograph, which only illustrates the variation in measured vibration parameter, i.e., displacement (Q) values on Y-axis and X-axis gives the frequency of vibration in Hz. As stated earlier, wave graphs in time domain data are intentionally eliminated from the vibration plots since it is hard to quantify the vibration levels with the help of wave graph. Each spectrum graph consists of the displacement values while drilling holes at 5th, 10th, 15th and 20th.

5. EXPERIMENTAL RESULTS AND DISCUSSION

Both wave graph and spectrum graph presented in this study give information while drilling 5th, 10th, 15thand 20thholes at a particular test combination as per the experiment plan. Displacement value varies depending on the workpiece hardness, drill length, cutting speed, feed rate, and the number of drilled holes. Displacement data measured at different levels of process parameters given in Table 5.

Tool life of drill bits while drilling holes on Ti-6Al-4V alloy with constant depth cut as 8 mm										
Colu mn	Experiment Run		Cutting force in feed direction (N)		Displacement in feed direction (µm)		Flank wear,VB (mm)		Tool life (min)	
	Vc, m/min (rpm)	f (mm/rev)	HSS	carbide	HSS	carbide	HSS	carbide	HSS	carbide
Ti-1	19.6 (625)	0.02	724	464	10.5	8.2	0.11	0.09	2.92	4.20
Ti-2	19.6 (625)	0.04	810	526	21.4	17.5	0.16	0.11	2.39	4.19
Ti-3	19.6 (625)	0.06	931	583	39.10	32.2	0.20	0.16	2.23	4.18
Ti-4	24.9 (795)	0.02	614	274	20.2	25.3	0.23	0.12	1.97	3.94
Ti-5	24.9 (795)	0.04	460	315	55.1	42.2	0.26	0.18	1.67	3.15
Ti-6	24.9 (795)	0.06	358	352	65.3	58.3	0.29	0.23	1.25	3.28
Ti-7	39.2 (1250)	0.02	180	150	39.2	30.9	0.25	0.19	0.79	1.28
Ti-8	39.2 (1250)	0.04	147	171	69.7	57.1	0.35	0.25	0.68	1.11
Ti-9	39.2 (1250)	0.06	114	193	85.5	62.1	0.42	0.32	0.60	1.05
Tool life of drill bits while drilling holes on Al7075 alloy with constant depth cut as 8 mm										
	Vc, m/min (rpm)	f (mm/rev)	HSS	carbide	HSS	carbide	HSS	carbide	HSS	carbide
Al-1	19.6 (625)	0.02	625	377	8.5	5.3	0.08	0.05	3.02	4.51
Al-2	19.6 (625)	0.04	750	433	16.6	12.2	0.12	0.10	2.88	3.81
Al-3	19.6 (625)	0.06	862	510	35.3	27.5	0.19	0.15	2.52	3.08
Al-4	24.9 (795)	0.02	516	182	12.5	10.4	0.15	0.12	2.01	1.67
Al-5	24.9 (795)	0.04	603	212	33.1	21.3	0.21	0.19	1.72	1.59
Al-6	24.9 (795)	0.06	669	241	56.1	46.1	0.25	0.26	1.5	1.34
Al-7	39.2 (1250)	0.02	287	118	37.5	31.6	0.22	0.18	1.28	2.30
Al-8	39.2 (1250)	0.04	332	138	61.1	52.7	0.29	0.26	1.18	1.63
Al-9	39.2 (1250)	0.06	371	153	77.3	64.1	0.36	0.31	1.09	1.35

Table 5. Tool life of drill bit at constant 8 mm depth of cut for Ti-6Al-4V as per FF

From the results presented in Table 5, it is realized at various process parameters at all levels and in the FF design test setup, as the number of holes increased, the displacement parameter values also increased. In some cases, the last holes drilled by the drills that completed their tool life before reaching the 20th hole, i.e., flank wear(VB) values is found to be more 0.3mm. In the hole drilling operations at different levels of process parameters, the lowest displacement value is measured as 5.3 µm while drilling 5thhole with carbide drill bit in the Al7075 workpiece. This value is measured while drilling performed with cutting speed 19.6 m/min (625 rpm) and feed rate as 0.02 mm/rev. The highest displacement value 85.5 µm while drilling 20th hole with high-speed steel drill bit

in the Ti-6Al-4V workpiece. This value found while drilling performed, with cutting speed 39.2 m/min (1250 rpm) and feed rate as 0.06 mm/rev. It understood from Table 5 that the selection of a lower cutting speed and higher feed rate would have been more appropriate.

Results in Table 5, it indicates that the cutting speed contributed to 51% of the variation of drilling vibrations, followed by the feed rate, which results in 35.3% of the total variation.

The present study on the drilling of Ti-6Al-4V and Al7075 alloys using high-speed steel and tungsten carbide twist drills demonstrated an increase of displacement value at feed rate 0.02 mm/rev, 0.04 mm/rev and 0.06 mm/rev.

5.1 Main effects of process parameters on displacement amplitude and tool wear

Main effect graphics show the types of effects of dependent variables (output parameters) at different levels of independent variables (input parameters) [54]. In the drilling of Ti-6Al-4V and Al7075 specimens with high-speed steel and tungsten carbide twist drills having same lengths, the main effects of the process parameters on displacement amplitude (Q) shown in figure 8.

Rotational speed(N)	Feed rate(f)	Hardness(H)	Depth of cut	L/d ratio
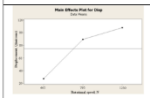	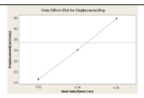	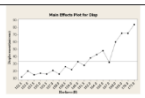	Kept constant. Its effect is assumed to be common.	Maintained the same ratio. Hence, no effect.

Fig. 8. Main effects of the process parameters on displacement amplitude

Effect of workpiece hardness on the variation of displacement amplitude values, depending on the number of holes and hole depth, is given in figure 8. The most important parameters affecting displacement amplitude were spindle rotational speed (N), feed rate (f), and workpiece hardness (H). There is no significant effect observed with drill length/tool overhang (L/d). A depth of cut is kept constant throughout the investigation due to this its effect is assumed to constant in all conditions. In the drilling of both of the work pieces, as the number of holes and hole depth increased, displacement amplitude values also increased. Cutting speed (V) is another important parameter on vibration which shortens tool life. The increasing tool wear at higher cutting speeds causes the cutting forces, chatter, and vibration to increase. Cutting tool lives are typically reduced by 50 to 80% at higher cutting speeds due to chatter vibrations [55]. While the displacement amplitude increased with the raising of the feed rate from 0.02 mm/rev to 0.06 mm/rev. It saw that in the drilling of Ti-6Al-4V, which possesses high hardness, higher displacement amplitude values obtained.

5.2.1 Displacement due to vibration – as a base for drill bit performance evaluation

In figure 9, vibration parameter displacement values measured at the minimum cutting speed of 625rpm (19.6 m/min) for high-speed steel drill bit. At similar test conditions, the performance of carbide drill bit is also evaluated based on displacement value. At the low cutting speed, depending on the increase in the number of holes, a gradual increase occurred in the displacement amplitude values. This trend is similar in the case of both high-speed steel and carbide drill bits as well, and it is clearly evident in figure 9. Vibration parameter displacement values measured at the maximum cutting speed 1250 rpm (39.2 m/min) for high-speed steel and carbide drill bits presented in figure 9.

At high cutting speed, displacement value on high-speed steel drill bit increases more rapidly than with carbide drill bit in all test conditions presented in this section. It is due to high rigidity associated with carbide drill bit with high hardness as well. With high-speed steel drill bit, displacement parameter value increases approximately by 165% while drilling Ti-6Al-4V and in the case of Al7075 alloys, an increase of 89% observed. In the event of carbide drill bit, displacement parameter value increases approximately 105% while drilling Ti-6Al-4V.

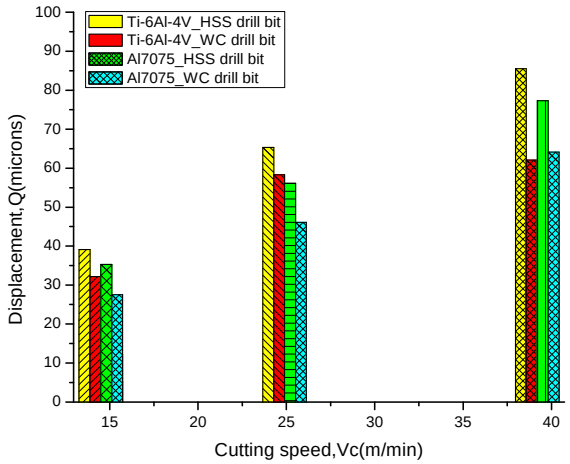

Fig. 9 Effect of cutting speed on drill bit performance (displacement)

When making holes on Al7075 alloys, the change in displacement value is observed as 49% approximately by raising the cutting speed from 19.6 m/min (625 rpm) to 39.2 m/min (1250 rpm). From the results table 5, it found that the maximum displacement value measured as 85.5 µm and its corresponding flank wear (VB) value is 0.42 mm while drilling holes on the Ti-6Al-4V specimen with high-speed steel drill bit at maximum cutting speed is, i.e., 39.2 m/min. According to vibration severity standard ISO 10816, any value of displacement beyond 60µm is not advisable for further machining. As the displacement value crosses beyond 60µm, then the corresponding tool flank wear (VB) also found to be above 0.3mm. The excessive wear occurred in the cutting tool at high cutting speed, and the steady built-up edge (BUE) formation were the main reasons for the increase in the displacement value. In the machining of T-6Al-4V and Al7075 alloys, the cutting speed affects the formation of BUE in three different regions. In this case, highest displacement values are observed as 55 µm while drilling the 20th hole on the Ti-6Al-4V alloy with high-speed steel drill bit. The minimum amount of displacement is the as 25 µm

while drilling the 20th hole on the Al7075 specimen with tungsten carbide drill bit. It is clear that when Ti-6Al-4V (349 HV) workpiece drilled with high-speed steel drill bit produces higher displacement values obtained when compared with tungsten carbide drill bit. From the figure 9, it found that the displacement parameter value increases as the as the number of holes increases. Orhan et al. [56] examined the changes in the vibration and the tool wear during the end milling operation. It observed that vibration amplitude is found to increase with the progression of tool wear and causes vibrations in the workpiece/cutting tool/machining center.

5.2.2 Effect of cutting speed on drill bit performance

Cutting speed (V_c) is another important parameter on vibration that shortens tool life. The increasing tool wear at higher cutting speeds causes the cutting forces, chatter, and vibration to increase [57]. Figure 10 gives the variation of flank wear value at various cutting speeds by using high-speed steel and carbide drill bits. The flank wear (VB) value of 0.3 mm considered as the criterion for judging the effective tool life of the cutting tool. The performance of cutting tool lives are typically shortened by 50% to 78% at higher cutting speeds due to [58] regenerative vibrations.

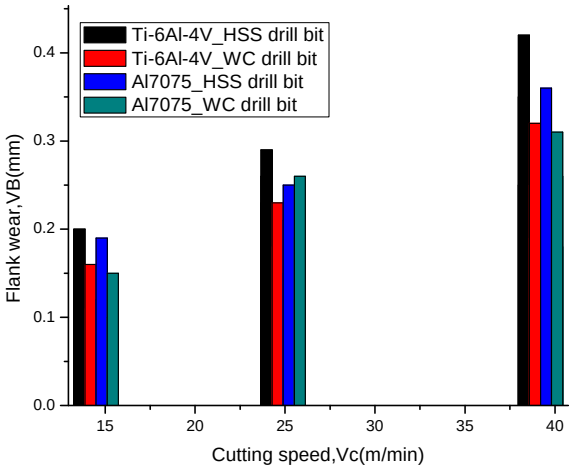

Fig. 10. Variation of flank wear at different cutting speeds

Figure 10 gives the growing of flank wear (VB) values found at cutting speed combinations. At low cutting speed, i.e., 19.6 m/min both high-speed steel and carbide tools showed the optimum tool life irrespective of workpiece materials. When cutting speed is maintained at 24.9 m/min (795 rpm), high-speed steel drill bit loses its life after drilling 147 holes on Ti-6Al-4V specimen whereas high-speed steel drill bit can retain its shape even after drilling 215 holes on the Al7075 specimen. High-speed steel drill bit performance is reduced by 78% while drilling holes on Ti-6Al-4V alloy and 52% when drilling Al7075 alloy at highest cutting speed, i.e., 39.2 m/min. From the figure 10, it observed that the flank wear values increases as the as the number of holes increases. It also found that displacement parameter value is growing with the progression of tool wear and causes vibrations in the drilling operation.

5.2.3 Effect of feed rate on drill tools life with displacement

Effect of feed rate on drill bit's tool life analyzed by varying the feed rate from 0.02 mm/rev, 0.04 m/min and 0.06 mm/rev. Effect of feed rate on drill bit life in all test condition presented in figure 11. As the friction generated per unit time increases the tool wear, which in turn shortens the tool life. As the feed rate increased from 0.02 mm/rev to 0.06 mm/rev along with cutting speed, which reduces the effective life of the drill bit.

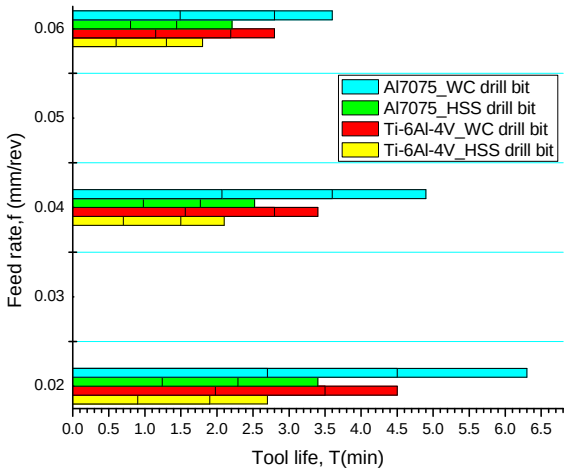

Fig. 11. Effect of feed rate on drill tool life

The useful life of high-speed steel drill bit when drilling Ti-6Al-4V represented by 'yellow' color and while drilling Al7075 alloy is identified with 'green' color in figure 11. In figure 11, bars with 'red' color gives the carbide drill bit life while drilling titanium alloy, whereas 'cyan' Colored bars show the life of carbide drill bit while drilling Al7075 alloy. Effect of feed rate is found to be maximum on high-speed steel drill bit while drilling holes on the Ti-6Al-4V alloy. Tool life of the high-speed steel drill bit recorded as less than 1 min, i.e., 41 seconds at cutting speed 39.2 m/min and corresponding displacement value are 85.5µm that is highest in the experimentation. Carbide drill bit exhibits the maximum tool file while drilling holes in the Al7075 specimen at all feed rates. In the drilling of the Ti-6Al-4V alloy during the experiment, flank wear, chisel edge wear, outer corner wear, and BUE were observed in the case of a high-speed steel cutting tool is presented in figure 12(a). Figure 12(b) gives the flank wear, chisel edge wear, outer corner wear, and BUE observed of carbide insert drill. The excessive wear occurred in the drill bit at higher cutting speeds, and the steady BUE [59] formation were the main reasons for the increase in the displacement value. In the machining, the cutting speed affects the formation of BUE in three different regions. The first region is the BUE initiation region, formed on the tool rake face at the low cutting speed of 19.6 m/min. In this region, due to chip fracture, cutting force oscillations, and significant variation of vibration amplitude in an irregular pattern occurs with increasing cutting speed.

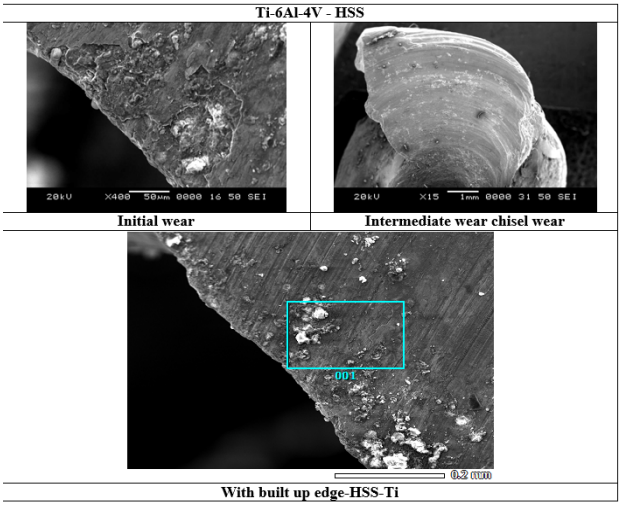

Fig. 12a. Tool wear mechanisms while Ti-6Al-4V drilled with high-speed steel drill

The steady BUE region occurred at the cutting speed of 24.9 m/min. In the steady BUE region, vibration amplitude steadily increases with increasing cutting speeds. In cutting tests, continuous chips with a tight chip curl observed.

The unsteady BUE region occurs at the relatively high cutting speed of 39.2 m/min. Due to the increase in cutting speed, the chips flowing over the tool rake face periodically fracture the BUE, and thus, the process of BUE formation occasionally broken.

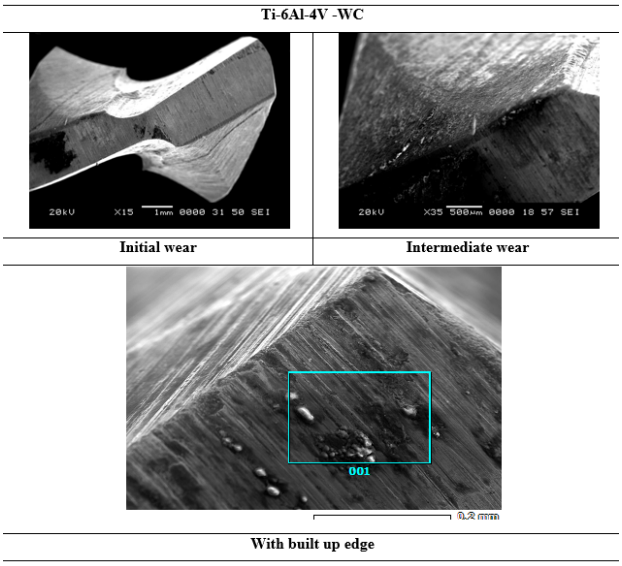

Fig. 12b. Tool wear mechanisms while Ti-6Al-4V drilled with tungsten carbide drill

The vibration amplitude keeps nearly constant with increasing cutting speeds. These observations were valid and applicable to for the wear mechanisms shown in figure 12(c) and figure 12(d). Figure 12(c) gives the tool wear mechanisms while Al7075 is drilled with high-speed steel drill and figure 12(d) presents the tool wear mechanisms while drilled with carbide insert drill. In the drilling of the Al7075 workpiece, having a hardness of 179HV, flank wear was observed on the cutting edges of the drill (figure 12c and figure 12d).

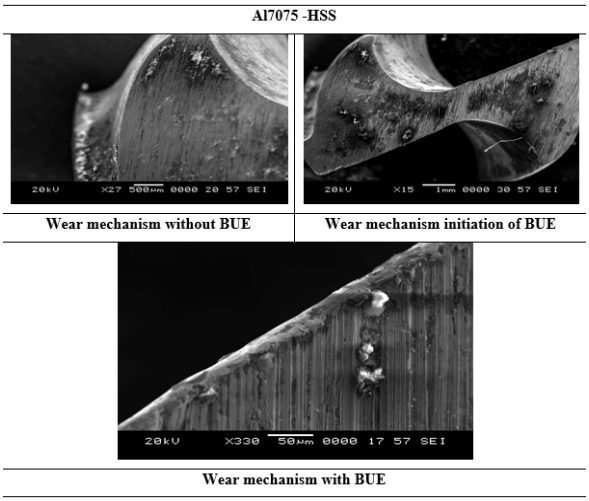

Fig. 12c. Tool wear mechanisms while Al7075 drilled with high-speed steel drill

In the drilling of the Ti-6Al-4V workpiece, with a hardness of 379 HV, formations of BUE, flank wear, outer corner wear, and chisel edge wear types were observed (figure 12a and figure 12b). It found that vibration amplitude increased with the progression of tool wear [57]. It known that in cutting operations, BUE formation accelerates tool wear, spoils the finished surface of the workpiece, and causes vibrations in the drilling. The flank wear occurred on the cutting edge of the cutting tool and the lower rigidity due to the lower workpiece.

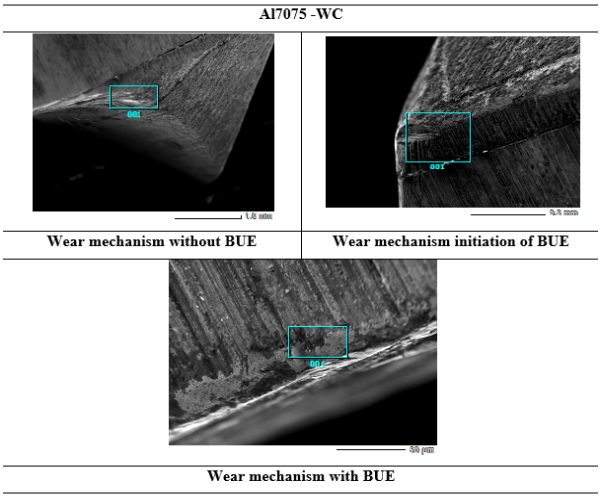

Fig. 12d. Tool wear mechanisms while Al7075 drilled with carbide insert drill

Variation of displacement values on changes in feed rate presented in figure 13. The reason for reaching the highest displacement value at feed rate 0.06 mm/rev and shorter tool life are due to an increase in the flank wear and outer corner wear of the cutting tool shown in figure 13.

With the increase in the feed rate from 0.02 m/rev to 0.06 mm/rev, flank wear, outer corner wear, chisel edge wear, and BUE increased as well. However, the cutting tool life did not complete until the drilling of the 15th hole.

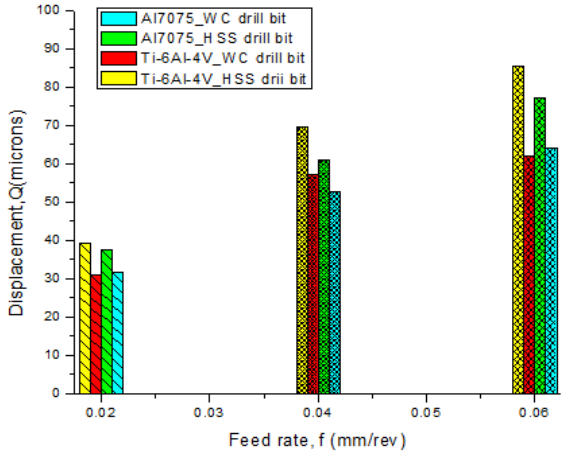

Fig. 13. Variation of displacement about feed rate

With the rise in the feed rate from 0.02 m/rev to 0.04 mm/rev, flank wear, and outer corner wear increases.

5.2.4 Effects of machining time on drill bit performance -Tool Life

The most critical parameter in the present study can be affected by the machining time (number of holes drilled) with each drill bit. As per the results are shown in figure 14 for all the cutting conditions, as the number of holes drilled increased (machining time), displacement value increases consistently.

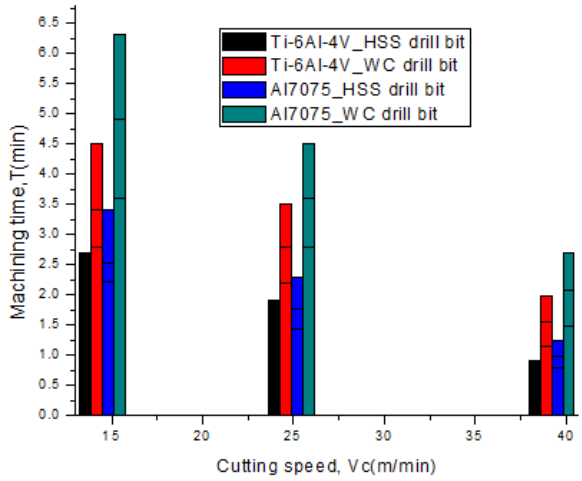

Fig. 14. Variation in machining time of drill bits

The main reason is the increase in drill bit tool wear, and it is dependent on the number of holes drilled. The corresponding increase in chatter formation due to the degree of difficulty of the cutting operation.

5.2.5 Predictive equation and analysis of variance for displacement amplitude and tool flank wear

In the present work, vibration displacement (Disp) and tool wear (VB) selected as the response variables. Feed rate (f), spindle rotational speed(N), depth of cut (d) at different levels of workpiece hardness (H) are the machining parameters. The machinability performance of displacement amplitude (µm) and tool wear (mm) are obtained, to analyze the machining parameters with the help of [58-59] response surface methodology (RSM). The relationship of preferred response and independent variables for input are represented in the appropriate form as follows. Feed rate, cutting speed, depth of cut, different hardness levels (independent variables) which vary during the experiments. For each factor, three stages are deliberately chosen and set during the experimentation according to the DOE. The response surface methodology (RSM) is also employed. Box–Behnken design is used to identify the cause and effect of the relationship between the control variables and the responses. Therefore, the degree of freedom model for displacement prediction in their investigation of the conformity between workpiece and cutting tool in the drilling process. The variation in displacement amplitude and corresponding tool wear with machining parameters (input parameters N, f, d, H) are being mathematically developed using the regression analysis method. Equations 5 (Disp) represents the displacement data whereas equations 6 represents (VB) the predicted tool flank wear data. Table 5 gives the experimental data results. To obtain scientific understandings of work materials and process variables effects on the tooling performance. An empirical relationship developed constructed on investigational data. The mathematical modeling did by polynomial equations that are very helpful in comparing the relationship between the process variables using Minitab software. In drilling, displacement (Disp) due to vibration expressed as a function of the process parameters and workpiece hardness as shown in equation 2.

$$Disp = f(N, f, d, H) \quad (9)$$

$$VB = f(N, f, d, H) \quad (10)$$

Where, Disp - machining response, f- response function and the drilling process variables such as N, f, d, H. In the analysis, a procedure for an approximation of response is derived using the built-in 2nd order polynomial regression as the quadratic model. The quadratic model for machining response as mentioned below. The second-order polynomial (regression) equation used to represent the response surface for displacement amplitude (Disp) is given by:

$$Disp = b_0 + \Sigma b_i X_i + \Sigma b_{ii} X_i^2 + \Sigma b_{ij} X_i X_j \quad (11)$$

and for four factors, the selected polynomial can be expressed as:

$$Disp = b_0 + b_1 N + b_2 f + b_3 d + b_4 H + b_{12} Nf + b_{13} Nd + b_{14} NH + b_{23} fd + b_{24} fH + b_{34} dH + b_{11} N^2 + b_{22} Nf^2 + b_{33} Nd^2 + b_{44} NH^2 \quad (12)$$

Where b1, b2, b3… b44 are regression coefficients [59-60], and b_0 is the average of the output responses. These coefficients depend on the respective linear, interaction, and squared terms of factors. The value of the coefficient was calculated using Minitab Software. The significance of each factor determined by 'p' values, which are presented in table 4 to table 7. The values of p less than 0.05 indicate that the model terms are significant. In this case, X1, X2, X4, X12, X22 and X1, X2 are significant model terms and X3 has less influence on the displacement. The values greater than 0.10 indicate that the model terms are not

significant [60]. The final empirical relationship is constructed using only these coefficients and developed the empirical relationship given below.

$$Disp = 50.26 - 12.72N + 6.24f + 2.94d + 57.2H - 4.72N2 + 20.54f2 + 0.9d2 + 45.83H2 + 45.7(N.f) + 17.02(N.d) - 74.16(N.H) + 12.16(f.d) - 47.42(f.H) - 11.16(d.H) \quad (13)$$

As shown in equations 5 and 6, a similar mathematical modeling is carried for flank wear and displacement data also. Coefficients shown in ANOVA tables 6 and 7 are used to develop empirical relationships for both the experimental and predicted flank wear data.

$$VB = 0.242 + 0.07N + 0.238f + 0.0102d + 0.015H - 0.024N^2 + 0.042f^2 - 0.004d^2 + 0.05H^2 - 0.059(N.f) - 0.028(N.d) + 0.709(N.H) + 0.0507(f.d) - 0.364(f.H) - 0.083(d.H) \quad (14)$$

The final empirical relationship is constructed using coefficients by equation 2, and the developed final empirical relationship is presented as above (14).

After obtaining the predicted values, these equations are used to correlate each other. The ANOVA tables for flank wear shown in the tables 6 and 7. Results in the tables clearly identify the significant factors that affect the tool wear in both experimental data and predicted data. These equations will give the expected values of displacement amplitude and flank wear for any combination of factor levels given that the levels are within the ranges stated in Table 1. From the above equations, it concluded that equations are approximately similar (3&4) and (5&6) to each other. Displacement amplitude and tool wear influenced by the factors on the right-hand side in both the cases. The above mathematical model can be used to predict the values of the displacement, and flank wear of the factors studied.

For the estimation of the displacement, amplitude occurred in the drilling of Ti-6Al-4V and Al7075 specimens using twist drills, a second-order polynomial equation involving the main and interaction effects of the process parameters was developed by regression analysis. The predicted R^2 (98.6 %) value and the adjusted R^2 value (97.8 %) matched with the experimental results.

The adjusted R^2 determines the amount of deviation about the mean which is described by the model. The predicted R^2 value and the adjusted R^2 value were found to be in good agreement. Normal probability plots given in figure 15 and 16.

From these figures, it seems that points are placed on a straight line or distributed close to a straight line; therefore, it concluded that the data exhibit a normal distribution. The reason that not all the data were in a straight line attributed to the significant number of tests in this study. It thought that during the experimental study, the uncontrollable factors increased the residuals.

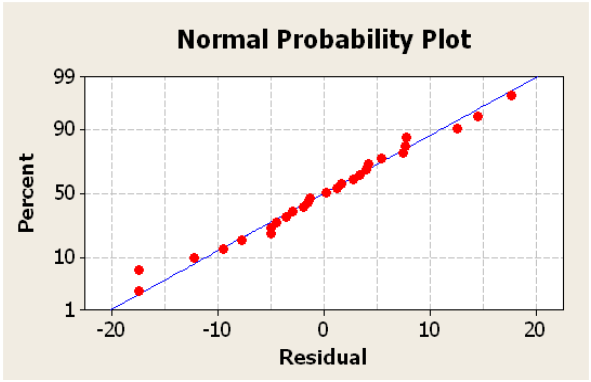

Fig. 15. Normal probability plot for displacement amplitude

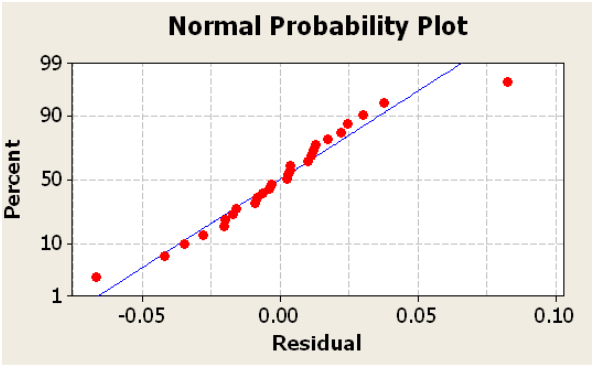

Fig. 16. Normal probability plot for flank wear

6. CONCLUSIONS

In the present study, effects of workpiece hardness, cutting speed, the number of holes drilled, and feed rate on the displacement amplitude in the drilling holes on Ti-6Al-4V and Al7075 alloys using high-speed steel and tungsten carbide twist drills at different test conditions investigated. The experimental results show that the progress of tool wear monitored by using the vibration parameter determined by the analysis of vibration signals. Predictive equation models have developed, and analysis of variance presented for displacement amplitude and tool flank wear. Based on this, the status of the tool predicted. The dominant failure modes for both high-speed steel and tungsten carbide tools while drilling Ti–6Al4V are non - uniform flank wear, chipping and catastrophic failure. Whereas while drilling of Al7075 both high-speed steel and carbide drill showed the consistent wear at all test conditions. Highest tool life was obtained with carbide drill when drilling at cutting speed of 39.4 m/min. The performance of carbide drill is superior to high-speed steel drill at all cutting speeds both regarding tool life and displacement due to vibration when drilling both Ti–6Al4V and Al7075. With an increase of feed rate from 0.02 to 0.06 mm/rev, an increase in the displacement amplitude recorded. As the number of holes rises, displacement value also increases. Flank wear and BUE observed on the worn drills. It concluded that drill wear increased the displacement

amplitude values. The vibration signals are measured which indirectly track tool wear. These signals are affected by the cutting conditions, workpiece material, and type of tool. For example, increasing the feed rate during the drilling process leads to a proportional rise in the measured signals. This situation could be confused with increased displacement due to tool wear in the system. Finally, the methods proposed in this paper can also be used for performance evaluation of drill tools effectively by monitoring vibration induced drilling.

7. REFERENCES

[1] Leyens Christoph and Peters Manfred, Titanium and Titanium Alloys Fundamentals and Applications WILEY-VCH Verlag GmbH& Co, 2005, Germany.

[2] Brewer William D, Bird R.Keith and Wallace Terryl A, Titanium alloys and processing for high speed aircraft, Materials Science and Engineering A. 243(1998) 299–304.

[3] Kandilli Ismet, Sönmez Murat, Ertunc Huseyin Metin, Çakır Bekir, Online monitoring of tool wear in drilling and milling by multi-sensor neural network fusion, Proceedings of the IEEE International Conference on Mechatronics and Automation. China. (2007) 1388-1394.

[4] W. Grzesik, An Investigation of the Thermal Effects in Orthogonal Cutting Associated with Multilayer Coatings, Annals of the CIRP. 50 (2001) 53-56.

[5] S. Dolinšek, J. Kopač, Mechanism and types of tool wear; particularities in advanced cutting Materials, Journal of Achievements in Materials and Manufacturing Engineering. 19(1) (2006) 11-18.

[6] Sikiru Oluwarotimi Ismail, HomNath Dhakal, Eric Dimla, Ivan Popov, Recent advances in twist drill design for composite machining: A critical review, Proceedings of the institution of mechanical engineers Part B Journal of Engineering Manufacture. (2016) 1–16. doi: 10.1177/0954405416635034.

[7] Brinksmeier E, Prediction of Tool Fracture in Drilling, Annals of CIRP. 39(1) (1990) 97-100.

[8] Kanai M, Fujii S, Kanda Y, Statistical Characteristics of Drill Wear and Drill Life for the Standardized Performance Tests, Annals of CIRP. 27(1) (1978) 61-66.

[9] Kaldor S, Lenz E, Investigation in Tool Life of Twist Drill, Annals of CIRP. 52 (1980) 30-35.

[10] Choudhury S. K, Raju G, Investigation into Crater Wear in Drilling, International Journal of Machine Tools & Manufacture. 40 (2000) 887-898.

[11] Harris S G, Doyle E D, Vlasveld A C, Audy J, Quick D, A Study of the Wear Mechanism of Ti_1-$_x$$Al_x$ N and $Ti_{1-x-y}Al_x$ Cr_yN Coated High Speed Steel Twist Drill Under Dry Machining Conditions, Wear. 254 (2003) 723-734.

[12] Tetsutaro H, Zhao H, Study of a High Performance Drill, Geometry Annals of CIRP. 38: (1989) 87-90.

[13] S.C. Lin, C.J. Ting, Tool wear monitoring in drilling using force signals, Wear. 180(1) (1995) 53-60.

[14] Muhammad Imran, Paul T Mativenga, Ali Gholinia, Philip J Withers, Comparison of tool wear mechanisms and surface integrity for dry and wet micro-drilling of nickel-base super alloys, International Journal of Machine Tools & Manufacture. 76 (2014) 49–60.

[15] H.S. Liu, B.Y. Lee, Y.S. Tarng, In-process prediction of corner wear in drilling operations, Journal of Materials Processing Technology. 101: (2000) 152-158.

[16] T.I. El Wardany, Gao D, Elbestawi M A, Tool condition monitoring in drilling using vibration signature analysis, International Journal of Machine Tools and Manufacture. 36(6) (1996) 687-711.

[17] Abuthakeer S.S, P.V Mohanram, G. Mohankumar, The effect of spindle vibration on surface roughness of workpiece in dry turning using ANN International, Journal of Lean Thinking. 2 (2011) 42–58.

[18] Izelu C.O, Eze S.C, Oreko B.U, Edward B.A, Garba D.K, Response surface methodology in the study of induced machining vibration and work surface roughness in the turning of 41Cr4 alloy steel, International Journal of Emerging Technology and Advanced Engineering. 3 (2013) 13–17.

[19] Khalili K and Danesh M, Investigation of overhang effect on cutting tool vibration for tool condition monitoring, Journal of Measurements in Engineering 1(2013) 171–177.

[20] Guillem Quintana, Joaquim Ciurana, Chatter in machining processes: A review, International Journal of Machine Tools & Manufacture. 51(2011) 363–376.

[21] S.A. Tobias, Machine tool vibration research, International Journal of Machine Tool Design Research. 1 (1961) 1-14.

[22] N.H. Hanna, S.A. Tobias, Theory of nonlinear regenerative chatter, Journal of Engineering for Industry Transactions of the ASME. 96 Ser B(1) (1974) 247–255.

[23] S. Ema, E. Marui, Theoretical analysis on chatter vibration in drilling and its suppression, Journal of Materials Processing Technology. 138 (1-3) (2003) 572–578.

[24] S. Ema, H. Fujii, E. Marui, Chatter Vibration in Drilling, Transactions of the ASME Journal of Engineering for Industry. 110 (1988) 309-314.

[25] Iman Maleki Mehrabadi, Mohammad Nouri, Reza Madoliat, Investigating chatter vibration in deep drilling, including process damping and the gyroscopic effect, International Journal of Machine Tools & Manufacture. 49 (2009) 939–946.

[26] T. Arvajeh, F. Ismail, Machining stability in high-speed drilling - part 1: modeling vibration stability in bending, International Journal of Machine Tools and Manufacture. 46(12-13) (2006) 1563–157259.

[27] T. Arvajeh, F. Ismail, Machining stability in high

speed drilling - part 2: time domain simulation of a bending-torsional model and experimental validations, International Journal of Machine Tools and Manufacture. 46 (12-13) (2006) 1573–1581.

[28] D.N. Dilley, P.V. Bayly, A.J. Schaut, Effects of the chisel edge on the chatter frequency in drilling, Journal of Sound and Vibration. 281 (1-2) (2005) 423–438.

[29] J.C. Roukema, Y. Altintas, Time domain simulation of torsional-axial vibrations in drilling, International Journal of Machine Tools and Manufacture. 46 (15) (2006) 2073–2085.

[30] Fang Ning, P. Srinivasa Pai, Mosquea S, The effect of built-up edge on the cutting vibrations in machining 2024-T351 aluminum alloy, International Journal of Advanced Manufacturing Technology. 49 (2010) 63–71.

[31] Abuthakeer S.S, P.V Mohanram, G. Mohan kumar, Prediction and control of cutting tool vibration in CNC lathe with ANOVA and ANN, International Journal of Lean Thinking 2: (2011) 1–23.

[32] Rahim E.A, Kamdani K, Sharif S, Performance evaluation of uncoated carbide tool in high speed drilling of Ti6Al4V, Journal of Advanced Mechanical Design, Systems and Manufacturing. 2 (2008) 522–531.

[33] Dornfeld D.A, Kim J.S, Dechow H, Hewson J, Chen L.J, Drilling burr formation in titanium alloy, CIRP Annals Manufacturing Technology. 48(1999) 73–76.

[34] Davoudinejad Ali, Ashrafi Sina Alizadeh, Hamzah Raja Ishak Raja, Niazi Abdol karim, Experimental analysis of wear mechanism and tool life in dry drilling of Al2024, Advanced Materials Research. 566 (2012) 217-221.

[35] Sakurai K, Adichi K, Ogawa K and Niba R, A study on drilling of Ti–6Al–4V by TiN coated drills, Proceedings of the International Conference on recent advances in science and engineering of light metals Sendai Japan. (1991)803–808.

[36] Rajesh Khanna, Anish Kumar, Mohinder Pal Garg, Ajit Singh, Neeraj Sharma, Multiple performance characteristics optimization for Al 7075 on electric discharge drilling by Taguchi grey relational theory, Journal of Industrial Engineering International 11(2015) 459–472.

[37] Erkki Jantunen, A summary of methods applied to tool condition monitoring in drilling, International Journal of Machine Tools & Manufacture. 42 (2002) 997–1010.

[38] Adam G. Rehorn, Jin Jiang, Peter E. Orban, State-of-the-art methods and results in tool condition monitoring: a review, International Journal of Advanced Manufacturing Technology. 26 (2005) 693–710.

[39] H.M. Ertunc, K.A. Loparo, A decision fusion algorithm for tool wear condition monitoring in drilling, International Journal of Machine Tools & Manufacture. 41(2001) 1347–1362.

[40] Sebastian Bombiński, Krzysztof Błażejak, Mirosław Nejman Krzysztof Jemielniak, Sensor signal segmentation for tool condition monitoring, 7th HPC CIRP Conference on High Performance Cutting Procedia CIRP. 46 (2016) 155-160.

[41] Jonathan Downey, Sebastian Bombiński, Mirosław Nejman, Krzysztof Jemielniak, Automatic multiple sensor data acquisition system in a real-time production environment, 9th CIRP Conference on Intelligent Computation in Manufacturing Engineering Procedia CIRP. 33 (2015) 215 – 220.

[42] A Volkan Atli, O Urhan, S Erturk, M Sonmez, A computer vision-based fast approach to drilling tool condition monitoring, Proceedings of the Institution of Mechanical Engineers Part B: Journal of Engineering Manufacture 220(9) (2006) 1409-1415.

[43] Bhuiyan M S H, Choudhury I A, Review of sensor applications in tool condition monitoring in machining, Comprehensive Materials Processing. 13 (2014) 539–569.

[44] Kuo R.J, Multi-sensor integration for on-line tool wear estimation through artificial neural networks and fuzzy neural network, Engineering Application of Artificial Intelligence 13 (2000) 249-261.

[45] B Srinivasa Prasad, MMM Sarcar, Analysis of face milling operation using acousto optic emission and 3D surface topography of machined surfaces for in-process tool condition monitoring, Jordan Journal of Mechanical and Industrial Engineering. 5(6) (2011) 509-519.

[46] Peter Norman, Mikael Backstrom, Matti Rantatalo, Ales Svoboda, Alexander Kaplan, A sophisticated platform for characterization, monitoring and control of machining, Measurement Science and Technology. 17(2006) 847–854.

[47] Srinivasa Prasad B, Prasad Siva D, Sandeep A, Veeraiah G, Condition monitoring of CNC machining using adaptive control, International Journal of Automation and Computing. 10(3) (2013) 202-209.

[48] Juhchin A. Yang, Venkatraman Jaganathan, Ruxu Du, A new dynamic model for drilling and reaming processes, International Journal of Machine Tools & Manufacture. 42 (2002) 299-311.

[49] S. S. Rao, Mechanical Vibrations 4th Edition Pearson publication. (2003) ISBN: 8177588745.

[50] Amit S. Wani, Gayatri S. Sagavkar, Vaibhav K. Bhate, Vibration analysis of drilling operation, International Journal of Students Research in Technology & Management. 1(2) (2013) 163-175.

[51] Repo J, Beno T, Pejryd L, New Aspects on Condition Monitoring of Machine Tools and Machining Processes, Proceedings of the 3rd Swedish Production Symposium. SPS'09 (2009) Göteborg Sweden.

[52] David A. Stephenson, John S. Agapiou, Metal Cutting Theory and Practice, CRC Press London. 3rd Edition, (2016) Taylor & Francis Group,

USA.
[53] Lazic´ ZR, Design of experiments in chemical engineering: a practical guide, Wiley (2004) VCH Weinheim.
[54] Yavuz Kaplan, Ali Riza Motorcu, Muammer Nalbant, Şenol Okay, The effects of process parameters on acceleration amplitude in the drilling of cold work tool steels, International Journal of Advanced Manufacturing Technology. 80 (2015) 1387-1401.
[55] Orhan Sadettin, Osman Er Ali, Camuşcu Necip, Aslan Ersan, Tool wear evaluation by vibration analysis during end milling of AISI D3 cold work tool steel with 35HRC hardness, NDT & E International. 40 (2007) 121–126.
[56] Ertunc Hüseyin, Metin, Sevim İbrahim, Studies on tool wear condition monitoring, Pamukkale University Journal of engineering sciences. 7 (2001) 55-62.
[57] Kayhan M, Budak E, An experimental investigation of chatter effects on tool life, Proceedings of the Institution of Mechanical Engineers Part B: Journal of Engineering Manufacture 223 (2009) 1455–1463.
[58] M.Y. Noordin, V.C. Venkatesh, S. Sharif, S. Elting, A. Abdullah, Application of response surface methodology in describing the performance of coated carbide tools when turning AISI 1045 steel, Journal of Material Processing Technology. 145 (2004) 46-58.
[59] Fazar Akbar, Paul T. Mativenga, M. A. Sheikh, An experimental and coupled thermo-mechanical finite element study of heat partition effects in machining, International Journal of Advanced Manufacturing Technology. 46 (2010) 491-507.
[60] Surinder Kumar, Meenu Gupta, P.S. Satsangi, Multiple-response optimization of cutting forces in turning of UD-GFRP composite using Distance-Based Pareto Genetic Algorithm approach, Engineering Science and Technology an International Journal. 18 (2015) 680-695.

Acknowledgements

This work funded by Ministry of Science and Technology, Department of Science and Technology, India as part of project work titled 'Development and implementation of Adaptive controller design for CNC milling' through funding order D.O: SB/FTB/ETA-0262/2013. Authors would like to appreciate Department of Science and Technology, India for the financial support.

Authors:

Y. Rama Mohan Reddy, Corresponding author, Ph.D. scholar, Dept.of Mechanical Engineering, GITAM Institute of Technology, GITAM University, Visakhapatnam, India-530045, Tel: +91-0-9553214909

Dr Balla Srinivasa Prasad, Research guide, Associate Professor, Dept.of Mechanical Engineering, GITAM Institute of Technology, GITAM University, Visakhapatnam, India-530045, Tel.: +91-0-98483210710 Fax: +91-891-2840250

e-mail: yrmreddy.3749@yahoo.com
bsp.prasad@gmail.com

http://doi.org/10.24867/JPE-2017-01-016

Journal of Production Engineering

Vol.20 No.1

JPE (2017) Vol.20 (1) Original Scientific Paper

Kovač, P., Rodić, D., Gostimirović, M., Savković, B., Ješić. D.

ADAPTIVE NEURO-FUZZY MODELING OF THERMAL VOLTAGE PARAMETERS FOR TOOL LIFE ASSESSMENT IN FACE MILLING

Received: 23 January 2017 / Accepted: 08 May 2017

Abstract: *The focus of this paper is to develop a reliable procedure to predict tool life during face milling process. This procedure involves a combination of Method of Least Squares and Neuro Fuzzy system. The factorial designs combined with the ANFIS techniques were applied to perform the prediction of thermal voltage. A least-squares linear regression is applied to perform the prediction of tool life from thermal-voltage signals. In this contribution we also discussed the construction of an ANFIS system that tends to provide a linguistic model for the estimation of thermal voltage obtained with different membership functions. This research focuses on developing ANFIS models using triangular and Gaussian membership functions. The work shows that the membership functions have the dominant effect among the on the accuracy model. The results indicate that the training of ANFIS with the Gaussian membership function obtains a higher accuracy rate in the prediction of thermal voltage, respectively tool life.*

Key words: *ANFIS, thermal voltage, tool life, face milling.*

Modelovanje termo-napona pomoću neuro-fazi sistema pri proceni postojanosti alata kod čeonog glodanja. *Cilj ovog rada je da se razvije pouzdan postupak za procenu postojanosti alata tokom procesa čeonog glodanja. Ovaj postupak obuhvata kombinaciju metode najmanjih kvadrata i neuro-fazi sistema. Za predvidjanje termo-napona korišćen je ANFIS postupak na osnovu faktorijalnog dizajna eksperimenta. Razvijena je regresiona jednačina koja se dobija metodom najmanjih kvadrata i služi za procenu postojanosti alata na osnovu vrednosti termo-napona. U ovom radu se takođe diskutuje o načinu formiranja ANFIS modela upotrebom različitih funkcija pripadnosti pri određivanju termo-napona. Korišćenjem trougaonih i Gausovih funkcija pripadnosti razvijeni su ANFIS modeli. Pokazalo se da izbor tipa funkcije pripadnosti utiče na tačnost modela. Rezultati istraživanja su potvrdili da obuka ANFIS modela sa Gausovim funkcijama pripadnosti daje tačnije predviđanje termo-napona, odnosno postojanosti alata.*

Ključne reči: *ANFIS, termo-napon, postojanost alata, čeono glodanje.*

1. INTRODUCTION

Tool life in the metal cutting process are very important factors affecting production optimization. The importance of tool life prediction for the machining processes has been well recognized in the machining research community primarily due to its constraints on the productivity [1]. Intelligent models of face milling processes provide the ability to predict stable cutting condition and increases tool life for a large combination of process [2].

The application of the Adaptive Neural Fuzzy Inference System (ANFIS) for the modeling purpose in various different areas including machining is used a widely by researchers [3, 4]. Several intelligent models for predicting as well as classifying tool life in machining operations have been developed [5, 6]. Zuper et al. developed a reliable method to predict flank wear during end milling process. They applied a neural-fuzzy system to perform the prediction of flank wear from cutting force signals [7]. A fuzzy logic based in-process tool-wear monitoring system is developed by Chen and Susanto. In this system the fuzzy membership function and rule bank were based on observations during cutting experiments using artificial tool-wear inserts in face milling operations [8]. Sokolowski introduced a new fuzzy rule acquisition method for tool wear estimation. It uses radial basis networks to find the optimal combination of rules to compose a fuzzy reasoning mechanism and options related to the membership functions [9]. ANFIS is a theory used to describe the relationship between system inputs and outputs. It is widely used to develop rule based expert systems in modeling of complex processes that difficult be modeled analytically under various assumptions [10]. Cutting forces and cutting conditions including speed, feed and depth of cut have been usually employed as input units in these prediction models. But very few researchers used the ANFIS to predict the tool life in face milling by thermal-voltage. Further, the impact of different membership functions which are utilized in the ANFIS model on the correct rate of prediction of tool life by thermal-voltage was not investigated yet. The selection of acceptable fuzzy membership function is generally a subjective decision, it is by trial and error and very time-consuming.

This paper focuses on developing ANFIS models using Triangular and Gaussian membership functions. The values of thermal voltage predicted by these models are then compared. In this research we attempt to solve this situation by using the adaptive neuro-fuzzy inference system (ANFIS) to predict the thermal voltage of the tool in face milling process. After obtained ANFIS models, tool life is predicted by the method of least squares.

2. EXPERIMENTAL SETUP

In order to develop the tool life prediction model, experimental results were used. Experimental investigation was conducted on a vertical milling machine without cooling lubrication fluid. A single-tooth face, milling cutter of 125 mm diameter, with a carbide P 25 insert SPAN 12 03 ER was used. The working material was a block of 100x120x600 mm of steel AISI 1060 and was fixed on milling machine table. The experiment was carried out for different combinations of cutting speed (v) [m/s], feed per tooth (f) [mm/t] and cutting depth (a) [mm] according to the planning of experiment, Table 1. Tool-work thermocouple thermal voltage was measured as shown in Fig. 1. To avoid thermal voltage leak, the workpiece was insulated from the machine tool on all contact surfaces. The carbide insert was insulated from the tool holder as well, to avoid thermal voltage noise. The cold junction on the tool was moved away from the cutting zone by adding carbide insert parts of the same kind of carbide used to avoid parasitic thermal voltage. This system is shown with detail enlarged in Fig.1. The cold junction temperature, at the end of the milling cutter, was monitored by artificial thermocouple to avoid scattering.

No.	Cutting speed (m/s)	Feed (mm/ tooth)	Depth of cut (mm)	Thermal Voltage (mV)	Tool Life (min)
1.	2.32	0.178	1	12.1	59
2.	3.67	0.178	1	13.4	20
3.	2.32	0.28	1	12.7	35
4.	3.67	0.28	1	14.2	11
5.	2.32	0.178	2.25	12.7	36
6.	3.67	0.178	2.25	14	13
7.	2.32	0.28	2.25	13.4	20
8.	3.67	0.28	2.25	14.8	7
9.	2.95	0.223	1.5	13.4	18
10.	2.95	0.223	1.5	13.4	22
11.	2.95	0.223	1.5	13.6	17
12.	2.95	0.223	1.5	13.7	18
13.	1.83	0.223	1.5	12.1	52
14.	4.65	0.223	1.5	14.9	7
15.	2.95	0.142	1.5	12.6	38
16.	2.95	0.351	1.5	14.1	12
17.	2.95	0.223	0.67	12.8	30
18.	2.95	0.223	3.37	15	6
19.	1.83	0.223	1.5	12.2	50
20.	4.65	0.223	1.5	15	6
21.	2.95	0.142	1.5	12.5	41
22.	2.95	0.351	1.5	14	13
23.	2.95	0.223	0.67	12.9	27
24.	2.95	0.223	3.37	14.9	6

Table 1. Experimental data

The measurement of thermal-voltage was performed by a natural thermocople tool-workpiece. From turning spindle of milling machine signal transmitting is made by slip rings. Reading of thermal-voltage was done digitally on the "digital thermometer" – TR 2112 instrument equipped. The factorial designs combined with the ANFIS techniques were applied. ANFIS modeling process starts by obtaining a data set (input–output data) and dividing it into training and checking data sets.

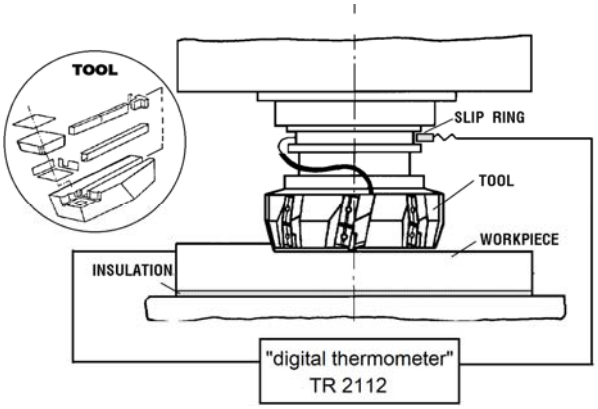

Fig. 1. The tool-workpiece thermocouple experimental setup

3. ANFIS MODELING

Figures Adaptive neuro-fuzzy inference system (ANFIS) is an architecture which is functionally equivalent to a Sugeno type fuzzy rule base. Both artificial neural network (ANN) and fuzzy logic (FL) are used in ANFIS architecture, figure 2 and 3.

ANFIS normally has 5 layers of neurons of which neurons in the same layer are of the same function family. Each node generates the membership grades of a linguistic label. In this paper an example of a membership functions are triangular and Gaussian membership functions:

$$Gaussian\ f(x,\sigma,c) = e^{\frac{-(I_e-c)^2}{2\sigma^2}}$$

$$Traingular\ f(x,a,b,c) = \max\left\{\min\left(\frac{x-a}{b-2},\frac{c-x}{c-b}\right),0\right\} \quad (1)$$

where (x, σ, c) and (x, a, b, c) are the parameter set. As the values of the parameters change, the shape of the membership functions varies. Parameters in that layer are called premise parameters.

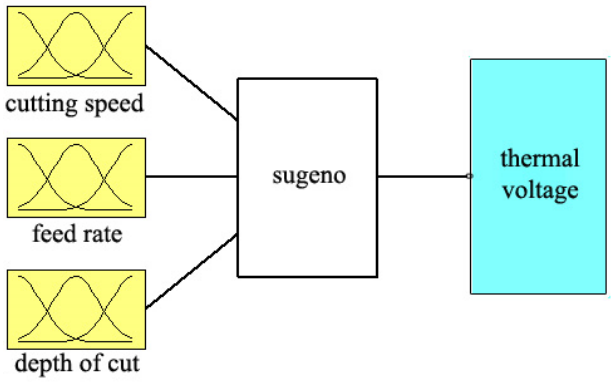

Fig. 2. Fuzzy inference system of ANFIS

In layer two, each node calculates the firing strength of each rule using the min or prod operator. In general, any other fuzzy AND operation can be used. The layer three enables to calculate nodes the ratios of the rule's

firing strength to the sum of all the rules firing strength. The result is a normalized firing strength. In layer four, the nodes compute a parameter function on the layer 3 output. Parameters in this layer are called consequent parameters. Finally in the layer five, normally a single node that aggregates the overall output as the summation of all incoming signals.

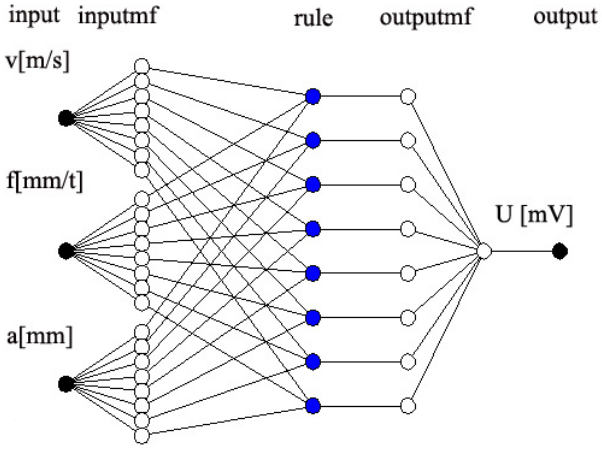

Fig. 3. Five-layer neural network of ANFIS

In our case ANFIS is a five-layer neural network that simulates the working principle of a fuzzy inference system. The ANFIS model generated from the membership functions and rules were data-driven by the process data for each mechanical property.

In this paper, a straightforward approach for designing an ANFIS model is presented to evaluate the effect of membership function in ANFIS model, and presents the performance comparison of ANFIS model with two different types of membership function. Though there are many numbers of membership functions available like triangular, trapezoidal, Gaussian, etc.

The modeling of the thermo voltage in this paper are using the triangular and the Gaussian types of membership functions as described by Klir and Folger [11]. Each set of process data collected from the extrusions consisted of 24 data points from which 20 and 4 were selected randomly for training and testing, respectively.

This paper presents a method for reduction in the fuzzy inference system, where the ANFIS model based on subtractive clustering is designed to predict for thermal voltage. Subtractive clustering is an extension of the mountain clustering method and which is more efficient at finding cluster centers. The subtractive clustering method assumes that each data point is a potential cluster center and, without prior knowledge of the default number of centers, it calculates the likelihood of a data point being defined as a cluster center according to the density of the surrounding data points [12]. The objective of using this approach is to design a ANFIS model with less number of rules leading to a smaller amount of computational time.

For example, in a three-input ANFIS model with 8 membership functions for each input, the possible rules are 8^3 =512, and if the number of inputs are increased, this number will quickly increase. To overcome this problem, the user may want to put constraints on the type membership functions or limit the rules. In this case, rather than 512 rules (conventional ANFIS with Triangular MF) adopted 8 (clustering based ANFIS with Gaussian MF), which are shown in figure 4.

Throughout the initial experiment, the parameter values used in the proposed ANFIS were set as follows. Parameters for clustering is: range of influence (0.5), squash factor (1.25), accept ratio (0.5) and reject ratio (0.15). The models were developed and implemented using 500 epochs. The input and output data sets contained three inputs [cutting speed, feed rate and depth of cut] and one output (thermal voltage).

The linguistic nodes in layers one and five represent the input and output linguistic variables, respectively. Nodes in layers two are term nodes acting as membership functions for input variables. Number of membership for each input parameters is eight. Each neuron in the third layer represents one fuzzy rule, with input connections representing preconditions of the rule and the output connection representing consequences of the rules. Initially, all these layers are fully connected, representing all possible rules. The hybrid batch learning rules are used in the training. Due to limitation of space, the results of conventional ANFIS are not included here.

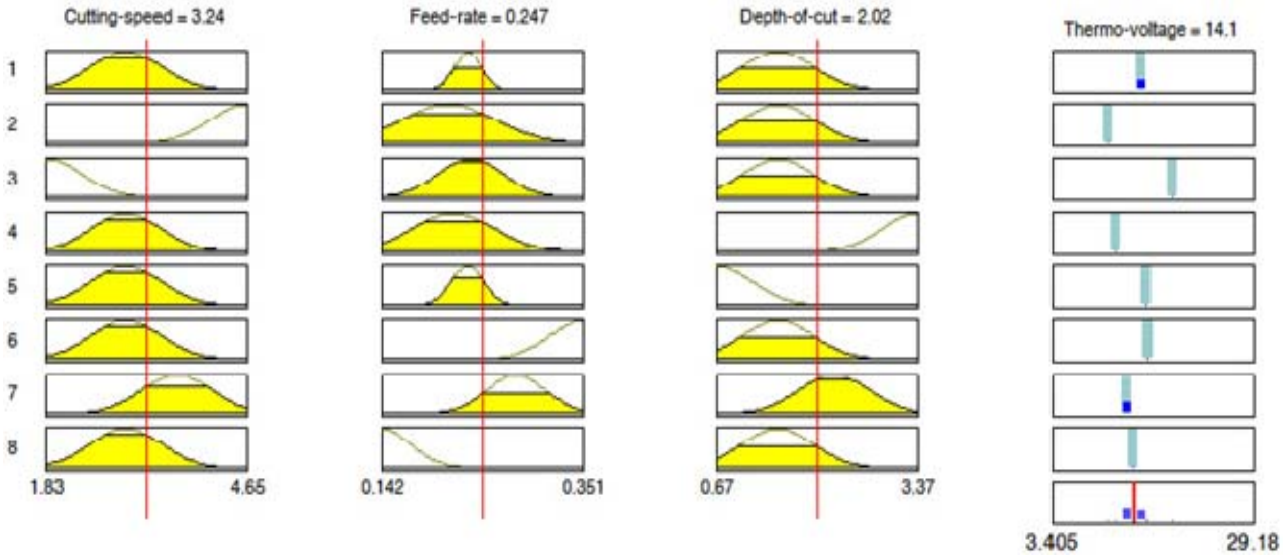

Fig. 4. Rule base (Gauss MF) of ANFIS model for predicting thermal-voltage

4. METHOD OF LEAST SQUARES FOR DETERMINING TOOL LIFE

The Method of Least Squares is a procedure to determine the best fit line to data. Least-squares linear regression is a statistical technique that may be used to estimate the tool life at the given level of thermal voltage based on experimental data, table 1. After experimental data processing, convenient mathematical models are evaluated by the coefficient of correlation value and on the basis of the magnitude of exponents in the exponential relationships and adequate linear regression model was obtained:

$$T = 1.5682919 \times 10^{13} \times U^{-10.56296} \qquad (2)$$

The scatterplot on figure 4. shows that the relationship between tool life and thermal voltage scores is linear.

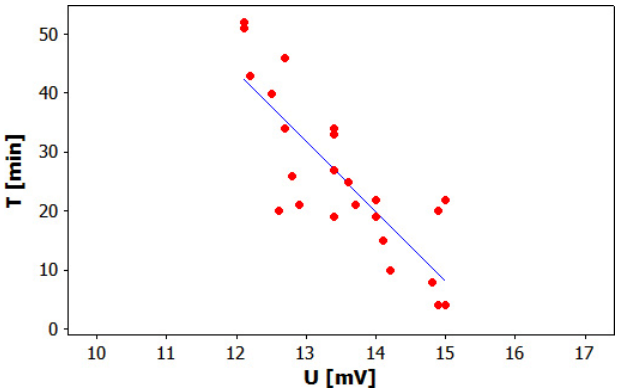

Fig. 5. The dependence on tool life of thermal voltage

In accordance with the presented we can generally conclude that, for proposed model, corresponding coefficient of correlation are sufficiently high (R=0.889), and the model can be used for predicting the tool life in machining of carbon steel.

5. RESULTS

In this research ANFIS system is used to predict the thermal-voltage in a face milling process. Based on the predicting thermal voltage using the least squares method can be calculated tool life. Because of thermal voltage signals have more information than other emission signals, the relationship between the thermal voltage and tool life was examined. The thermal-voltage value predicted by ANFIS are compared with the measurement values derived from the 24 data sets in order to determine the error of ANFIS. A comparison between the clustering based ANFIS with Gaussian MF and conventional ANFIS with Triangular MF is presented. The results indicate that the training of ANFIS with the Gaussian membership function obtains a higher accuracy rate in the prediction of thermal voltage. The experimental results indicate that the proposed ANFIS model has a high accuracy for estimating thermal-voltage with small computational time.

Figure 6-8 shows the effect of cutting parameters on the thermal voltage based on ANFIS model. According to Fig. 6, 7 and 8 cutting speed, feed rate and depth of cut had considerable effect on thermal voltage, while an increase in both cutting speed and/or feed rate, when depth of cut held constant, led to an increase in thermal voltage, but feed rate had a minor effect on thermal voltage. The ANFIS model show that the maximum thermal voltage is at the highest levels of cutting speed and depth of cut, figure 7.

No.	Cutting speed (m/s)	Feed (mm/t)	Depth of cut (mm)	Thermal voltage (mV)		
				Exp.	Gauss. MF	Trian. MF
1.	2.32	0.178	1	12.1	11.2	10.1
2.	2.32	0.28	2.25	13.4	13.8	14.2
3.	2.95	0.142	1.5	12.6	12.5	13.6
4.	2.95	0.351	1.5	14	14.1	14.9
Average error [%]:					***3.11***	***9.7***

Table 2. Predicted value of thermal voltage for gaussian and triangular membership functions

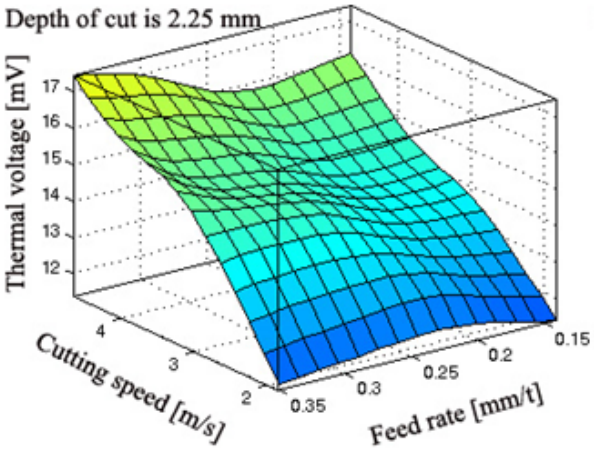

Fig 6. Effect of cutting speed and feed rate on thermal voltage where is depth of cut constant

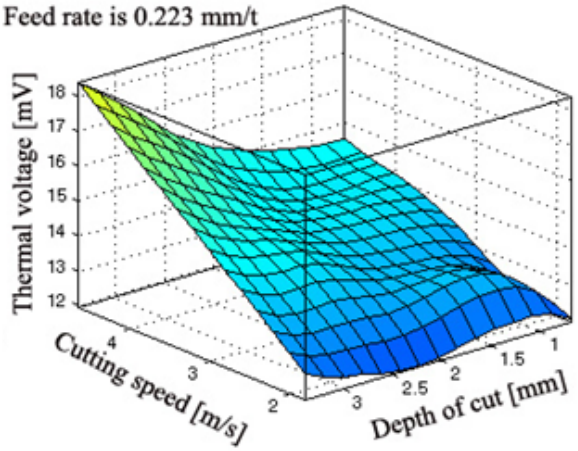

Fig. 7. Effect of cutting speed and depth of cut on thermal voltage where is feed rate constant

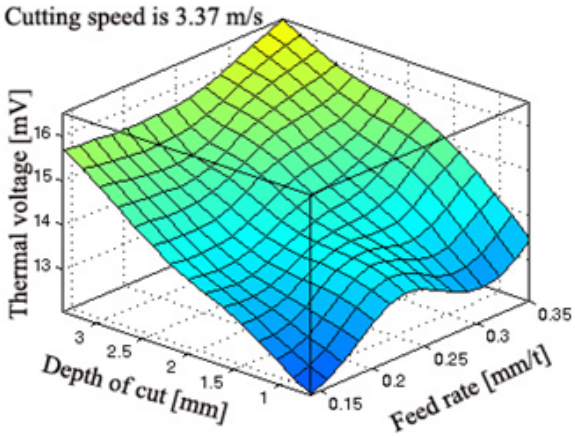

Fig. 8. Effect of depth of cut and feed rate on thermal voltage where is cutting speed constant

6. CONCLUSION

This study concludes that the cutting speed and feed rate are the most significant parameters affecting the thermal voltage, respectively tool life. The depth of cut has minor effect on the thermal voltage. ANFIS was successfully used to develop an empirical model for modeling the relation between the predictor variables (v, f and a) and the performance parameter thermal voltage. ANFIS model with Gaussian membership functions is accurate and can be used to predict thermal voltage in face milling operation with average percentage errors 3.11%.

7. REFERENCES

[1] Kovac, P., M. Gostimirovic, and D. Milikic, Prediction of the Tool Life Function Based on the Tool-Work Thermocouple Temperature During Milling. International Journal For Manufacturing Science And Production.Vol. 2(4): pp. 199-206, 1999.

[2] Kovac, P., et al., Multi-output fuzzy inference system for modeling cutting temperature and tool life in face milling. Journal of Mechanical Science and Technology.Vol. 28(10): pp. 4247-4256, 2014.

[3] Dinakaran, D., S. Sampathkumar, and N. Sivashanmugam, An experimental investigation on monitoring of crater wear in turning using ultrasonic technique. International Journal of Machine Tools and Manufacture.Vol. 49(15): pp. 1234-1237, 2009.

[4] Maher, I., et al., Investigation of the effect of machining parameters on the surface quality of machined brass (60/40) in CNC end milling—ANFIS modeling. The International Journal of Advanced Manufacturing Technology.Vol. 74(1-4): pp. 531-537, 2014.

[5] Massol, O., et al. An exTS based neuro-fuzzy algorithm for prognostics and tool condition monitoring. in Control Automation Robotics & Vision (ICARCV), 2010 11th International Conference on. 2010. IEEE.

[6] Rizal, M., et al., Online tool wear prediction system in the turning process using an adaptive neuro-fuzzy inference system. Applied Soft Computing.Vol. 13(4): pp. 1960-1968, 2013.

[7] Uros, Z., C. Franc, and K. Edi, Adaptive network based inference system for estimation of flank wear in end-milling. Journal of Materials Processing Technology.Vol. 209(3): pp. 1504-1511, 2009.

[8] Chen, J. and V. Susanto, Fuzzy logic based in-process tool-wear monitoring system in face milling operations. The International Journal of Advanced Manufacturing Technology.Vol. 21(3): pp. 186-192, 2003.

[9] Sokołowski, A., On some aspects of fuzzy logic application in machine monitoring and diagnostics. Engineering Applications of Artificial Intelligence.Vol. 17(4): pp. 429-437, 2004.

[10] Gill, S.S., et al., Adaptive neuro-fuzzy inference system modeling of cryogenically treated AISI M2 HSS turning tool for estimation of flank wear. Expert Systems with Applications.Vol. 39(4): pp. 4171-4180, 2012.

[11] Klir, G.J. and T.A. Folger, Fuzzy sets, uncertainty, and information. 1988.

[12] Chen, M.-Y., A hybrid ANFIS model for business failure prediction utilizing particle swarm optimization and subtractive clustering. Information Sciences.Vol. 220: pp. 180-195, 2013.

ACKNOWLEDGMENT

This paper is the result of the research within the project TR 35015 financed by the Ministry of Science and Technological Development of the Republic of Serbia.

Authors: **[1]Professor Pavel Kovač PhD, [1]Research Associate Dragan Rodć MSc, [1]Professor Marin Gostimirović PhD, [1]Assist. Professor Borislav Savković PhD, [2]Professor Dušan Ješić PhD.**

[1]University of Novi Sad, Faculty of Technical Sciences, Institute for Production Engineering, Trg Dositeja Obradovica 6, 21000 Novi Sad, Serbia, Phone.: +381 21 450-366, Fax: +381 21 454-495.

[2]MTM Academia, Novi Sad, Serbia.

E-mail: pkovac@uns.ac.rs
rodicdr@uns.ac.rs
maring@uns.ac.rs
savkovic@uns.ac.rs
dusanjesic@hotmail.com

http://doi.org/10.24867/JPE-2017-01-021

Journal of Production Engineering

Vol.20 No.1

JPE (2017) Vol.20 (1) Original Scientific Paper

Rao, A. S., Rao, K.V.

AN EXPERIMENTAL STUDY ON EFFECT OF PROCESS VARIABLES ON SURFACE ROUGHNESS, TOOL VIBRATIONS AND ELASTIC SPRING BACK IN MILLING OF AISI 316 STAINLESS STEEL

Received: 23 February 2017 / Accepted: 05 April 2017

Abstract: *In this paper, effect of process variables like cutting speed, feed rate and depth of cut has been studied. The multi variable responses like surface roughness, tool vibrations and elastic spring back effect on CNC end milling operation of AISI 316 Stainless Steel is analyzed. The AISI 316 Stainless Steel is taken as a sample for our work. The experiments are performed on a 3 axis CNC vertical milling machine with two flute tungsten carbide end mills at high rotational spindle speeds and optimized the process parameters. The elastic spring back is referred to as the change in shape of the work piece after removing the tool. The surface roughness is measured by diamond point stylus and vibrations are measured by Laser Doppler Vibrometer (LDV). The elastic spring back is calculated as the difference between any two corresponding points in metal cutting and the value is measured by using Scanning Electron Microscope (SEM). Based on the experimental data from the specified instruments, the process variables have been optimized. This paper shows the influence of process parameters on the spring back on surface roughness and vibrations. In online tool condition monitoring, the optimized process parameters would give better tool life, maintain good machining time and gives higher machining efficiency.*

Key words: *AISI 316 stainless steel, surface roughness, tool vibrations, elastic spring back and CNC milling*

Eksperimentalna studija uticaja promenljivih procesa na hrapavost površine, vibracije alata i elastične deformacije prilikom glodanja AISI 316 nerđajućeg čelika. *U ovom radu je ispitivan, efekat više varijabli procesa kao što su brzina rezanja, pomak i dubina rezanja. Više promenljivih utiče na hrapavost površine, vibracije alata i elastično pomeranje delova pri CNC vretenastom glodanju nerđajućeg čelika AISI 316. Od nerđajućeg čelia AISI 316 su pravljeni uzorci za ispitivanje. Eksperimenti se izvode na 3 osnoj CNC vertikalnoj glodalici sa visokim brzinama obrtanja vretena sa alatom od tvrdog metala sa dva žljeba i optimizirani su parametari procesa. Elastična deformacija nazad, naziva se promena u obliku obradka nakon vađenja alata. Površinska hrapavost je merena dijamantskim vrhom alata a vibracije se mere pomoću Laser Doppler Vibrometera (LDV). Elastična deformacija se izračunava kao razlika između bilo koje dve tačke pri rezanju metala i vrednost se meri pomoću elektronskog mikroskopa (SEM). Na osnovu eksperimentalnih podataka iz navedenih instrumenata, varijable procesa su optimizovane. Ovaj rad pokazuje uticaj parametara procesa na elestične deformacije, na hrapavost površine i vibracije. U online praćenju stanja alata, optimizovani parametri procesa će dati bolju postojanost alata, održavati dobro vreme obrade i dati veću efikasnost mašinske obrade.*

Ključne reči: *AISI 316 nerđajući čelik, hrapavost površine, vibracije alata, elastične deformacije i CNC glodanje*

1. INTRODUCTION

AISI 316 Stainless Steel has wide applications include pumps, valves, marine fittings, fasteners, paper and pulp machinery, petro chemical equipment and surgical implants that demand a good combination of high strength, good corrosion resistance and low stress. The mechanical properties lead to challenges in machining operations such as high process temperature as well as rapidly increasing tool wear. In this work, tungsten carbide end mills have been used in machining of AISI 316 Stainless Steel. The surface roughness, vibrations and elastic spring back have been experimentally investigated and put into relationship with the process parameters under dry machining condition. The quality of the machined surfaces has been evaluated by measuring the roughness of the machined surfaces. Finally the correlation among vibrations, surface roughness and elastic spring back has been analyzed and discussed.

Literature to date has shown that limited work has been carried out to analyze the consequence of machining process variables on cutting of AISI 316 Stainless Steel. Vibration is defined as the relative motion of an object or objects relative to a stationary frame referred to as the equilibrium of the vibration. Since the vibration of mill cutter is a result of relative motion between work piece and tool, it is required to measure vibration of cutter as close as to machining. We used LDV to measure vibration of mill cutter the LDV's are used as non contact methods to measure vibrations of cutting tool or work piece accurately. The LDV is capable of giving reliable information of tool vibration.

Among the online tool wear monitoring methods, the vibrations are a tool wear indicator during automated manufacturing because the measurement of vibration is fairly simple. With the widely used CNC machine tools together with high performance computer aided design and computer aided

manufacturing systems, HSM has demonstrated advantages over traditional machining techniques such as increased productivity, high quality surface, burr-free edges and virtually stress free components. The increasing demand for higher machining efficiency has led to a much more reliable monitoring condition of the machining process. A recent study shows that a coated carbide tools may be used to machine AISI 316 Stainless Steel for a wide range of cutting conditions by producing variation in chip morphologies.

Alberti et al. [1] developed an algorithm based system to select optimal cutting parameters in conventional as well as high speed milling process. They have used the algorithm based system to select optimum parameters for reduction in production time in both conventional milling and high speed milling operations while ensuring optimal finishing conditions. Optimization of cutting parameters helps to improve production rate by reducing production time with improved tool life and less power consumption. This gives less production time and maximum profit in manufacturing. Albrecht. P [2] stated that the desirability function was introduced in 1980 to optimize cutting parameters. The desirability function uses a gradient algorithm and it finds desirability with maximum value between 0 and 1. If the desirability value closes to 0, then the response is completely unaccepted and if the desirability value is 1 or close to 1, then the response is accepted.

Response surface methodology (RSM), artificial neural networks and support vector regression were used by Amit Kumar [3] to develop the empirical models for prediction of surface roughness, tool wear and power consumption in turning process. RSM was used to optimize cutting parameters for minimum surface roughness and amplitude of cutter vibration. Baskar et al. [4] have developed optimization strategy with hill climbing algorithm and genetic algorithm for the optimization of parameters in face milling, corner milling, pocket milling and slot milling. They have obtained maximum profit with the help of developed strategy through optimization of cutting parameters. Production cost of a unit is affected by direct and indirect costs. Bhardwaj et al. [5] have used RSM with center composite rotatable design in turning of AISI 1019 steel to find out influence parameter on surface roughness. Prediction models were also developed for accurate prediction of surface roughness. Feed rate was found as significant parameter on surface roughness, while the depth of cut has no significant effect. In RSM, the quantitative relationship between input and output variables is presented as follows

$$y = f(x_1, x_2, x_3, \ldots, x_n) \pm e_r \quad (1)$$

where ''y'' is the desired response; ''f'' is the response function, dependent variable; x_1, x_2, x_3, ., x_n are independent variables; and ''e_r'' is the fitting error.

The increased feed rate in any machining process will lead to generation of heat and therefore it contributes high surface roughness. A prediction model was developed by Choudhuri and El-Baradie [6] using RSM for prediction of surface roughness in machining of EN 24T steel. They have conducted dry machining with uncoated carbide inserts and studied the effect of cutting speed, feed and depth of cut on surface roughness. RSM shows effect of individual factors and two factors interaction on the responses and it also identifies significant factors. The RSM combined with factorial design of experiments is a better alternative to the traditional one variable at a time approach for studying the effects of cutting variables on responses such as surface roughness and tool life. Karagu¨zel et al. [7] analyzed turn milling process is a new technology that combines two conventional machining processes like turning and milling. This new technology is an alternative process that gives improved productivity especially in machining of hard and large diameter work pieces. Many authors reported that there is a correlation between surface roughness and vibrations of cutter in any machining process. Kirby et al. [8] and Lin SC et al. [9] found a strong correlation between vibrations and surface roughness in turning process. In metal cutting, there is a relative motion between work piece and cutting tool. The cutting tool is getting dynamic excitation due to deformation of metal that results in vibration of tool. The relative motion and vibration of tool affect the surface quality of the product. These vibrations are to be maintained minimum to reduce surface roughness and tool wear. Vibration is defined as the repetitive motion of an object or objects relative to a stationary frame referred to as the equilibrium of the vibration. Vibrations are measured in terms of displacement, velocity or acceleration. Maiyar et al. [10] stated that increased cutting speed and feed rate will remove high amount of material, but it leads to wear on cutting edges due to abrasion between cutting edges and work piece. Muthukrishnan et al. [11] studied the surface roughness, the ANOVA has been used to find out significant cutting parameters and interaction of cutting parameter on the amplitude of cutter vibration. The ANOVA was performed at the confidence level of 95%, and the cutting parameters which are having ‘p’ value less than 0.05 are significant. There is no significant effect of depth of cut on surface roughness. Previous researchers have also claimed the similar results that cutting speed and feed rate have more effect on the surface roughness. Newmann et al. [12] stated that 6%-40% of energy savings can be achieved in metal cutting with optimum cutting parameters. Pettersson et al. [13] also proved that the cutting speed has significant effect on the cutter vibration. Prasad et al. [14] have used LDV’s to measure vibration of mill cutter in milling process. Fast Fourier Transformation (FFT) is used for generating features from an outline Acousto Optic Emission (AOE) signals to develop a data base for appropriate decisions. The FFT transforms the AOE signals into time domain with different time frequency zones. In this work, the LDV was adopted for online data acquisition of mill cutter vibration and a high speed FFT analyzer was used to process the AOE signals obtained from LDV. Prasad babu GHV et al. [15] analyzed tool vibration and surface roughness in orthogonal turn milling of ASTM B139 Phosphorous Bronze as per Taguchi design of experiments. Total 16 experiments were conducted on

four axes CNC milling machine and experimental results of tool vibration and surface roughness were collected. Response surface methodology (RSM) was used to find out the effect of process parameters such as cutting speed, feed and depth of cut on responses. A multi response optimization technique was used to optimize process parameters for minimum surface roughness and tool vibration. They have concluded that vibration increases with increase of feed. At the same time the surface roughness has found to be increased as speed was increased. Rantatalo et al. [16] have used the LDV in milling process to measure vibrations of rotating arbor in horizontal milling machine. Sahin. [17] has prepared design of experiments with cutting parameters and experiments were conducted according to design of experiments. Signal to noise ratios of experimental results were calculated by Taguchi method and analysis of variance (ANOVA) was used to analyze the ratios to identify cutting parameters which having more influence on tool life. Sahin and Motorcu [18] studied the effect of cutting parameters such as cutting speed, feed rate and depth of cut on turning of hard material with cubic boron nitride tool. They used RSM to predict surface roughness and a good correlation was found between them. Savas and Ozay [19] have used genetic algorithms for optimization of cutting parameters to get good surface quality in tangential milling. Different optimization strategies were developed by different researchers using algorithms to optimize cutting parameters. Schaal N.et al. [20] explained the spring back in metal cutting with high cutting speeds. They proved the influence of the cutting speed on the spring back is significant. Senthil Kumar et al. [21] have used genetic algorithms to select optimum cutting parameters in order to reduce production cost by improving tool life. They found that the Zirconia toughened alumina ceramic cutting tool has more life and it is able to machine at lower production cost. Sriram et al. [22] discussed the use of LDV's in the field of light weight structures. Frequency domain of LDV output signal is scanned to obtain deflection shape of the vibrating structure. Tatar and Gren[23] stated that the measurement of spindle and tool vibration is more important for tool condition monitoring in high speed milling process. Since the vibration of mill cutter is a result of relative motion between work piece and tool, it is required to measure vibration of cutter as close as to machining. They have used Laser Doppler Vibrometers (LDVs) to measure vibration of mill cutter. In recent applications, LDVs are used as non contact methods to measure vibration of cutting tool or work piece accurately. Venkatarao et al. [24] have used LDV to measure vibration of rotating work piece in boring of steels on horizontal computer numerical control (CNC) lathe machine. LDV was developed by Yeh and Cummins [25] as the measuring process involves measuring the Doppler's shift of the laser radiation that is scattered by the moving particles. Later the technique was developed as LDV. Spring back energy density is proposed by Zhu et al. [26] for evaluation of the amount and direction of spring back. Spring back in the present context refers to the elastically driven change of shape that occurs following a metal cutting operation when loads are removed from the work piece. Spring back involves small strains, similar in magnitude to other elastic deformation of metals. As such it was formally considered a simple phenomenon relative to the large strain deformation required for forming. Spring back is inevitable during the process of metal cutting. It can cause the shape and size of the final part to be in discordance with the shape and size of the end mill. The factors that affect the spring back generally include the mechanical parameters of AISI 316 Stainless Steel, anisotropy, grain arrangement, process conditions, work hardening phenomenon etc. A large no of studies on the spring back have been conducted by scholars and various solutions and simulation algorithms have been presented. Due to the diversity the materials used as sheets, structures and sizes of work pieces, different metal sheets have different spring back rules. According to the essence nature of mechanics, spring back is caused by non uniform stress distribution along the metal thickness direction and the spring back amount is decided by spring back energy.

The main objective of this work is to experimentally investigate the elastic spring back effect during milling of AISI 316 Stainless Steel with carbide end mills under dry machining condition. The quality of the machined surfaces has been evaluated by means of roughness. Finally the correlation among spring back effect, vibrations and surface roughness has been analyzed and discussed.

2. MATERIAL AND CUTTER

The work piece material used in the experiment was AISI 316 Stainless Steel with chemical composition shown in Table 1. Its mechanical properties are shown in Table 2.

Elements	Percentage (%)
C	0.08 Max
Mn	2.0
Si	0.75
P	0.045
S	0.03
Cr	16-18
Ni	10-14
N	0.1
Fe	Balance

Table. 1 Chemical composition of AISI 316 Stainless Steel

Mechanical Properties	Value
Ultimate Tensile strength (MPa)	620-795
Yield strength (MPa)	206
Elongation at Break (%)	30
Modulus of Elasticity (GPa)	164
Hardness(BHN)	146

Table 2. Mechanical properties of AISI 316 Stainless Steel

The tungsten carbide end mill cutters were used for milling of AISI 316 Stainless Steel. The tools have

been rapidly fixed to a tool holder with a nominal diameter of 10mm. Geometric parameters of the tools are given in Table 3.

Diameter (mm)	10
Rake angle (^{o})	10
Clearance angle (^{o})	10
No of tooth	2
Helix angle (^{o})	30

Table 3. Geometric parameters of end mills

3. EXPERIMENTAL PROCEDURE

The experiments have been carried out on Chandra BFW CNC milling machine as shown in the Figure 1. The following sequential procedure was used to carry out the experiment under dry condition.

1. Each trail was started with a new end mill with one new test condition (trail) and machining was stopped at the end of each pass.
2. An LDV was placed in front of the machine and the LDV produces a laser beam to the rotating mill cutter to measure vibration signals and the setup of experiment is shown in the Figure 1.
3. After each pass, the work piece was removed and its surface roughness was measured.
4. The above steps were repeated and remained the same in the experiment with a new end mill.
5. Experimental data of 27 experiments, surface roughness R_a and vibrations along x and y directions and spring back effect are shown in the Table.4

Fig. 1. Three axis CNC vertical milling machine with Laser Doppler Vibrometer (LDV)

The surface roughness of the work piece was measured by a stylus instrument. To measure roughness of the surface of the work piece, the cut off length was taken as 100mm and the sampling length as 150mm.

Samples of AISI 316 Stainless Steel with dimensions of 150mm X 120mm X 15mm have been tested. Three levels of cutting speed (95, 110 and 126 m/min), three levels of feed rates (0.1, 0.2 and 0.3mm/rev) and three levels of depth of cut (0.3, 0.6 and 1mm) have been taken into account. The machined sample of work piece is shown in Figure 2.

Fig. 2. The machined AISI 316 Stainless Steel work piece

4. RESULTS AND DISCUSSION

The experimental cuts have been performed in random sequence, in order to reduce the effect of any possible systematic error. The titanium sample is fixed in a vice and the Laser Doppler Vibrometer (LDV) is used to measure vibrations through data logger. As per Taguchi design of experiments (DOE), total 27 experiments have been performed on a machine follows and experimental results shown in the Table 4(a) and (b).

In each experiment, cutter vibration, surface roughness and elastic spring back effect on machined surface were measured in microns. The analysis is done by response surface methodology in Design expert software 10. Laser Doppler Vibrometer (LDV) measures vibrations in ways that other sensors cannot. The LDV measures the vibrations of a milling cutter in the laser beam direction. In this work, LDV was used for online acquisition of cutter vibration data in the form of AOE signals as shown in the Figure 3.

Exp. No.	Design of experiments			Surface roughness (μm)					Cutter displacement in X direction (μm)				
	C S m/min	F R mm/rev	DOC mm	R_a 1	R_a 2	R_a 3	R_a 4	R_a Avg	V_x 1	V_x 2	V_x 3	V_x 4	V_x Avg
1	95	0.1	1.0	0.21	0.19	0.17	1.60	0.54	9.93	10.0	9.30	9.61	9.71
2	95	0.2	1.0	0.22	0.17	0.37	1.65	0.60	9.91	10.2	10.32	9.94	10.00
3	95	0.3	1.0	0.65	0.22	1.76	1.74	1.09	9.01	9.88	10.11	9.94	9.74
4	95	0.1	0.6	0.22	0.25	0.78	0.76	0.49	9.73	8.20	8.93	10.37	9.31
5	95	0.2	0.6	0.24	0.31	1.60	1.33	0.87	9.62	9.39	9.41	10.20	9.67
6	95	0.3	0.6	1.15	1.66	1.74	1.72	1.57	8.45	9.85	9.33	9.19	9.21
7	95	0.1	0.3	0.26	0.31	1.36	1.08	0.75	8.21	8.58	10.33	10.39	9.38
8	95	0.2	0.3	0.28	0.92	1.69	1.47	1.09	8.57	8.37	10.02	10.37	9.33
9	95	0.3	0.3	1.41	1.76	1.74	1.72	1.66	8.33	8.27	8.92	10.04	8.89
10	110	0.1	1.0	0.21	0.22	0.27	0.23	0.23	9.92	9.69	8.22	8.52	9.09
11	110	0.2	1.0	0.22	0.23	0.24	0.17	0.21	9.90	9.50	9.27	10.08	9.69
12	110	0.3	1.0	0.49	0.80	0.58	0.32	0.55	9.15	8.52	9.69	10.32	9.42
13	110	0.1	0.6	0.22	0.24	0.31	0.16	0.23	9.88	8.42	8.21	10.23	9.19
14	110	0.2	0.6	0.22	0.24	0.23	0.21	0.22	9.88	9.23	8.76	10.12	9.50

15	110	0.3	0.6	0.67	1.09	0.45	1.71	0.98	8.93	8.64	9.32	9.25	9.04
16	110	0.1	0.3	0.31	0.29	0.16	0.18	0.24	8.71	8.15	10.35	10.39	9.40
17	110	0.2	0.3	0.22	0.27	0.17	1.56	0.55	9.54	8.36	10.15	10.29	9.59
18	110	0.3	0.3	0.84	0.89	0.60	1.76	1.03	8.61	8.86	8.57	8.54	8.65
19	126	0.1	1.0	0.21	0.23	0.26	0.34	0.24	9.91	9.48	8.67	8.12	9.05
20	126	0.2	1.0	0.22	0.25	0.26	0.29	0.25	9.87	9.34	9.13	8.64	9.25
21	126	0.3	1.0	0.25	0.32	0.40	0.27	0.31	9.62	9.01	8.92	10.17	9.43
22	126	0.1	0.6	0.22	0.24	0.32	0.16	0.23	9.89	8.84	8.11	10.10	9.24
23	126	0.2	0.6	0.22	0.24	0.27	0.17	0.22	9.90	9.28	8.25	10.20	9.41
24	126	0.3	0.6	0.27	0.38	0.30	0.18	0.28	9.63	8.91	9.85	9.74	9.53
25	126	0.1	0.3	0.43	0.40	0.17	0.16	0.29	9.12	8.12	9.80	10.39	9.36
26	126	0.2	0.3	0.23	0.26	0.17	0.16	0.21	9.80	8.22	10.10	10.33	9.61
27	126	0.3	0.3	0.30	0.40	0.17	0.18	0.26	9.53	8.98	9.76	9.59	9.47

Table 4 (a). DOE and experimental results of surface roughness and cutter displacement

Exp. No.	Cutter displacement in Y direction (µm)					Elastic spring back (µm)				
	V_y 1	V_y 2	V_y 3	V_y 4	V_y Avg	S 1	S 2	S 3	S 4	S Avg
1	6.11	5.81	5.72	6.58	6.06	0.131	0.131	0.132	0.132	0.132
2	6.03	5.06	5.03	6.52	5.66	0.131	0.131	0.132	0.137	0.133
3	5.44	4.89	5.21	5.69	5.31	0.150	0.155	0.16	0.171	0.159
4	6.32	6.59	6.59	6.55	6.51	0.131	0.133	0.135	0.147	0.137
5	6.27	6.48	6.58	6.49	6.46	0.132	0.132	0.144	0.158	0.142
6	6.07	5.59	6.36	6.45	6.12	0.166	0.152	0.177	0.179	0.169
7	6.59	6.59	6.59	6.60	6.59	0.152	0.144	0.179	0.180	0.164
8	6.58	6.60	6.60	6.60	6.60	0.141	0.143	0.180	0.181	0.179
9	6.50	6.60	6.58	6.59	6.57	0.174	0.178	0.181	0.181	0.179
10	6.10	5.65	5.99	6.42	6.04	0.131	0.133	0.152	0.136	0.138
11	6.07	5.27	5.07	5.28	5.28	0.131	0.138	0.146	0.132	0.137
12	5.84	5.01	4.89	4.89	5.16	0.139	0.174	0.166	0.150	0.157
13	6.15	6.57	6.55	5.16	6.10	0.131	0.133	0.142	0.143	0.137
14	6.12	5.98	6.23	5.65	6.00	0.131	0.135	0.14	0.143	0.137
15	5.91	5.08	4.95	6.14	5.52	0.144	0.172	0.175	0.176	0.167
16	6.53	6.6	6.08	6.50	6.43	0.169	0.145	0.168	0.179	0.165
17	6.39	6.59	5.59	6.59	6.29	0.132	0.134	0.159	0.179	0.151
18	6.21	5.78	5.69	6.59	6.07	0.155	0.170	0.180	0.181	0.172
19	6.07	5.25	5.35	6.57	5.81	0.131	0.139	0.152	0.154	0.144
20	5.98	5.09	5.06	6.16	5.57	0.131	0.145	0.15	0.140	0.142
21	5.70	5.03	4.99	4.91	5.16	0.134	0.157	0.163	0.148	0.151
22	6.09	6.22	6.58	5.11	6.00	0.132	0.136	0.159	0.140	0.142
23	6.06	5.32	6.41	5.03	5.71	0.131	0.14	0.148	0.139	0.139
24	5.90	5.05	4.95	4.96	5.22	0.133	0.159	0.153	0.165	0.153
25	6.13	6.6	5.78	5.43	5.99	0.181	0.176	0.165	0.172	0.174
26	6.13	6.55	5.17	5.18	5.76	0.133	0.142	0.142	0.154	0.143
27	6.00	5.23	4.98	5.04	5.31	0.134	0.156	0.165	0.174	0.157

Table 4 (b). Experimental results of cutter displacement and elastic spring back

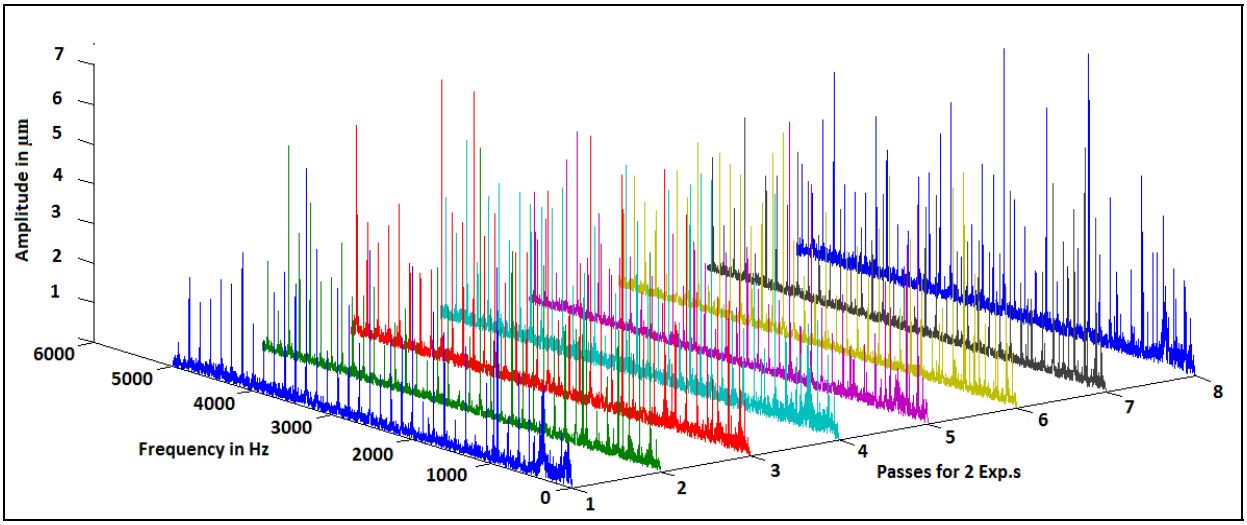

Fig. 3. Frequency domains for the experiment 1 and 2

FFT analyzer was used for generating features from online AOE signals to develop a data base for appropriate decisions. The trends of effect of these machining parameters help to identify which parameter and interaction of parameters are significant on the surface roughness and mill cutter vibration.

Based on the experimental results and experimental parameters shown in Table 4, four factor interaction response function for elastic spring back effect, surface roughness and vibrations along x and y can be expressed as function of process parameters. The quadratic model for the elastic spring back is given by the following equation (2).

$$s=0.27847-9.20921E-0.04v+0.017955f-0.24799d- -3.94475E-0.03vf+9.21643E-0.04vd+0.10360fd+ +4.30108E-0.06v^2+1.06111f^2+0.073280d^2 \quad (2)$$

Effect of parameters on R_a

Interaction effect of cutting speed, feed rate and depth of cut on the amplitude of cutter vibration in feed direction is shown in the Figure 4. Figure 4 (a) represents normal probability plot of the residuals for the surface roughness, most of the residuals are almost close to the straight line. That indicates that there is normal distribution of errors for the surface roughness. As per the Figures 4 (b), the surface roughness is found to be low at 113.6m/min of cutting speed and 0.25 mm/rev of feed rate. If feed rate increases, the surface roughness will also increase. If the cutting speed increases, the surface roughness will also increase. When the cutting speed increases from 113.6m/min, the surface roughness will also increase. When the feed rate increases from 0.25mm/rev the surface roughness will also increase. As per the Figure 4 (c and d), it is observed that when the feed rate at0.18mm/rev and depth of cut at 0.6 mm, the surface roughness is low. When the depth of cut is above 0.6 mm and feed rate is 0.3mm/rev the surface roughness is high. When the cutting speed increases from 113.6m/min the surface roughness will also increase. The feed rate has a significant parameter on surface roughness.

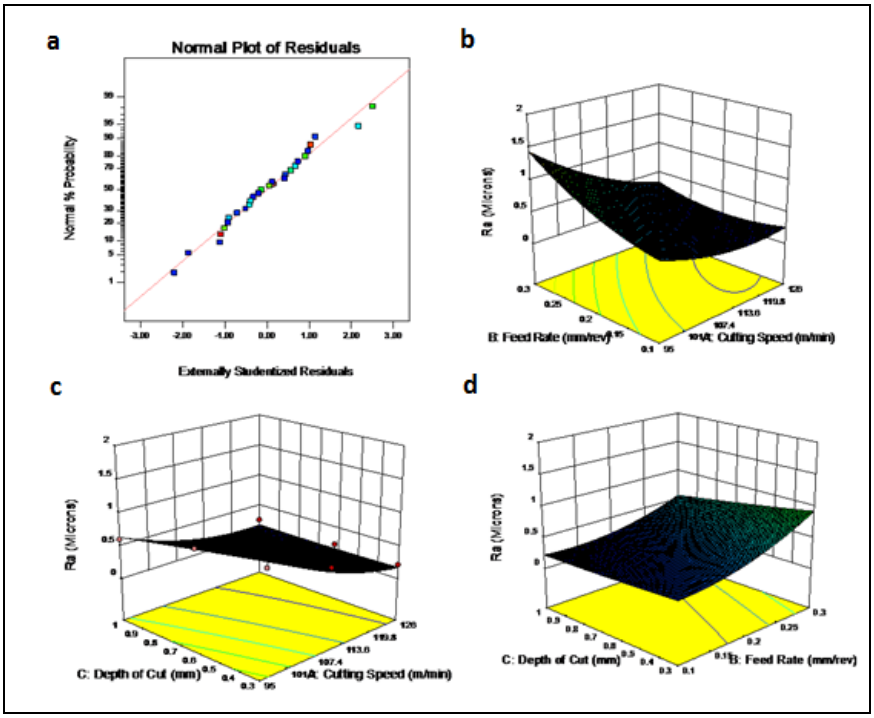

Fig. 4. (a) Normal probabilities of residuals for R_a. (b) Effect of feed and cutting speed on R_a, (c) effect of depth of cut and cutting speed on R_a, and (d) effect of depth of cut and feed rate on R_a

Effect of parameters on V_x

Interaction effect of cutting speed, feed rate and depth of cut on the amplitude of cutter vibration in feed direction is shown in the Figure 5. Figure 5 (a) represents normal probability plot of the residuals for the amplitude in feed direction, most of the residuals are almost close to the straight line. That indicates that there is normal distribution of errors for the amplitude in feed direction. As per the Figures 5 (b), when the feed rate and cutting speed increases, the amplitude of cutter vibration will increase. It is also observed that at high feed rates and low cutting speeds, the amplitude of cutter vibration is very high. As per the Figure 5 (c and d), the amplitude is found to be high at 1mm of depth of cut and cutting speed at 95 m/min. The amplitude of cutter vibration is getting reduced when the depth of cut is decreased. When the depth of cut is 0.3 mm and cutting speed is 95m/min and the feed rate is 0.1mm/rev, the amplitude of cutter vibration is very low.

When the depth of cut is at 1mm, it gives higher amplitude of cutter vibration. The higher depth of cuts is a significant parameter on cutter vibrations. There is no significant of cutting speed and feed rate on the amplitude of cutter vibration in feed direction. Among the cutting speed and feed rate, the feed rate has significant effect on the vibration.

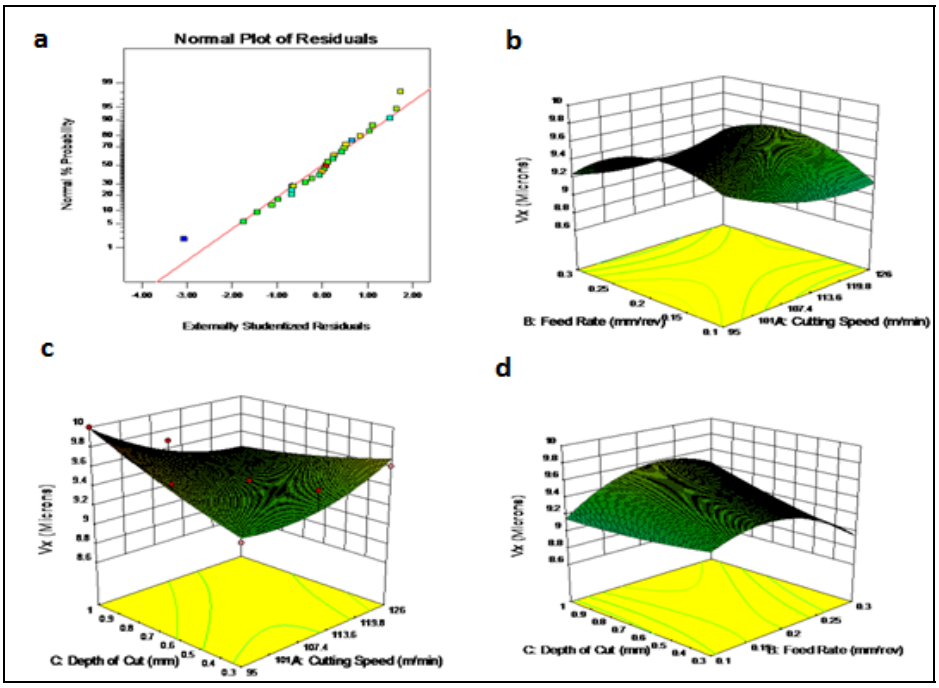

Fig. 5. (a) Normal probabilities of residuals for V_x (b) Effect of feed and cutting speed on V_x, (c) effect of depth of cut and cutting speed on V_x, and (d) effect of depth of cut and feed rate on V_x

Effect of Parameters on V_y

Interaction effect of cutting speed, feed rate and depth of cut on the amplitude of cutter vibration in depth of cut direction is shown in the Figure 6. Figure 6 (a) represents normal probability plot of the residuals for the amplitude of cutter vibration in depth of cut direction, most of the residuals are almost close to the straight line. This indicates that there is normal distribution of errors for the amplitude of cutter vibration along y direction. As per the Figures 6 (b,c,d), When the feed rate is 0.3mm/rev and at cutting speed 95 m/min the V_y is very high. At same time it is observed that at feed rate of 0.3mm/rev and cutting speed 95m/min, the V_y is very low. At the depth of cut of 1mm and cutting speed at 95m/min the V_y is high. At depth of cut at 1mm and feed rate 0.1 mm/rev, the V_y is very high. At the depth of cut of 0.3mm and feed rate of 0.3mm/rev, the V_y is high. There is no much variation in the amplitude of cutter vibration for further changes in the cutting speed and feed rate.

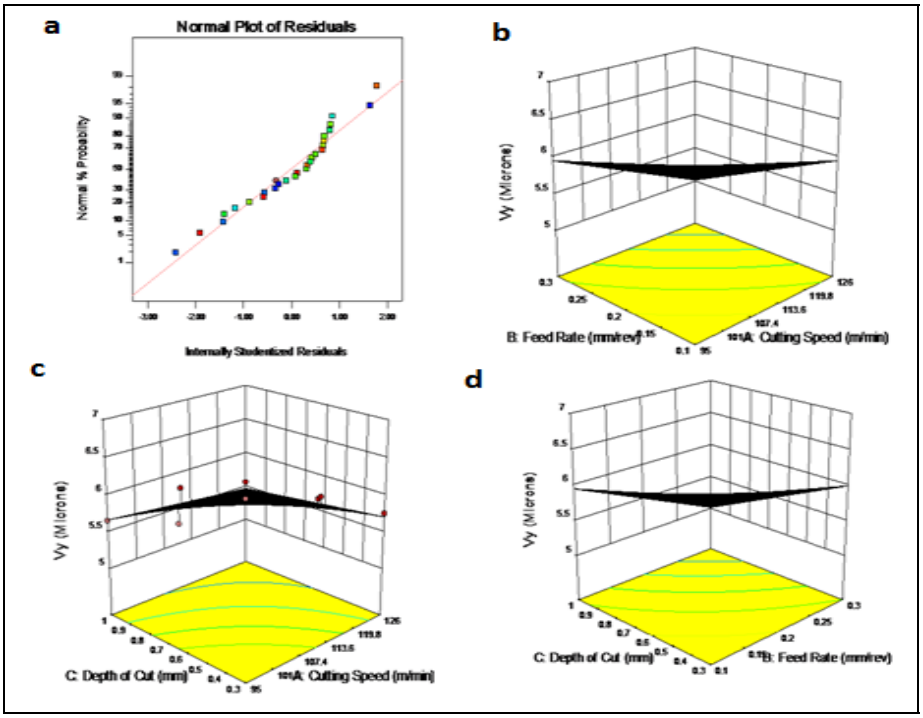

Fig. 6. (a) Normal probabilities of residuals for V_y (b) Effect of feed and cutting speed on V_y, (c) effect of depth of cut and cutting speed on V_y, and (d) effect of depth of cut and feed rate on V_y

Effect of Parameters on 'S'

Interaction effect of cutting speed, feed rate and depth of cut on the elastic spring back effect is shown in the Figure 7. Figure 7 (a) represents normal probability plot of the residuals for the elastic spring back effect, most of the residuals are almost close to the straight line. That indicates that there is normal distribution of errors for the elastic spring back effect. As per the Figure 7 (b), the feed rate of 0.3 mm/rev and cutting speed of 95m/min the elastic spring back effect is very high. At the feed rate of 0.1mm/rev and cutting speed of 95m/min, the elastic spring back is very low. As per the Figure 7 (c and d), the depth of cut of 1mm and cutting speed of 95m/min, the lower elastic recovery is noticed. At the feed rate of 0.3mm/rev and depth of cut of 0.3 mm, the elastic recovery is very high. The cutting speed and depth of cut have a significant contribution in high elastic recovery of the materials.

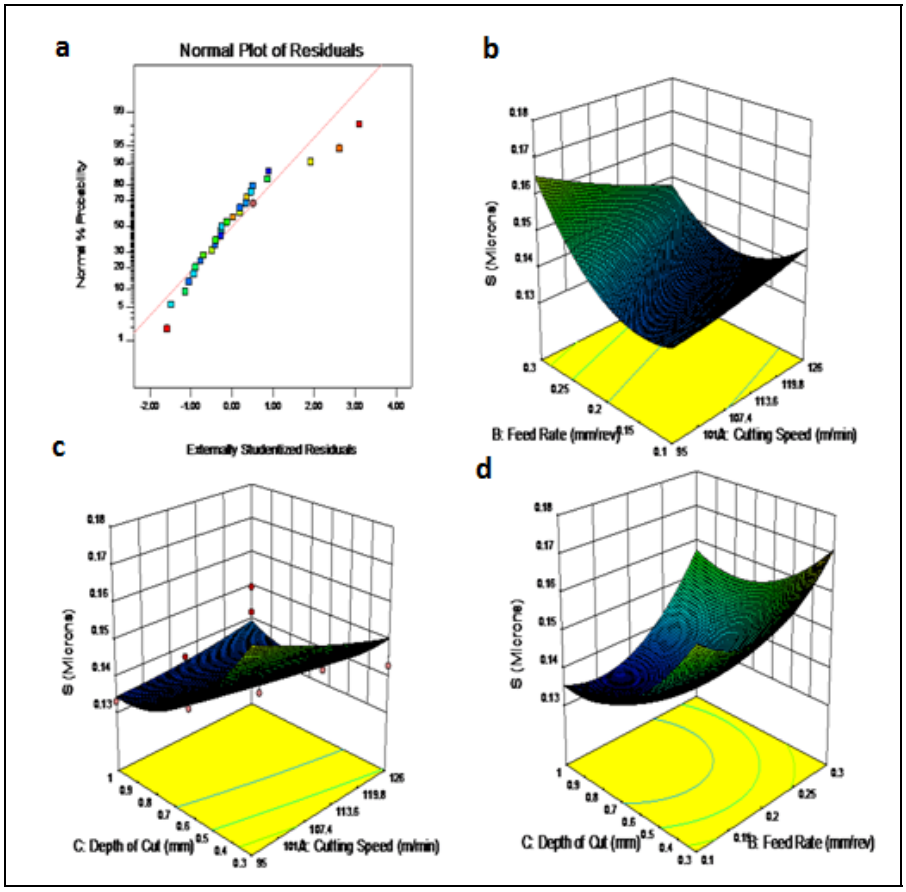

Fig. 7. (a) Normal probabilities of residuals for 'S' (b) Effect of feed and cutting speed on 'S', (c) effect of depth of cut and cutting speed on 'S', and (d) effect of depth of cut and feed rate on 'S'

Optimum values of multi objective function

The objective of this work is to find out optimum cutting parameters to achieve less surface roughness and amplitude of cutter vibration in order to reduce power consumption, production time and to improve tool life.

Optimum values for multi objective of surface roughness and amplitude of cutter vibrations were done using response surface methodology and spring back effect is being measured by Scanning Electron Microscope (SEM) and the results are shown in the figure 8.

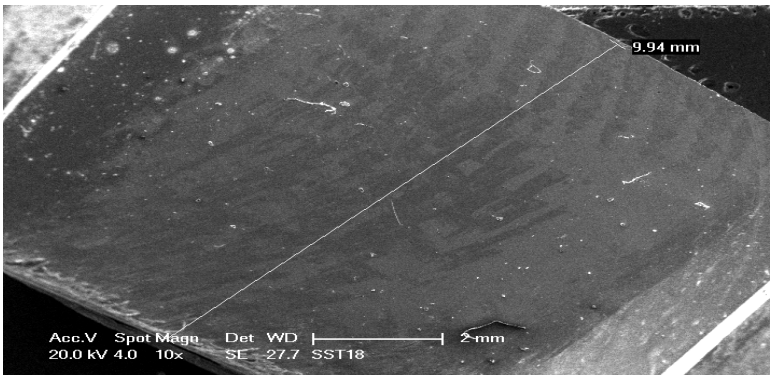

Fig. 8. Measurement of spring back of a AISI 316 Stainless steel sample using Scanning electron Microscope (SEM)

In this study, smaller the better function was used for surface roughness and amplitude of cutter vibration and larger the better function for elastic spring back because these responses should be optimum for any product to obtain good product quality and tool life. The amount of spring back during unloading depends on the Young's modulus of the material. Based on the experimental and numerical analysis, it is concluded that the 'R_a' has a lower value at cutting speed of 113m/min, feed rate of 0.25mm/rev and depth of cut of 0.6 mm. The amplitude 'V_x' has a lower value at cutting speed of 95m/min, feed rate of 0.1mm/rev and at depth of cut of 0.3mm. The amplitude 'V_y' is also lower at cutting speed of 126m/min, feed rate of 0.3 mm/rev and depth of cut of 0.6 mm. The elastic spring back 'S' has higher value at cutting speed of 95m/min, feed rate of 0.3 mm/rev and at depth of cut of 1mm.

5. CONCLUSIONS

Optimization of cutting parameters to improve surface quality and production rate at low power consumption was found using multi objective optimization technique. The milling experiments were conducted on AISI 316 Stainless Steel with two flute carbide end mill on three axis milling machine. Response Surface Methodology (RSM) approach Design Expert Version 10 is used to identify significant parameters where affecting surface roughness, amplitude of cutter vibration and spring back effect of the material. The following conclusions can be drawn from this study:

1. Effect of cutting parameters on amplitude of mill cutter vibration was measured with LDV by focusing optic signal on rotating cutter. Changes in the amplitude of cutter vibration due to tool wear can be used for online tool condition monitoring.

2. The AOE signals are very sensitive and they identify changes in cutting zone due to vibrations.

3. Surface roughness, amplitude of cutter vibration and elastic spring back were analyzed by using RSM. The cutting speed, feed rate and depth of cut were found to be significant cutting parameters on surface roughness, amplitude and elastic spring back has been proved.

4. The multi objective technique shows at a particular cutting speed, feed rate and depth of cut are the optimal combination of milling parameters for minimum surface roughness (R_a), amplitude of cutter vibration along feed and depth of cut directions (V_x,V_y) and maximum elastic spring back effect(S) has been proved in our study. This data can help to improve simulation result of cutting processes and to understand the importance of elastic-plastic effects of materials.

6. REFERENCES

[1] Alberti M, Ciurana J and Casadesu´ s M. A system for optimizing cutting parameters when planning milling operations in high-speed machining. J Mater Process Tech 2005; 168(1): 25–35.

[2] Albrecht.P. New developments in the theory of the metal cutting process part 1, the ploughing process in metal cutting, ASME journal of engineering for industry, Vol 81; 1960:348-358

[3] Amit Kumar G. Predictive modeling of turning operations using response surface methodology, artificial neural networks and support vector regression. Int J Prod Res 2010; 48(3): 763–778.

[4] Baskar N, Asokan P, Saravanan R, et al. Selection of optimal machining parameters for multi-tool milling operations using a memetic algorithm. J Mater Process Tech 2006; 174(1–3): 239–249.

[5] Bhardwaj B, Kumar R and Singh PK. Surface roughness prediction model for turning of AISI 1019 steel using response surface methodology and Box–Cox transformation. Proc I Mech E, Part B: J Engineering Manufacture 2014; 228(2): 223–232.

[6] Choudhuri IA and El-Baradie MA. Surface roughness prediction in the turning of high-strength steel by factor-ial design of experiments. J Mater Process Tech 1997; 67(1–3): 55–61.

[7] Karagu¨zel U, Uysal E, Budak E, et al. Analytical modeling of turn-milling process geometry, kinematics and mechanics. Int J Mach Tool Manu 2014; 91: 24–33, http://www.sciencedirect.com/science/article/pii/S08906955 14001618

[8] Kirby ED, Chen JC, Zhang JZ, et al. Development of a fuzzy-nets-based in process surface roughness adaptive control system in turning operations. Expert Syst Appl 2006; 30(4): 592–604.

[9] Lin SC and Chang MF. A study on the effects of vibrations on the surface finish using a surface topography simulation model for turning. Int J Mach Tool Manu 1998; 38(7): 763–782.

[10] Maiyar LM, Ramanujam R, Venkatesan K, et al. Optimization of machining parameters for end milling of Inconel 718 super alloy using Taguchi based grey relational analysis. Proc Eng 2013; 64: 1276–1282.

[11] Muthukrishnan N and Davim JP. Optimization of machining parameters of Al/SiC-MMC with ANOVA and ANN analysis. J Mater Process Tech 2009; 209: 225–232.

[12] Newman ST, Nassehi A, Imani-Asrai R, et al. Energy efficient process planning for CNC machining. CIRP J Manuf Sci Techn 2012; 5(2): 127–136.

[13] Pettersson L, Hakansson L, Claessonans I, et al. Active control of machine-tool vibration in a CNC lathe based on an active tool holder shank with embedded piezo ceramic actuators. In: Proceedings of the 8th international Congress on Sound and Vibration, Hong Kong SAR, China, 2–6 July 2001. IIAV Publisher.

[14] Prasad BS, Sarcar MMM, Satish Ben BB, et al. Surface textural analysis using acousto optic emission- and vision-based 3D surface topography—a base for online tool condition monitoring in face turning. Int J Adv Manuf Tech 2011; 55(9–12): 1025–1035.

[15] Prasad Babu GHV, BSN Murthy, K Venkatarao

and Ch Ratnam. Multi response optimization in orthogonal turn milling by analyzing tool vibration and surface roughness using response surface methodology, Proc I Mech E Part B: J Engineering Manufacture 1–10 I Mech E 2016

[16] Rantatalo M, Tatar K, Norman P, et al. Laser Doppler vibrometry measurement of a rotating milling machine spindle. In: Proceedings of the international conference on vibrations in rotating machinery—I Mech E conference transactions, Swansea, 7–9 September 2004, pp.231–240. Professional Engineering Publishing Ltd.

[17] Sahin Y. Comparison of tool life between ceramic and cubic boron nitride (CBN) cutting tools when machining hardened steels. J Mater Process Tech 2009; 209(7): 3478–3489.

[18] Sahin Y and Motorcu AR. Surface roughness model in machining hardened steel with cubic boron nitride cutting tool. Int J Refract Met H 2008; 26(2): 284–290.

[19] Savas V and Ozay C. The optimization of the surface roughness in the process of tangential turn-milling using genetic algorithm. Int J Adv Manuf Tech 2008; 37: 335–340.

[20] Schaal N.et al, spring back in metal cutting with high cutting speeds, 15th CIRP conference on modeling of machining operations, Zurich, Switzerland, 2015.

[21] Senthil Kumar A, Adam Khan M, Thiraviam R, et al. Machining parameters optimization for alumina based ceramic cutting tools using genetic algorithm. Mach Sci Technol 2006; 10(4): 471–489.

[22] Sriram P, Hanagud S, Craig J, et al. A new laser Doppler technique for velocity profile sensing. Appl Optics 1990; 29(16): 2409–2417.

[23] Tatar K and Gren P. Measurement of milling tool vibrations during cutting using laser vibrometry. Int J Mach Tool Manu 2014; 48(3–4): 380–387.

[24] Venkatarao K, Murthy BSN, Mohanrao N, et al. Cutting tool condition monitoring by analyzing surface roughness, work piece vibration and volume of metal removed for AISI 1040 steel in boring. Measurement 2013; 46: 4075–4084.

[25] Yeh Y and Cummins HZ. Localized fluid flow measurements with a He-Ne laser spectrometer. Appl Phys Lett 1964; 4: 176.

[26] Zhu D.B, L. Ma, D.C. Li, B.H. Lu On spring back evaluation for 3-D sheet metal stamping parts Mech. Sci. Technol.,19 (2000),pp.953-955

Note: This work (Major project) was funded by Science and Engineering Research Board, Department of Science and Technology, Government of India. Grant No.: SERB/F/1761/2015-16. Dr. K Venkata Rao is PI of the Project and co author of the manuscript.

Author: **A. Sreenivasa Rao**, Corresponding Author:
A. Sreenivasa Rao, Department of MechanicalEngineering, MLR Institute of Technology, Hyderabad, India.
E-Mail: asrao2k14@gmail.com
Mobile: +91 8465022671
K Venkata Rao, Department of Mechanical Engineering, PBR Visvodaya Institute of Technology & Science, Kavali, India.

http://doi.org/10.24867/JPE-2017-01-031

Journal of Production Engineering

Vol.20 No.1

JPE (2017) Vol.20 (1) Original Scientific Paper

Vasilko, K.

MODIFIED QUATION T=f(v_c) AND IST IDENTIFICATION

Received: 22 March 2017 / Accepted: 27 April 2017

Abstract: *Recent development of the application of new kinds of material in transport and production technology places higher requirements on the technologist at the determination of cutting conditions. The assortment of recent kinds of cutting material enables to intensify cutting conditions while maintaining acceptable tool durability. The dependence of tool durability on cutting speed, or „basic law of machining", is the basic means to determine tool durability at selected cutting conditions. The paper contains a suggestion to modify the original Taylor equation on recent conditions of productive machining.*

Key words: *machining, tool life, tool wear, sintered carbide*

Modifikovana jednačina T=*f*(v_c) i njena identifikacija. *Nedavni razvoj primene novih vrsta materijala u transportu i proizvodnim tehnologijama stavlja sve veće zahteve tehnologi pri određivanju režima rezanja. Asortiman novih vrsta materijala za rezanje omogućava da se intenziviraju režimi rezanja uz održavanje prihvatljive postojanosti alata. Zavisnost postojanosti alata od brzine rezanja ili "osnovni zakon obrade", je osnovno sredstvo za utvrđivanje postojanosti alata za izabrane uslove rezanja. U radu se nalazi predlog za izmenu originalne Tailorove jednačine za nove uslove produktivne obrade.*

Ključne reči: *mašinska obrada, postojanost, habanja alata, sinterovani karbida*

1. HISTORY OF THE DESCRIPTION OF EQUATION T = f(v_c)

In 1906, after the invention of high-speed cutting steel, Taylor [1] constructed graphic dependences VB = f(τ_s) at different cutting speeds (Fig. 1). He selected the criterion of blunting, equal for all curves VB_k.

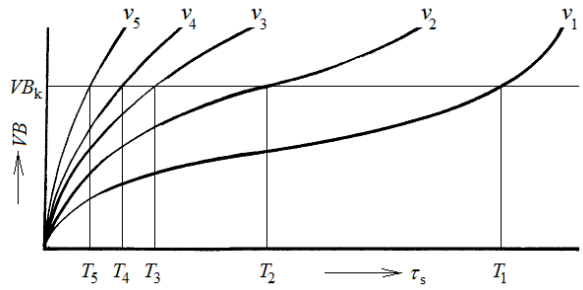

Fig. 1. Curves of tool wear at different cutting speeds $v_5 \rangle v_4 \rangle ... \rangle v_1$

For this criterion, the values of durability VB_1 – VB_5 are subtracted and a graph of dependence T = f(v_c), is constructed (Fig. 2). In the Figure, an actual diagramme, which has been obtained in an experiment, is shown.

As it is difficult to describe a curve mathematically, after its transformation into double logarithmic network, a straight line is obtained (Fig.3).

The dependence presents a visually precise straight line, which confirms Taylor´s theory.

The straight line equation in double algorithmic system will have the following form:

$$\log T = \log C_T - m.\log v_c \qquad (1)$$

where m = arctg φ is slope of the straight line.

After de-taking a logarithm of the equation, a well-known Taylor equation appears [2-5]:

$$T = \frac{C_T}{v_c^{\,m}}. \qquad (2)$$

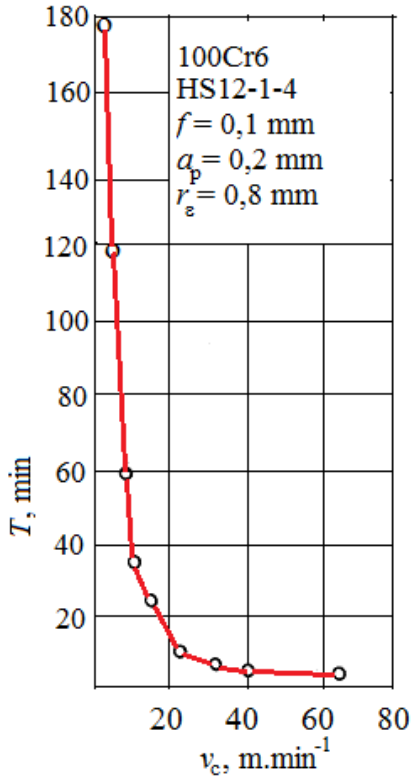

Fig. 2. Theoretical (a) and experimental (b) dependence of tool durability on cutting speed

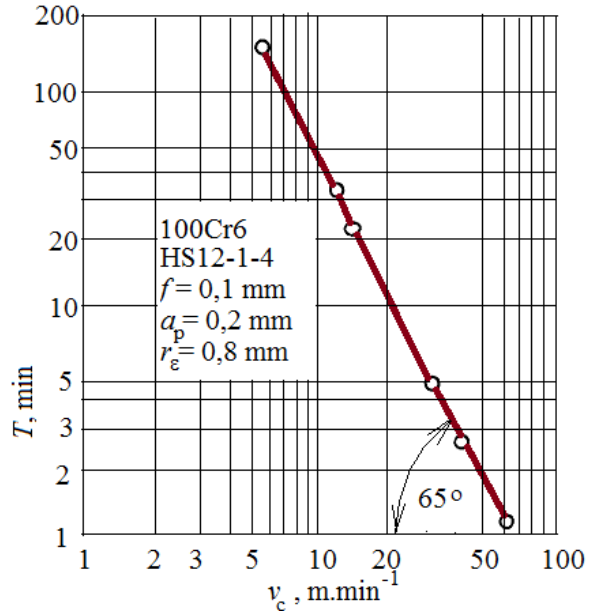

Fig. 3. Theoretical and actual dependence $T = f(v_c)$ in double algorithmic system

2. MODIFICATION OF DEPENDENCE T-v_c

In the course of the century, a development of high-performance cutting materials on the base of sintered carbids, ceramics, complemented with wear resistance coats has realised [6-9]. Therefore it is necessary to modify the original Taylor equation.

When machining with a tool made of sintered carbid, T-v_c dependence has much more complex course. At selected criterion of blunting VB_k = 0.3mm, values of relative durabilities have been subtracted and a graph in Fig. 4 has been constructed. The conditions which have been used correspond with finishing turning.

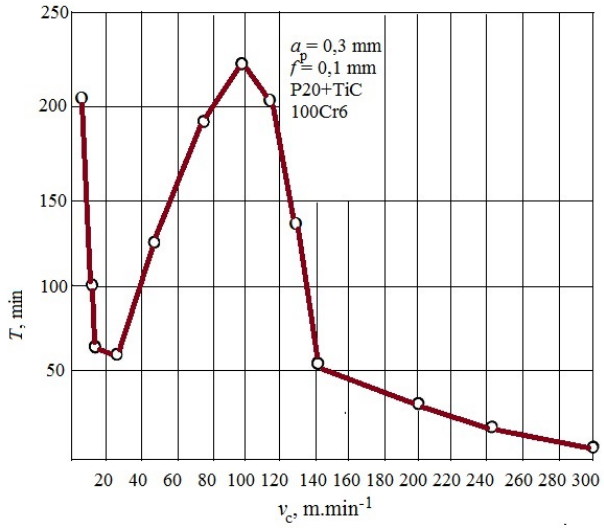

Fig. 4. Experimental dependence of tool durability on cutting speed when machining with a tool made of sintered carbid in a linear coordinate system

It can be seen that at minimal values of cutting speeds, there occurs the increase of durability as a result of a small area of contact of the chip with the tool face. Cut material is firm but brittle. A segmented chip, which does not adhere with cutting material, is created. At higher cutting speed, the durability decreases (local minimum is probably at $v_c \approx 20$ m.min^{-1}). Further increase of cutting speed leads to the creation of a built-up edge and its protective effect on cutting wedge shows. Durability increases sharply and reaches its maximum at approximately v_c = 90 m.min^{-1}. Then it decreases continually and at cutting speeds above 200 m.min^{-1} it reaches several min.

It can be seen that the course of the curve is rather complex. There exist two areas of high durability – at minimal cutting speed and, in presented case, at cutting speed of approximately 100 m.min^{-1}. At cutting speed about 20 m.min^{-1} the durability is minimal, similar phenomenon occurs after crossing the cutting speed 140 m.min^{-1}. If the dependence is trasformed into double logarithmic system (Fig. 5), one can get a graph which can be interpolated by abscisses. As in practice cutting speeds of over 80 m.min^{-1} are usually used, Taylor equation (2) can be used to describe decreasing branches of the curve. However, it is necessary to realise that there exist cases when whole range of cutting speeds are used (cutting off, drilling, turning with combination tools, etc.) and where tool durability changes considerably and it is necessary to know them.

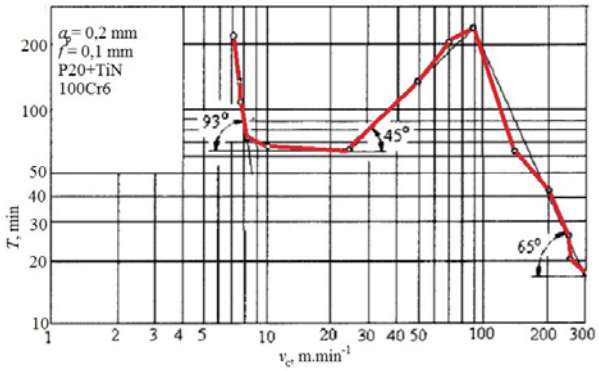

Fig. 5. Dependence from Fig. 4 in double logarithmic coordinate system

3. ANALYTIC DESCRIPTION

In an attempt ot describe such a dependence mathematically it has been found out that it is a non-linear function [2]:

$$T = C.\exp(-v).((v^4)+(v^{-1})) \qquad (3)$$

where

$$v_c = (\ln v_c); v \in (0,\infty); v_c \in (1,\infty); C = C(a_p, f, r_\varepsilon); C = 50$$

The non-linear function T= f(v_c) depends on non-linear parameters. It is possible to statistically analyse the dependence from n-realised experimental dependences of tool durability $T_1, T_2, ...T_n$ on cutting speed:

$$T_t = T(v_c.\theta) + \varepsilon_t, \qquad (4)$$

where $\theta = (\theta_1, ...\theta_p)^t$; $\theta \in R^p$ is the vector of suggested parameters.

Cutting speed v_c is expressed by a single-column vector;

ε_1 is required preciseness: $\varepsilon_t = N(0, \sigma^2)$.

t = 1,...n, partial derivations $\frac{\partial^2 \theta}{\partial \theta_i . \partial \theta_j}$. t = 1,...n are continuous functions.

The original equation is expressed in the following form:

$$T = \frac{\ln v_c^4 + \frac{1}{\ln v_c}}{e^{\ln v_c}}. . \qquad (5)$$

Its graphic description can be found in Fig. 6.

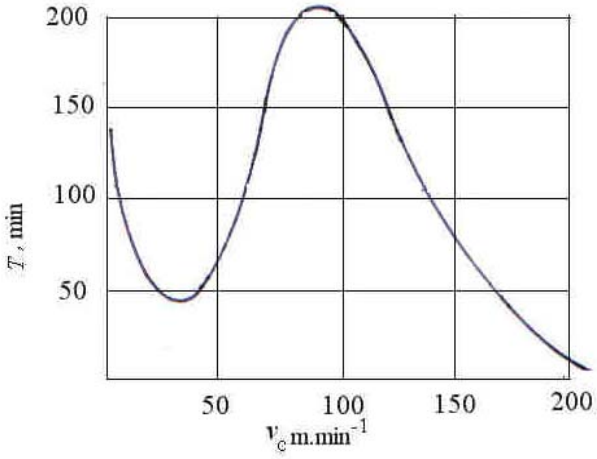

Fig. 6. Diagramme T = f(v_c) from analytic expression (conditions equal to those in Fig. 5

*Op*timal cutting speed can be determined by a derivation of the equation (5) according to v_c or its adjustment respectively (6) and setting a derivation equalling -1, i.e. constructing a tangent line to the curve under the angle – 45^0 [10, 11].

$$T = \frac{50}{e^{\ln v_c}}\left((\ln v_c)^4 + (\ln v_c)^{-1}\right) \qquad (6)$$

$$\frac{dT}{dv_c} = -1$$

There are two solutions. The first corresponds to maximum, the second to minimum (uninteresting) durability. After adjustment an equation is being solved:

$$50.\ln(v_c) + 50.v_c.\ln(v_c) - 200.\ln(v_c) + 50 + v_c.\ln(v_c) = 0 \qquad (7)$$

The equation has two solutions: $v_{c\,opt}$ = 100 m.min^{-1} and $v_{c\,min}$ = 22 m.min^{-1}. It is in interaction with Fig. 4.

4. SOME ESSENTIAL DEPENDENCES

In another experiment, the influence of the cut depth on the course of observed dependence has been followed. The diagramme is shown in Fig. 7.

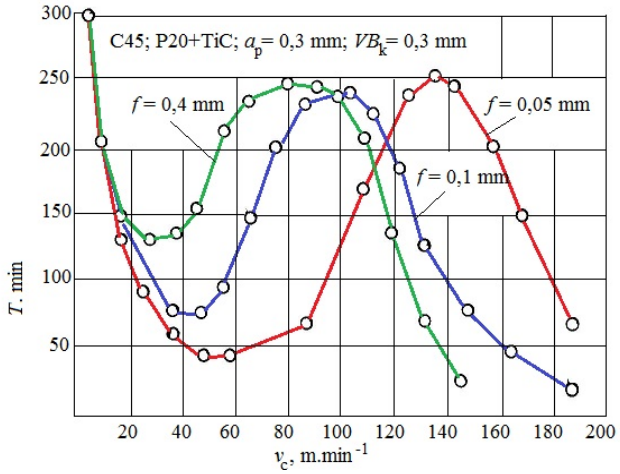

Fig. 7. Experimental curves of dependence T-v_c, obtained ar different shifts

It can be seen that with increased shift the curves move towards lower cutting speeds. At minimal cutting speeds they merge. Maximum values T do not differ, they increase minimally with the increase of shift.

In Fig. 8 there is an experimental course of dependence obtained when turning with ceramic tools.

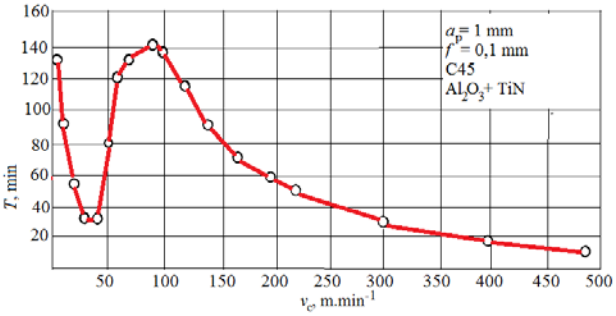

Fig. 8. Experimental dependence T-v_c, obtained when turning with coated ceramic tool

In comparison with machining made by sintered carbid, the values are shifted towards higher cutting speeds.

It is interesting to observe the course of T-v_c dependence at super high cutting speeds. Corresponding diagramme in double logarithmic system is shown in Fig. 9.

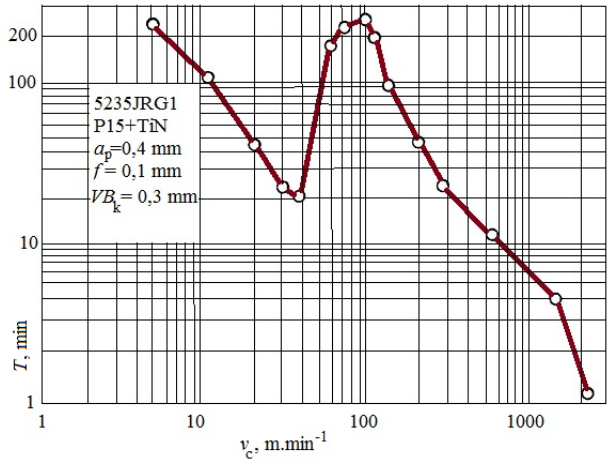

Fig. 9. Experimental dependence T-v_c in maximum obtainable range of cutting speeds

In comparison with previous dependences, a considerable decrease of durability at high cutting speeds can be seen. At $v_c \geq 100$ m.min tool durability reaches values of few seconds.

5. SUGGESTION OF RATIONAL EXPERIMENT

Finding out T-v_c dependence in wide range of cutting speeds requires a lot of time and material. A hypothesis can be formed that the same function can be fulfilled also by dependence $VB - v_c$, constructed after some machining time τ_s = const.

Such a dependence is shown in Fig. 10. It corresponds with continuous machining during the time of 20 min.

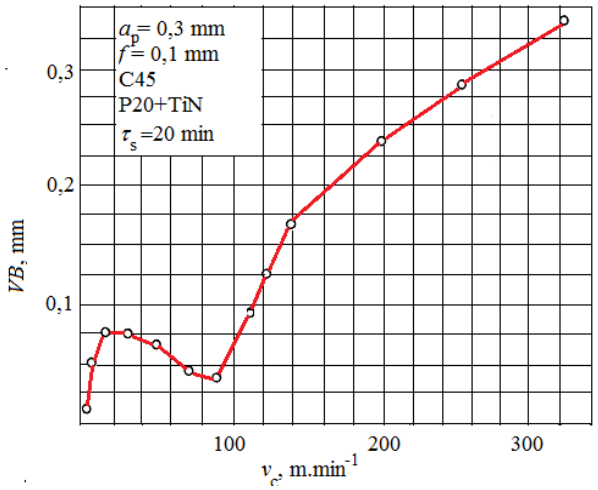

Fig. 10. Experimental course of dependence of wear on the back on cutting speed

As it can be seen, this dependence is in fact an inverse function of $T - v_c$ dependence from Fig. 4. Equally, as $T - v_c$ dependence enables to determine optimal cutting speed which provides the smallest intensity of tool wear.

6. CONCLUSION

Identification of dependence of tool durability on cutting speed for given pair cut – cutting material is of special importance in determination of cutting conditions, mainly cutting speed. Taylor solved this problem in a genius way as early as the beginning of the last century when high-speed cutting steel was invented. The development of new tool and cut materials requires modification of Taylor equation of constant durability as one of the conditions for effective material machining.

7. REFERENCES

[1] Taylor, F, W.: On the art of cutting metals. *Transaction of the ASME,* 28, November 1906, s. 31-279, 281-350

[2] Vasilko, K., Macurová, A.: Identifikácia rovnice $T = f(v_c)$ pre spekaný karbid, *Technologické inžinierstvo*, III, č.2/2006, s.8-11

[3] Bobrov, V.F., et all.: *Razvitije nauki o rezanii metallov*. Moskva: Mašinostrojenije, 1967, 414

[4] Buda, J., Békés, J.: *Teoretické základy obrábania kovov.* Bratislava: ALFA, 1967, 698 s.

[5] Granovskij, G. I., Granovskij, V. G.: *Rezanije metallov.* Moskva: vyššaja škola 1985, 304 s.

[6] Grzesyk, W.: *Podstawy skawania materialow metalowych.* Warszawa: Wydawnictwa, Naukowo-Techniczne, 1998, 380 s.,ISBN 83-204-2311-2

[7] Kalpakjian, S.: *Manufacturing engineering and technology.* New York: Addison Wesley Publishing Company, 1989, pp.1999, ISBN 0-201-12849-7

[8] Kovač, P., Mmiličič, D.: *Rezanje metala* Novi Sad: Univerzitet u Novom Sadu, 240 s., ISBN 86.899-0015-1

[9] Přikryl, Z., Musílková, R.: *Teorie obrábění.* Praha: SNTL, 1982, 235 s.

[10] Smar, E. F – Trent, E. M.: Distribution des temperatures dans les outils de couple utilizes pour l´ usinage du far, du titane et du nickel. *Bull. Cerlce étud. Métaux,* 1985, num. spac., 443-447. Discuss., 478-479.

[11] Weber, H., Loladze, T.N.: *Grundlagen des Spanens.* Berlin: VEB Verlag Technik, 1986, 255 s.

Authors: **Dr.h.c. prof. Ing. Karol Vasilko, DrSc.,** Technical University of Košice, Faculty of Manufacturing Technologies, 080 01 Prešov, Bayerova 1, Slovakia. E-mail: karol.vasilko@tuke.sk

http://doi.org/10.24867/JPE-2017-01-035

Journal of Production Engineering

Vol.20 No.1

JPE (2017) Vol.20 (1) Original Scientific Paper

Vrabeľ, M., Viňáš, J., Maňková, I., Brezinová, J., Savkovič, B., Kovač, P.

ANALYSIS OF TOOL WEAR PATTERNS IN ROUGH TURNING OF CHROMIUM HARDFACING MATERIAL

Received: 02 April 2017 / Accepted: 10 May 2017

Abstract: *Weld cladding represents one of the major remanufacturing technology employed in renovation of the worn machine tool components used in steel industry. Welded layer deposited on roller, originating from hot rolling mill improve its properties such as wear resistance, corrosion resistance and oxidation resistance in elevated temperatures. Machining processes must by applied on the part after the process of deposition to achieve desired dimensional accuracy and required surface integrity of the final parts. Dynamic mechanical loads acting on a cutting tool due to variable chip cross-section, nature of carbides, their size and distribution makes rough machining of martensitic materials difficult to cut, especially with the respect to rapid tool wear. This paper discusses and summarizes various cutting tool wear patterns occurring in turning of high content chromium hardfacing layers. The results show that tool edge and tip breakage, as well as flank wear are typicall features of failured carbide tool under the consideration.*

Key words: *rough turning, martensitic alloy, hardfacing, tool wear, remanufacturing.*

Analiza tragova habanja alata pri grubom struganju navarenog materijala hroma. *Navarivanje predstavlja jedanu od glavnih tehnologija reproizvodnje primenjenih u renoviranje potrošenih komponenti alatnih mašina koje se koriste u metaloprerađivačkoj industriji. Zavareni sloj deponovan na valjak, poreklom iz vruće valjaonice poboljšava osobine kao što su otpornost na habanje, otpornost na koroziju i otpornost na oksidaciju na povišenim temperaturama. Procesi obrade moraju da se primene na delu nakon procesa deponovanja i postizanja željene dimenzionalne preciznosti i potrebnog integriteta površine finalnih delova. Dinamičko mehanička opterećenja deluju na rezni alat zbog promenljivog poprečnog preseka strugotine, prirode karbida, njihove veličine i distribucije koja čini mašinsku obradu martenzitnog materijala teškog za obradu, posebno se javlja pojava brzog habanja alata. Ovaj rad razmatra i rezimira različite pojave habanja alata pri struganju koji se javljaju kod slojeva hroma posle navarivanje sloja. Rezultati pokazuju da se ivica alata i vrh krza, kao i da je pojas habanja tipične karakteristike za otkaza alata kod obrade tvrdog metala.*

Ključne reči: *grubo struganje, martenzitna legura, navarivanje, habanje alata, reproizvodnja.*

1. INTRODUCTION

The challenge for modern machining industries is to achievement of product quality in terms of superior surface integrity, high dimensional accuracy, less tool wear, reduced manufacturing cost, and lessened environmental impact [1]. Remanufacturing technology has been used in practice for production of new parts with overlays, which have specific properties, and for renovation of the abraded, fatigued and fractured surfaces. In some cases, the use of suitable overlay can save materials and energy, optimize the part's performance, and expand the service life [2]. High chromium hardfacing materials are widely used in industry due to its excellent wear resistance. The wear resistance of these materials is mainly achieved by a high hardness and high carbide contents and this makes machining of these hardfacings extremely difficult [3]. Hardfacing materials are often applied to a substrate by welding to provide wear-resistant layers several millimetres thick. Subsequent machining is usually necessary to achieve required standards of dimensional accuracy and surface finish [4]. During turning one of the important factors is tool wear whether it is soft or hard machining. Flank wear is the most important wear which will affect the smoothness of the product, cost of operation and performance [5]. Tool wear mechanisms are generally influenced by four phenomenons namely: abrasion, thermal softening, diffusion and notching at depth of cut and trailing edge [6]. Jawaid et al. [7] in their research concluded, that significant nose wear was the common failure mode observed at higher speed conditions in machining of martensitic stainless steel with coated carbides. Moreover, plastic deformation and chipping/fracture at the cutting edge were additional failure modes observed within experimental trials. In this work, tool wear patterns and wear mechanisms when machining high chromium hardfacing material with TiAlN coated carbide tools were investigated and discussed.

2. EXPERIMENTAL SETUP

The aim of the experimental testing within this study was to analyze and document cutting tool wear occurring in machining of martensitic hardfacing material. Worn continuous caster roll originating from hot rolling mill was used as a workpiece material, whose nominal diameter was about 150±0, 1 mm and total length was 1100 mm. The initial diameter was

increased to the value of approximately 160 mm by cladding process in which hardfacing overlay is applied on worn cylinder surface, see Fig. 1. Therefore, thickness of the overlay was about 5 mm.

Renovation process of the roll was as follows:

- turning (removing the worn surface layer),
- cladding process
- post weld heat treatment,
- turning (roughing),
- turning (finishing).

Fig. 1. Workpiece - roller after cladding process

Martensitic filler material Weldclad 3 (WLDC 3) with diameter of 2.4 mm from Corewire manufacturer was used in cladding process, see Tab. 1. This type of material is recommended by manufacturer for surfacing of continuous caster rolls by process of submerged-arc welding (SAW) with oscillating movement of the electrode tip. Recommended welding parameters are listed in Tab. 2. Cladding operation was performed using equipment from Lincoln Electric company. The welding process is illustrated in the Fig. 3 and Fig. 4, respectively.

C	Mn	Si	Cr	Ni	Mo	Nb	V
0.1	1	0.6	12.2	2.5	0.8	0.15	0.15

Table 1. Nominal All Weld Composition, wt% (WLDC3) [8]

Pre heat [℃]	Wire Feed Speed [in/min]	Amps [A]	Volts [V]
250	2,97	400	29
Travel speed [mm/min]	**Stick out [mm]**	**Bead Width [mm]**	**Overlap [mm]**
150	35	40	10

Table 2. Welding parameters [8]

Post weld heat treatment (warming up to 520 °C for 4 hours and holding time for 8 hours) was applied to soften hardened metal. According to annealing curve of the filler material in Fig. 2, it is possible to determine the weld hardness, which in this case was in the range 44 to 50 HRc.

The TOS SUI 63-80 universal lathe was used to machine the roll after welding. Important parameters of the employed machine tool are summarized in Tab. 3. The Korloy PSSNR3232-P19 cutting tool was used in rough turning operations and was clamped into Multifix tool holder, see Fig. 6. The whole experimental configuration is illustrated in Fig. 5. Main dimensions of the cutting insert CNMG160616 are shown in Fig. 7. Cutting material of the insert was TiAlN coated carbide (PC9030).

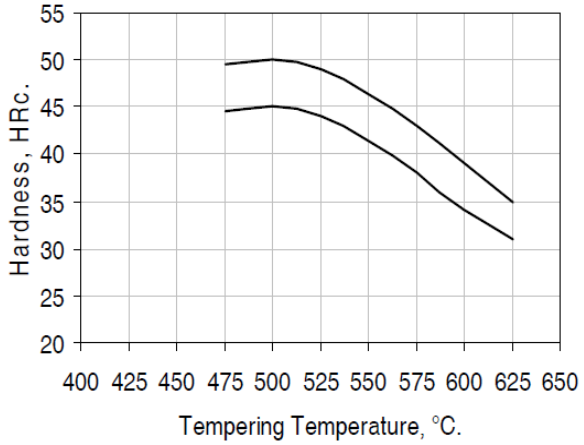

Fig. 2. Temper response [7]

Fig. 3. Cladding layer formation process

Fig. 4. Roller with hardfacing layer before machining process

Fig. 5. Experimental configuration (1 – 3 jaws chuck, 2 – workpiece, 3 – coolant supply, 4 – tailstock quill, 5 – tailstock assembly, 6 – cutting tool, 7 – tool post)

Swing diameter [mm]	Turning diameter [mm]	Stroke in Z axis [mm]	Bar capacity [mm]
630	350	1500	71
Main spindle power [kW]	**Speed range max.** [rpm]	**Workpie ceweight max.** [kg]	**Max. dimensions of the cutting tool (holder cross - section)**
15	1800	1600	40 x 32

Table 3. Selected parameters of the universal lathe TOS SUI 63 - 80

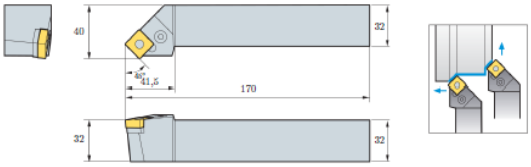

Fig. 6. Tool holder Korloy PSSNR3232-P19 [9]

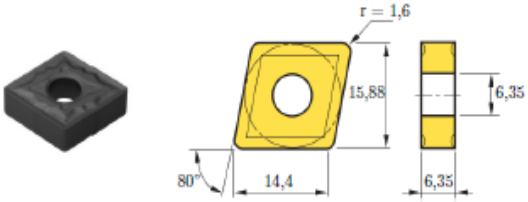

Fig. 7. Cutting insert Korloy CNMG160616-HS [9]

The welding parameters were used as those recommended by the manufacturers, except speed (160 mm·min^{-1}), volts (35 V) and wire feed speed (4,62 m·min^{-1}). The cutting conditions used for turning are compared with the recommended values by producer as listed in Tab. 4. An oil based cutting fluid of 8% concentration was used in machining tests.

	Recommended	Used
ap [mm]	2 - 6	4
f [mm/rev]	0.15 – 0.6	0.33
$\mathbf{v_c}$ [m/min]	70 - 180	40

Table 4. Cutting conditions employed within experimental trials

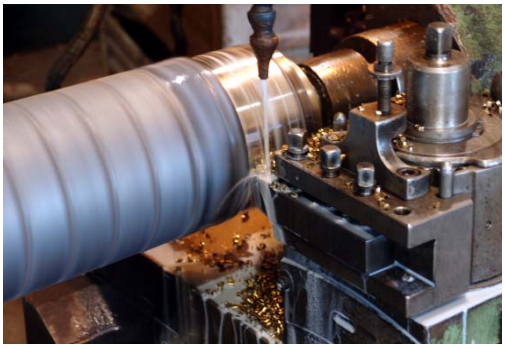

Fig. 8. Machining of the hardfacing layer

Side rake angle	Clearance angle	Side cutting edge angle	Back rake angle	Nose radius
- 8°	8°	45°	0°	1.6

Table 5. Cutting tool geometry

3. RESULTS AND DISCUSSION

During the experiments, several types of cutting tool wear have been observed when machining chromium hardfacing overlay (Fig. 10 - 12):

- flank wear,
- cutting edge chipping,
- notch wear,
- BUE formation,
- cutting edge and tool tip breakage/fracture.

As a predominant types of wear on the cutting wedge occurred:

- flak wear due to abrasive mechanism,
- main cutting edge an insert nose fracture
- built up edge formation
- notch wear corresponding to depth of cut.

Fig. 9. Roller after roughing operation

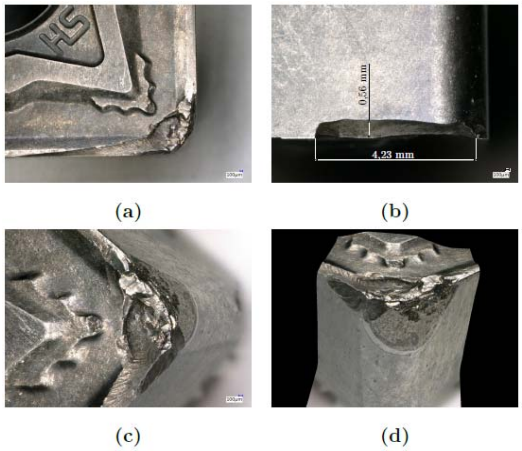

Fig. 10. Observed wear on the cutting insert No.1 (a, b – flank wear; c, d – nose chipping/breakage)

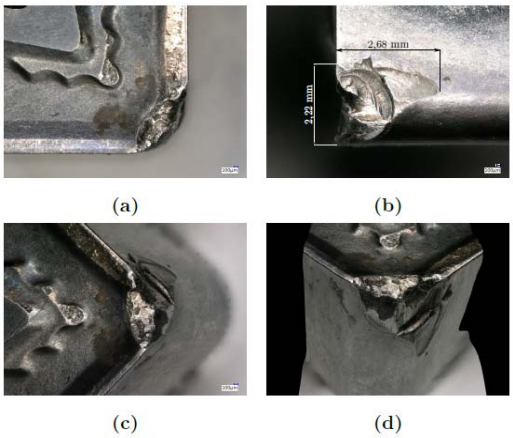

Fig. 11. Observed wear on the cutting insert No.2 (plastic deformation, built up edge – BUE, tip breakage)

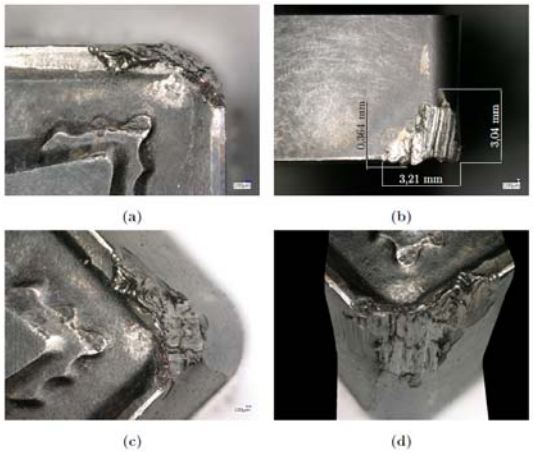

Fig. 12. Observed wear on the cutting insert No.2 (flank wear, built up edge)

4. CONCLUSION

Renovation of the continuous caster roll from hot mill used in steel industry was realised in this work. With regard to the welding and machining process parameters, tool wear of the coated carbide inserts in rough turning operation of the hardfacing layers (44 – 50 HRc) with martensitic structure was evaluated. A common wear of the cutting edge was fracture/ breakage, which means sudden change in the geometry of the cutting wedge. This type of failure is particularly undesirable because it is not possible to reliably predict its occurrence, thus risk of the workpiece damage is significant. Insert brittle failure is caused in discontinuous cutting due to the varying depth of cut, which results to dynamic mechanical loads. In addition, this kind of wear may be the result of vibration as a consequence of insufficient rigidity of the machine tool, workpiece and fixture employed. Abrasion is also very common and often occurring wear mechanism when machining hard materials. During metal cutting of martensitic hardfacing overlays is abrasion and tool damage caused by hard carbide particles distributed in the workpiece material. Tool fatigue fracture occurs as a result of cylindrical workpiece run-out, which also markedly contributes to variable mechanical load and therefore results in unstable cutting.

5. REFERENCES

[1] Liu, Z. Q., Zhao, P. F.: *An experimental and numerical analyses of hard turning AISI 440C Martensitic Steel*, Materials Processing and Technoogy, Vol. 1, pp. 1-11, 2010.

[2] Wang, M., Xu, B., Zhang, J., Dong, S.: *Experimental observations on surface roughness, chip morphology, and tool wear behavior in machining Fe-based amorphous alloy overlay for remanufacture*, International Journal of Advanced Manufacturing Technology, Vol. 67, pp. 1537-1548, 2013.

[3] Ren, X. J., R., Yang, Q. X., James, R. D., Wang, L.: *Cutting temperatures in hard turning chromium hardfacings with PCBN tooling*, Journal of Material Processing Technology, Vol. 147, pp. 38-44, 2004.

[4] Ren, X. J., James, R. D., Brookes, E. J., Wang, L.: *Machining of high chromium hardfacing materials*, Journal of Material Processing Technology, Vol. 115, pp. 423-429, 2001.

[5] Hasan, S., Thamizhmanii, S.: *Tool flank wear analysis of AISI 440C martensitic stainless steel by turning*, International Journal of Material Forming, Vol. 3, pp. 427-430, 2010.

[6] Thamizhmanii, S., Hasan, S.: *Effect of tool wear and forces by turning process on hard AISI 440 C and SCM 440 materials*, International Journal of Material Forming, Vol. 3, pp. 531-534, 2009.

[7] Jawaid, A., Olajire, K. A., Ezugwu, E. O.: *Machining of martensitic stainless steel (JETHETE) with coated carbides*, Journal of Engineering Manufacture, Vol. 1, pp. 769-779.

[8] WLDC 3 Material data sheet (2017). www.corewire.com

[9] KORLOY (2017). www.korloy.com

ACKNOWLEDGEMENT

This work was supported by the Slovak Research and Development Agency under the contract of bilateral project APVV SK-SRB-2016-0045 and research project APVV-16-0359 as well as the project VEGA 1/0434/15. Moreover, authors wish to thank Faculty of Mechanical Engineering of TU in Košice for the material and financial support within the project "Development of the intelligent monitoring system for zero defect production". We are also grateful to Ing. Juraj Ondaš from Corwire Surface Technology s.r.o who provided expertise that greatly assisted the research.

Authors: **Dr. Marek Vrabeľ., Assist. Prof. Dr. Ján Viňáš., Prof. Dr. Ildikó Maňková., Prof. Dr. Janette Brezinová.,** Technical University of Košice, Faculty of Mechanical Engineering, Deptartment of Manufacturing Technology and Materials, Mäsiarska 74, 040 01 Košice, **Assist. Prof. Dr. Borislav Savkovič., Prof. Dr. Pavel Kovač.,** University of Novi Sad, Faculty of Technical Sciences, Institute for Production Engineering, Trg Dositeja Obradovica 6, 21000 Novi Sad, Serbia, Phone.: +381 21 450-366, Fax: +381 21 454-495.

E-mail: marek.vrabel@tuke.sk
jan.vinas@tuke.sk
ildiko.mankova@tuke.sk
janette.brezinova@tuke.sk
savkovic@uns.ac.rs
pkovac@uns.ac.rs

http://doi.org/10.24867/JPE-2017-01-039

Journal of Production Engineering

Vol.20 No.1

JPE (2017) Vol.20 (1) Original Scientific Paper

Batinić, B., Rodić, D., Gostimirović, M., Kulundžić, N., Laković, N.

MONITORING OF THE DISCHARGE CURRENT BY HALL-EFFECT SENSOR

Received: 20 January 2017 / Accepted: 05 May 2017

Abstract: *The paper describes the use of Hall-effect sensor to monitor the discharge current in electrical discharge machining (EDM). The discharge current across the gap between tool and workpiece is fed into developed acquisition system for the recording of impulses during processing. The data acquisition system consists of a sensor that works on the Hall element principle and microcontroller which collects and sends data on the PC that performs data acquisition. Experimental results have shown that discharge current and discharge duration can be clearly classified even with different machining conditions. The integration of the acquisition system can substantially improve the performance of the EDM process trought the analysis of discharge current.*

Key words: *discharge current, Hall-effect sensor, microcontroller, electrical discharge machining.*

Praćenje procesa elektroerozivne obrade primenom Holovog senzora. *Ovaj rad opisuje primenu Holovog senzora za praćenje struje pražnjenja tokom elektroerozivne obrade. Struja pražnjenja koja se pojavljuje između alata i obratka prolazi kroz akvizicioni sistem i vrši se njeno praćenje i snimanje tokom procesa obrade. Akvizicioni sistem se sastoji od senzora koji radi na principu Holovog efekta i mikrokontrolera koji prosleđuje signal za prikaz i snimanje na računaru. Eksperimentalni rezultati pokazuju da struja pražnjenja i dužina trajanja impulsa mogu jasno klasifikovati pri različitim uslovima obrade. Integracijom sistema za akviziciju podataka omogućuje se analiza struje pražnjenja čime se postiže značajno poboljšati performance procesa elektroerozivne obrade.*

Ključne reči: *struja pražnjenja, Holov senzor, mikrokontroler, elektroerozivna obrada.*

1. INTRODUCTION

Electrical discharge machining is one of the most widely applied process for machining and shaping hard, fragile and difficult-cutting alloyed tool steel in the tool industry [1]. Material is removed by means of repetitive spark discharges across the gap between the tool and workpiece [2]. Hence, the discharge current, discharge duration and pause time of the tool-workpiece gap form EDM pulses, which are often used to monitor the EDM process.

Generally, pulses of discharge current can be classified into several types, that is, open, spark, arc, off, and short pulses. Therefore, it is very important to develop a monitoring technique to classify various EDM pulses. Several well-known monitoring techniques including a transistor-controlled power supply [3], short-time-Fourier-transform [4], an emitted radio frequency analyserand a data dependent system modelling analyser [5, 6] have been reported in the EDM literature. These monitoring techniques use the preset and classifying various EDM pulses. A system for acquisition of current and voltage signals is presented in [7], which provides easy and reliable storage of the data acquired under various machining conditions. The system is based on a commercial data-acquisition board which performs data acquisition at very high frequencies (up to 10 MSamples/s). As part of a more complex system for detection of parameters that influence efficiency of the machining process, a virtual instrumentation system (VIS) is developed in [8], which measures relevant magnitudes, related to the occurrence of an increase in peak current, as well as increases and/or decreases in ignition delay time. The proposed real time acquisition system containes expensive NI6115 acquisition card, with 12-bit resolution analog channels and sampling rate of 5 Msamples/s. Systems for data acquisition described in the above mentioned papers represent effective solutions, however using expensive equipment.

In order to improve the machining efficiency, stability and quality the main objective of this paper is to create a low-cost monitoring system based on the Hall effect and microcontroller. The monitoring system is designed to monitor the performance of discharge current.

2. PRINCIPLE OF DISCHARGE CURRENT MEASUREMENT

Current impulses coming from the machining center are recorded using a sensor based on the Hall element. Hall element consists of a thin sheet of semi-conducting material through which a current is passed. The output connections are perpendicular to the direction of current. When a perpendicular magnetic field is present, a potential difference (voltage) across the output is created and it is proportional to the applied magnetic field. This potential difference is very small, on the order of μV, thus additional amplification is required in order to obtain desired voltage levels.

Fig.1 shows the current flow through the sheet. When no magnetic field is present, current distribution is uniform and no potential difference is seen across the output. When a perpendicular magnetic field is present, a Lorentz force is exerted on the current. This force

disturbs the current distribution, resulting in a potential difference (voltage) across the output.

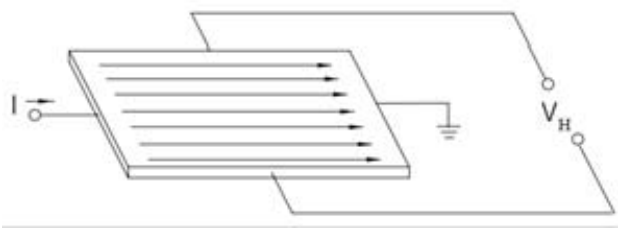

Fig. 1. Hall's element [9]

This voltage is the Hall voltage (VH). Hall element combined with an appropriate interface forms the sensor that utilizes Hall effect.

$$V_H = I \times B \quad (1)$$

Hall voltage is equal to the cross product of current intensity I and magnetic field B (1). This voltage is on the order of μV. The necessary signal amplification is provided by the integrated on-chip differential amplifier [9]. The sensor used in this paper provides output voltage that is proportional to the applied magnetic field. The sensed magnetic field can be either positive or negative. As a result, the output of the amplifier will be driven either positive or negative, thus requiring both plus and minus power supplies. To avoid the requirement for two power supplies, a fixed offset or bias is introduced into the differential amplifier. The amplifier shown in Figure 2. must be a differential amplifier so as to amplify only the potential difference the Hall voltage.

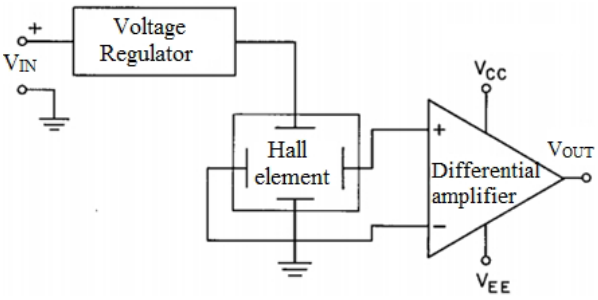

Fig. 2. Halls's sensor inside chipset [9]

This offset value appears on the output when no magnetic field is present and is referred to as a null voltage. When a positive magnetic field is sensed, the output increases above the null voltage as illustrated in Fig. 3.

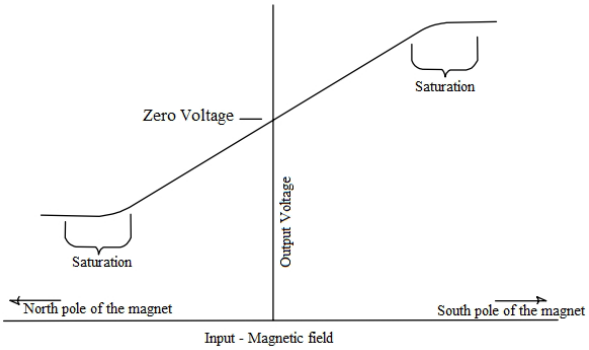

Fig. 3. Output signal of sensor vs. magnetic field [9]

The output of the amplifier cannot exceed the limits imposed by the power supply. The amplifier will begin to saturate before the limits of the power supply are reached. Hence, the saturation takes place in the amplifier, not in the Hall element. Therefore, large magnetic fields will not damage the Hall effect sensor, but rather drive it into saturation.

3. ACQUISITION SYSTEM

Hardware of the measuring device consists of a current measuring module based on the Hall effect ACS712 and a microcontroller dsPIC30F4012 whose role is to process the measured data and provide communication with PC. ACS712 sensor is selected because of its operating range (up to 30A), and the microcontroller dsPIC30F4012 was chosen because its integrated A/D converter has sufficient resolution to process impulses coming from the EDM device. It is important to point out that the electronic module that performs acquisition is galvanically isolated from the EDM device, hence there is no danger from occurrence of highcurrent or high-voltage impulses.

The current measuring module is connected in series with the electrode. Analog signal from the sensor module ACS712 is converted using an integrated A/D converter. Then this information is buffered within certain timeframe and then forwarded to the PC using serial RS232 communication, where it is further processed and stored using appropriate software. A/D converter is based on the successive approximation architecture (SAR) and allows maximum sample rate of 1 Msps (using 10-bit resolution). In order to further increase the sample rate, reference voltages are provided to the converter, which limit the expected voltage from zero voltage to the saturation voltage of the sensor. The machining center with the connected measuring system consists: microcontroller, current measuring sensor, interface for communication with PC and software for data acquisition.

3.1 Algorithm of microcontroller firmware

Microcontroller code is written in the C programming language, and the corresponding algorithm is shown in Fig. 4. In the initialization phase, the clock frequency is set and the RS232 serial communication and A/D converter are initialized. The speed of RS232 serial communication is set to 525 kbps. A/D converter generates interrupt routine after each conversion and stores the data in the buffer.

Programme is executed in an infinite loop, where it is checked if the buffer with the data from A/D conversion is ready, and if the condition is met the buffered data is sent to PC using serial communication after which the buffer is reset. Programme then resumes execution in the loop.

3.2 PC software

The microcontroller forwards the data to the PC with processing software developed on the LabVIEW platform. The application consists of the front panel presented in Fig. 5 and the block diagram, which controls the operation of the application in the

background by receiving data from the serial port and calculating the intensity of current impulses based on the data from the A/D converter. This calculation is not performed directly on the microcontroller in order to save time for additional conversions.

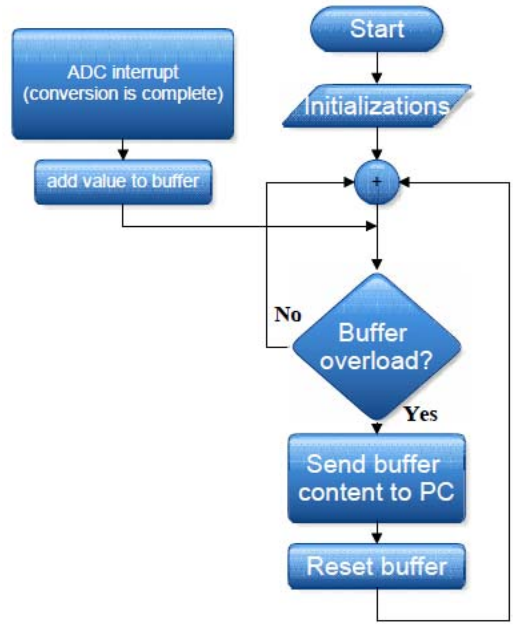

Fig. 4. Firmware Algorithm of Microcontroller

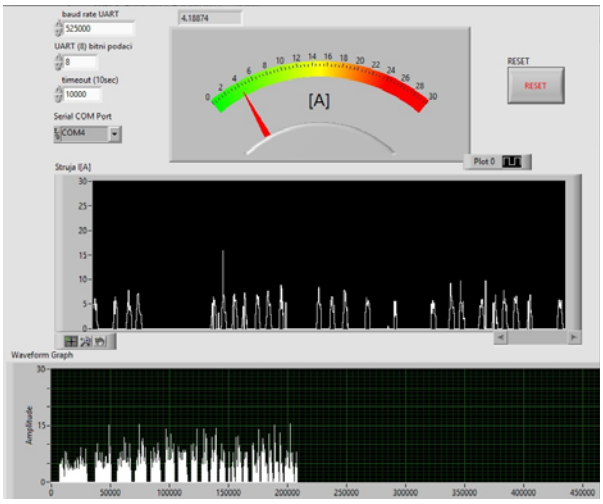

Fig. 5. Interface for communication with PC

Data about current impulses is presented on the display using analog scale and graphically using current view and continual view. After the processing is done, the data is exported in an excel fire for further analysis.

4. RESULT AND DISCUSSION

The experiments were performed on a CNC EDM SP1U machine. Rectangular graphite was used for an electrode to erode a workpiece of ductile iron DI 400. The discharge current between the tool and workpiece was directly measured from the EDM machine.

The most important electrical pulse parameters of EDM are discharge current and pulse duration [10]. These parameters directly influence the machining performance, and that is why their monitoring is important.

Experimental results have shown that the developed system can correctly for recording various EDM pulses. Several examples are shown in the following.

The peak current is the maximum intensity of the current passing through the electrodes for a given pulse. The average peak discharge current is the mean of the peak discharge current values measured in a period of time. It is known that the discharge energy is influenced by the discharge voltage, discharge current, and pulse duration. The discharge current directly impacts the discharge energy [11]. If the discharge current oversteps the limit for the given machining conditions like on figure 8, the stability of the impulse discharge will be threatened. This process initiates continuous current flow and occurrence of arcing or short circuiting. This lengthens the time required to deionize the discharge channel, thus reducing the efficiency of EDM. In the other words, the deionization of the discharge zone would be affected, resulting in either low or uncontrolled output machining caracteristcs. The pulse duration is another parameter which allows direct control of discharge energy. However, here too the independent regulation of process parameters is limited. It is known from experience that pulse duration must be limited for a particular discharge current. Otherwise, electric arcing occurs, damaging both the tool and workpiece.

Figure 6 shows the discharge current 6A and discharge duration 12 µs. The average discharge current pulse duration can be used to distinguish between different types of discharges. It was evaluated for all the current pulses as the distance between current pulse end time and current pulse start time identified as shown in Fig. 7. Figure 7 also show an example of discharge stability. Unstable machining is show on figure 8.

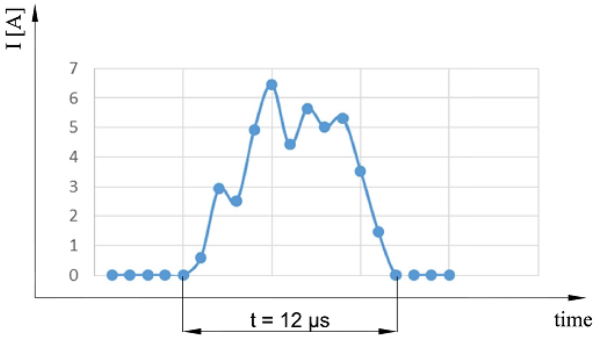

Fig. 6. Impulse measured during EDM machining

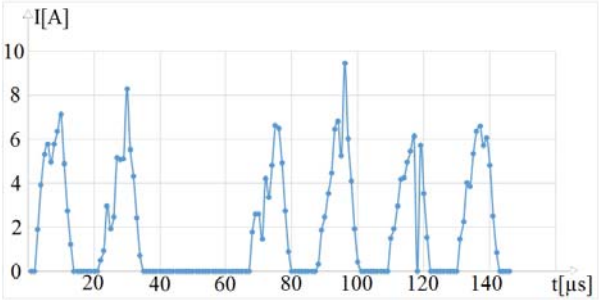

Fig. 7. An example of discharge stability

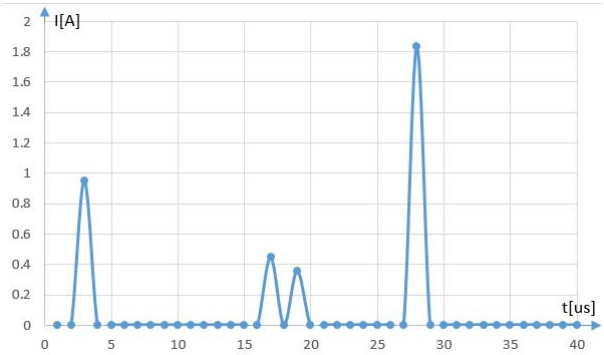

Fig. 8. An example of discharge unstability

5. CONCLUSION

In this paper a low-cost system for acquisition of current impulses measured on the basis of Hall sensor is presented. The acquisition system is paired with a machining center. The machining center does not provide functionality of detailed acquisition of current impulses, hence not offering detailed insight in the machining process. The proposed acquisition system has proven to provide a reliable way of monitoring the result of the machining process at a low-cost by means of data acquisition. The obtained data enables us to observe if the result of the machining process is in accordance with the parameters provided by the manufacturer. Furthermore, the data is stored for future analysis. A potential improvement of this methodology is the realization of a pulse classification algorithm based on artificial intelligence.

6. REFERENCES

[1] J. Schey, Introduction to Manufacturing Processes-3rd, New York: McGraw-Hill, 2000.

[2] H. Liu, Y. Tarng, Monitoring of the electrical discharge machining process by abductive networks, The International Journal of Advanced Manufacturing Technology, 13 (1997) 264-270.

[3] M.-T. Yan, H.-T. Chien, Monitoring and control of the micro wire-EDM process, International Journal of Machine Tools and Manufacture, 47 (2007) 148-157.

[4] S. Yu, B. Lee, W. Lin, Waveform monitoring of electric discharge machining by wavelet transform, The International Journal of Advanced Manufacturing Technology, 17 (2001) 339-343.

[5] D. Dauw, R. Snoeys, W. Dekeyser, Advanced pulse discriminating system for EDM process analysis and control, CIRP Annals-Manufacturing Technology, 32 (1983) 541-549.

[6] S. Pandit, T. Mueller, Verification of on-line computer control of EDM by data dependent systems, J. Eng. Ind., 109 (1987) 117-121.

[7] E. Portillo, I. Cabanes, M. Marcos, D. Orive, J.A. Sánchez, Design of a Virtual-Instrumentation System for a Machining Process, IEEE Transactions on Instrumentation and Measurement, 56 (2007) 2616-2622.

[8] I. Cabanes, E. Portillo, M. Marcos, J. Sánchez, On-line prevention of wire breakage in wire electro-discharge machining, Robotics and Computer-Integrated Manufacturing, 24 (2008) 287-298.

[9] Honeywell, "MICRO SWITCH Sensing and Control", Freeport, Illinois 61032, 005715-2-EN IL50 GLO.

[10] H. Kansal, S. Singh, P. Kumar, Performance parameters optimization (multi-characteristics) of powder mixed electric discharge machining (PMEDM) through Taguchi's method and utility concept, (2006).

[11] M. Gostimirovic, P. Kovac, M. Sekulic, B. Skoric, Influence of discharge energy on machining characteristics in EDM, Journal of Mechanical Science and Technology, 26 (2012) 173-179.

ACKNOWLEDGMENT

This paper is the result of the research within the project TR 35015 financed by the Ministry of Science and Technological Development of the Republic of Serbia.

Authors: **Research Associate Branislav Batinic MSc, Research Associate Dragan Rodć MSc, Professor Marin Gostimirović PhD, Research Associate Nenad Kulundžić MSc, Nikola Laković MSc.**
University of Novi Sad, Faculty of Technical Sciences, Trg Dositeja Obradovica 6, 21000 Novi Sad, Serbia, Phone.: +381 21 450-366, Fax: +381 21 454-495.
E-mail: banebb@uns.ac.rs,
rodicdr@uns.ac.rs
maring@uns.ac.rs
kulundzic@uns.ac.rs,
lakovicn@uns.ac.rs.

http://doi.org/10.24867/JPE-2017-01-043

Journal of Production Engineering

Vol.20 No.1

JPE (2017) Vol.20 (1) Original Scientific Paper

Sodhi, H S.

PARAMETRIC OPTIMIZATION OF ELECTRIC DISCHARGE MACHINE USING RESPONSE SURFACE METHOD

Received: 09 December 2016 / Accepted: 01 March 2017

Abstract: *Present work has been done for the parametric optimization of process parameters such as discharge current, pulse on time, gap voltage and duty cycle on a Electric Discharge Machine for high speed steel for getting maximum material removal rate and at the same time to get minimum surface roughness. Experiments has been performed an a matrix formulated by Response Surface Method and further analysis work has been done by using regression test and ANOVA to get the optimized range of parameters to get the desired results on EDM machine.*
Key words: *Electric Discharge Machine, surface roughness, optimization.*

Parametarska optimizacia mašine za elektroerozionu obradu pomoću metode odzivne površine. *U ovom radu je urađena optimizacije parametara na mašini kao što su struje pražnjenja, puls u vremenu, napon prekida i radnog ciklusa na mašina za elektroerozionu obradu za obradu brzoreznog čelika u cilju dobijanja maksimalne količine skidanja materijala i istovremeno dobijanje minimalne površinske hrapavosti. Eksperimenti su izvedeni prema matrici metode odziva površine, a dalje analize su urađene pomoću testa regresije i ANOVA analize da se dobije optimalni opseg parametara, odnosno da bi se dobili željeni rezultati na EDM mašini.*
Ključne reči: *mašina za elektroerozionu obradu, hrapavost površine, optimizacija.*

1. INTRODUCTION

Electric discharge machine is electro-warm machining process, in which electric vitality is utilized to produce the start between the work piece and terminal. The material is expelled because of warm vitality which is created by the electric start. Electric release machine is utilized for a machining of high quality temperature safe combinations and the material which are hard to machine in other machining forms. In EDM, since there is no immediate contact between the work piece and the cathode, consequently there are no mechanical powers existing between them. Any kind of conductive material can be machined utilizing EDM independent of hardness or sturdiness of material.

Each assembling industry expect the most astounding material evacuation rate and at same time least device wear rate and least surface harshness. Keeping in mind the end goal to accomplish that it is critical to streamline the EDM procedure parameters. The procedure parameters of EDM which impact these reactions are release current, voltage, beat on-time, beat off-time, obligation cycle, circular segment crevice, breadth of terminal, overcut, ecological conditions, coolant utilized, administrator abilities and so forth. In the present work, the advancement of four EDM handle parameters like release current, beat on –time, voltage and obligation cycle for high Speed steel (AISI-M2) is finished by performing tests utilizing reaction surface method (RSM) with a specific end goal to amplify the material expulsion rate and at same time minimize the apparatus wear and minimize the surface unpleasantness. After the improvement results are evaluated through ANOVA test.

2. ELECTRIC DISCHARGE MACHINE

The universe of metal working has made considerable progress. Previously, smithy were compelled to sledge bits of metal, yet in this new age, we have a fast procedure to shape the metal to our plan. So EDM is one of them assembling process where coveted shape is accomplished utilizing sparkles or electrical release. Fundamentally there are two sorts of EDM machine: 1. Die sinking EDM

2. Wire EDM

In this trial work the machine utilized is electronica's elecktra puls PS 50 which is bite the dust sinking EDM.

Fig. 1. Electronica’s elecktra puls PS 50 electric discharge machine

3. PROCESS PARAMETERS FOR EDM

In this experiment, the effect of following process parameters have been taken into account to measure the material removal rate, tool wear rate and surface roughness.

3.1 Discharge Current

It is one of most critical machining parameter in EDM in light of the fact that it identifies with power utilization while machining. The release current is specifically corresponding to material evacuation rate. Higher current will enhance material evacuation rate yet at the cost of hardware wear rate and surface harshness. It is measured in amp permitted to per cycle.

3.1 Pulse-On-Time

It is span of time in small scale seconds(μs) when the current is permitted to stream per cycle. Material evacuation rate is additionally specifically relative to measure of vitality connected amid this on-time. This vitality is truly controlled by the pinnacle current and length of on-time.

3.3 Gap Voltage

It is the open circuit voltage which is connected between the terminals. The release voltage de-ionizes the dielectric medium, which rely on cathode hole and the quality of di-electric, preceding stream of current. Once the present stream begin, the open circuit voltage drops and balance out the anode hole. It is fundamental element that impacts the start vitality, which is in charge of higher material expulsion rate.

3.4 Duty Cycle

It is the proportion of heartbeat on-time and the beat time frame. Obligation cycle is characterized as a condition given beneath:

$$Tau = \frac{ton}{ton + toff} \times 100 \qquad (1)$$

At higher *Tau*, the spark energy is supplied for longer duration of the pulse period which resulting in higher machining efficiency.

4. INTRODUCTION TO RESPONSE SURFACE METHOD (RSM)

Response surface methodology (RSM) is gathering of scientific and factual system for exact model building. The goal is to upgrade the a response (output factors) which is impacted by a few free factors (input factors). Reaction surface system involves an assortment of strategies for investigating for ideal working conditions through test techniques. Ordinarily, this includes doing a few trials, utilizing aftereffect of one trial to give bearing to what to do next. This next activity could be to center the trial around an alternate arrangement of conditions, or to gather more information in current test area to fit a higher request demonstrate or affirm what appears to have found. The use of RSM is likewise planned to lessen the costs of other troublesome expository methods (like: limited component technique, or CFD investigation and so on.) and their related numerical noises. The issue can be approximated with smooth elements of focal composite outline of RSM that enhance the joining of the advancement procedure since they diminish the impact of commotions and characteristic blunders, generously. The reactions can be spoken to graphically, either in three dimensional space or as shape plots that further picture connection of reaction surfaces with information factors all the more obviously.

5. LITERATURE REVIEW

Lee et al. [1] have done test and found that the aftereffects of MRR and surface harshness increments with the estimations of heartbeat current however after certain esteem SR and MRR decrease due to development of electric plasma. Bhattacharyya et al. [2] has created scientific models for surface harshness, white layer thickness and surface split thickness in light of reaction surface philosophy (RSM) approach using test information. M.M. Rahman et al. [3] explored the impact of the pinnacle current and heartbeat term on the execution qualities of the EDM. I. Rajurkar et al. [4] did comes about which demonstrated that the force and heartbeat time variable were the most essential if there should arise an occurrence of SR while the obligation cycle component was not noteworthy by any stretch of the imagination. The power consider was again compelling instance of TWR. The imperative calculates instance of MRR were the force took after by obligation cycle and the beat time. Bhattacharyya.B et al. [5] explored the machining of tungsten carbide with copper tungsten as anode. The full factorial outline of examinations was utilized for breaking down the parameters. In the event of SR, the vital elements were voltage and heartbeat off time while current and heartbeat on time were not huge. curre D. Kanagarajan et al. [6] found that SR of work piece and terminal were impacted by current and heartbeat on time, higher estimations of these parameters expanded the surface unpleasantness. Rahman M.M et al. [7] arrived at the accompanying conclusions: with increment in pinnacle current MRR, TWR and ROC expanded altogether in a nonlinear manner; MRR and ROC expanded with the expansion in heartbeat on time and hole voltage was found to have some impact on the three reactions. Chen. S. L et.al [8] concentrated the impacts of EDM parameters on surface qualities of a sort of tungsten carbide. They have reasoned that MRR and surface unpleasantness of the work piece are specifically corresponding to the release current power. Puertas I.,. [9] utilized non-overwhelmed sorting hereditary calculation (NSGA-II) to acquire a Pareto ideal arrangement of info factors in an exchange off way. Sodhi H S etal Discussed that in present manufacturing scenario, quality and quantity are two challenging aspects to be looked upon. Quality is important according to customer point of view, whereas quantity is required for the industry to maximise profit earnings. For the sustainability of machining industry, there should be an optimised path which should be followed to satisfy not only the aspect of higher material removal rate (MRR) but also to achieve lower surface roughness (Ra) simultaneously. MRR and Ra are inversely related machining characteristics and in case of non-ferrous materials these mainly depends upon input variables like: cutting speed, feed and depth of cut. Therefore in this study, optimisation of multi-response CNC turning parameters has been done by using central composite design technique of ‘response surface methodology’ (RSM) through Minitab 16 Software. Further statistical testing of results is verified through ANOVA. The paper discusses an experimental study on Al-7020

alloy turned with un-coated carbide tip tool with a 'CNC TL-250 turner' that has a wide application in aerospace, machine tools and automobiles sector. It focuses more on software-based approach for implementing RSM on machining parameters, in contrast of conventional methods [10].

6. RESEARCH GAP

The high speed steel is most ordinarily utilized cutting instruments and they are equipped for cutting the metal at much higher rate than the carbon apparatus steel and keeps on cutting and hold its hardness notwithstanding when the purpose of hardware is warmed to a low red temperature. M2 review of HSS have great wear resistance, durability, machinability and its hardness is same as that of T1 review of HSS. It is normally used to produce an assortment of apparatuses, for example, boring tools, taps and reamers. Presently in this investigation the impact of release current, beat on time, crevice voltage and obligation cycle on the material expulsion rate, instrument wear rate and surface harshness can be gotten to subsequent to surveying the writing. Keeping in mind the end goal to improve the test comes about, utilization of Design of Experiments (full factorial or halfway), Taguchi's Method, RSM, Finite Element Method and so on are adequately found in writing. The impact of every parameter were decide for the material, instrument and machining operations. A portion of the analyst set up the relationship between the reliant and autonomous machining parameters through this relapse models. In the wake of spurring from above review, an exertion has been made to bring the advancement of essential info parameters of the electric release machine (EDM) for rapid steel M2 review (AISI-M2) while machining with electronica's elecktra puls PS 50 which is kick the bucket sinking EDM.

7. PROCESS VARIABLES AND THEIR LIMITS

Process parameters has been decided by referring. Experimentations has been done by considering the following levels of process variables. These Table 1 process variables and their limits.

Parameters	Lower limit	Upper limit
Discharge current (Amp)	4	40
Pulse-on-time (µsec)	100	250
Gap voltage (V)	3	6
Duty cycle(%)	1	11

Table 1. Process variables and their limits

StdOrder	RunOrder	PtType	Discharge current (Amp)	Pulse on time (µs)	Gap voltage (volt)	Duty cycle (%)	TWR (gm/min)
13	1	1	4	100	6	11	0.012
26	2	0	22	175	4.5	6	0.008
16	3	1	40	250	6	11	0.002
15	4	1	4	250	6	11	0.004
18	5	-1	58	175	4.5	6	0.016
5	6	1	4	100	6	1	0.002
10	7	1	40	100	3	11	0.032
19	8	-1	22	25	4.5	6	0.006
25	9	0	22	175	4.5	6	0.004
8	10	1	40	250	6	1	0.004
29	11	0	22	175	4.5	6	0.006
21	12	-1	22	175	1.5	6	0.008
9	13	1	4	100	3	11	0
20	14	-1	22	325	4.5	6	0
24	15	-1	22	175	4.5	16	0.008
1	16	1	4	100	3	1	0
7	17	1	4	250	6	1	0.002
2	18	1	40	100	3	1	0.008
14	19	1	40	100	6	11	0.032
6	20	1	40	100	6	1	0.012
22	21	-1	22	175	7.5	6	0.006
30	22	0	22	175	4.5	6	0.008
31	23	0	22	175	4.5	6	0.018
28	24	0	22	175	4.5	6	0.008
12	25	1	40	250	3	11	0.002
4	26	1	40	250	3	1	0.008
3	27	1	4	250	3	1	0
23	28	-1	22	175	4.5	-4	0.008
27	29	0	22	175	4.5	6	0.006
17	30	-1	-14	175	4.5	6	0.002
11	31	1	4	250	3	11	0.004

Table 2. Orthogonal matrix of response surface method

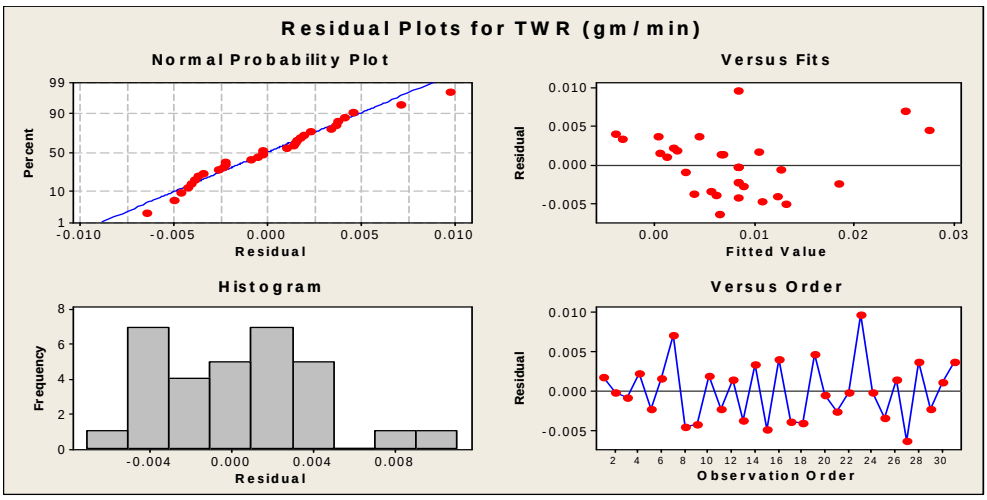

Fig. 2. data normality test for tool wear rate (TWR)

8. ORTHOGONAL MATRIX OF RSM

The investigations have been led utilizing reaction surface technique, trial outline which comprises of 31 blends of release current, beat on-time, voltage and obligation cycle. The analyses are executed according to the orthogonal grid produced by reaction surface technique with four variables and two levels while 0 blocking and reproduce estimation of 1 (allude table 2 for outlined analysis) of experimental order as far as second response tool wear rate (TWR) is concerned.

Reaction surface approach for instrument wear rate has been connected at 95% certainty, so all variables and their cooperations having p (likelihood) esteem under 0.05 will be factual huge for apparatus wear rate (TWR) and must be further dealt with. Allude table 4. for more detail of measurable examination of RSM for TWR. As p qualities are more than 0.05 for (hole voltage ×gap voltage) and (crevice voltage ×duty cycle) and consequently can be disregarded amid enhancement of TWR on account of their unimportant explanatory impact. Coefficients speak to the relative effect of every component and its cooperations on TWR that have been dissected at 96.96% R-sq and R-sq (balanced) esteem.

Term	Coef	SE Coef	T	P	Significant/ Not significant
Constant	0.008286	0.001956	4.236	0.001	Significant
Discharge current(Amp)	0.008667	0.002113	4.102	0.001	Significant
Pulse on time(µs)	-0.007000	0.002113	-3.314	0.004	Significant
Gap voltage(volt)	0.001000	0.002113	0.473	0.046	Significant
Duty cycle(%)	0.004333	0.002113	2.051	0.037	Significant
Dis. current*dis. Current	0.001381	0.003871	0.357	0.072	Significant
Pulse on time*Pulse on time	-0.004619	0.003871	-1.193	0.025	Significant
Gap voltage*Gap voltage	-0.000619	0.003871	-0.160	0.875	Not Significant
Duty cycle(%)*Duty cycle(%)	0.000381	0.003871	0.098	0.023	Significant
Discharge current*pulse on time	-0.016000	0.005175	-3.092	0.007	Significant
Discharge current*gap voltage	-0.004000	0.005175	-0.773	0.045	Significant
Discharge current*duty cycle	0.005000	0.005175	0.966	0.034	Significant
Pulse on time*Gap voltage	-0.005000	0.005175	-0.966	0.084	Significant
Pulse on time*Duty cycle	-0.014000	0.005175	-2.706	0.016	Significant
Gap voltage(volt)*Duty cycle(%)	0.002000	0.005175	0.387	0.704	Not Significant
R-Sq = 96.96%	R-Sq(pred) = 90.26%		R-Sq(adj) = 93.46%		

Table 3. statics for tool wear rate (TWR)

9. GRAPHICAL INFERENCES FOR TOOL WEAR RATE (TWR)

The software has deduced the result in graphical form also. The figure 3 highlights the one factor at a time effect on tool wear rate response. The first plot of figure 3 represents the increase in tool wear rate with rise of discharge current. The tool wear rate is directly proportional to the discharge current. If discharge current increases then tool wear rate is also increases with respect to it and if discharge current decreases then tool wear rate is also decreases. The second plot of figure is TWR versus pulse on time. In this figure the tool wear rate is increased firstly with rise in pulse on time upto 100µs and then after 100µs the tool wear rate start decreasing with increase in pulse on time and it become very low at 325µs. The third plot of figure is TWR versus gap voltage.

The gap voltage does not have much effect on the tool wear rate. First when gap voltage increases upto 3

volt the TWR decreases and after that if gap voltage is increases upto 6volt then the TWR start increases and in last when gap voltage increases upto 7.5 volt then TWR again become start decreasing and become least at 7.5volt. The fourth plot is TWR versus duty cycle which is very important as duty cycle is major parameter of EDM. In this plot TWR first decreases with increase in duty cycle upto 1% and after that TWR start increases rapidly from 1% to 11%. And become maximum at 11%.

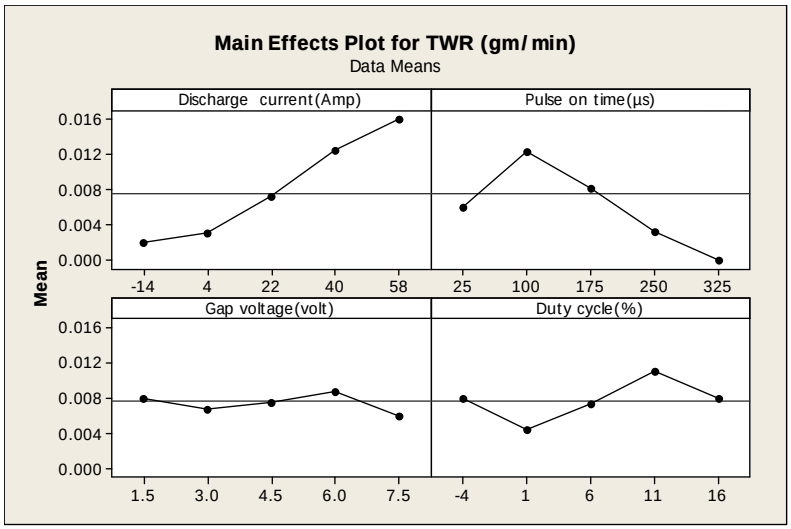

Fig. 3. main effect plots for TWR

10. CONCLUSION

In optimization of machining parameters generally taguchi's method is used but in the present case central composite design of response surface methodology (RSM) is being applied on electric discharge machine parameters for AISI-M2 high speed steel, successfully. The optimized result obtained by RSM are closely matched with actual one and further verified by ANOVA. The best combination of EDM parameters for AISI-M2 high speed steel are; discharge current 20.19 (Amp), pulse on time 221.96 (µs), gap voltage 3.56 (Volt) and duty cycle 16 (%). It has been also found that individual parameters like discharge current and duty cycle are more influencing than other parameters like gap voltage and pulse on time.

11. REFERENCES

[1] S. H. Lee, X. P. Li,"Study of the effect of machining parameters on the machining characteristics in electrical discharge machining oftungsten carbide", J. Mater. Process Technol., 115 (2001), pp. 344-358.

[2] B. Bhattacharyya, S. Gangopadhyay, B. R. Sarkar,"Modelling and analysis of EDMed job surface integrity", Journal of Materials Processing Technology, Vol. 189, pp. 169-177, 2007.

[3] Rahman M.M., Khan M.A.R., Kadirgama K., Noor M.M., Bakar R.A.,Experimental Investigation into Electrical Discharge Machining of Stainless Steel 304, Journal of Applied Sciences, 11: pp. 549-554.

[4] K. P. Rajurkar, S. M. Pandit,"Quantitative expressions for some aspects of surface integrity of electro discharge machined components", Journal of Engineering for Industry, vol. 106, No. 2, pp. 171–177, 1984.

[5] B. Bhattacharyya, S. Gangopadhyay, B. R. Sarkar,"Modelling and analysis of EDMed job surface integrity", Journal of Materials Processing Technology, Vol. 189, pp. 169-177, 2007.

[6] D. Kanagarajan, R. Karthikeyan, K. Palanikumar, J. Paulo Davim, "Optimization of electrical discharge machining characteristics of WC/Co composite using non-dominated sorting genetic algorithm (NSGA-II)", Int. J. Adv. Manuf. Technol., 36 (2008), pp. 1124-1132.

[7] Rahman M.M., Khan M.A.R., Kadirgama K., Noor M.M., Bakar R.A.,Experimental Investigation into Electrical Discharge Machining of Stainless Steel 304, Journal of Applied Sciences, 11: pp. 549-554.

[8] Chen . S. L, Hsi eh . S. F, Li n . H. C, Li n. M. H, Huang J.S,"Electrical discharge machining of TiNiCr and TiNiZr ternary shape memory alloys", Materials Science and Engineering A 445-446 (2007) 186-492.

[9] Puertas I., Luis C.J., Alvarez L.,"Analysis of the influence of EDM parameters on surface quality, MRR and EW of WCCo", Journal of Materials Processing Technology, 153-154 (2004), pp. 1026-1032.

[10] Bikram Jit., Sodhi H S "Parametric optimisation of CNC turning for Al-7020 with RSM"IJOR ,Vol 20, No 2, PP 180-205.

Author: Mr **Harsimran Singh Sodhi** is Post Graduate in Production Engineering and Pursuing his PhD. He is working as Assistant Professor in Mechanical Engineering Department of Chandigarh University Gharuan. Author is having a vast teaching experience of eight years. Authour is having more than twenty five publications in various international/ national conferences and International Journals. Key research areas of intrest of author are machining processes and industrial engineering.

E-mail: harsimransodhi86@gmail.com

http://doi.org/10.24867/JPE-2017-01-048

Journal of Production Engineering

Vol.20 No.1

JPE (2017) Vol.20 (1) Original Scientific Paper

Abdulkarim, K.O., Abdulrahman, K.O., Ahmed, I.I., Abdulkareem, S., Adebisi, J.A., Harmanto, D.

FINITE ELEMENT ANALYSES OF MINI COMBINED HARVESTER CHASSIS AND HITCH

Received: 26 December 2016 / Accepted: 18 March 2017

Abstract: *The perennial problems associated with harvesting of agricultural products in sub-Sahara Africa are not unconnected with financial limitations of the farmers. The design of low cost mini combine harvester was aimed at ameliorating the challenges of agricultural products harvest in Nigeria. The work presented here was a detailed analysis of low cost mini combine harvester chassis and hitch. The need for cost effectiveness, affordability, durability and efficiency of the designs necessitated detail analysis of the design to achieve the above objectives. Solidworks Finite Element Analysis (FEA) software was employed in carrying out both static and fatigue analysis of a low-cost mini combine harvester chassis and hitch design. The results were compared and contrasted, with appreciable improvements on available existing data. The stresses, displacements and strains on the chassis were significantly low with factors of safety of 2.48 and 2.80 for chassis and hitch respectively.*

Key words: *analyses, chassis, factor of Safety, FEA, harvester, hitch*

Analiza šasije i kuke mini kombajna za žetvu pomoću metode konačnih elemenata *Višegodišnji problem u vezi sa berbom poljoprivrednih proizvoda u oblasti sub-Saharne Afrike nisu nepovezana sa finansijskim ograničenjima poljoprivrednika. Dizajn jeftinih mini kombajna je imao za cilj ublažavanje izazova žetve poljoprivrednih proizvođača u Nigeriji. Rad predstavljen ovde je detaljna analiza šasija i kuka jeftinih mini kombajna. Potreba za isplativost, dostupnost, trajnost i efikasnost dizajna zahtevala je detaljnu analizu dizajna za postizanje gore navedenih ciljeva. Solidvorks softver metoda analize konačnih elemenata (FEA) je korišćena za obavljanju analize šasije kombajn i za kuke za vuču kako statičke tako i analize zamora jeftinog mini kombajna. Rezultati su dali značajnija poboljšanja u odnosu na postojeće podake. Naprezanja, pomeranje i deformacije su značajno niži sa faktorima sigurnosti 2,48 i 2,80 za šasiju i vučnu kuku respektivno.*

Ključne reči: *analiza, šasija, faktor sigurnosti, FEA, kombajn, kuka*

1. INTRODUCTION

The recent downward turn in the prices crude oil in international market has given a wake-up call to a number of governments especially in sub-Sahara Africa on the need to strengthen agriculture as a mainstay of economy. In Nigeria, despite the neglect agriculture had suffered over time due growing dependence on oil, Nigeria can still be considered an agrarian economy with sizeable number of Nigerian, particularly in the Northern part still rely on agriculture for livelihood and as Small and Medium Enterprise [1]. It is against this backdrop that successive governments particularly the current economic transformation agenda is being focused around agriculture and rural development with strategic planning and adequate policy measure focusing on improved productivity and value addition, to move the sector out of stagnation [2].

Mechanization has ever remains one of the biggest challenges facing average Nigerian farmer, and Lamidi and Akande [3] was of the opinion that, the main constraint to successful farm mechanization in Nigeria is non-affordable farm machineries to farmers. Hitherto, majority of farmers still employ hand tools for cultivation and harvesting processes [4]. This predicament is not unconnected with lack of access to loan facilities and higher interest rate. The high yield grains and seedling made available to farmers by government must be complimented by affordable machinery especially for harvesting and transportation from farm to the markets. Abdulkareem [5] was however optimistic on the varieties of indigenous technological objects recently developed in various forms. Among these emerging technologies was the work of Olukunle [6] who developed an indigenous self-propelled combine harvester for cowpea and soya bean. The machine is capable of operating at 0.33 ha/h at estimated feed rate of 322.22 kg/h between 100 to 600 rpm. The performance of the machine in various operational conditions was satisfactory but the estimated costs of the machine at ₦450,000 and ₦1,200,000 for one and it full scale three rows capacity respectively were beyond the reach of small scale farmers. Hence the need for cheaper, cost effective and durable alternative combine harvester capable of serving the need of the local farmers, which is achievable through Finite Element Analysis (FEA).

1.1 Finite Element Analysis (FEA) on Frame

Modern engineering practices have been revolutionized by the rise of Finite Element Analysis. It is a computational technique used to obtain approximate solutions of boundary value problems in engineering [7]. The basic procedure for completing any basic FEA involves four major steps namely: assigning of geometry, application of boundary

constraints and loads, meshing of object, and running the solver. It is noteworthy that engineering success in innovative products in today's competitive environment requires FEA simulation power. SolidWorks simulation technology ensures the quality and performance of design before dabbling to production. Comprehensive analysis tools allow models to be tested digitally for valuable insight in the design process. The tools has capability of establishing leverage between various competing parameters including weight and cost reduction, improve durability and manufacturability, optimize margins, and compare design alternatives to meet specific customer requirements.

Wakeham [8] carried out study and presented a good knowledge on fundamental requirements of chassis, stating how to start and optimised design making use of FEA software. The study ascertains the performance requirements of the automotive chassis. Among others, the chassis holds firmly all components while transferring lateral and vertical loads on the chassis via the suspension and to the wheels.

The ladder frame which is the oldest and the simplest style of frame is still employed in the construction of modern vehicles. It was formally used in the horse and buggy type carriages due to its good strength and stability under load. The ladder frame comprises of two beams running the total length of the vehicle, with other members cross linking the frame rail so as to hold it firmly together. Cars from the ladder frame era make use of braces at the sides of the frame, which add large amount of strength to the ladder chassis frame. X-bracing or cross-bracing is an effective way of strengthening the ladder frame. Fig. 1 shows the FEA images of both the ladder frame and the X-bracing frame.

Reina [10] did a study on the analysis of a bicycle frame using of finite element method to verify the validity of finite element approach. The experiment showed great extent of the functionality, implementation and high accuracy of the finite element method when compared to the experimental values. It was then concluded that the finite element results are greatly dependent on authenticity of the modelling methods and decisions employed. Jurgens Caravans Company performed an analysis using finite element analysis to analyse stress on chassis. The work was used to identify locations of high stress concentration to ensure prerequisite strengthening measures are put in place. Fig. 2 below shows the FEA static result obtained, in analysing the effect of load on the frame chassis.

The above case studies have shown that using solid works FEA simulation help to: provide accurate, efficient solution to difficult analysis problems; accelerate time-to-market; minimize design uncertainty, reduce error in production; and helps to reduce returns/warranty claims, thereby enhances productivity and profitability.

The major challenge in today's ground vehicle industry is how to overcome the increasing demands for higher performance, lower weight, and longer life of components at a reasonable cost and in a shortest period of time [12]. Several works have been done on the analyses of frame ladder chassis including modifications on reduction of weight using different FEA software [8, 13-15]. However, in this work, modeling of low cost combine harvester component parts precisely chassis and hitch was carried out for static and fatigue analyses using SolidWorks FEA.

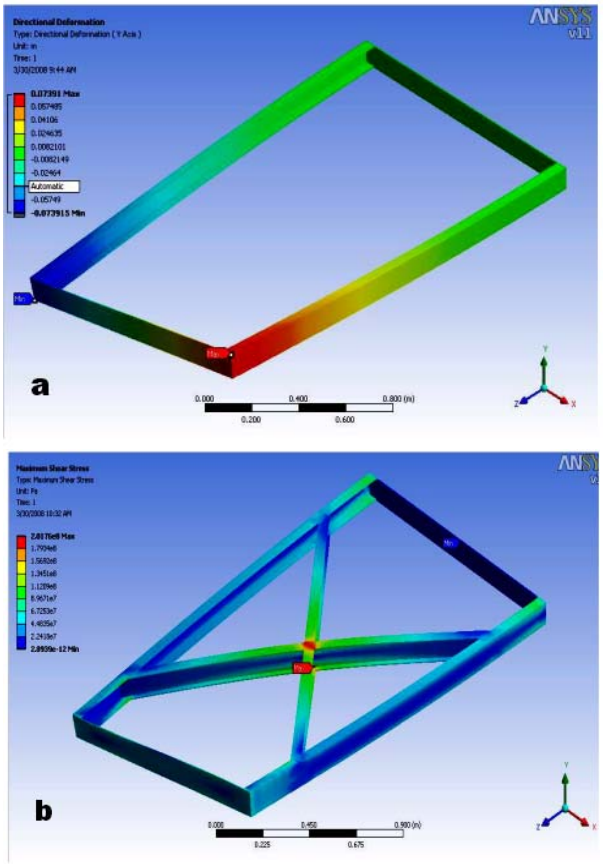

Fig. 1. Ansys simulation of: Steel ladder frame (a) and Large X-bracing frame (b) [8, 9]

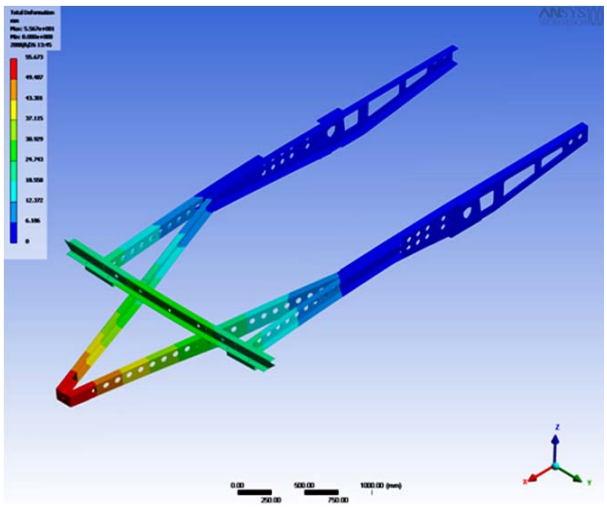

Fig. 2. FEA stress analysis on frame chassis [11]

2. METHODOLOGY

The flow chart in Fig. 3 illustrates the various steps followed towards static and fatigue analysis in this work. The detailed methodology for FEA analyses are detailed below.

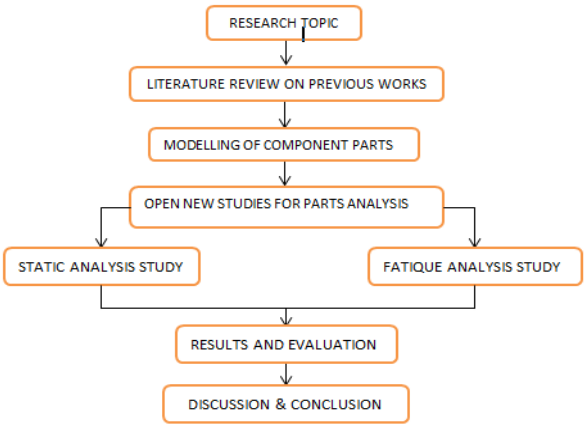

Fig. 3. Study Methodology Flow Chart

2.1 Methodology for the FEA analysis

The procedures below were followed during the Finite Element Analysis on the chassis and hitch:

1. Set the analysis units: Activation of simulation new study
2. Creating study for the analysis: Static study icon from the simulation menu was activated.
3. Assigning material: Material is applied to the model using custom icon from material window to specify the required material properties from design calculation.
4. Meshing: The model is meshed using default setting.
5. Applying fixtures: Fixed geometry icon is selected for restraining both ends.
6. Applying forces: External loads icon is active to apply load and direction to the model.
7. Run for analysis: After desire result from meshing the run icon is active to analyse the model
8. Visualizing and verifying the result: Checking on the results for stress and strain, displacement, and factor of safety by comparing to hand calculation.
9. Compile the report: After satisfactory result, report was compiled for recommendation.

2.2 FEA Analysis on Chassis and Hitch

The frame (chassis) being one of the most important components of the harvester, supports the entire load of the machine and this makes it an integral part that have to be analysed to determine how well it is able to carry the load being subjected to. Also the hitch which provides a link or attachment also needed to be analysed to ascertain that it does not fail during course of operation.

The design for the chassis was adopted from [14] with similar analysis carried out. Both statics and fatigue analysis were conducted on the chassis and hitch to determine how well the chassis had been designed. The ability of the chassis and hitch to withstand damage and deformation based on the designed load was also determined. The static analysis performed involved fixing the chassis in areas where it is to be supported by tyres and shafts.

The modeled chassis was assigned a material of AISI 1045 after thorough material consideration. The loads were applied onto two sections of the chassis considering the load uneven distribution. Load of 1994.92 N was applied to the front section while load of 3989.84 N was applied to rear section taking into consideration the gravitational force through the sections. The study was then simulated. Both the chassis and hitch were modelled using Solidworks (2014) . New simulation studies were performed for static and fatigue analysis on the components. The stages and results obtained in the analysis are discussed below.

3. RESULTS AND DISCUSSION

To have a clear view of the various analyses, the different views of the combined harvester from the design images are contained in Fig. 4. The analyses will be restricted to the chassis frame and the hitch as detailed below.

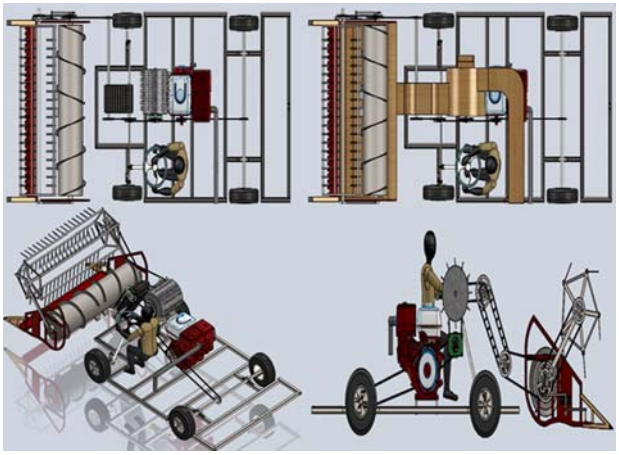

Fig. 4. Different Views of Combined Harvester Chassis and Components

3.1 Chassis Static Analysis Result

Fig. 5 showed the chassis frame, the chassis supporting fixtures (arrows pointing upwards) and the loading points (arrow pointing downwards) including the location of centre of gravity. The loading was not uniformly distributed. The load of about 2 kN applied to the front of the chassis was to account for the engine and the frontal loadarge chunk of 3989.8 N was applied to the rear portion of the chassis while about half of the rear load applied to the front portion.

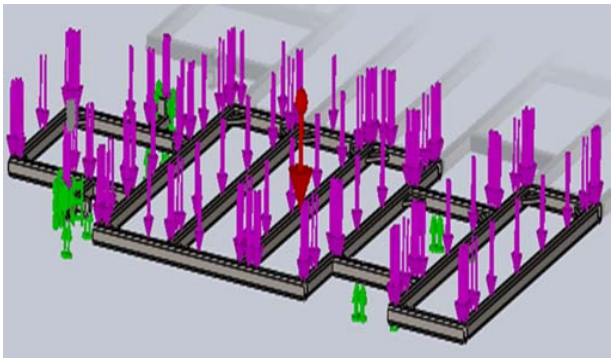

Fig. 5. Fixtures and load Application on the chassis for FEA Analysis

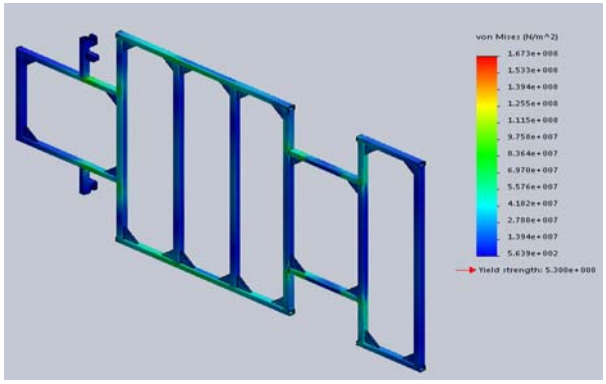

Fig. 6. Stress Distribution Result of the FEA Analysis

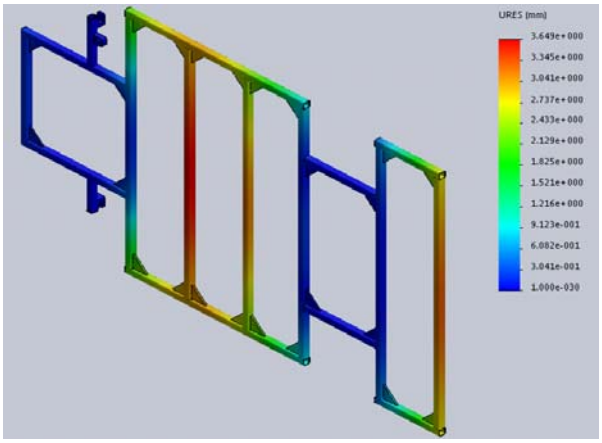

Fig. 7. Displacement Distribution Result of the FEA Analysis

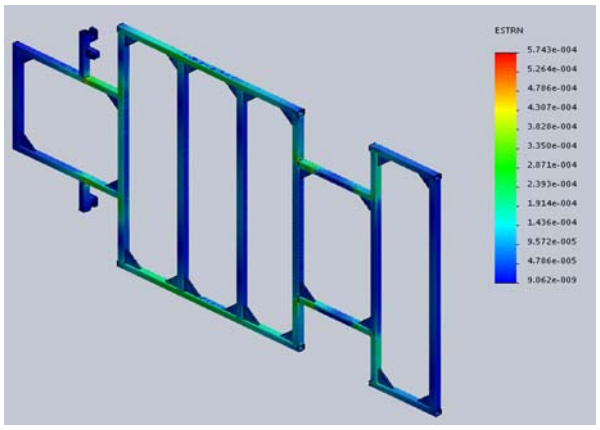

Fig. 8. Strain Distribution Result of the FEA Analysis

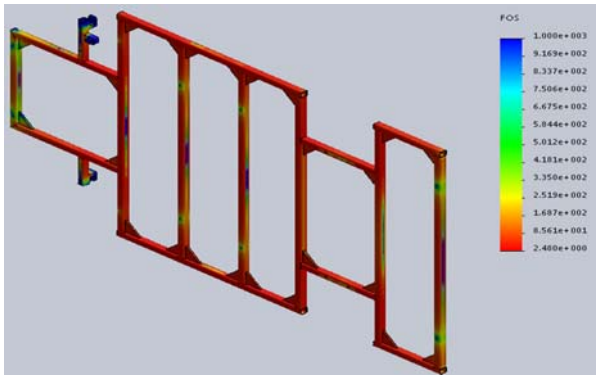

Fig. 9. Factor of Safety Result of the FEA Analysis

The greenish yellowish area in some part of the chassis as shown in Fig. 6 revealed the most stressed region on the chassis. Red coloured regions in Fig. 7 are depicting region of high displacement. Fig. 8 also revealed greenish yellowish area representing highly strain region just similar to the one shown in Fig. 6. The last result on static analysis gave a minimum factor of safety of 2.48 (see Fig. 9).

3.2 Chassis Fatigue Analysis Results

The detailed results of fatigue analyses of the chassis are given below.

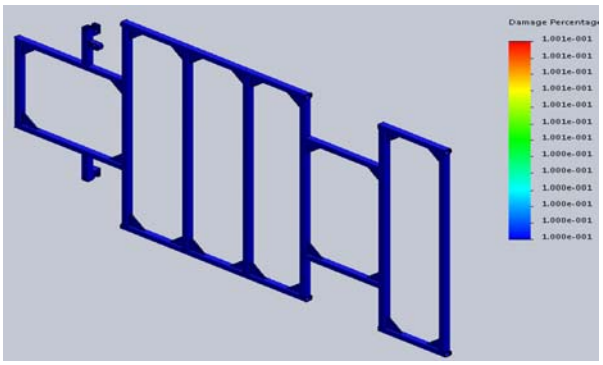

Fig. 10. Damage Percentages Result of the fatigue Analysis

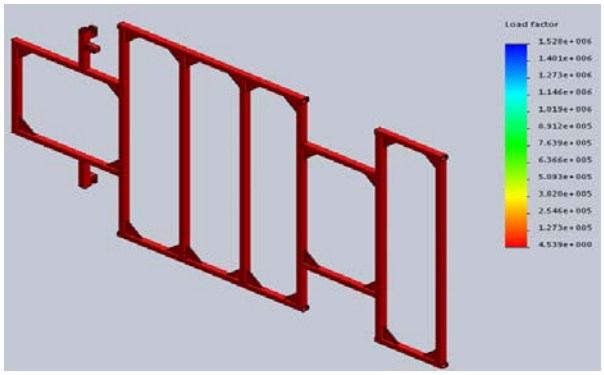

Fig. 11.Load Factor Result of the Fatigue Analysis

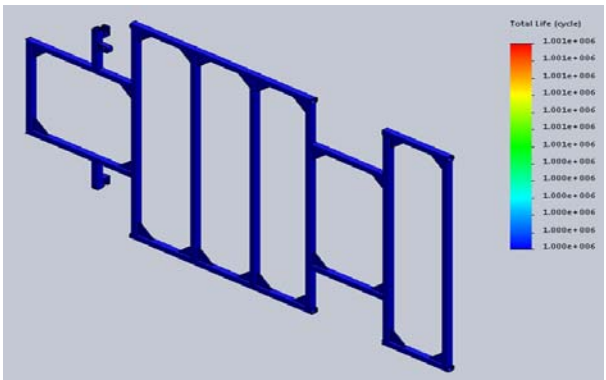

Fig. 12.Total Life Cycle Results for the Chassis

From Fig. 10, the chassis maximum damage percentage is 0.1. Fig. 11 shows a maximum load factor of 1.528×10^6 with the maximum total life of the chassis at 1.001×10^6 cycles as shown in Fig. 12.

Looking at the chassis insignificant damage percentage, load factor greater that one and the total life cycle, all clearly pointed out that the chassis have been well designed.

Table **1** and 2 showed the comparison of results done based on present work and adopted work of Abdulrahman [14], for static and fatigue analysis of the chassis respectively. From the Table **1**, it will be seen that there was a considerable difference in the results obtained. These differences are attributed to type of material selected for the chassis and slight improvement in the chassis design. The improvements led to an improved chassis of higher factor of safety. The analysis done by Kotari and Gopinath [17] on chassis frame, adding stiffener at region of maximum stress in other to improve it payload, revealed results of 7.3 mm deformation and factor of safety of 1.27.

FEA Analysis (Static)	Abdulrahman FEA		Present Work FEA	
	Min	Max	Min	Max
Stress	1.43×10^2 N/m^2	2.43×10^8 N/m^2	5.6×10^2 N/m^2	1.67×10^8 N/m^2
Strain	7.40×10^{-10}	8.70×10^{-4}	9.06×10^{-9}	5.743×10^{-4}
Displacement	1.0×10^{-30} mm	5.57mm	1.0×10^{-30} mm	3.649 mm
Factor of safety	1.66		2.48	

Table 1. Chassis FEA Static Analysis Results Comparison

Fea Analysis (Fatigue)	FEA Results	
	Abdulrahman (2014)	Present Work
Max. Damage Percentage (%)	0.705	0.1
Max. Load Factor	5.21×10^6	1.528×10^6
Total Life	1.0×10^6	1.0×10^6

Table 2. Chassis Fatigue Analysis Results

3.3 Hitch Static Analysis Results

There are various types of hitches currently available in the market differing with type of application. For this design, is a standard rear drawbar hitch that can carry load up to one tonne.it will allow rotation of two axes and will be bolted to the chassis. This type of hitch will not only allow all the attachments to be mounted or dismounted easily but also removable quickly and safely.

It can be evidenced from various researchers, design and analysis companies that several work has been done on different types of hitches. To mention few, Adnoor et al. [18] performed non-linear buckling analysis on tow bar. Alimardani et al. [19] and Khannade et al. [20] goes further from performing the FEA analysis to design dynamometer and transducers that can measure forces on hitches during operation using three point hitches of a tractor.

Since hitch is the critical component that allows the harvester and the trailer to move together. The great importance of hitch makes it justifiable to perform analysis on the component, to determine it strength during the operation. Like that of the chassis analysis, similar steps were followed in other to carry out statics analysis on the hitch. Cast iron material of yield strength of 526 Mpa was selected for the hitch.

Fig. 13a shows the fixed region (with green arrows) of the hitch while the pink arrow region depicts region of applied load. Fig. 13b shows the meshed image of the hitch.

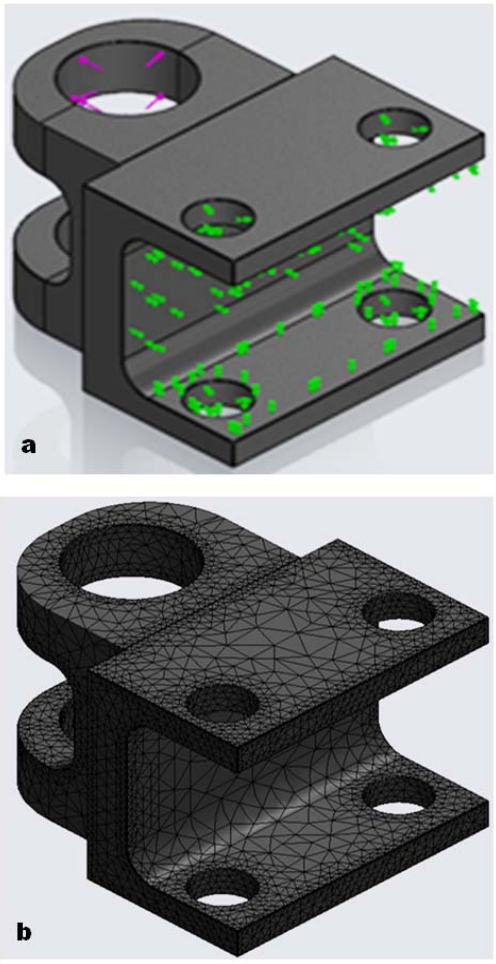

Fig. 13. Image of Hitch: Fixture and Load Application (a) and Meshed Image (b)

The results obtained from the simulation, revealed a maximum stress of 4.866 × 10^7N/m^2 with highly stressed region around the region of applied load as shown in Fig. 14a. The same region also shows region of greatest displacement and strain, with maximum displacement of 1.532 × 10^{-2} mm and maximum strain of 5.669 × 10^{-4} as shown in Fig. 14b and Fig. 14c respectively. Fig. 14c revealed factor of safety of 2.

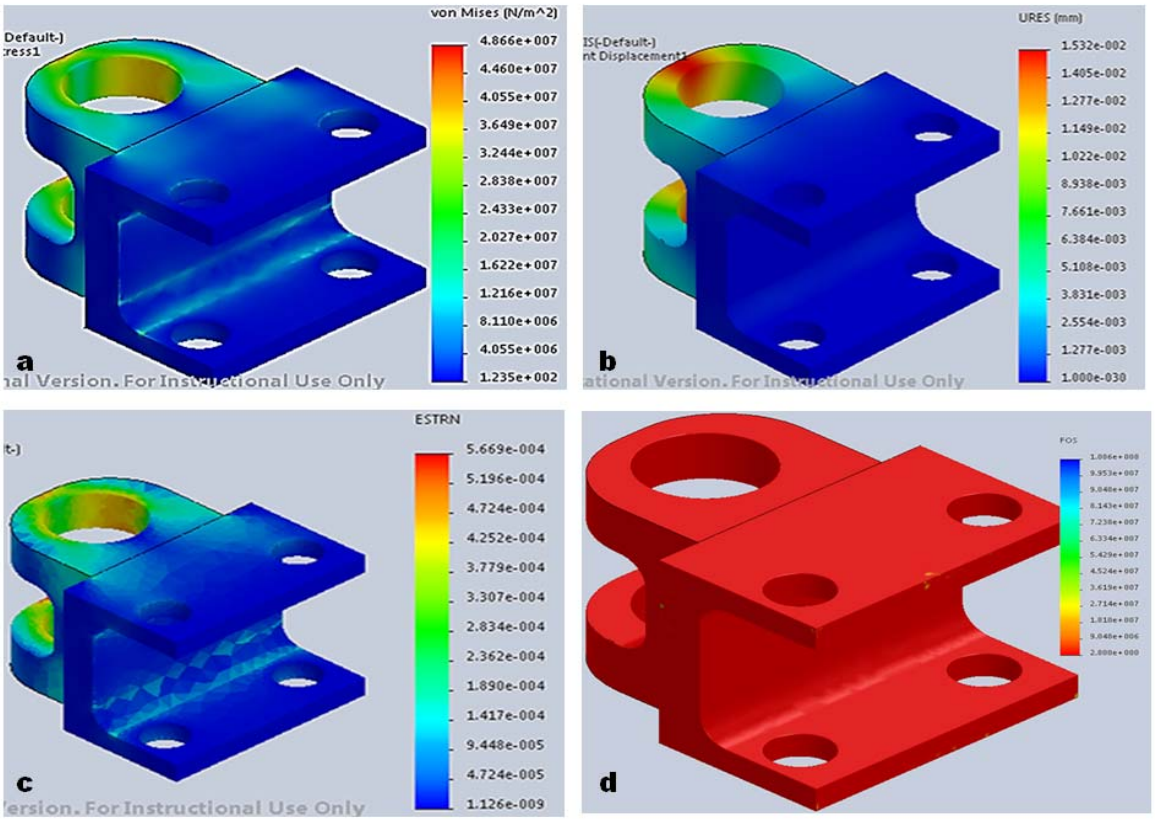

Fig. 14. FEA Analysis showing Distributions of: Stresses (a), Displacement (b), Strain (c), and Factor of Safety (d).

The fatigue analysis carried out for the hitch revealed the results shown in the Table 3. Tables 1-4 has clearly presented summary of the results obtained from the chassis and hitch FEA analysis. Looking at the results showing negligible displacement with good factor of safety, it can therefore be said that both the chassis and hitch have been designed to withstand subjected loads and resist damage.

FEA Analysis (Fatique)	**FEA Results**	
	Min	**Max**
Damage Percentage (%)	0.1	1.832
Load Factor	3.641	1.284× 10^6
Total Life Cycle	5.457× 10^4	1.0× 10^6

Table 3. Hitch Fatigue Analysis Results

FEA Analysis (Static)	**FEA Results**	
	Min	**Max**
Stress (N/m^2)	1.235×10^2	4.865×10^7
Displacement(mm)	1.0×10^{-30}	1.53×10^{-2}
Strain	1.126×10^{-9}	5.669×10^{-4}
Factor of safety	2.8	

Table 4. Hitch FEA Static Analysis Results

4. CONCLUSIONS

Finite element analysis (FEA) results obtained for the chassis and hitch clearly revealed that the models have been adequately designed to withstand maximum subjected load the components may be carrying provided high yield strength materials are used in the construction of such components.

The static analysis of the chassis revealed maximum displacement of 3.6mm and a factor of safety of 2.48. The fatigue analysis gave a damage percentage of 0.1 and maximum load factor of 1.52 ×

10^6 when subjected to maximum load. The hitch gave a maximum displacement of 1.53×10^{-2}mm and a factor of safety of 2.8 when subjected to maximum load. FEA simulation software (SolidWorks 2014) have clearly demonstrated that it is a viable tool in analyzing models as it showed areas of possible failures that needed additional strengthening mechanism to prevent imminent failure.

In conclusion, the analysis was successful on account of better results obtained when compared to previous work. The analysis also showed that it is possible to design for manufacture, chassis of a multi-purpose low-cost combine harvester that will make use of locally sourced materials like the square hollow pipe.

5. REFERENCES

[1] Talabi, S. O. and Onasanya, O. *Agricultural Introduction*. 2013 22/09/2014]; Available from: http://www.onlinenigeria.com/agriculture/?blurb=480.

[2] Aderohunmu, M., Is Nigeria's agricultural sector improving?, 2012.

[3] Lamidi, W. A. and Akande, L. O., A Study of Status, Challenges and Prospects of Agricultural Mechanization in Osun State, Nigeria. 1(1): p. 001-008, 2013.

[4] Takeshima, H., Pratt, A. N., and Diao, X., Agricultural Mechanization Patterns in Nigeria: Insights from Farm Household Typology and Agricultural Household Model Simulation., IFPRI, 2013.

[5] Abdulkareem, Y. A., Indigenous Technology, Past, Present and Futures, in Workshop for the Processing Of Raw Materials: Raw Materials Research and Development Council, 1992.

[6] Olukunle, O. T., *Developments in Grain Harvesting Mechanisation.* Journal of Agricultural Engineering and Technology (JAET). 18(1), 2010.

[7] David, V. H., *Fundamentals of Finite Element Analysis*. First ed.: McGraw-Hill, 2004.

[8] Wakeham, K. J. *Introduction To Chassis Design*. 2009 14/04/2014]; Available from: http://www.keithwakeham.com/Files/ChassisDesign.pdf

[9] Wakeham, K. J. *Ansys simulation of Steel ladder frame and Large X-bracing frame* 14 April, 2014]; Available from: http://www.keithwakeham.com/Files/ChassisDesign.pdf.

[10] Reina, J., Structural Analysis of a Bicycle Frame using Finite Element Techniques, 2007.

[11] Jurgens. *Chassis Stress Analysis*. 2010 [cited 06 October, 2016]; Available from: http://jurgens.com.au/Range/Smart-Technology.aspx

[12] Patel H, Pancha, K. C., and Jadav, C. S., *Structural Analysis of Truck Chassis Frame and Design Optimization for Weight Reduction.* International Journal of Engineering and Advanced Technology (IJEAT). 2(4), 2013.

[13] Patil, H., Kachave, S. D., and Deore, E. R., *Stress Analysis of Automotive Chassis with various Thicknesses.* Journal of Mechanical and Civil Engineering. 6(1): p. 44-49, 2013.

[14] Abdulrahman, K. O., Design of Low-Cost Vehicle for Nigerian Rural Farmers for Transportation of Farm Produce, 2014.

[15] Singh, A., Soni, V., and Singh, A., *Structural Analysis of Ladder Chassis for Higher Strength.* International Journal of Emerging Technology and Advanced Engineering. 4(2), 2014.

[16] SolidWorks, 2014.

[17] Kotari, S. and Gopinath, V., *Static and Dynamic Analysis on Tatra Chassis.* International Journal of Modern Engineering Research (IJMER). 2(1): p. 086-094.

[18] Adnoor, A., Guruprasd, H. L., and Maurthi, B. H., *Nonlinear Buckling Analysis of a Tow Bar.* Indian Journal Science. 9(1): p. 088-095, 2014.

[19] Alimardani, R., Fazel, Z., Akram, A., Mahmoudi, A., and Varnamkhasti, M. G., *Design and Development of a three-point hitch dynamometer.* Journal of Agricultural Technology. 4(1): p. 37 - 52, 2008.

[20] Khannade, P., Chitnis, A., and Jagdale, G., *Design and Stress Analysis of Tow Bar for Medium Sized Portable Compressors.* International Journal of Research in Engineering & Advanced Technology. 2(3): p. 1-6, 2014.

Authors: **Researcher. Mr Kazim Olawale Abdulkarim**, Department of Mechanical Engineering, University of Derby, Derby. DE22 1GB, UK. +447553081438. **Lecturer. Mr Kamardeen Olajide Abdulrahman,** Department of Mechanical Engineering, University of Ilorin, P.M.B. 1515, Nigeria, +2348061596252. **Lecturer. Dr Ismaila Idowu Ahmed,** Department of Materials and Metallurgical Engineering, University of Ilorin, P.M.B. 1515, Nigeria, +2347018271354. **Lecturer. Sulaiman Abdulkareem,** Department of Mechanical Engineering, University of Ilorin, P.M.B. 1515, Nigeria, +2348058219222. **Lecturer. Mr Jeleel Adekunle Adebisi,** Department of Mechanical Engineering, University of Ilorin, P.M.B. 1515, Nigeria, +2348030422330. **Lecturer. Dani Harmanto,** Department of Mechanical Engineering, University of Derby, Derby. DE22 1GB, UK, +447773057610.

E-mail: zeem2002@yahoo.com
olajideabdulrahman@yahoo.com
ismaila.ahmed@yahoo.com
sulkarm@yahoo.com
adebisijeleel@gmail.com
d.harmanto@derby.ac.uk

http://doi.org/10.24867/JPE-2017-01-055

Journal of Production Engineering

Vol.20 No.1

JPE (2017) Vol.20 (1) Original Scientific Paper

Abdulkarim, K.O., Abdulrahman, K.O., Ahmed, I.I., Abdulkareem, S., Adebisi, J.A., Harmanto, D.

DESIGN OF MINI COMBINED HARVESTER

Received: 26 December 2016 / Accepted: 19 March 2017

Abstract: *In this research, various problems associated with harvesting of agricultural food grains by local farmers in Nigeria were identified. The aim of the research was to design low cost multipurpose mini combined harvester for production using locally available materials at affordable cost. The research was to ensure improved performance and low cost maintenance of harvester for use by farmers in developing nations. The modelling of the chassis and other components of the combined harvester was done using Solid works 2014. The selection of materials for the design was achieved using Cambridge Engineering Selector (CES) 2014. Calculations for the design of each components and power requirements to determine the engine specifications were carried out to ensure optimal performance. The output of the research was the development of mini combine harvester which is a microcosm of large capital intensive harvester, at affordable cost to small scale farmer in developing nations. The research ensures the use of mechanised farming equipments designed and developed from local materials for effective harvesting and transportation of agricultural produce.*

Key words: *chassis, design, grains, harvester, material selection, modelling.*

Konstrukcija mini kombajna za žetvu. *U ovom istraživanju, identifikovani su različiti problemi u vezi berbe poljoprivrednih žitarica od strane lokalnih poljoprivrednika u Nigeriji. Cilj istraživanja je bio da se dizajnira jeftin višenamenski mini kombajn, a za proizvodnju se koristi lokalno dostupni materijali po pristupačnoj ceni. Istraživanje je bilo usmereno da se obezbede bolje performanse i jeftino održavanje kombajna za upotrebu od strane poljoprivrednika u zemljama u razvoju. Modeliranje šašije i drugih komponenti kombajna je urađeno pomoću Solid Vorks 2014. Izbor materijala za konstrukciju je vršen korišćenjem Cambridge Engineering Selectora (CES) 2014. Proračuni u cilju projektovanje svake komponente kombajna kao i potrebne snage je bio da se utvrde specifikacije motora kako bi se osigurale optimalne performanse. Izlazni rezultat istraživanja je bio razvoj mini kombajna koji je mikroverzija velikog i skupog kombajna, po pristupačnoj ceni za obim rada kod malog farmera u zemljama u razvoju. Istraživanje osigurava upotrebu mehanizovane poljoprivredne opreme konstruisane i razvijene od strane lokalnih materijala za efikasno sakupljanje i prevoz poljoprivrednih proizvoda.*

Ključne reči: *šasija, dizajn, žitarice, kombajn, izbor materijala, modeliranje.*

1. INTRODUCTION

Agricultural in Nigeria still remains the source of raw material to both local and international industries despite years of neglect following the emergence of oil economy [1, 2]. According to Engineering Export Promotion Council (EEPC) [3] report, it was indicated that 82 million hectares out of Nigeria‘s total land area of 91 million hectares are arable and only about 34 million are being cultivated. But despite the setback in agricultural sector in Nigeria on account of oil boom, agricultural still account for a significant shares both in Gross Domestic Product (GDP) and total export [4].

Mechanization remains one of the biggest challenges especially to the local farmers. Faborode [5] reported that agricultural mechanization in Nigeria is less than 2%, while 98% of the production is done by traditional methods and the effect of this methods is low output [6]. Lamidi and Akande [7] indicated that the major constraints to successful farm mechanization in Nigeria are non-affordable farm machineries to local farmers. Hitherto, majority of farmers still employ hand tools for cultivation and harvesting processes [8]. This predicament is not unconnected with lack of access to loan facilities and higher interest rate. The high yield grains and seedling made available to farmers by government must be complimented by affordable machinery especially for harvesting and transportation from farm to markets. Abdulkareem [9] was however optimistic on varieties of indigenous technological tools recently developed in various forms.

As part of the government initiative towards becoming one of top 20 economies in the world by year 2020. Nigeria government has challenged the indigenous engineers among others, on the design of low cost farm machineries and equipment [10]. This is in a bid to increase productivity and to enhance quality of farm operation and effective land usage [11]. In addition, government of Nigeria also set up several institutes like, The Lake Chad Research Institute (LCRI) working alongside with Support To Agricultural Research For Development Of Strategic Crop (SARD-DC) to research into the production problems of popularly grown crop such as rice, wheat, millet, barley, cassava and sorghum at the same time find a generic improvements. Also, some institutes were set up to encourage local farmers on mechanized farming through agricultural scheme.

Harvesting among the major operations, is the culmination of the farming processes and could be

achieved through different methods depending on the type of the crop to be harvested; it involves cutting, gathering threshing, cleaning, transporting and stacking of the grains. In Nigeria, Harvest of grains is traditionally done manually using sickle, knife or scissors which involve intensive labour, cost and time consuming (see Fig. **1**).

Fig. 1. Harvesting [12] and Transportation of Harvested Grains

2. COMBINE HARVESTERS

Grain harvesters can be described as various designs of tools, machine and system used during the harvest of grains. It can be classified into two categories such as traditional methods and mechanical methods. However, the entire operation can be divided into four stages such as cutting, threshing, separating and cleaning depending on the methods used.

The world first engine operated combine harvester was built by George Stockton Berry in the year 1888, a self-propelled machine that burned fuel off the land. The machine was the first and the largest header of 40 feet tractor that work both forward and backward, also, the first to harvest over100 acres of land in a day with the aid of head light at night time, it took five year to build and was sold at cost of $4500 apiece [13].

Several development trends was followed after the discovery of the machine, many leading manufactures were merged and international harvester company was formed in 1902.Due to increase in demand and performance of the machine several development has occur ever since by different manufacturers. The trends of Improvements from the size of the machine to work rate, improvement of threshing, separating and cutting efficiency, reduction of gathering loss, reduction of grain damages, reduction of operation fatigues have been witness. However, other important improvement like usage comfort and safety, automatic adjustment, electronic controls and it ergonomics has evidence that combine harvester witnesses a significant transformation.

There are several types of combine harvester current available but their selection depends on the factors like size of the farm, types of the crop, and the available capital. It is a very unique machine as it cuts, transports, threshes, separates and as well stores the grain [14].

From all review of grain harvester it was evidence that a good amount of work has been done in developed countries. But taken the cost into account it is an obstacle to the local farmers and needs of the small scale farmers remained unmet which is a challenge to indigenous engineers in developing countries [14].

However, in some other developing countries such as Thailand, Pakistan, and India a great response to the challenge have been made. In India, an indigenous combine harvester have been tested and introduced to market, the Swaraj- 8100 manufactured by Punjab tractors limited. The machine was tested for 75 hours on different field at operating speed of 2-3 km/hr in first gear at 1850 rpm. The overall performance of the machine was found to be satisfactory but still expensive for small scale farmers [15].

Meanwhile in Africa, particularly Nigeria a lot of research work and development into grain harvesters has been done. Abdulkareem [9] currently stated that there are many indigenous technological objects developed in various forms. For grain harvesters, machine such as thresher and strippers are available in the market. Researchers are currently working on improving threshing machines into combine, according to Ademosun et al. [16] who stated that development of grain harvesters is in progress.

Olukunle [14] developed an indigenous self-propelled combine harvester for cowpea and soya bean. The machine is capable of operating at 0.33ha/h at estimated feed rate of 322.22kg/h between 100 to 600 rpm. Although, machine was tested in various operational conditions and the cost of the machine was estimated to ₦450, 000 and it full scale 3 row will cost ₦1, 200,000. Comparing the machine to the modern combine harvester it is very cheap. However,

considering the small scale farmers the cost is very high which require further development.

Therefore, the design of multipurpose low cost combine harvester was aimed at fulfilling the above challenge. Although, currently there is no engine manufacturing company in Nigeria but it is locally available at affordable price. Some of the design targets of the low cost combine harvester include it ability to operate under different weather conditions efficiently, suitability for temporary storage on farm and transportation of farm products.

3. DESIGN METHODOLOGY AND MATERIAL SELECTION

3.1 Design methodology flow chart

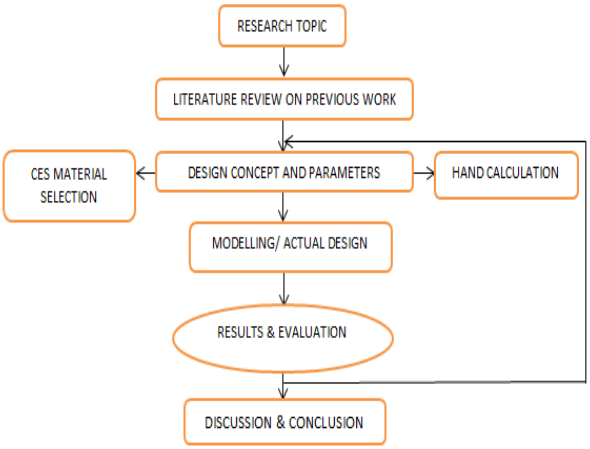

Fig. 2. Design Methodology Flow Chart

The research is followed by in-depth knowledge of concept design with assumed parameters, hand calculations, 3D modelling, material selections, operation systems of the harvester taking into consideration the aim and objectives with the background knowledge. Results from the design were evaluated and discussed. Finally, a comprehensive conclusion is drawn based on all the results obtained.

3.2 Hand calculations of Design Parameters:

The following are the parameters used for the calculation of stress and strain on the chassis:

- Total Length of required chassis pipe, L=11.371m, Approximated to 12m.
- Total Surface Area of chassis, A=12 x 0.03 = 0.36m^2
- Material: AISI 1045
- Density of the material, ρ = 7850kg/m^3
- Young modulus of the material, E= 210 GPA
- Yield strength: 530x 10^{6}N/m^2
- Mass of the chassis, M=28.62kg
- Approximated total weight on the chassis, W=640kg = 62784N
- Moment of inertia, I=3.5977 x10^{-4}m^4

The engineering stress and strain on the chassis were calculated with Equations 1 and 2 respectively:

$$\sigma_c = \frac{W_c}{A_c} \qquad (1)$$

$$\varepsilon_{ch} = \frac{\sigma_{ch}}{E} \qquad (2)$$

Treating the chassis as uniformly distributed load to calculate for deflection, y

$$y = \frac{5WL^4}{384 \times EI} \qquad (3)$$

Substituting for W = 6278.4N, L = 2.01m, E = 210GPA, I = 3.5977 X 10 $^{-4}$ m^4 in Equation 3, gave the value of deflection, y = 1.76 mm.

The Factor of safety was calculated according to Equation 4, and given the ultimate and actual stresses of 53000 N/m^2 and 17000 N/m^2.

$$FOS = \frac{Ultimate\ Stress}{Actual\ Stress} \qquad (4)$$

The power required for Threshing, P_1 was calculated from Equation 5.

$$P_1 = \frac{MV^2}{1-f} + A_{w1} + B_{w^3} \qquad (5)$$

The following parameters were considered for calculation of power:

M: Total Mass of the Material Feed to the Drum (kg/S), i.e. Mass of the Grain +Mass of the Straw.
Using Wheat for Calculation: 450 kg/h
Approximated Grain Straw Ratio in Mass is 1.5
Total Mass of the Wheat = 450+1.5×450 = 1125kg/h
= 0.31kg/S

V: Tip Speed of the Drum (m/s) = 35m/s

F: Friction Coefficient Range between 0.7-0.8 for this type of Material

A_{W1}: Factor Accountable to the Resistance of Bearing taken to be 3.0 X10^{-2} kgfm

$B_W{}^3$: Factor Accountable For the Air Resistance Taken to Be 0.48 X10^{-2} kgfm

Grain	Straw Ratio	Average Weight (kg)
Barley Straw	**1.2**	**21.74**
Corn Straw	**1.0**	**31.75**
Oat Straw	**1.3**	**14.515**
Sorghum Straw	**1.4**	**25.40**
Wheat Straw	**1.5**	**27.22**
Wheat Straw (Winter)	**1.7**	**27.22**

Table 1. Different Grain Straw Ratio and their Average Weights [17]

W: Angular speed of the drum (rad/s) assumed to be 800 rpm = 84 rad/sec

Calculating for the power using Equation 5, showed that Power, P_1 = 1.27 kW

It was assumed that the same amount of power will be required to operate the auger and the reel, so the combined power sum is 2.54 kW.

And the power need of the conveyor was calculated from Equations 6-9.

$$P_2 = T_e \times \frac{V}{1000} \quad (6)$$

$$T_e = TC + TL + TH \quad (7)$$

$$TC = F_1 \times L \times CW \quad (8)$$

$$TL = F_2 \times L \times MW \quad (9)$$

T_e = The effective tension on the belt
V = Velocity
TC = Sum of tension required to move the empty belt
TL = Tension required to move the load on the belt horizontally
TH= Tension required to lift the load
F_1 = Coefficient of friction=0.02
L = Length of the belt =1.68m
CW =Total weight of conveyor belt components=12 kg
TC = 0.02×1.68×12 = 0.40N
F_2 = Friction factor to move the load horizontal
L = Length of the belt
M_W =Material weight =0.31KG/S
TL = 0.02 × 1.68 X0.31= 0.010N
TH = H × M_W
H = Difference in the elevation of the pulleys (M)
= 0.37m
TH=0.37 × 0.31 = 0.11N
Therefore
T_e = 0.40+0.011+0.11 = 0.52N
P_2 = 0.52 ×35 /1000 = 0.0182 HP or 0.014 kW

And the power required for blower was calculated from Equation 10

$$P_3 = Q \times \frac{PF}{33000} \times \mu \quad (10)$$

The following parameters were used for the calculation of power required for the blower:
Q = Flow Rate = 125.6 m/s
PF = Atmospheric Pressure =101325 N/m^2
M = Efficiency Coefficient =1.7
P_3 = 125.6 ×101325/33000 × 1.7 = 12726420/5610=
= 2.26 kW

The Power requirement for Shaft transmission was calculated from Equation 11.

$$P = F \times V \quad (11)$$

F = Total weight of mini combine harvester
= 640 kg = 6278 N
V = Assumed to be 1.2 m/s
P = 6278 X 1.2 = 7533 Nm/s = 10.10HP or 7.53 kW

The total power sum required:
= 7.53+2.26+0.014+2.54
=12.34 kW

The total power was rounded up to 13 kW considering all the transition loss

The design capacity of the container was calculated as shown below:

The container was rectangular box with internal dimensions given as 0.9 × 0.45 × 0.30 m
Volume of container, Vc was 0.128 m^3

Converting the volume to bushels and then to kilogram through following expression:
0.128/0.36 = 3.5 bu
While 1 bu = 27.22 kg
3.5 bu = 95.25 kg
To calculate for amount of grain per m^2.

And considering wheat for the calculation, an average mass of 1000 grains (extra strong) range form 0.040-0.044 kg at 210 m^2.

The total amount of grains contained in 95.25 kg was estimated at 23000 grains.

3.3 Selection of materials

For engineering applications, selection of materials is considered an important and challenging task. Choosing materials wrongly may increase the product cost and possible failure of the product. During the selection, properties and behaviour of the material depends on several factors that needed to be considered to ensure the quality of the product is not compromise [18]. The selection process are often simplified into 4 categories namely: manufacturing processes, functional requirement, cost considerations and operational parameters [19]. All the four categories were considered in the design of the low cost harvester using Cambridge Engineering Selector (CES) 2014 software while the criteria for the design were adapted from [20-23]. There are thousands of different materials available in the market and it will be difficult to process all the detail knowledge of the materials [24].

The material selections for the machine components were carried out, setting the variable limit of the parameters. Density was first set against the yield strength, the results obtained was narrowed down by setting the price against young modulus. Then yield strength against young modulus. After all the analyses were conducted, appropriate materials most suitable for the machine were chosen. The chosen materials considered are shown in Table 2.

Engine specifications

Based on the power requirements from the calculation of approximately 13 kW, a Honda G630 air cooled 4 stroke OHV petrol engines; electric starter of net power of 15.5 kW (20.8 HP)/3600 RPM was selected. The engine was mounted at the center of the chassis in other to drive the rear shaft and other components (auger, reel, cutter, conveyor, blower and thresher) with the aid of pulleys. It was designed to start from the entrance door to the engine compartment next to the driver, this makes it easier to stop the engine, for easy maintenance of the engine and other components.

Fig. 3. Honda G630 Engine [25]

4. CAD MODELING AND ASSEMBLY

4.1 Concept Design

With the present agricultural mechanization situation in Nigeria, the idea of low cost multipurpose mini combine harvester came up as a result of the current demand by Nigerian farmers. The harvester was designed with back wheel drive and consists of chassis, main body and engine unit in conjunction with reeling, cutting, threshing and storage units. The machine will in addition to providing better operation condition for the operator with availability of seat and cover, it was also designed to provide good visibility lighting when required. With the aid of attachment, combine harvester can as well serve as mower, plough, seeder and the engine can be used for irrigation.

The power transmissions was achieved through the use of B type 2 V-groove pulley and rubber belt to transmit power from the engine to the wheel shaft, then to cutter blades along with rotational motions of auger, reel, conveyor belt and thresher. The conveyor, auger and thresher rollers were designed using standard seam tube steel of 10 m thickness with different diameters. Also, basic type food grade belt was selected for the conveyor while most of the fasteners used for the design were nails apart from special connection areas like body to chassis, engine, tires to shaft etc.

During the design, consideration for past design types, operations, efficiency, materials and cost were examined, several factors such as weather, topography and farming system about the region of operations were also considered in order to meet the demand of the local farmers.

Based on the design assumptions, the concept design of low cost multipurpose mini combine harvester was modelled using Solidworks 2014. The Fig.4 shows the side view of the combine harvester.

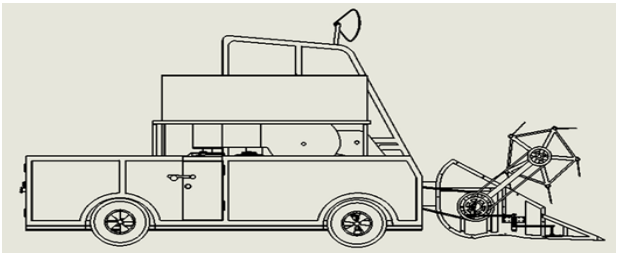

Fig. 4. Side View of the Combine Harvester

4.2 Chassis

There are different types of chassis, and they vary from ladder, twin tube to space frame types. For this design, the concept for the harvester chassis was adopted from Abdulrahman [26]. The chassis was a conventional type space frame ladder structure with two long side member and 7 sides cross members. It was designed for easy fabrication by welding using square steel pipe of 30 × 30 × 2.6 mm and 2000 mm length ×1220 mm Width, it could be fasten to the body by bolts 60.50 mm.

And according to the calculation the total square steel pipe length required was approximated to be 12 m with the total weight of 640 kg .Other fixtures such as shaft, steering, steering arms, engine and hitch will be attached to the chassis also with the aid of different bolt sizes.

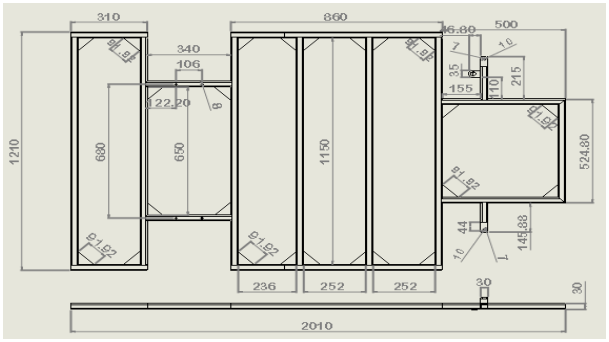

Fig. 5. Sketch of combined harvester chassis

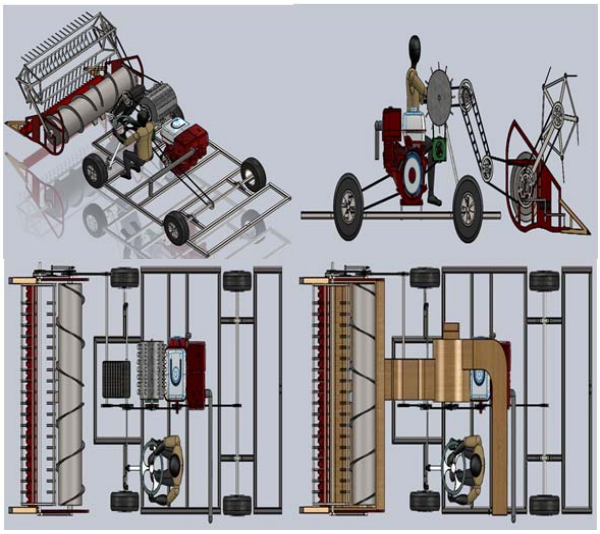

Fig. 6. Different Views of Combined Harvester Chassis and Components

4.3 Harvester body

One of the design requirement is to make the harvester compacted, the main body of the harvester was 1170 × 1008 × 440 mm at the front end (driver side) while the rest of the body was 2000 × 1220 × 440 mm. The body was designed using Mahogany and other attachments (such as conveyor cover, threshing housing and cutting bucket) using oak wood. A plastic sheet was also attached to the body in order to protect the storage unit and the engine during operation. Accessibility for engine maintenance was also considered which leads to provision of entrance door to the engine compartment. The storage unit was designed to be accessible both from inside and outside as may be required.

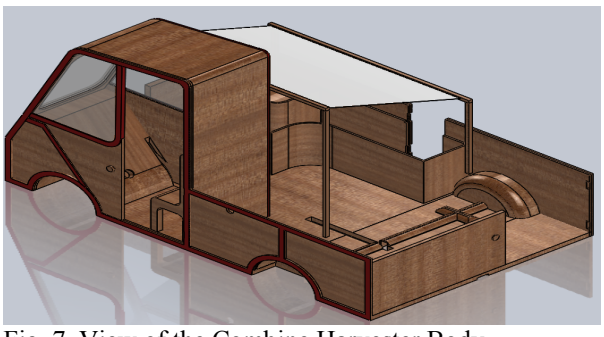

Fig. 7. View of the Combine Harvester Body

4.4 Machine operation system

The design adopted for the harvester was based on the existing designs but different in size, materials and cost. Major operating system of the harvester is made up of five compartments: The Header consisting of reeling unit, cutting unit, bucket and the auger. The feeder comprising the conveyor belt and driven roller. The Threshing unit consist of threshing drum, sieve and the blower. Transmission system unit which consists of Engine, shafts, Pulleys Belts, wheels and Hub, brakes and suspension system and finally, the storage Unit consisting of grain pan and cover.

The cutting and gathering process of the grain will be accrued from the reeling unit and cutting unit, which will then be conveyed from the auger to the feeder and presented to the threshing unit. The grain will be threshed at rotational force with the aid of threshing combs attached to threshing drum at line intervals. These threshing combs comprise of small rod made of metal called tongs and each of it is carved into small arc. The small clearance between the sieve and the comb will allow detachment of the grains

After detachment of the grains from the ears, the sieve will separate the grains directly to the storage and the straw will be blown out through the straw channel to the ground. Although, general threshing problem is either over threshed or under threshed. Over threshing, which could damage grains due to high speed of the thresher is taking care of by the speed of the engine but with possibility of fine straws escaping with the grains which can easily be cleaned later before storage. However, all these processes cannot be achieved without the transmission system.

For the suspension system, it is not generally necessary to have suspension in place for the harvester based on the design speed of the machine. The design is single axle back wheel drive with engine in the middle operating at the speed of 1-2 m/s. More so, the types of tyre and wheels used for the harvester were the most common car type which can provide certain amount of shock absorption on the road, reduction of unnecessary motion and support for the harvester weight.

The tires used for the harvester was common pneumatic type which can both change and maintain directions, it also allow tractions and brake force to the road surface. They will be mounted on the hubs welded to the axle in the front and shaft at the rear end. Apart from the tires, other components were fabricated at low cost.

Although, the harvester does not have standard braking system because of it speed but a provision for stopping mechanism was provided. The entrance door beside driver seat leads to the engine compartment for driver to have access to the engine at any point in time in case of emergency. Also, there is provision for hand lever near the driver seat link to the rear tires that can bring the harvester to a halt. The harvester will also have supportive components such as lightning, hitch, windows and shield cover and belts cover.

For the Hitch, it mechanism allow rotation of two axes in other to accommodate attachment such as furrows, seeders and rakers and possibly a trailer within the capacity range of 8-10 HP. The lightning will also provide good visibility during night time for farmer to work this is sourced directly from the engine coil unit while the shields and cover belt did not only provide protection for driver and the engine during bad weather conditions but also protect them from accident against foreign objects.

5. RESULT AND DISCUSSION

Calculations of stress, strain, deflection of the chassis and the total power required by the combine harvester was done. From the calculated results obtained, it was observed that the chassis will definitely withstand the design load.

The calculated stress, strain and deflection on the chassis using steel material AISI 1045 with yield strength of 530 MN/m^2, gave 1.7×10^4 N/m^2, $8.305x\ 10^{-8}$ and 1.76 mm respectively. The displacement of the chassis can be seen as negligible considering it with a higher factor of safety of 3.1 and compared with previous work of Abdulrahman [26] on static analysis on similar chassis with displacement of 5.57mm and a factor of safety of 1.7. The total calculated power required by the combine harvester was 12.34 kW (approximated to 13 kW) to cater for transmission losses.

The selection of material for the combine harvester was done with the aid of CES. It is an effective and precise tool that helps in arriving at an appropriate and cost effective material. The results obtained from the material selection are shown in the Table 2. From the power requirement of the combine harvester, the motor recommended and readily available in the market was a Honda G630 air cooled 4 stroke OHV petrol engines; electric starter of net power of 15.5 kW (20.8 HP)/3600 rpm.

6. CONCLUSION

This research has clearly demonstrated that it is quite possible to design for manufacture of a multipurpose mini combine harvester aimed at solving farmer's problem of harvesting and transportation in developing nations. The combine harvester is designed not only to harvest, thresh and store grains but also to drive other farm implements and used for irrigation purpose when engine is connected to a pump.

The calculated results obtained showed that the chassis was able to withstand the design load the harvester may be subjected to as long as high strength material is used for the chassis construction. The result also revealed a deflection of 1.76 mm when the chassis is subjected to maximum load, which it was safe to use considering a factor of safety of 3.1 incorporated in the design.

Finally, the materials that have been carefully selected for the combine harvester design were those available locally. Low price square hollow pipe have been used in the designed for construction of chassis. Other materials selected namely: plywood, polythene and plastics for vehicle body and single cylinder engine to drive the harvester could be sourced locally for

manufacturing. All these were attempted to ensure the cost of production was significantly reduced and the combine harvester is readily accessible to small scale farmers.

Components	Size (mm)	Materials	Density (kg/m^3)	Young Modulus (MPa)	Yield Strenght (MPa)
Chassis	30x30 × 2.6	AISI 1045 steel	7850	205000	530
Shafts	666.35 × 20	AISI 1045 steel	7850	205000	530
Conveyors	447x180	Natural rubber	930	1.2	21
Auger	1213 × 250	Carbon stainless steel (sheet)	7858	205000	282.69
Reels	1250 × 20	Cast iron	6800	172000	526
Cutter Blades	1165×120×10 1105×120×10	Tool steel	7600	206000	1680
Main Body	Various	Mahogany	640	10.60	49
Bucket	-	Oak	850	20600	43.2
Conveyor Cover	-	Oak	850	20600	43.2
Hitch	-	Cast iron	680	172000	526
Pulleys (Various)	Various sizes	Cast iron	680	172000	526
Bolts	Various sizes	Cast iron	680	172000	526

Table 2. Different Selected Materials for the Design [20]

7. REFERENCES

[1] Apata, T. G., Linkages between Crude-oil Exploration and Agricultural Development in Nigeria: Implications for relevant qualitative data collection and analysis to improve rural economy., 2010.

[2] Olajide, O. T., Akinlabi, B. H., and Tijani, A. A. *Agriculture Resource And Economic Growth In Nigeria*. 2012.

[3] Engineering Export Promotion Council (EEPC), Agricultural Machinery, Parts and Tractors Market in Nigeria., 2013.

[4] Talabi, S. O. and Onasanya, O. *Agricultural Introduction*. 2013 22/09/2014]; Available from: http://www.onlinenigeria.com/agriculture/?blurb=480.

[5] Faborode, M. O. Strategies for sustainable National Agricultural Infrastructures Development. in Sustainable Engineering Infrastructures development. Port Harcourt: The Nigerian Society of Engineers,2001.

[6] Akande, L. O., Empowerment of the Rural People through Agricultural Mechanization, Osun State College of Education, 2006.

[7] Lamidi, W. A. and Akande, L. O., A Study of Status, Challenges and Prospects of Agricultural Mechanization in Osun State, Nigeria. 1(1): p. 001-008, 2013.

[8] Takeshima, H. and Salau, S., Agricultural Mechanization and the Smallholder Farmers in Nigeria; Nigeria strategy support program, 2010.

[9] Abdulkareem, Y. A., Indigenous Technology, Past, Present and Futures, in Workshop for the Processing Of Raw Materials: Raw Materials Research and Development Council, 1992.

[10] Adamade, C. A. and Jackson, B. A., *Agricultural mechanization: a strategy for food sufficiency*. Scholarly Journal of Agricultural Science. 4(3): p. 152-156, 2014.

[11] Asoegwu, S., Agricultural Field Implements and Mechanization., 1998.

[12] André-Michel, E. Despite recovery, Africa needs more jobs, says ECA. 2016.

[13] Quick, G. R. and Buchele, W. F., *The Grain Harvesters.* American society of agricultural engineers., 1978.

[14] Olukunle, O. T., *Developments in Grain Harvesting Mechanisation.* Journal of Agricultural Engineering and Technology (JAET). 18(1), 2010.

[15] AMRI, *Test Report Indian Combine Harvester SWARAJ-8100*, Agricultural Mechanization Research Institute (AMRI), Multan Government of the Punjab, Lahore, 2014.

[16] Ademosun, O. C., Adewumi, B. A., Olukunle, O. J., and Adesina, A. A., *Development of Indigenous Machines for Weeding and Grain Harvesting: FUTA Experience.* . FUTAJEET 3(2): p. 77-84, 2003.
[17] BioSat Agricultural Biomass Sources. 2016.
[18] Karande, O., Gauri, S. K., and Chakraborty, *Applications of Utility Concept and Desirability Function for Materials Selection.* Material and Design Journal 45: p. 349-358, 2012.
[19] Shackelford, J. F., *Introduction to Materials Science for Engineers*. Fifth ed.: Prentice Hall, 2000.
[20] Granta, *Cambridge Engineering Selector (CES)*, Granta Design Limited, UK, 2014.
[21] Childs, P. R. N., *Mechanical Design*. Second ed.: Oxford: Butterworth-Heinemann, 2003.
[22] Khurmi, R. S. and Gupta, J. K., *A Textbook of Machine Design*. Ram Nagar, New Delhi: Eurasia Publishing house, 2005.
[23] Pahl, G., Beitz, W., Feldhusen, J., and Grote, K.-H., *Engineering Design: A system Approach*. Third ed., London: Springer-Verlag 2007.
[24] Sapuan, S. M., A knowledge-based system for materials selection in mechanical engineering design. Materials & Design. 22(8): p. 687-695, 2001.
[25] Honda *Engine Models*. 2016.
[26] Abdulrahman, K. O., Design of Low-Cost Vehicle for Nigerian Rural Farmers for Transportation of Farm Produce, 2014.

Authors: **Researcher. Mr Kazim Olawale Abdulkarim**, Department of Mechanical Engineering, University of Derby, Derby. DE22 1GB, UK. +447553081438. **Lecturer. Mr Kamardeen Olajide Abdulrahman,** Department of Mechanical Engineering, University of Ilorin, P.M.B. 1515, Nigeria, +2348061596252. **Lecturer. Dr Ismaila Idowu Ahmed,** Department of Materials and Metallurgical Engineering, University of Ilorin, P.M.B. 1515, Nigeria, +2347018271354. **Lecturer. Sulaiman Abdulkareem,** Department of Mechanical Engineering, University of Ilorin, P.M.B. 1515, Nigeria, +2348058219222. **Lecturer. Mr Jeleel Adekunle Adebisi,** Department of Mechanical Engineering, University of Ilorin, P.M.B. 1515, Nigeria, +2348030422330. **Lecturer. Dani Harmanto,** Department of Mechanical Engineering, University of Derby, Derby. DE22 1GB, UK, +447773057610.
E-mail: zeem2002@yahoo.com
olajideabdulrahman@yahoo.com
ismaila.ahmed@yahoo.com
sulkarm@yahoo.com
adebisijeleel@gmail.com
d.harmanto@derby.ac.uk

http://doi.org/10.24867/JPE-2017-01-063

Journal of Production Engineering

Vol.20 No.1

JPE (2017) Vol.20 (1) Original Scientific Paper

Panda, S.B., Nayak, N.C., Mishra, A.

ENGINEERING POLYMERS IN AUTOMOBILE SEAT BELT LOCK APPLICATIONS: IT'S DEVELOPMENT, INVESTIGATION AND PERFORMANCE ANALYSIS

Received: 22 January 2017 / Accepted: 10 April 2017

Abstract: *Almost all vehicles use seat belts for occupant's safety. The seat belt locking system consists of buckle assembly where the tongue plate enters the buckle assembly and locks automatically. The tongue plate is made by over molding injection process to a metal plate, which requires two distinct & different process techniques to produce. In this research, the tongue plate is completely redesigned into a single piece injection molded part replacing the sheet metal part. The parts are produced using 'Delrin' and 'Nylon 6-GF 30%' material separately by injection molding machine strictly following the International standard. Then, pertinent data were collected from mold flow analysis. The injection molding process is used to produce the component as a single part, which eliminates the sheet metal process, hence eliminating sheet metal die, process, post finishing operations, inventory etc. that reduces production cost, time and multiple numbers of parts. The tongue plate which is made by sheet metal and then polymer is being over molded into it, increases the process cost and also the chance of QC failure. This research concludes that the tongue plate may be produced as a single injection molded part with high accuracy, finish, strength and at a lower cost.*

Key words: *injection molding, mold flow analysis, composites, derlin, nylon, strength*

Inženjerski polimeri primenjeni u automobilskoj bravi za pojaseve: njihov razvoj, istragživanje i analiza performansi. *Skoro sva vozila koriste pojaseve za bezbednost putnika. Sistem zaključavanja pojaseva se sastoji od kopče pojasa gde jezičak pločice ulazi u sklop kopče i automatski se zaključava. I jezičak pločice je napravljen preko procesa oblikovanja na metalnu ploču, koja zahteva različite tehnike procesa proizvodnje. U ovom istraživanju, jezičak pločice je kompletno redizajniran i u jednom komadu dobija se brizganjem i zamenjuje presovan metalni deo. Delovi su proizvedeni upotrebom "delrin" i "Nilon 6-GF 30%" materijala posebno na mašini za brizganje strogo poštujući međunarodne standarde. Zatim, su relevantn podaci prikupljeni iz analize protoka kalupa. Proces brizganja se koristi za proizvodnju komponenti kao jedan deo, koji eliminiše proces dobijanja iz lima, kalupe, završne operacije, inventar i sl što smanjuje troškove proizvodnje, vreme i višestruki broj delova. Jezčak pločice se sastoji od lima, preko koga se zatim uliva polimer, povećava troškove procesa i istovremeno je daje šansu za lošiji kvalitet. Ovo istraživanje zaključuje da se jezičak pločice može dobiti kao jedan deo ubrizgavanjem sa visokom preciznošću, završnim oblikom, odgovarajućom čvrstoćom i po nižoj ceni.*

Ključne reči: *brizganje, analiza protoka kalupa, kompozit, derlin, najlon, čvstoća*

1. INTRODUCTION

Composite materials have been the better substitute for past few years ranging from everyday products to sophisticated engineering applications. At present high performance FRP, engineering plastics can be used to resist explosive impacts, automotive applications, windmill blades, industrial drive shafts, support beams of highway bridges and even paper making rollers. In certain applications, composites have replaced metals that resulted in saving both cost and weight. Particularly in automotive industries it has a great impact to save the fuel and subsequently increasing the performance.

The seat belt lock system consists of buckle assembly, tongue plate, knit fabric belt as shown in fig. 1. The tongue plate is made of steel and then over molded with polymer. It may so happen that the 'tongue plate' will be made of a single piece injection molded part, avoiding the sheet metal one, as many stages of operations could be eliminated such as the sheet metal production process, post finishing operation, surface treatment, inventory, etc. Moreover, the cost and time could be saved to a great extend also.

The objectives of this research work is to redesign and test using various CAE software to arrive at a single piece optimum design which could be produced as a single shot injection molded part. It should possess greater strength and practical application condition that finally could replace the existing part. As seat belt is meant for safety of the occupants during accidents, so special attention need to given towards achieving the strength and durability of the part.

Though there exist many polymers, engineering polymers, and high performance polymers (HPP), composites are widely used for automobile components where some of them also replace metals. In this research, we have taken four types of composite polymers for the discussed part aiming to replace the metal part.

2. LITERATURE REVIEW

From the existing literature, it is observed that

research has been done on composites especially for automobile applications to replace metal components. High Performance polymers and engineering plastics is used to get the advantages such as corrosion resistance, better durability, high strength related to weight, design flexibility, dimensional stability etc.

Airbus Helicopters door fitting bracket is replaced by injection molded fiber-reinforced high performance polymer instead of aluminum, resulted a 40% reduction in weight and costs [1]. Researcher claims that injection molded glass fiber reinforced phenolic cylinder housings deliver the same performance as die cast aluminum components. They suggests that the composite casing delivers a weight reduction of up to 20% and manufacturing costs are approximately 10% lower. In addition, life cycle assessments demonstrate that the environmental impact of phenolic composite components over their entire lifetime is lower than that of aluminum alternatives [2]. Researcher [3] suggests an experimental vehicle engine featuring fiber-reinforced plastic (FRP) parts that could be lighter than aluminum. The engine parts, such as the cylinder casing, could shed up to 20% of its weight if it was made of fiber-reinforced plastic rather than aluminum, without extra costs. The injection-molded parts could even be suitable for mass production. Fiber reinforced thermoplastic composites produced by injection molding process could be used for aircraft fuselage clips and brackets [4]. The less mass it carries around, power train has to work less, and with less fuel use. In other words, for every one percent reduction in mass, we gain half a percent in fuel economy [5]. Metal replacement saves weight from 35% - 50%, eliminates material waste, reduces secondary operations which could be possible with single shot molding process. The above has advantages over simple loaded metal parts [6]. The brazed metal manifold components swapped out for V6 engines with a lightweight plastic part made from Nylon composites family that reduce weight and cost [7]. Automotive industry growth is being driven by the continued focus on lightweight construction, greater fuel efficiency and lower emissions, which is possible with carbon fiber reinforced plastic (CFRP) components [8]. High performance polymers (HPP) used to replace metals in the automotive industry that offers specific strengths, chemical resistance over metals. These materials could be low cost solutions to fuel tanks in past. High temperature capable HPP's (up to 300° C) exhibit outstanding friction and wear performance, used in applications like replacing metal-polymer bushings with a full polymer solution [9]. Metal components could replace with lighter plastics such as fiber reinforced nylon family products that are durable in high-heat, harsh-chemical environments found in under hood applications [10]. Composite materials offer their light weighting benefits than steel and aluminum. Using glass-filled polypropylene (PP) one can replace a more expensive metal version of door module [11]. In an experiment, the feasibility of replacing the metal coil spring with the composite coil spring has been demonstrated [12]. Metal replacement to engine cover components using mineral-reinforced nylon resin and Zytel nylon resin for two cast-aluminum parts resulted in less weight and cost, without affecting function or performance [13]. Fibers are used to strengthen thermoplastic compounds, improving physical properties such as modulus, tensile strength, heat deflection temperature and dimensional stability. The fiber reinforced thermoplastics continues to replace metals for better performance. Well-known advantages of thermoplastics over metals include design freedom, reduced weight and corrosion resistance [14]. The study demonstrated that elliptical spring made of composites can be used for light and heavy truck suspension systems with substantial weight saving [15]. Another study find composites to have significant economic potential when considering the polymer composite body-in-white design against the mild-grade steel body that serves vehicle light-weighting and thereby improved fuel efficiency [16]. Palmyra fruit fiber reinforced composite has been developed and its strength has been tested for automobile applications [17]. A four-leaf steel spring at rear suspension system of light vehicles can be replaced with a composite made from fiberglass with epoxy resin [18].

3. THEORY & METHODOLOGY

In this research, the tongue plate (Fig. 1) is completely redesigned to a single piece injection molded part replacing the sheet metal and subsequently its process, post finishing operations. It eliminates sheet metal die, post finishing, operation time, reducing the cost of the product, its weight and increasing the performance of the seat belt locking system. Various steps for manufacturing the lock are as follows:

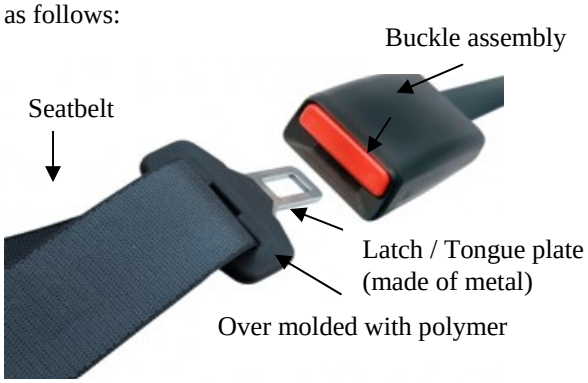

Fig. 1. Seat belt locking

3.1 Part Design

The tongue plate made up of sheet metal is to be prepared from polymer and over molded into it, made into a single part, which is designed & validated by the ProE & Mold Flow software. The part is first designed by ProE with all engineering validations such as tensile strength, load carrying capacity, etc.

The 3D CAD model is developed by ProE by considering all the dimensions with reference to the existing buckle assembly, and then little modifications incorporated to improve the strength at the load application areas, as shown in Fig. 2(a). Fig. 2(b) show detail drawings, being generated to check & validate the 3D CAD model.

(a) 3D CAD model

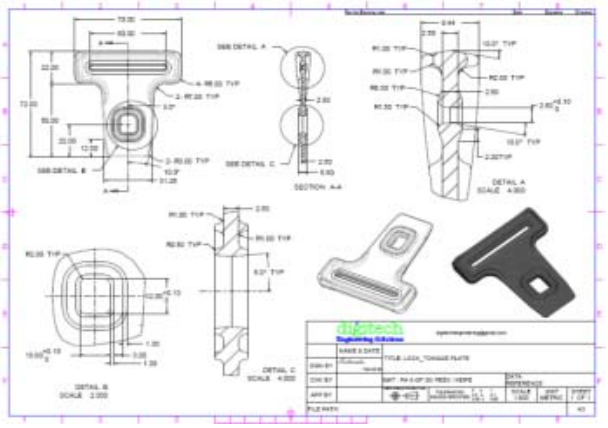

(b) 2D detail drawing

Fig. 2. Tongue plate

3.2 Mold Design

Injection mold is designed with Pro-E software and subsequently the tool drawings are created for mold manufacturing. CNC machining of core, cavity and other parts of the mold is being made to get the complete mold. Simultaneously an UTM sample piece is also being designed within the mold to carry out the tensile test of the part. This is being done to get the accurate results of the tongue plate part as the same processing parameters are involved for both the parts, as shown in Fig. 3 (a) & (b). Fig. 3 (c) & (d) shows the details of the mold prepared to manufacture seat belt lock.

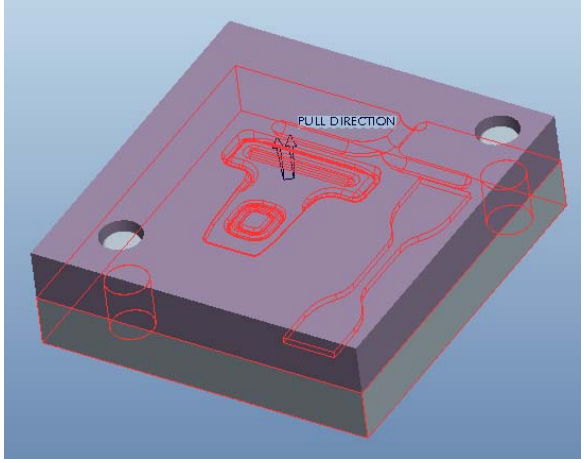

a) 3D Mold design assembly

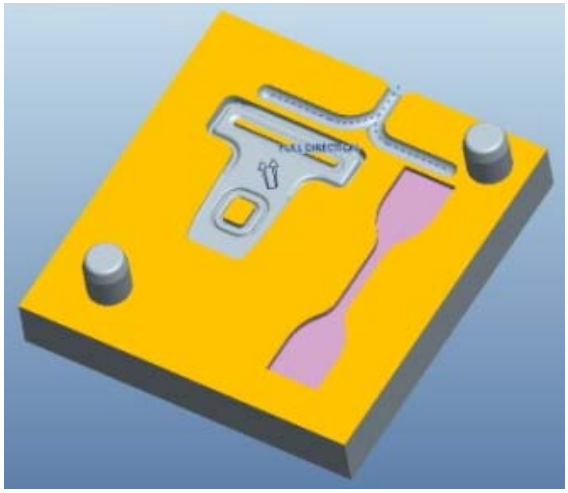

(b) 3D CAD of Cavity plate

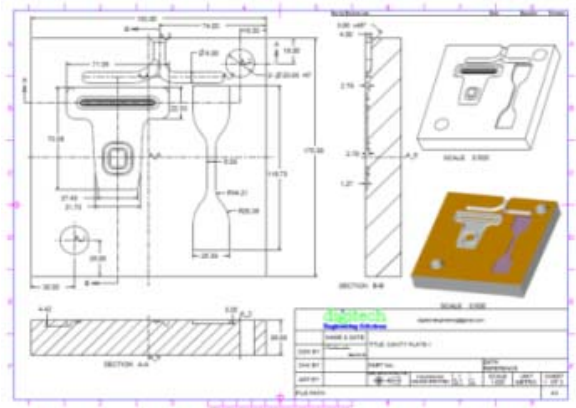

(c) Detail drawing of mold cavity plate

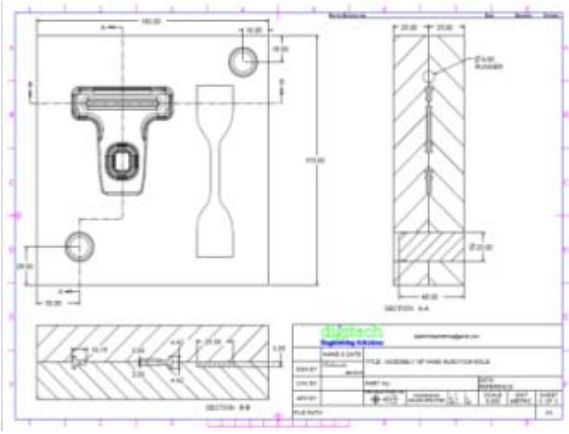

(d) 3D detail drawing of mold assembly

Fig. 3. Mold design

3.3 Analysis & Optimization

As new and advanced technology/software is available to validate the digital model prior to manufacturing, one should take advantage of that. While the part is being designed by the software, concurrently analysis followed by optimization being carried out to get the best engineered part. Thus, one can save much more cost & time carrying out this project.

3.1.1 Mold Floww Analysis

As the part is going to be injection molded in a single shot, so it need to carry out the required

analysis to predict the possible injection molding process difficulties in advance. The 'Mold Flow Plastic part advisor' is used here to validate injection molding process parameters. Many trials have been taken for gate location, and other parameters, and then the results for the mold flow analysis are shown in Fig. 4, as above.

(a) Flow Front Temperature: As shown in fig. 4 (a), the part shows with red in color has the maximum temperature during filling and gradually reduced to minimum at the blue color areas. So that we can decide the cooling circuits accordingly.

(b) Sink marks: As shown in fig. 4 (b), the part shows the sink mark severity in the color code red as maximum and blue gradually minimum, but there is no red color marking area. Though sink marks are present over at the extreme ends of the part, we need to give extra care to those areas by cooling first over to those portions then to other areas of the part.

(c) Weld lines: The most important criteria are how the polymer melts and supposed to join inside the mold during packing or filling. As shown in fig. 4 (c), the weld lines are in 2-3 places, which have been minimized by several attempts to gate location & other technical parameters.

(d) Air traps: If the air in the mold cavity is being trapped, so there is the chance of voids present inside the part, which weakens the quality & durability of the part during application. So it is needed to give air escape passages with respect to the air trap points, as shown in fig. 4(d).

Moreover, we can conclude that the mold flow analysis is done to a great extent to optimize the process parameters to design and validate the part for the injection molding process.

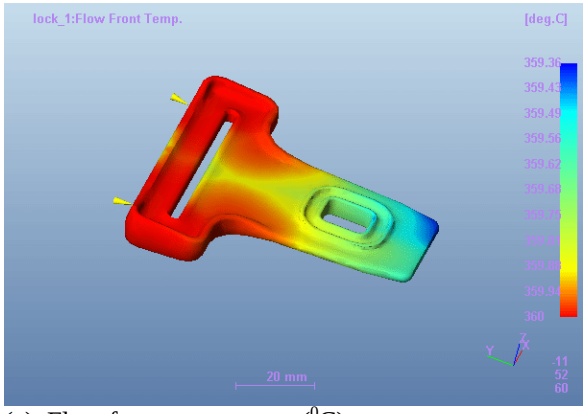

(a) Flow front temperature (^{0}C)

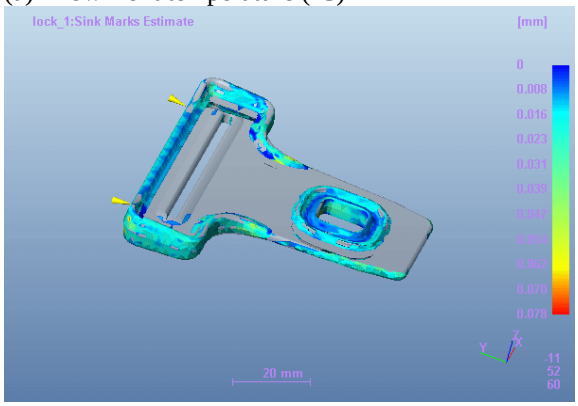

(b) Sink marks

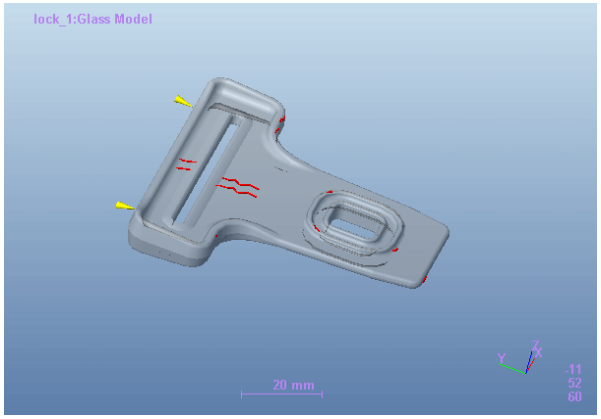

(c) Weld lines

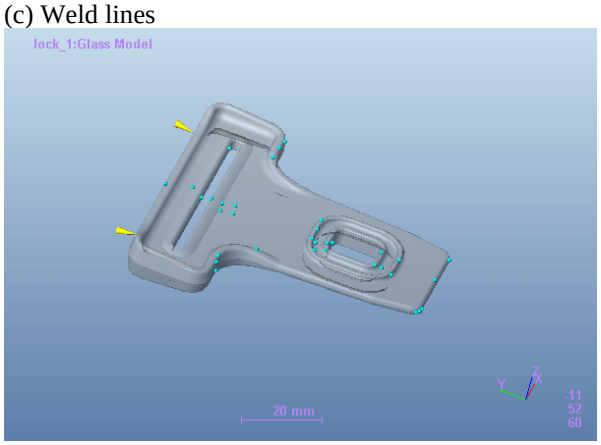

(d) Air traps

Fig. 4. Mold Flow analysis

3.4 Mold Cavity Manufacturing

Once the mold design is over followed by the mold flow analysis with satisfactory optimization of the part design & mold design, then it is time to manufacture the mold. Out of 3D CAD data, CNC programming has been done for CNC machining operations to prepare the complete mould (Fig. 5).

(a) Cavity machining

(b) Final machining

Fig. 5. Mold manufacturing

Fig. 6. Mold trial setup

3.5 Part Production

To get the defect free parts out of the injection molding process we had carefully maintained the intended process parameters for the particular polymer materials as specified by the IS manufacturers (Fig. 6). The process parameters maintained for manufacturing seat lock from four different polymers are as provided in Table 1.

Process parameters	POM GF 30	PA6 GF 30	PA66 GF 30	PP GF 30
Injection Pressure(MPa)	110	85	70	80
Injection Temp. (^{0}C)	210	260	280	240
Melt Temp. (^{0}C)	178	221	260	210
Injection Time (sec.)	3	2	3	2
Clamping force (tone)	105	80	65	75
Cycle time (sec.)	5	4	5	5

Table 1. Injection molding process parameters

Fig. 7. Part production

The parts get produced using all the four materials separately by injection molding machine strictly following the data in Table 1, using ‘mold flow analyses’.

4. RESULTS & DISCUSSION

The seat lock which is made of four different engineering polymers has been undertaken different tests for the durability of the product as shown in Fig. 8.

Though all the composite polymers shown satisfactory results, but PA6GF30 has better results as compared to all the rest 3 types of polymers in all respects.

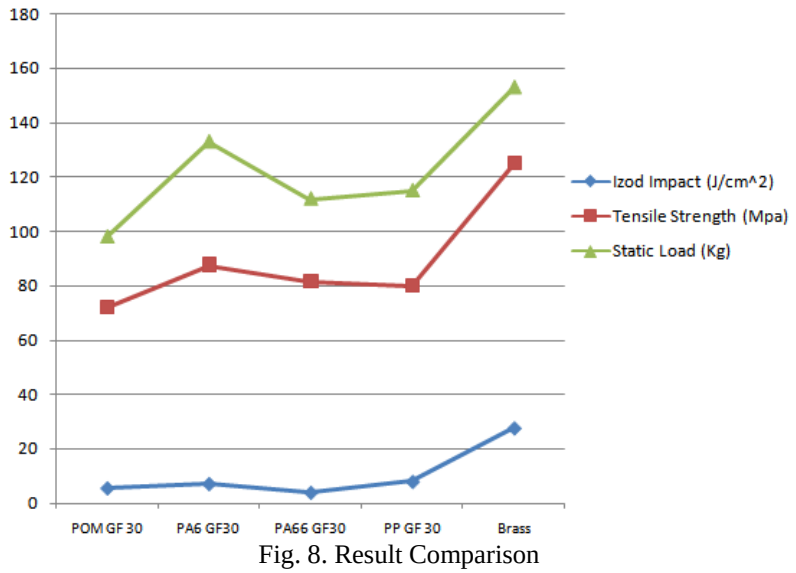

Fig. 8. Result Comparison

5. CONCLUSION&SCOPE OF FUTURE WORK

The tongue plate which is made of complete injection molding process has significant result that has replaced the existing metal with polymer over-molded part. The above eliminates the sheet metal process & cost for finishing the product. It also reduces the chances of rejection of QC failure using optimization technique. This also reduces the post finishing operations on sheet metal press part. Moreover, this research manufactures and tests the tongue plate which has been produced as injection molded component as a single finished part with same strength as earlier seat locking system.

5. REFERENCES

[1] Wolf, C. 40% weight reduction with carbon fiber part, *Reinforced Plastics*, Vol. 59, No. 6, pp. 258–259, 2015.

[2] Austin, T., Morgan, F., Keyser, H.D., Caliendo, H., and Farish, M. Composite future for cylinder housings, *Reinforced Plastics*, Vol. 59, No. 4, pp. 152–153, 2015.

[3] Berg, L.F., Koch, B. and Niesing, B. FRP engine parts could reduce vehicle weight, *Reinforced Plastics*, Vol. 59, No. 4, pp. 154-163, 2015.

[4] Gardiner, G., Herr, T. and Kneath, T. Overmolding expands PEEK's range in composites, *Composites World*, Vol. 1, No. 7, pp. 19-21.

[5] Murray, C. Carbon Fibers Spearhead Automotive Light weighting Effort, *Science Journals: Design news*, Vol. 70, No. 7, pp. 42-42, 2015.

[6] Eby, J., Schenk, G., Labatut, V. and Schenk, G. Tweed and Aerolia validate thermoplastic composite replacement for complex-shape metallic, *Reinforced Plastics*, Vol. 21, No. 3, pp. 32-38, 2014.

[7] Hopperton, L., Granowicz, P. and Terrell, T. Plastic manifold to feature on Ford's latest V6 engine, *Eureka Engineering Design*, Vol. 12, No. 1, pp. 12-19, 2014.

[8] Jacob, A. and Gray, N. Carbon fibre and cars - 2013 in review, *Reinforced Plastics*, Vol. 58, No. 1, pp. 18–19, 2014.

[9] Gurchinoff, S., Fish, D. and Stern, B. High Performance Polymers for Small Engine Applications, *Engineering Design*, Vol. 11, No. 3, pp. 52-69, 2013.

[10] LeGault, M., Conkey, J., Schlicker, S., Newill, B. and Conkey, S. High-temp Thermoplastics: Higher expectation, *Composite world*, Vol. 18, No. 5, pp. 26-28, 2012.

[11] Stewart, R. and Bowland, C. Automotive composites offer lighter solutions, *Reinforced Plastics*, Vol. 54, No. 2, pp 22–28, 2010.

[12] Budan, D.A. and Manjunatha, T.S. Investigation on the Feasibility of Composite Coil Spring for Automotive Applications, *International Journal of Mechanical, Aerospace, Industrial, Mechatronic and Manufacturing Engineering*, Vol. 4, No. 10, pp. 1035-1039, 2010.

[13] Ederlan, F. and Ghosn, C. Nissan replaces metal engine covers, *Reinforced Plastics*, Vol. 52, No. 6, pp. 4-13, 2008.

[14] Markarian, J., Eckert, C., Hoppe, K. and Watkins, C. Strengthening compounds through fiber reinforcement, *Reinforced Plastics*, Vol. 51, No. 2, pp. 36–39, 2007.

[15] Goudah, G., Mahdi, E., Talib, A.R., Mokhtar, A.S. and Yunuset R. Automobile Compression Composite Elliptic Spring, *International Journal of Engineering and Technology*, Vol. 3, No.2, pp. 139-147, 2006.

[16] Fuchs, E.R.H., Field, F.R., Roth, R. and Kirchain, R.E. Strategic materials selection in the automobile body: Economic opportunities for polymer composite design, *Composites Science and Technology*, Vol. 68, No. 9, pp. 1989-2002, 2005.

[17] Nayak N. C. and Mishra A, Development and mechanical characterization of Palmyra fruit fibre reinforced epoxy composites, *Journal of Production Engineering*, Vol. 16. No. 2, pp. 69-72, 2013.

[18] Mahmood M.S. and Rezaei, D. Analysis and optimization of a composite leaf spring, *Composite Structures*, Vol. 21, No. 2, pp. 23-29, 2003.

Authors: **Sudhanshu B. Panda,** Research Scholar in Mechanical Engineering Department, Indira Gandhi Institute of Technology (An Autonomous Institute of Govt. of Odisha), Sarang, India - 759146.

Ph D Narayan C. Nayak, Reader in Mechanical Engineering Department, Indira Gandhi Institute of Technology (An Autonomous Institute of Govt. of Odisha), Sarang, India - 759146. (Corresponding Author)

Ph D Antaryami Mishra, Professor in Mechanical Engineering Department, Indira Gandhi Institute of Technology (An Autonomous Institute of Govt. of Odisha), Sarang, India - 759146.

E-mail: sudhanshu.panda@gmail.com
nayak.iem@gmail.com
igit.antaryami@gmail.com

http://doi.org/10.24867/JPE-2017-01-069

Journal of Production Engineering

Vol.20 No.1

JPE (2017) Vol.20 (1) Original Scientific Paper

Adegbola, J. O., Adedayo, S. M., Ohijeagbon, I. O.

DEVELOPMENT OF COW BONE RESIN COMPOSITES AS A FRICTION MATERIAL FOR AUTOMOBILE BRAKING SYSTEMS

Received: 06 March 2017 / Accepted: 18 April 2017

Abstract: *Cow bone resin composites as a friction material for automobile breaking systems have been developed. Increasing interfacial bonding was observed as the cow bone particle size decreased from 850 to 250 µm, resulting in better mechanical properties of brake pads produced with 250µm particle size relative to higher particle sizes investigated. Experimentally produced brake pads with cow bone composites were found to compare favourably with conventional brake pads and those from previous studies; consequently, cow bones particles are suitable replacements for asbestos-free brake pad due to the fact that asbestos dust poses health hazards.*

Key words: *cow bone, breaking system, brake pad composites, asbestos-free*

Razvoj kompozita od kravljih kostiju kao frikcioni materijal za kočioni sistem automobila. *Razvijeni su od kompozita od kravljih kostiju kao materijala za automobilske kočione sisteme. Povećanje međusobnog vezivanja je primećeno kod obloga od kravlje kosti sa smanjenjnjem veličine čestica od 850 do 250 µm, što rezultira boljim mehaničkim svojstvima kočionih pločica proizvedenih od veličine 250µm čestica u odnosu na veće veličine ispitivanih čestica. Eksperimentalno je utvrđeno da kočnice proizvedene od kompozita od kravlje kosti su bolje u poređenju sa konvencionalnim kočionim pločicama iz prethodnih studija; prema tome, kočnice od kompozita od kosti krava su odgovarajuća zamene za azbestne kočnice zbog činjenice da azbest prašina postavlja opasnosti po zdravlje.*

Ključne reči: *kravlje kosti, kočioni sistem, kompozitne obloge, bezazbestne*

1. INTRODUCTION

Automobile friction pads are of very high significance in braking systems, and are one of the most important safety and performance systems in automobiles. It is essential for all types of vehicles that are equipped with brake disc. Brake pad is a friction material typically attached to a metal backing plates with rivets or high-temperature adhesives facing the brake disc [1, 2]. Brake pads convert the kinetic energy of a car to thermal energy through friction, thereby fading-out due to operating wear and tear. This makes it one of the most commonly replaced components in the brake system [3]. Components of the brake pad are the lining materials, which are categorized as metallic, semi-metallic, organic and carbon-based, depending on the composition of the constituent elements. Typical formulations consist of different ingredients; however, exact compositions of commercial friction materials are rare in open literature [2, 4]. Ingredients used for brake pads can be grouped as binders, reinforcing fibres, fillers, and frictional additives, based on the major function they perform which includes controlling friction and wear performance. The binder is used to hold the ingredients together, to maintain structural integrity of the brake pads subjected to mechanical and thermal stresses; the structural materials provide the structural reinforcement to the composite matrix; the fillers make up the free volume of the brake lining; and the friction modifiers stabilize the coefficient of friction and wear rates [5].

In the past, asbestos was the standard brake pad material. The composition generally consists of asbestos fibres embedded in polymeric matrix along with other ingredients. It offers good friction qualities, long wear, and low noise. But new materials are being used because of the health hazards of asbestos dust [6]. The use of asbestos fiber is been avoided due to its carcinogenic nature and related asbestos-induced diseases, such as malignancies, asbestosis, lung cancer and pleural mesothelioma [7, 8, 9]. Therefore it is imperative to develop an asbestos-free friction material as brake pads.

Different studies have been carried out in the area of development of asbestos-free brake pad. The use of periwinkle, coconut shell, banana peel, palm kernel shell (PKS) has been developed for asbestos free brake pads materials. The trends in researches are focusing on ways of utilizing either industrial or agricultural wastes as source of raw materials in the industry. [2, 3, 4, 5]. Several benefits have been discovered in employing alternative constituent materials for brake pad production amongst others. Bhane *et al.* [10] proposed combining two or more materials to determine the tribological properties for brake pad material in order to develop alternatives to conventional materials that would result in composite materials of lower cost, reduced weight and increased life of brake materials. Keskin [11] investigated the use of natural zeolite in brake pad production by adding different amount of zeolite in the mix of other regular ingredients in brake pad production. Zeolite contains silica which gives the pad materials a ceramic like behavior. The friction assessment and screening test (FAST) conducted by

Keskin [11], shows that the sample with 10% zeolite rate provided higher friction coefficients, because its wear ratio and standard deviations were considerably lower; while lower value of friction coefficients were obtained for 30 and 35% zeolite. Similarly, fly ash obtained from power plant in Neyveli Lignite Corporation was used by Vijay *et al.* [12] to incorporate 50%wt of fly ash particles in automotive brake lining friction composites; and developed brake lining composites was found to exhibit consistent coefficients of friction in the range of 0.3-0.4, and wear rates lower than 12%wt. Also, the selection and production of composite brake pad with varied constituent's composition was investigated by Dan-Asabe *et al.* [13] to determine the tensile, compressive, hardness, impact, wear and corrosion to ascertain composition with the optimum property compared with a commercial Honda brake pad (Enuco) model widely used in Nigeria. Asabe *et al.* [13] observed that higher percentage of grounded coconut shell powder induces brittleness, and lower percentage produced higher breaking strength and lower wear rate.

Cow bones constitute a waste in developing countries. In the rearing and consumption of cows, cow meat is considered a major source of protein, while cow bone is bio-degradable, free from asbestos molecules, ecologically friendly and consists of high strength. Consumption of cow meat on a daily basis is very high and as a result most of the cow bones are discarded as waste in most abattoirs in Nigeria [14]. Development of a sustainable raw material for production of brake pads will contribute in addressing global climatic problems and several socioeconomic related issues. This work is aimed at developing a new asbestos-free friction brake pad which is environmentally friendly using cow bones as the base material.

2. EXPERIMENTAL PROCEDURES

2.1 Materials and equipment

The materials and equipment used in this study are: phenolic resin (phenol formaldehyde), cow bones, engine oil (SAE 20W/50), water, designed brake pad mould, band heater, digital weighing balance, a set of sieves, digital weighing machine, bunsen burner, polisher machine with load, inclined planes and computerized metallurgical microscope. The chemical compositions of cow bones comprises of 23.326% calcium and 2.602% Iron [15].

2.2 Production of brake pad composites

Cow bones as sourced from the abattoir in Ilorin, Nigeria was washed, cleaned and sun dried for 21 days, followed by oven drying at 105°C for 5 hours until the moisture and oil content was almost completely eliminated. The dried bones were then charged into a hammer mill that reduces the size of the bones into smaller particle sizes [16]. The product was transferred into a set of sieve of; +850 µm, +500 µm, +250 µm. While the oversize of +850µm was returned or recycled for regrinding until it passes through the sieves.

Grinded bones with particle sizes of 250 µm, 500 µm and 850 µm, were mixed with the 35%wt phenolic resin. Digital weighing balance was used for precision weight measurements. Twenty five (25) test samples from each of the sieve size were then produced. Each composition was blended homogeneously. The mixed samples were then transferred to the designed mould kept at a temperature of 150^{o}C. Mixtures were compacted at a pressure of 15MPa for 2 minutes using a 1560KN unaxial, hydraulic compression machine. Mould surface was polished with mould-releasing agent prior to loading to ease removal of produced composite from the mould. At the end of the hot-pressing process, the composite brake pad samples were taken out of the moulds, allowed to cool at room temperature, and cured in an oven at a temperature of 120^{o}C for 8 hours [16, 17, 18].

2.3 Physical characteristics and mechanical tests procedure

2.3.1 Brinell hardness test

The resistance of the composites to indentation was examined through the hardness testing equipment based on BS240. A Tensometer was used to press a hardened steel ball with diameter D into a test specimen. Based on ASTM specification, a 10 mm diameter steel ball was used, and the load applied P was kept stable at 3000 kgf. The diameter of the indentation d was measured along two perpendicular directions, using an optical micrometer screw gauge. The mean value was taken and incorporated into equation 1 to obtain the Brinell Hardness Number (BHN) [5].

$$BHN = 2P \div \pi D(D - \sqrt{D^2 - d^2}) \qquad (1)$$

P is the load applied, D is the diameter of hardened steel ball into a test specimen and d is the diameter of indentation.

2.3.2 Coefficient of friction

Each sample of produced brake pads with different sieve sizes was placed on inclined plane of known angle and a 90^{o} wedge. Wedge of a known height was positioned and varied to increase the angle of inclination until specimen was just about to slide down the plane. Equation 2 was used to calculate resulting coefficient of static friction [5].

$$\mu = \tan\theta \qquad (2)$$

where, θ is an angle of repose at instant of sliding

2.3.3 Water and oil absorption test

The water and oil (SAE 20W/50) absorption of the samples were determined by soaking the samples in water and oil for 24 hours. The initial weight of each specimen was taken and recorded as W_0 before soaking in engine oil and water. After 24 hours, specimens were brought out of oil and water, thoroughly cleaned to remove water and oil on surfaces, reweighed and recorded as W_1. Differences in initial and final weights for each specimen were then used to determine absorption rate [2, 4-5].

$$\text{Absorption rate}\,(\%) = \frac{W_1 - W_0}{W_0} \times 100\% \qquad (3)$$

2.3.4 Flame resistance test

The flame resistance of the samples was carried out by placing produced samples on wire gauze positioned directly on the blue flame of a Bunsen burner. The sample weight before and after burning was taken after 10 minutes and was used in obtaining the percentage of flame resistance [2, 3, 4, 5].

2.3.5 Wear characteristics

The wear characteristics were determined using a polisher machine with load. The set up was similar to the concept of the pin-on-disc test. The tested samples have a dimension of 40mm in diameter and 10mm in height. The samples were placed in the rotating wheel of the polisher machine. All tests were conducted at room temperature. The pin with a 8mm diameter with a load of 10N was placed on each sample rotating with a speed of 100rpm. The samples were weighed before and after testing to determine weight loss within an accuracy of 0.0001mg. Wear rates was determined using equation 4.

$$\text{Wear rate} = \frac{W_a - W_b}{S} \qquad (4)$$

where, W_a is initial weight and W_b is the final weight after wear.

2.3.6 Density test

The ASTM standard D792-00 specification was used to calculate the density of the composite specimens. A clean sample is weighed accurately in air using an electronic pocket scale model: EHA901, and then suspended in water. The weight of the sample when suspended in water was determined, and the volume of the sample was determined from the effect of displacement by water [19].

$$\text{Density}, \rho = \frac{M}{V} \qquad (5)$$

where, M is the mass of test piece (g) and V is the measuring volume of test piece (cm^3) by liquid displacement method.

2.3.7 Morphological test

The microstructural examination of the samples was carried out by grinding the samples using 200, 300, 400, and 600 grit papers respectively. Dry polishing was then carried out on the samples and the internal structures were viewed under the computerized metallurgical microscope [2].

3. RESULTS AND DISCUSSIONS

3.1 Results

The friction brake pads developed were subjected to various tests; these are hardness, water and oil absorption, wear characteristics, flame resistance, density and microstructural examination. The results of tests carried out were analyzed to determine the potential of the asbestos free brake pad for application as a brake pad material. The test results were compared with corresponding properties of conventional asbestos based brake pads and from previous studies. The results made clear the effect of the physical and mechanical constituent properties of the developed friction material considering the manufacturing procedure employed.

3.2 Brinnel hardness test

Figure 1 shows the result of the Brinell hardness test with three different sieve size particles in comparison with three other brake pad products from previous studies [2]. The sample with 250µm sieve grade has the highest hardness value of 102.62BHN. A gradual drop in hardness was observed in the samples with higher sieve grades (500µm, 850µm). The high hardness observed for the 250µm sieve grade was as a result of reduced particle size of cow bones which results in increase in contact surface area and subsequent increase in bonding ability with the resin. This is lower than hardness value of 100µm PKS based of 125BHN. It is slightly higher than commercial brake pad (asbestos based) (101BHN) and bagasse based (100.5BHN) brake pad [2, 4, 5]. The PKS based showed a higher hardness value which may be as a result of the 20% binder and lower sieve size of 100µm and other materials used in its formulation compared to the 35% used for the formulation of produced cow bone based brake pad . This results in increasing bonding and glue line between the brake pad materials thereby improving its hardness properties. It can be inferred from the result trend that smaller bone particles sizes enhances the hardness value.

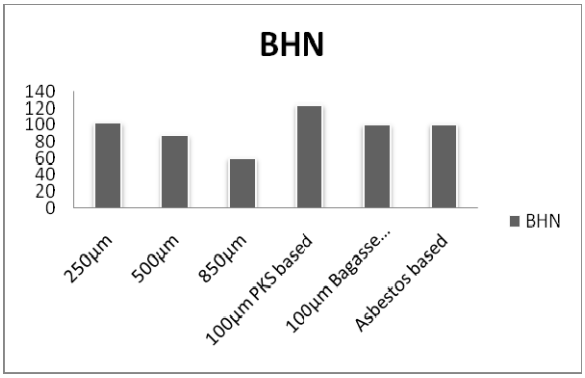

Fig. 1. Comparison of hardness of developed friction brake pad

3.3 Coefficient of friction (µ)

Figure 2 presents the results of the average coefficients of friction for each of the sieve size cow bone-based brake pad compositions with the parameters used. The coefficient of friction decreased as sieve sizes of the cow bones increased in each composition. The coefficient of friction of each produced sieve sizes compares favourably with that of conventional brake pad obtained by standard method [2, 5]. The value for brake pad with 250µm cow bones sieve sizes was the highest with friction coefficient of 0.42 while 500µm and 850µm sieve sizes had 0.39 and 0.36 respectively. The coefficient of friction of conventional brake pad is usually in the range 0.3 - 0.4 [5]. It can be concluded, that the developed brake pad satisfy the requirement with 250µm excelling above the range for conventional brake pads. By comparison, friction coefficient of the developed brake pad 250µm, 500µm and 850µm varied above the mean values of

that of commercial brake pad (0.35.) by 20%, 11.43% and 2.86% respectively. The friction coefficient of developed pad of 250µm was slightly higher than those obtained in previous studies [2, 4, 5, 19].

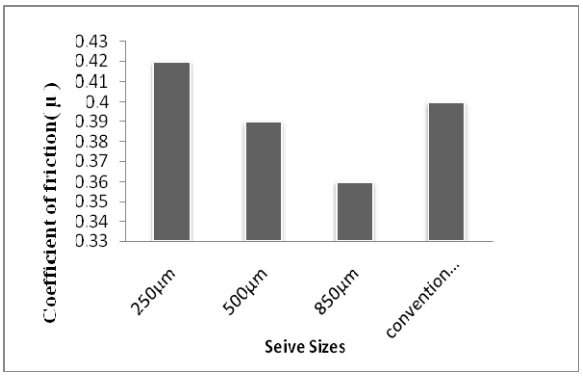

Fig. 2. Coefficient of friction (µ) of different sieve sizes

3.4 Water and oil absorption test

Figure 3 shows the test results obtained from the experiment after 24 hours. The water and oil adsorbent property of the developed brake pad tends to increase as the sieve sizes increase from 250µm to 850µm in the formulation. This increased water and oil absorption rate was due to the decreased interfacial bonding between binder and filler particle which results in increased porosity. The result compared favourably with that of the earlier observation of Aigbodion *et al.* [2] of bagasse based brake pad. The water absorption value for the produced brake pad was 5.07 % and this value compares favourably with that of optimum formulation brake pad PKS and bagasse based which had water absorption values of 5.03% and 3.48% respectively as shown in figure 3. The commercial brake (asbestos based) with a water absorption value of 0.9% [1, 2, 5] showed an extremely better water absorption property than the experimentally produced brake pad. The oil absorption value for the produced brake pad was 1.3 % and this value compares with that of optimum formulation brake pad PKS and bagasse based which had oil absorption values of 0.44% and 1.11% respectively as shown in figure 3. However the commercial brake (asbestos based) with an oil absorption value of 0.3% [1, 2, 5] showed an extremely better oil absorption properties as well, than the produced brake pad. The brake pad absorption rate could be improved if other additives are added with lower sieve sizes.

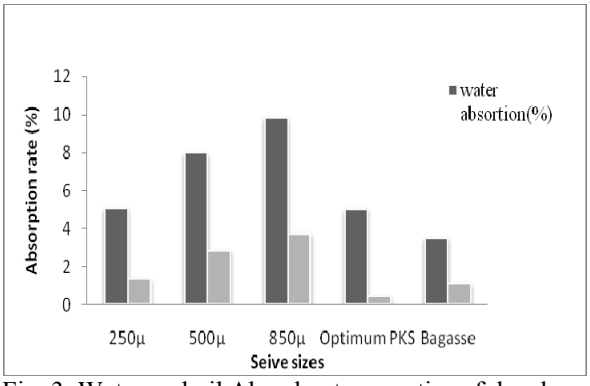

Fig. 3. Water and oil Absorbent properties of developed brake pad

3.5 Flame resistance

A good brake pad should possess good resistance to high heat and temperature [2, 6]. From the test performed, flame resistance test after 10 minutes showed that the produced brake pad of sieve size 250µm is charred with only 12% ash. This makes it of better heat and temperature resistance than PKS-based and bagasse-based brake pad with 46% and 34% ash content respectively [1, 5]. Figure 4 shows the flame resistant results obtained from the experiment after 10mins heating time.

It can also be inferred from the tests that the developed brake pad competes favourably with the conventional brake pads with small variance of 4%. This implies that, if lower bone particle sizes is used it will result in better resistance to heat and temperature. The percentage charred properties increased as the sieve grade increases which can be attributed to the increase in pores as sieve size increases. These results are at par with earlier observations [1, 2, 3, 4, 5].

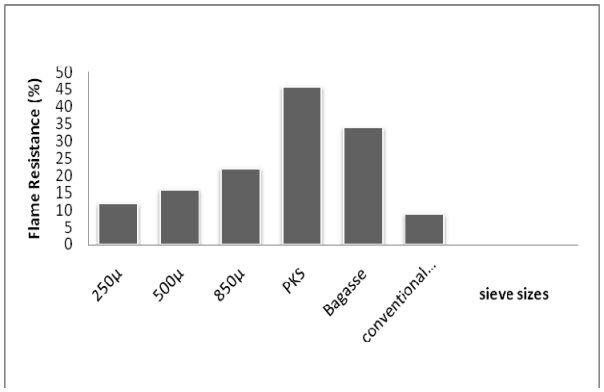

Fig. 4. Flame resistance of developed braked with others

3.6 Density test

Figure 5 shows the variation of density with bone particle sizes. The density decreased as the bone particle sizes of the developed brake pad increased. The increase in density can be attributed to the decrease in particle sizes, that is, increased packing of cow bone particle. The 250µm has the highest density which is as a result of closer packing of cow bone particles creating more homogeneity in the entire phase of the composite body [5].

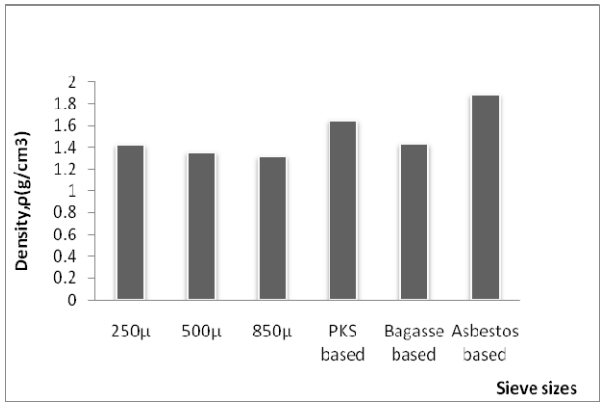

Fig. 5. Densities of developed brake pad with other brake pads

The density results were determined and plotted against the compositions of specimens as shown in figure 5 where density decreased as the sieve size of the developed brake pad increased. This value compares favorably with that of optimum formulation brake pad PKS and bagasse based which had water absorption values of 1.65 and 1.43 respectively as shown in figure 5. Though, the weight/volume of specimens was less than that of commercial brake pad (1.890g/cm^3) however is in par with standard [1, 2, 5]. The density of each developed auto-system friction brake pad of 250µm, 500µm and 850µm varied from that of the conventional brake pad by 24.77%, 28.22% and 30.31% respectively.

3.7 Wear characteristics

Figure 6 shows the wear of the developed brake pad samples. The wear increases as the particles size of the cow bone increased from 250-850 µm. The lower wear rate at lower particle size of the brake pad formulation can be attributed to interfacial bond between the particle and the resin, which reduces the possibility of a particle pull out. This observation is at par with the work of Aigbodion *et al* [2]. From previous studies it was observed that, increase in pores formed between particles sizes, significantly affected wear characteristics [20].

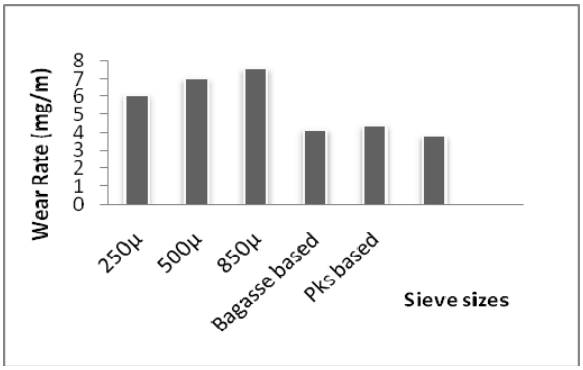

Fig. 6. Wear rate of developed brake pad and other allied products

3.8 Microstructure analysis

Figures 7-9 show the microstructure of 250µm, 500µm and 850µm bone particle sizes. Figure 7 shows an almost even dark region of resin and white region of cow bones of 250µm. Figure 8 Shows slight uniform dark region of resin and white region of cow bone region.

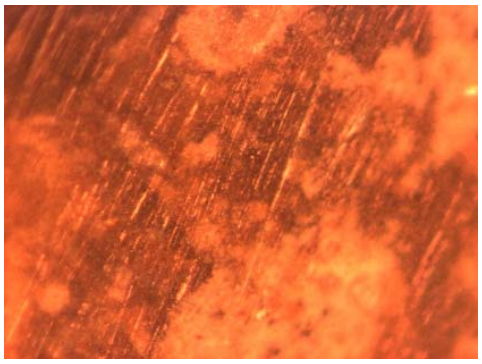

Fig. 7. Microstructure of 250µm sieve grade sample(X100).

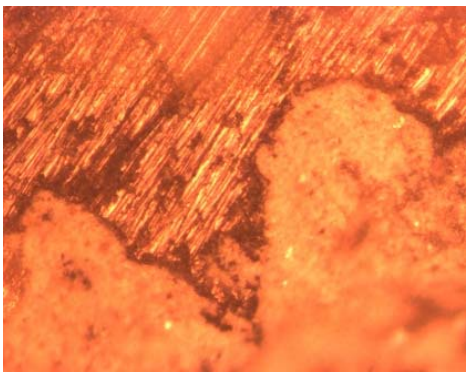

Fig. 8. Microstructure of 500µm sieve sample(X100).

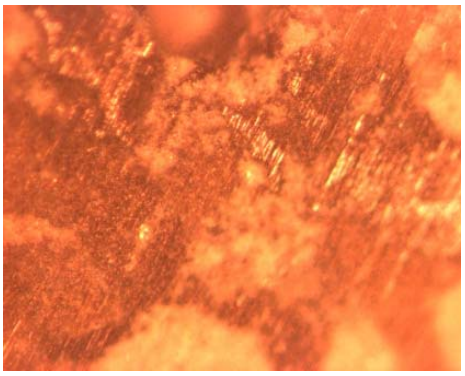

Fig. 9. Microstructure of 850µm sieve grade sample(X100).

From the microstructure there is more uniform distribution of the resin with the cow bone as the particles size of the cow bones decreased. This is as a result of proper bonding between the cow bone particles and the resin as the sieve grade decrease and also closer inter-packing distance. It can be predicted that if lower bone particle sizes are used, the inter-packing distance will also reduce thereby giving better properties.

The result of this study indicates that samples containing 250µm (65% cow bones- 35% resin) gave better properties than other samples tested. Hence, the lower the sieve grades of cow bones, the better the properties. The 250µm sieve size results were compared with those of commercial brake pad (asbestos based) and optimum formulation laboratory brake pad (Palm Kernel Shell based (PKS) from previous studies [1, 5].

4. CONCLUSION

Cow bone particle (65% cow bone partcles- 35% phenolic resin) composite material friction brake pad was successfully developed using a compressive moulding process. There was increasing interfacial bonding as the cow bone particle size decreases from 850 to 250 µm. The 250µm cow bone particle size gave better properties relative to higher particle sizes studied. The wear rate increases with increasing cow bone particle sizes. The co-efficient of friction obtained were within the recommended standard for automobile friction brake pad. Hardness and densities of the produced samples were seen to be decreasing with increase in cow bone particle sizes, while oil, water

soak, wear rate and percentage charred increased as cow bone particle size increased. It is hereby recommended that produced brake pad from cow bone composites be coated with a hydrophobic substance like paraffin wax to reduce its water absorption value, thereby greatly improving the physical stability of the produced brake pads. The results of this study indicates that cow bone particles composite materials can be used as a suitable replacement for asbestos in the manufacturing of brake pads.

5. REFERENCES

[1] Deepika, K., Bhaskar, R.C., Ramana, R.D.: *Fabrication and performance evaluation of composite material for wear resistance application*, International Journal of Engineering Science and Innovative Technology, 2 (6), pp. 66-70, 2013

[2] Aigbodion, V.S., Akadike, U., Hassan, S.B., Asuke, F., Agunsoye, J.O.: *Development of asbestos free brake pad using bagasse, Tribology in Industry*, 32 (1), pp.12-17, 2010.

[3] Erjavec, J.: *Automotive technology: a system approach*, 5th Edition, Cengage Learning, USA, pp.1424-1426, 2010.

[4] Idris, U.D., Aigbodion, V.S., Abubakar, I.J., Nwoye, C.I.: *Eco-friendly asbestos free brake-pad: using banana peels*, Journal of King Saud University-Engineering Sciences, 27, pp.185–192, 2013.

[5] Elakhame, Z.U., Alhassan, O.A., Samuel, A.E.: *Development and production of brake pads from palm kernel shell composites*, International Journal of Scientific and Engineering Research, 5 (10), pp. 734-744, 2014.

[6] Maleque, M.A., Atiqah, A., Talib, R.J., Zahurin, H.: *New natural fibre reinforced aluminium composite for automotive brake pad*, International Journal of Mechanical and Materials Engineering (IJMME), 7 (2), pp. 166-170, 2012.

[7] Doll, W., Peto, J.: *Effects on health of exposure to asbestos*, Health and Safety Commission, HSE Books, 1996.

[8] Kim, S.J., Williams, D., Cheresh, P. Kamp, D.W.: *Asbestos-induced gastrointestinal cancer: an update*, Gastrointestinal and Digestive System, 3 (3), pp. 1-6, 2013. http://dx.doi.org/10.4172/2161-069X.1000135

[9] Olabisi, A.I., Adam, A.N., Okechukwu, O.M.: *Development and assessment of composite brake pad using pulverized cocoa beans shells filler*, International Journal of Materials Science and Applications, 5 (2), pp. 66-78, 2016. doi: 10.11648/j.ijmsa.20160502.16

[10] Bhane, A.B., Kharde, R.R., Honrao, V.P: *Investigation of tribological properties for brake pad material: a review*, International Journal of Emerging Technology and Advanced Engineering, 4 (9), pp. 530-532, 2014.

[11] Keskin, A.: *Investigation of using natural zeolite in brake pad*, Scientific Research and Essays, 6 (23), pp. 4893-4904, 2011. DOI: 10.5897/SRE10.1072

[12] Vijay, R., Kumar, S.R., Satish, V., Thiyagarajan, V., Subramaniam, L.: *Development and testing of asbestos free brake pad material*, International Journal of Manufacturing Science and Engineering, International Science Press, 2 (2), pp. 57-63, 2011.

[13] Dan-Asabe, B., Madakson, P.B., Manji, J.: *Material selection and production of a cold-worked composite brake pad*, World J of Engineering and Pure and Applied Sci., 2 (3), pp. 92-97, 2012.

[14] Oladele, I.O., Adewole, T.A.: *Influence of cow bone particle size distribution on the mechanical properties of cow bone-reinforced polyester composites*, Biotechnology Research International, Hindawi Publishing Corporation, Article 725396, pp.1-5, 2013.

[15] Agunsoye, J.O., Talabi, S.I., Awe, O., Kelechi, H.: *Mechanical properties and tribological behaviour of recycled polyethylene/cow bone particulate composite*, Journal of Materials Science Research, 2 (2), pp. 42-50, 2013.

[16] Dagwa, I.M., Ibhadode, A.O.: *Determination of optimum manufacturing conditions for asbestos-free brake pad using Taguchi method*, Nigerian Journal of Engineering Research and Development, Basade Publishing Press Ondo, Nigeria, 5 (4), pp. 1-8, 2006.

[17] Mathur, R.B., Thiyagarajan, P., Dhami, T.L.: *Controlling the hardness and tribological behaviour of non – asbestos brake lining materials for automobiles*, Journal of Carbon Science, 5 (1), pp. 6-11, 2004.

[18] Kim, S.J., Kim, K.S., Jang, H.: *Optimization of manufacturing parameters for brake lining using Taguchi method*, Journal of Material Processing Technology, no.136, 2003, pp. 202-208, 2003.

[19] Nuhu, A.A., I.O. Adeyemi, I.O.: *Development and evaluation of maize husks (asbestos-free) based brake pad*, Industrial Engineering Letters, 5 (2), pp. 67-80, 2015.

[20] Yakubu, A.S., Amaren, S.G., Yawas, D.S.: *Evaluation of the wear and thermal properties of asbestos free brake pad using periwinkles shell particle*s, Usak University Journal of Material Sciences, 1, pp. 99-108, 2013.

Authors: **Professor Segun M. Adedayo PhD, Senior Lecturer Idehai O. Ohijeagbon PhD, James O. Adegbola M.Eng.** University of Ilorin, Department of Mechanical Engineering, P.M.B. 1515, Ilorin, Nigeria, Phone: 234-7030092411,

E- mail: adyos1@yahoo.com,
idehaiohi@yahoo.com,
adegbolajames01@gmail.com

http://doi.org/10.24867/JPE-2017-01-075

Journal of Production Engineering

Vol.20 No.1

JPE (2017) Vol.20 (1) Original Scientific Paper

Nageswara, R.M., Narayana, R.K.., Ranga, J.G.

INTEGRATED SCHEDULING OF MACHINES AND AGVS IN FMS BY USING DISPATCHING RULES

Received: 17 April 2017 / Accepted: 20 May 2017

Abstract: *Recent advancement in meta-heuristics for simultaneous scheduling of machines and AGV studies have applied various techniques such as Differential evaluation (DE), Simulated Annealing (SA) and Ant Colony Optimization (ACO) to solve the simultaneous scheduling problem. All of these technique requires an initial scheduler in order to initiate the scheduling process and the priority rule algorithms will typically be used. However, from the literature, none of these studies elaborate and justify their selection of a particular priority rule algorithms over another. Since the initial scheduler can significantly affect the entire scheduling process, it is important that the correct initial scheduler be selected. In this paper we quantitatively compared three initial scheduler algorithms to determine the best algorithm performance. We believe the performance comparison would enable users to utilize the best initial scheduler to fit their meta-heuristics simultaneous scheduling studies.*
Key words: *simultaneous scheduling, priority rules, performance*

Integrisano raspoređivanje mašina i AGVs u FMS korištenjem dispečerska pravila. *Nedavni napredak u meta-heuristici za istovremeno raspoređivanje mašina i AGV studije su primenjeni u raznim tehnikama, kao što je diferencijalno vrednovanje (DE), Simulano žarenje (SA) i Optimizacija uz pomoć kolonije mrava (ACO) da reši istovremeno raspoređivanje problem. Sve ove tehnike zahtevaju inicijalni planer kako bi se započeo proces za raspoređivanje i algoritmi prioriteta pravila koja će se obično koristiti. Međutim, iz literature, nijedna od ovih studija ne elaborira i opravdava izbor određenog prioriteta pravila algoritama nad drugim. Pošto početni raspored može značajno uticati na čitav proces za raspoređivanje, važno je da se izabere ispravn početni planer. U ovom radu su kvantitativno upoređena tri početna planer algoritma da bi se odredile najbolje performanse algoritma. Veruje se da će poređenje performansi omogućiti korisnicima da postave najbolji početni planer da bi odgovarao njihovoj meta heuristikoj simultanoj studiji raspoređivanja.*
Ključne reči: *simultano raspoređivanje, prioritetna pravila, performanse*

1. INTRODUCTION

FMS is a highly automated and sophisticated system in the field of manufacturing to achieve high flexibility and productivity in mid-variety and mid-range of products [1, 2]. The great demand for goods needs new way to enhance productivity with existing manufacturing system and available resources. FMS has emerged as a viable alternative to the conventional manufacturing system and showed benefits in cost reduction, enhanced utilizations, reduced work-in-process levels, etc. The problems encountered in the life cycle of a FMS are classified in to design, planning, scheduling and control [3]. The task of scheduling and controling problems plays an important role during operation owing to the dynamic nature of the FMS such as flexible parts, tools, AGV routings [4] and AS/RS storage assignments[5].scheduling of machines in FMS is made through sequencing of jobs on machines, and routing of jobs through the system [6,7]. Other resources in the system,(e.g. material-handling devices like AGVs and AS/RS) need to be considered. To have flexible and efficient production, automated guided vehicle systems (AGVS) and the material-handling system (MHS) are being employed [8,9]. The AGVs effectiveness depends on several factors. Function of a well-designed vehicle management are: Dispatching the process of selecting and assigning tasks to AGV; Routing the process of selecting specific paths by AGVs; and Scheduling – the process of determining the arrival and departure dates. The demand for goods enhances pressure on manufacturing systems seeking ways to increase productivity with available resources. Scheduling is a critical function for the control and operation of any FMS [10].

1.1 Dispatching rules

Over the last four decades, the sequencing and scheduling problem has been solved using dispatching rules (also called scheduling rules, sequencing rules, decision rules, or priority rules). These dispatching rules are used to determine the priority of each job. The priority of a job is determined as a function of job parameters, machine parameters, or shop characteristics. When the priority of each job is determined, jobs are sorted and then the job with the highest priority is selected to be processed first. Baker [11] and Morton and Pentico [12] classified dispatching rules as follows:

Local rules

Local rules are concerned with the local available information.

Global rules

Global rules are used to dispatch jobs using all

information available on the shop floor.

Static rules

Static rules do not change over time, and ignore the status of the job shop floor.

Dynamic rules

Dynamic rules are time dependent, and change according to the status of the job shop floor.

Forecast rules

Forecast rules are used to give priority to jobs according to what the job is going to come across in the future, and according to the situation at the local machine. Several dispatching rules have been reported by many researchers. The following are some of the dispatching rules that have been developed, investigated, and implemented by several researchers and practitioners:

1. **SPT or SEPT**: Shortest Processing Time or Shortest Expected Processing Time. The job with the smallest operation processing time is processed first.
2. **LPT or LEPT**: Longest Processing Time or Longest Expected Processing Time. The job with the largest operation processing time is processed first.
3. **EDD**: Earliest Due Date. The job with the smallest due date is processed first.
4. **JST**: Job Slack Time. The job with minimum slack is processed first. The job slack time is computed as the difference between the job due date, the work remaining, and the current time.
5. **CR**: Critical Ratio. The job with the smallest ratio is processed first. The CR is determined by dividing job's allowance by the remaining work time.
6. **RANDOM**: Service in Random Order. A job is randomly selected from the set of jobs which are queued at the machine.
7. **FCFS or SORT**: First Come, First Served or Smallest Ready Time. The job which arrives first at the machine will be served first.
8. **LCFS**: Last Come, First Served. The job which arrives last will be served first.
9. **LFJ**: Least Flexible Job. The job with the least flexibility is processed first.
10. **FOFO**: First Off, First On. The job with the operation that could be completed earliest will be processed first even if this operation is not yet in the queue. In this case, the machine will be idle until the operation arrives.
11. **LAWINQ**: Least Anticipated Work in Next Queue. From the set of jobs waiting for a specific machine, a job will be selected that will encounter the smallest queue at the next machine in its route.
12. **COVERT**: Cost OVER Time. COVERT is a composite rule that puts the job with the largest COVERT ratio in first position. The COVERT ratio is computed by dividing an anticipated tardiness for the associated job and its operation processing time.
13. **Most Operation Remaining Rule (MOPNR):** Every job has a number of operations and according to this rule the operation which has more number of succeeding operations will be given the first priority.
14. **Preferred Customer Order (PCO):** Sometimes jobs belonging to a particular customer may be given priority for different reasons like the business offered by them is more than that offered by others or because of their regular business orders etc.
15. **Least Slack (LS):** Generally there is always a difference between actual finishing time of the job and the due date by which it is supposed to be finished, which is known as "slack". According to this rule the job with the least slack is given first priority as mentioned earlier.

2. SCHEDULING WITH DISPATCHING RULES

Scheduling provides a basis for assigning jobs, whereas sequencing (also referred as dispatching) specifies the priority for completion of jobs in a systematic way at WorkCentre.Hanssmann and Hess [13] have adopted the Linear Programming (LP) in a model to achieve maximum profit or lowest cost. Held and Karp [14] have applied the dynamic programming (DP) while solving a large problem. Ignall and Schrage [15] have developed branch and bound algorithms for the permutation flow shop problem with makespan minimization. Bomberger [16] has followed the DP approach considering the production scheduling of different items over the same facility in the system on a repetitive basis. The facility in the system is: only one item can be produced at a time associating with setup cost and setup time under constant demand rate. Campbell *et al.* [17] have applied heuristic algorithm in stages. Lockett and Muhlemann [18] have used the branch and bound algorithm for scheduling jobs with sequencing suitable for small size problems. Crowin and Esogbue [19] have considered two different flow shop scheduling problems for minimizing makespan. After establishing the optimum permutation schedules, an efficient DP formulation has been developed. Holland [20] has invented the algorithms based on Darwin's theory of natural selection and survival. These were invented by. Rinnooy Kan [21] has formulated mathematical programming models and obtained unsatisfactory results. Majority of these techniques are unable to provide feasible solutions and have limited practical use. Panwalkar and Iskander [22] have utilized have classified 100 scheduling rules into static and dynamic rules. Tripathy [23] and, Arani et al. [24] have shown better results applying the integer programming on vehicle scheduling problem. Holthaus and Rajendran [25] have utilized the dispatching rules to optimize the job-shop scheduling problems in the manufacturing world. Pan and Fan [26]have used branch and bound algorithm for the problem and reduced the size of the problem including dominance properties. However, the algorithm is limited to 18 jobs. Chen *et al.* [27] have applied DP approach to Lagrangean relaxation for complex scheduling problems and found optimal solution for single and parallel machine problem. Papakostas and Chryssolouris [28] have proposed a dispatching rule (viz., RTSLACK) by maximizing the slack time of the remaining tasks in the manufacturing resources in a series of single machines and hybrid flow shop scheduling instances. Barman and Lisboa [29] have utilized a combination of dispatching rules for cost performance and minimized both mean and variable

waiting cost. Ko et al. [30] have proposed a dispatching rule for non-identical parallel machines with sequence dependent setups and quality restrictions. Kayvanfar et al. [31] have examined a single machine scheduling problem with controllable processing times. Ying et al. [32] have studied the single-machine scheduling problem with a Common Due Window (CDW) having constant size and position to minimize the total weighted earliness and tardiness penalties in jobs completion. Ling et al. [33] minimizing total deviation of job completion time on a single machine scheduling. Dispatching rules have a significant role due to ease of implementation and compatibility with the dynamic nature of manufacturing systems.

3. FMS DESCRIPTION

The FMS considered in this work has the configurations as shown in Fig 1. There are four Machines having Computer Numerical Controlled Machines (CNCs) each equipped with an independent and self sufficient tool magazine, one Automatic Tool Changer (ATC) and one Automatic Pallet Changer (APC).

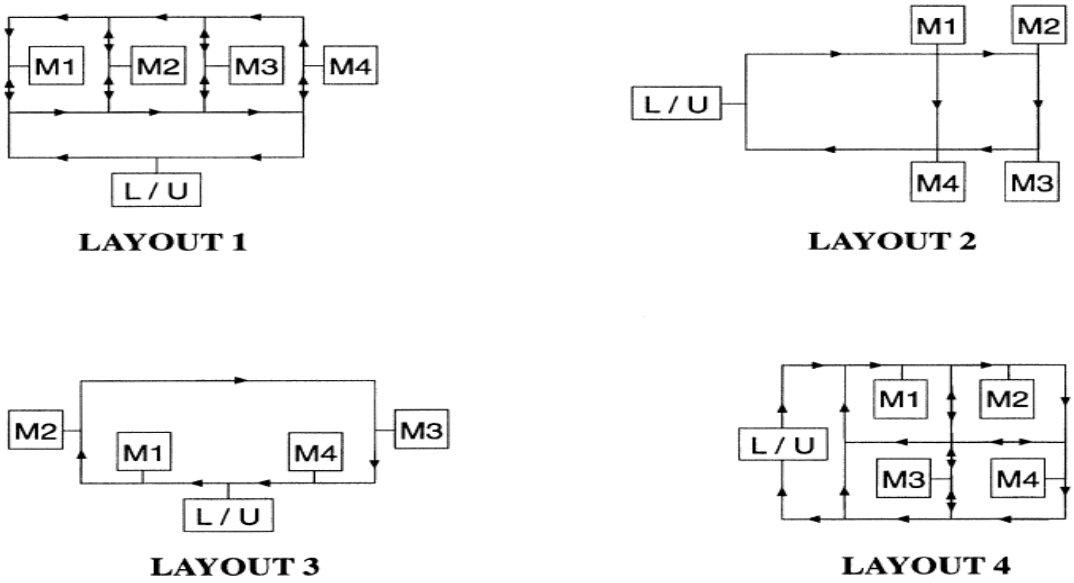

Fig. 1. the layout configurations adopted in example problems

3.1 FMS Envirnoment

The environment within which the FMS under consideration operates can be described as follows:

1. The types and number of machines are known. Operations are no preemptive. There is sufficient input/output buffer space at each machine
2. Processing, set-up, loading and unloading times are available and are deterministic.
3. Number of AGVs is given and the AGVs are all identical in the sense that they have the same speed and load carrying characteristics.
4. Flow path layout is given and travel times on each segment of the path are known.
5. A load/unload (L/U) station serves as a distribution center for parts not yet processed and as a collection center for parts finished. All vehicles start from the L/U station initially and return to after accomplishing all their assignments. There is sufficient input/output buffer space at the (L/U) station.
6. AGVs carry a single unit-load at a time. They move along predetermined shortest paths, with the assumption of no delay due to congestion. Preemption of trips is not allowed. The trips are called loaded or deadheading (empty) trips depending on whether a part is carried or no part is carried during that trip, respectively. The durations for the deadheading trips are sequence dependent and are not known until the vehicle route is specified.
7. It is assumed that all the design and set-up issues within the hierarchy of OR/MS problems in an FMS as suggested by Stecke [34] have already been resolved. Machine loading, i.e., the allocation of tools to machines and the assignment of operations to machines, is made. Pallets and other necessary equipment are allocated to parts. The set of part types to be produced during the planning period and the routing of each part type are available before making scheduling decisions. In other words, routing flexibility is not considered. The routing for a part type can be selected based on considerations of technological feasibility and processing efficiency, or by formulating the set-up phase problems in a manner that can also handle the routing decisions.
8. Ready-times of all jobs are known. Initially, partially processed parts might be available at machines waiting for further processing, and they can be treated as jobs having zero ready times and their routing consists of the remaining operations.
9. Such issues as traffic control, congestion, machine failure or downtime, scraps, rework, and vehicle dispatches for battery change are ignored here and

left as issues to be considered during real-time control.

3.2 Assumptions

a. The types and no. of machines are known
b. There is sufficient input/output buffer space for each machine
   Machine loading
   i. Allocation of tools to machine has been done
   ii. Assignment of operation to machine are made
c. Pallet and other necessary equipment are allocated
d. The speed of AGV kept at 40 m/min
e. The distance between the two machines and distance between loading/ unloading machines are known

3.3 Input data

The input data i.e. travelling time matrix from table 1.1 and Job sets for the problem is taken from a paper by Bilge U and Ulusoy G [35]. Data given in Table 1. gives the distances from load/unload stations to machines and distances between machines in metres for all the four layouts .The Ten job sets are given in Table 2. given below each containing four to eight different job sets, machines in each job set to be used and numbers with in the parenthesis is the processing time of particular job on specified machine. The load/unload (L/U) station serves as a distribution center for parts not yet processed and as a collection center for parts finished. All vehicles start from the L/U station initially. Trips follow the shortest path between two points either between two machines or between a machine and the L/U station. Preemption of trips is not allowed the trips are called loaded or deadheading (empty) trips. The durations for the deadheading trips are sequence dependent and are not known until the vehicle route is specified.

Layout-1	L/U	M1	M2	M3	M4
L/U	0	6	8	10	12
M1	12	0	6	8	10
M2	10	6	0	6	8
M3	8	8	6	0	6
M4	6	10	8	6	0
Layout-2	L/U	M1	M2	M3	M4
L/U	0	4	6	8	6
M1	6	0	2	4	2
M2	8	12	0	2	4
M3	6	10	12	0	2
M4	4	8	10	12	0
Layout-3	L/U	M1	M2	M3	M4
L/U	0	2	4	10	12
M1	12	0	2	8	10
M2	10	12	0	6	8
M3	4	6	8	0	2
M4	2	4	6	12	0
Layout-4	L/U	M1	M2	M3	M4
L/U	0	4	8	10	14
M1	18	0	4	6	10
M2	20	14	0	8	6
M3	12	8	6	0	6
M4	14	14	12	6	0

Table 1. Travel time matrix for this particular problem

JobSet-1 Job 1: Ml(8); M2(16); M4(12) Job 2: Ml(20); M3(10); M2(18) Job 3: M3(12); M4(8); Ml(15) Job 4: M4(14); M2(18) Job 5: M3(10); Ml(15)	JobSet-2 Job 1: Ml(10); M4(18) Job 2: M2(10); M4(18) Job 3: Ml(10); M3(20); Job 4: M2(10); M3(15); M4(12) Job 5: Ml(10); M2(15); M4(12) Job 6: Ml(10); M2(15); M3(12)
JobSet-3 Job 1:Ml(16); M3(15) Job 2:M2(18); M4(15) Job 3:Ml(20); M2(10) Job 4:M3(15); M4(10) Job 5:Ml(8);M2(10);M3(15);M4(17) Job 6: M2(10);M3(15);M4(8);Ml(15	JobSet-4 Job1: M4(11); Ml(10); M2(7) Job2: M3(12); M2(10); M4(8) Job3: M2(7); M3(10); Ml(9); M3(8) Job4: M2(7); M4(8); Ml(12);M2(6) Job5:Ml(9);M2(7);M4(8);M2(10);M3(8)

JobSet-5 Job 1: Ml(6);M2(12);M4(9) Job 2: Ml(18);M3(6); M2(15) Job 3: M3(9);M4(3);Ml(12) Job 4: M4(6);M2(15) Job 5: M3(3);Ml(9)	JobSet-6 Job 1: Ml(9); M2(11); M4(7) Job 2: Ml(19); M2(20); M4(13) Job 3: M2(14); M3(20); M4(9) Job 4: M2(14); M3(20); M4(9) Job 5: Ml(11); M3(16); M4(8) Job 6: Ml(10); M3(12); M4(10)
JobSet-7 Job 1: Ml(6); M4(6) Job 2: M2(11); M4(9) Job 3: M2(9); M4(7) Job 4: M3(16); M4(7) Job 5: Ml(9); M3(18) Job 6: M2(13); M3(19); M4(6) Job 7: Ml(10); M2(9); M3(13) Job 8: Ml(l1); M2(9); M4(8)	JobSet-8 Job 1: M2(12); M3(21);M4(11) Job 2: M2(12); M3(21);M4(11) Job 3: M2(12); M3(21);M4(11) Job 4: M2(12); M3(21);M4(11) Job 5: Ml(10); M2(14);M3(18);M4(9) Job 6: Ml(10);M2(14); M3(18);M4(9)
JobSet-9 Job 1: M3(9);Ml(12);M2(9);M4(6) Job 2: M3(16);M2(11); M4(9) Job 3: Ml(21); M2(18); M4(7) Job 4: M2(20); M3(22); M4(11) Job 5:M3(14);Ml(16);M2(13); M4(9)	JobSet-10 Job1:Ml(11);M3(19);M2(16);M4(13) Job2: M2(21);M3(16); M4(14) Job3:M3(8); M2(10); Ml(14); M4(9) Job4: M2(13); M3(20); M4(10) Job5: Ml(9); M3(16); M4(18) ; Job6:M2(19);Ml(21); M3(11);M4(15)

Table 2. Data for the Job Sets Used in Example Problems

3.4 Objective function

Operation completion time=Oij=Tij+Pij

T_{ij}=Traveling time for j^{th} operation and i^{th} job

P_{ij} =operation processing time

Mean Tardiness = $\frac{1}{n}\sum_{i=1}^{n} T_i$ n = number of jobs;

Ti = Tardiness

Optimization parameters considered

Population Size = Double the no of operations

Iterations completed = 1000

3.5 Vehicle scheduling methodology

Jobs are scheduled based on the operation sequence derived by the Sheep Flock Heredity algorithm. Initially AGVs carry jobs from the load/unload station to the respective workstations where the first operations are scheduled. AGVs make two types of trips, a loaded trip where it carries a load and a deadheading trip where the vehicle moves to pick up a load. Deadheading trip can start immediately after the delivery and vehicle demand at different workstations are considered and the subsequent assignments are made. If both AGVs are available task is assigned to the earliest available vehicle. If no vehicle is available, the earliest available times of the AGVs are computed and the assignment is made. If the vehicle is idle and no job is ready, assign the operation that is going to be completed early and is identified the vehicle is moved to pick up that job. This type of vehicle scheduling methodology helps in reducing the waiting times and thus helps in improving the resource utilization and the throughput. The flow chart of the vehicle assignment methodology is given in Fig. 2.

4. IMPLEMENTATION OF SEQUENCING RULES

Scheduling provides a basis for assigning jobs to a work center. Sequencing (also referred to as dispatching) specifies the order in which jobs should be completed at each centre. The sequencing methods are referred to as priority rules for sequencing or dispatching jobs to a work center. In the manufacturing world, scheduling problems are extensively adopting the dispatching rules to provide good solutions to complex problems in a real-time production environment.

4.1 First cum First Serve(FCFS)

For implementation of First cum first serve rule, Job set 5 and Layout1 is considered.

Job Set 5

Job1		Job2			Job3			Job4		Job5		
M_1	M_2	M_4	M_1	M_3	M_2	M_3	M_4	M_1	M_4	M_2	M_3	M_1
1	2	3	4	5	6	7	8	9	10	11	12	13

In FCFS continuous numbers are marked initially for the operations in a job set by following precedence relation, i.e., operation of the same job set must be in increasing order but anywhere in the sequence. According to this rule the sequence is.

1 2 3 4 5 6 7 8 9 10 11 12 13

4.2 Shortest processing time (SPT)

For implementation of shortest processing time rule, Job set 3 and Layout 2 are considered.

In SPT continuous numbers are marked initially for the operations in a job set by following precedence relation. And the total process time for each and every job is found out. For example in the above Job set total

processing times are job1-31, job2-33, job3-30, job4-25, job5-50, and job6-44. According to this rule the priority of job is 4, 3, 1, 2, 6, 5 and the sequence is:

8 5 6 12 3 4 14 15 16 9 10 11 12

Job set 3

Job 1		Job 2		Job 3		Job 4		Job 5				Job 6			
M1	M3	M2	M4	M1	M2	M3	M4	M1	M2	M3	M4	M2	M3	M4	M1
16	15	18	15	20	10	15	10	8	10	15	17	10	15	8	15
1	2	3	4	5	6	7	8	9	10	11	12	13	14	15	16

4.3 Longest processing time (LPT)

For implementation of longest processing time rule, Job set 9 and Layout 3 are considered.

In LPT continuous numbers are marked initially for the operations in a job set by precedence relation. The total process time for each and every job is found. For example in job set No 9 total processing times are job1-36, job2-36, job3-46, job4-53, and for job5-52, since both the process times are same first one is selected as priority. According to this rule the priority of job is 4, 5, 3, 1, 2 and the sequence is:

11 12 13 14 15 16 17 8 9 10 1 2 3 4 5 6 7

And the test results obtained by simulating FCFS, SPT and LPT for simultaneous scheduling problems are given below in Table 3. and Table 4.

Job set 9

Job 1				Job 2			Job 3			Job 4			Job 5			
M3	M1	M2	M4	M3	M2	M4	M1	M2	M4	M2	M3	M4	M3	M1	M2	M4
9	12	9	6	16	11	9	21	18	7	20	22	11	14	16	13	19
1	2	3	4	5	6	7	8	9	10	11	12	13	14	15	16	17

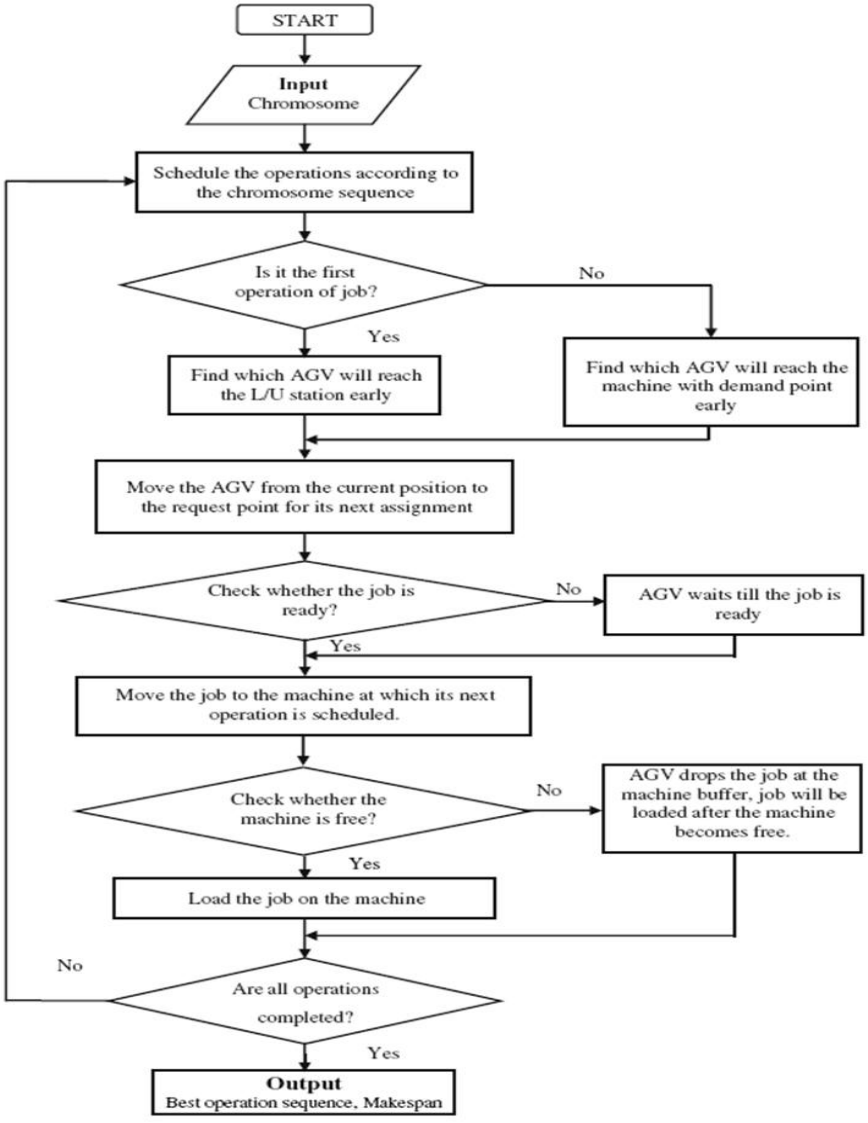

Fig. 2. flow chart for Simultaneous scheduling machines and AGVs

3. RESULT AND DISCUSSION

Ten different job sets with different processing sequences, and process times are generated and presented. Different combinations of these ten job sets and four layouts are used to generate 82 example problems. In all these problems there are two vehicles. Table 3. consists of problems whose t_i/pi ratios are greater than 0.25, and whose t_i/pi ratios are lesser than 0.25 ratios are represented in Table 4. A code is used to designate the example problems which are given in the first column. The digits that follow 1.1 indicate the job set and the layout. In Table 2 another digit is appended to the code. Here, having a 0 or 1 as the last digit implies that the process times are doubled or tripled, respectively, where in both cases travel times are halved.

Job. No	t/p	FCFS	SPT	LPT
1.1	0.59	173	193	177
2.1	0.61	158	158	177
3.1	0.59	202	224	198
4.1	0.91	263	267	264
5.1	0.85	148	164	148
6.1	0.78	231	240	227
7.1	0.78	195	210	201
8.1	0.58	261	261	266
9.1	0.61	270	277	268
10.1	0.55	308	308	310
1.2	0.47	143	173	165
2.2	0.49	124	124	130
3.2	0.47	162	188	160
4.2	0.73	217	223	224
5.2	0.68	118	144	131
6.2	0.54	180	169	165
7.2	0.62	149	160	149
8.2	0.46	181	181	198
9.2	0.49	250	249	244
10.2	0.44	290	288	287
1.3	0.52	145	175	167
2.3	0.54	130	130	136
3.3	0.51	160	190	162
4.3	0.8	233	237	230
5.3	0.74	120	146	133
6.3	0.54	182	171	167
7.3	0.68	155	166	151
8.3	0.5	183	183	200
9.3	0.53	252	251	246
10.3	0.49	293	294	293
1.4	0.74	189	207	189
2.4	0.77	174	174	174
3.4	0.74	220	250	212
4.4	1.14	301	301	298
5.4	1.06	171	189	171
6.4	0.78	249	252	237
7.4	0.97	217	242	151
8.4	0.72	285	285	200
9.4	0.76	292	311	290
10.4	0.69	350	350	345

Table 3. Performance evaluation for t/p>0.25 considering FCFS, SPT and LPT procedures

Job.No	t/p	FCFS	SPT	LPT
1.10	0.15	207	248	252
2.10	0.15	217	217	225
3.10	0.15	257	327	282
4.10	0.15	303	328	317
5.10	0.21	152	190	187
6.10	0.16	304	281	297
7.10	0.19	231	240	264
8.10	0.14	338	338	347
9.10	0.15	390	367	359
10.10	0.14	452	429	444
1.20	0.12	194	238	246
2.20	0.12	194	194	206
3.20	0.12	241	311	270
4.20	0.12	285	312	298
5.20	0.17	142	180	184
6.20	0.12	292	260	284
7.20	0.15	212	218	249
8.20	0.11	306	319	334
9.20	0.12	380	355	347
10.20	0.11	445	423	439
1.30	0.13	195	239	247
2.30	0.13	197	197	209
3.30	0.13	240	312	271
4.30	0.13	292	317	301
5.30	0.18	141	181	183
6.30	0.24	296	261	285
7.30	0.17	215	221	250
8.30	0.13	307	320	335
9.30	0.13	381	356	348
10.30	0.12	448	426	442
1.40	0.18	213	255	254
2.41	0.13	307	307	319
3.40	0.18	261	330	282
3.41	0.12	370	476	411
4.41	0.19	434	471	451
5.41	0.18	218	269	270
6.40	0.19	310	288	299
7.40	0.24	239	251	270
7.41	0.16	329	344	385
8.40	0.18	343	343	349
9.40	0.19	396	379	370
10.40	0.17	466	445	455

Table 4. Performance evaluation for t/p<0.25 considering FCFS, SPT and LPT procedures

5. CONCLUSIONS

In this paper the optimal sequence of machines and AGVs are determined by using FCFS, SPT and LPT from Table no 3. and table 4. it is observed that from table 3. out of 40 problems 22 problems gives better results using FCFS when compared with SPT and LPT, 8 problems gives better results using SPT when compared with FCFS and LPT and 24 problems gives better results using LPT when compared with SPT and FCFS and also it can be observed that from table 4. out of 42 problem 30 problems gives better results using FCFS when compared with SPT and LPT, 14 problems gives better results using SPT when compared with

FCFS and LPT and 4 problems gives better results using LPT when compared with SPT and FCFS.

6. REFERENCES

[1] Akturk M.S., Yilmaz H.: Scheduling of automated guided vehicles in a decision making hierarchy, International Journal of Production Research, 32, 577–591 (1996)

[2] Sabuncuoglu. I, Hommertzheim D.L.: Experimental investigation of FMS machine and AGV scheduling rules against the mean flow time criterion. Inter: journal of production research, 30(7) 1617-1635 (1992).

[3] Karabtik.S. Sabuncuolu I.: A beam search based algorithm for scheduling machines and AGVs in an FMS. In: Proceedings of the Second Industrial Engineering Research Conf, Los Angeles, 308–312 (1993).

[4] Kusiaka. Material Handling in Flexible Manufacturing Systems. Material Flow, 2, 90-95 (1985).

[5] El-Maraghy.H.A., Ravi.T. Modern tools for the design, modelling and evaluation of flexible manufacturing systems, Int J Robot Comput Integr Manuf, 9(4), 335–340 (1992).

[6] Orhan.E., Alper.D. : A new approaches to solve hybrid flow shop scheduling problems by artificial immune system, Future Generation Computer Systems, 20 1083–1095 (2004)

[7] Lee S.M, Jung.H.J.: A multi-objective production planning model in a flexible manufacturing environment. Int J Prod Res, 27(11), 1981–1992 (1989)

[8] Raman. N., Talbot F.B., Rachamadgu. R..: Simultaneous scheduling of machines and material handling devices in automated manufacturing, In: Proc Second ORSA/TIMS Conf.on FMS (1986)

[9] Blazewicz. J., Eiselt. H.A, Finke. G., Laporte. G., Weglarz. J.: Scheduling tasks and vehicles in a flexible manufacturing system, Int J Flex Manuf Syst,4,5–16 (1991)

[10] Sabuncuogluand. I., Hommertzheim D.L.: Dynamic dispatching algorithm for scheduling machines and automated guided vehicles in a flexible manufacturing system,Int J Prod Res,30,1059–1079 (1992)

[11] Baker, K.R..: Introduction to Sequencing and Scheduling, Wiley, New York, (1974)

[12] Thomas Morton and David Pentico.: A Volume in the Wiley Series in Engineering and Technology Management, (Ed.) D.Kocaoglu, Chapter 13.2.2,(1993)

[13] Hanssmann. F., Hess.S. W.: A linear programming approach to production and Employed scheduling. Management Technology, 1, 46-54 (1960)

[14] Michael Held., Richard M.Karp.: A Dynamic Programming Approach to Sequencing Problems. Journal of the Society for Industrial and Applied Mathematics, 10 (1), 196-210 (192)

[15] Ignall, E., Schrage, L.: Applications of the branch and bound techniques to some flow shop scheduling problems Operations Research, 13,400-412 (1965)

[16] Bomberger.E.E.: A Dynamic Programming Approach to A Lot Size Scheduling Problem, JSTOR: Management Science, USA, 12(11), 778-784 (1966)

[17] Campbell, H.G., Dudek, R.A. and Smith, M.L.: A heuristic algorithm for the n-job m-machine sequencing problem. Management Science 16(10), 169-174(1970)

[18] Lockett, A.G. and Muhlemann, A.P.: Technical notes: a scheduling Problem involving sequence dependent changeover times. Operation Research 20, 895- 902(1972)

[19] Corwin, B. D. and Esogbue, A. O.: Two machine flow shop scheduling problems with sequence dependent setup times: A dynamic programming approach. Naval Research Logistics Quarterly, 21,515-524(1974)

[20] Holland, J. H.: Genetic algorithms and the optimal allocation of trials. SIAM Journal on Computing, 2 (2), 88-105(1973)

[21] Rinnooy Kan. A.: Machine Scheduling Problem: Classification, Complexity and Computation. Martinus Nijhoff,Hague, (1976)

[22] Panwalkar.S.S., Iskander.W.: A Survey of Scheduling Rules. Operations Research, 125(1), 45-62 (1977)

[23] Arabinda Tripathy.: Integer linear programming, management science, 30(12), 1473-1489 (1984)

[24] Taghi Arani, Mark kerwan, and vahid lotfi.: Integer programming on exam scheduling problem, European journal of operations research,34,372-383(1988)

[25] Holthaus, O. and Rajendran, C.: Efficient dispatching rules for scheduling in a job shop, International Journal of Production Economics, 48, 87-105 (1997)

[26] Pan, J.C.H., Fan, E.T.: Two-machine flow shop scheduling to minimize total tardiness. International Journal of Systems Science 28, 405-414 (1997)

[27] Chen,H., Chu,C. and Proth,J.M..: An Improvement of the Lagrangean Relaxation Approach for Job Shop Scheduling: A Dynamic Programming Method, IEEE Transaction on Robotics and Automation..14(5), 786-795 (1998)

[28] Chryssolouris, G., Mavrikios, D., Papakostas, N., Mourtzis, D., Michalos, G., and Georgoulias, K.: Digital manufacturing: history, perspectives, and outlook. Proc. IMechE, Part B: J. Engineering Manufacture, 223(5), 451–462 (2009)

[29] Samir Barman, Joao V. Lisboa.: Cost performance of simple priority rule combinations, Journal of Manufacturing Technology Management, 21 (5), 567 – 584 (2010)

[30] Ko.H-H., Kim J., Kim .S.S., Baek. J.G.: Dispatching Rule for Non-identical Parallel Machines with Sequence-dependent Setups and Quality Restrictions, Computers & Industrial Engineering 59, 448-457(2010)

[31] Kayvanfar V., Mahdavi I., Komaki GM.: Single machine scheduling with controllable processing

times to minimize total tardiness and earliness. Computers & Industrial Engineering , 65(1): 166–175(2013)
[32] Kuo-Ching Ying., Chung-Cheng Lu., Jhao-Cheng Chen.: Exact algorithms for single-machine scheduling problems with a variable maintenance, Computers and Industrial Engineering, 98,427-433(2016)
[33] Ling-Huey Su., Hui-Mei Wang.: Minimizing total absolute deviation of job completion times on a single machine with cleaning activities, Computers and Industrial Engineering,103 (C), 242-249 (2017)
[34] Stecke, K.E. and J.J. Solberg (1981), "Loading and Control Policies for a Flexible Manufacturing System." International Journal of Production Research, 19 (5), 481-490.
[35] Bilge U, Ulusoy G.: A time window approach to simultaneous scheduling of machines and material handling system in an FMS. Operation Research , 43(6),1058–1070 (1995)

Acknowledgments
The authors acknowledge with thanks the financial assistance offered by DST-SERB, Govt.of India wide file. No: SB/EMEQ-501/2014 for carry out this work.

Authors: **Nageswara Rao Medikondu,** Mechanical Department, JNTUK, Kakinada, Andhra Pradesh 533003, India.
Narayana Rao K., Mechanical Department, Govt Polytechnic, Vijayawada, Andhra Pradesh, 520008 India
Ranga Janardhana G., Mechanical Department, JNTUA, Anantapur, Andhra Pradesh 533003, India
E-mail: medikondu1979@gmail.com

http://doi.org/10.24867/JPE-2017-01-085

Journal of Production Engineering

Vol.20 No.1

JPE (2017) Vol.20 (1) Original Scientific Paper

Siva Kumar, B., Charan Theja, P.

STUDY OF WEAR & MICROSTRUCTURAL BEHAVIOR OF HYBRID ALUMINIUM METAL MATRIX COMPOSITE MANUFACTURED BY STIR CASTING TECHNIQUE

Received: 27 February 2017 / Accepted: 10 May 2017

Abstract:. *Aluminium is one of the most widely used metals due to its desirable physical, chemical and mechanical properties and it characterizes an important category of technological materials. Because of its high strength-to weight ratio, besides other desirable properties e.g. high corrosion resistance, desirable appearance, nonmagnetic, non-sparking, non-toxic, ease of fabrication and high thermal and electrical conductivities, aluminium and its alloys are used in a wide variety of industrial applications. These properties led also to the association of aluminium and its alloys with transportation mainly with aircraft and space vehicles, containers and packaging and electrical transmission lines, construction and building. Nowadays Al-based composites are used due to their superior mechanical properties. The reinforcements are ceramic, metallic and non-metallic used in the form of particles, fibers, and laminates. The reinforcements added to MMC will improve the properties of the composite like yield strength, hardness, density and wear behavior. There are several studies done on the non-metallic and ceramic reinforcements. This paper attempts to study the different combination of reinforcing materials used in the processing of hybrid aluminium matrix composites and how it affects the wear performance & Microstructure of the materials.*

Key words: *Composite, Hybrid Aluminium Metal Matrix Composite, Reinforcement, Stir Casting.*

Studija habanja & mikrostrukturno ponašanje kompozita hibridnih aluminijuma sa metalnom osnovom proizvodenih uzburkanim livenjem. *Aluminijum je jedan od najšire korišćenih metala zbog poželjanih fizičkih, hemijskih i mehaničkih svojstava i on spada u važnu kategoriju tehnoloških materijala. Zbog svoje visoke čvrstoće za određenu težinu, pored drugih poželjnih osobina npr. visoka otpornost na koroziju, poželjan izgled, nemagnetičnost, ne varničnost, netoksičanost, lako se obrađuje i ima visoku termičku i električnu provodljivost, shodno tome aluminijum i njegovih legura se koriste u raznim industrijskim oblastima. Ove osobine su dovele da se danas aluminijum i njegove legure koriste pri izradi transportnih sredstva, uglavnom aviona i svemirskih vozila, kontejnera i ambalaža i izgradnju električnih dalekovoda, i izradu kompozita. Kompoziti bazirani na aluminijumul se koriste zbog njihovih superiornih mehaničkih osobina. Pojačavaju se pomoću keramike, metala i nemetala u obliku čestica, vlakana, i laminata. Pojačanje je dodato u metalnu osnovu i poboljšava svojstva kompozita kao što su tečenja, tvrdoća, gustina i habanje. Postoji nekoliko studija koje su rađene sa nemetalnim i keramičkim pojačanjima. Ovaj rad pokušava da prouči različitu kombinaciju ojačanih materijala koji se koriste u izradi hibridnih aluminijumskih matrica kompozita i kako to utiče na performanse tj. habanje & mikrostrukturu materijala.*

Ključne reči: *Kompoziti, hibridni kompoziti aluminijuma sa metalnom matricom, armatura, uzburkano livenje.*

1. INTRODUCTION

In the last two decades research has shifted from monolithic materials to composite materials to meet the global demand for light weight, high performance, environmental friendly, wear and corrosion resistant materials. Metal Matrix Composites (MMC) are suitable for applications requiring combined strength, thermal conductivity, damping properties and low coefficient of thermal expansion with lower density. In the field of automobile, MMC's are used for pistons, brake drum and cylinder block because of better corrosion resistance and wear resistance.

Manufacturing of MMC's has several challenges like porosity formation, poor wettability and improper distribution of reinforcement. Achieving uniform distribution of reinforcement is the foremost important work. A new technique of manufacturing cast Aluminium Matrix Composite has been proposed to improve the wettability between alloy and reinforcement. In this, all the materials are placed in graphite crucible and heated in an inert atmosphere until the matrix alloy is melted and followed by two step stirring action to obtain uniform distribution of reinforcement. The manufacturing techniques of MMCs play a major role in the improvement of mechanical and tribological properties.. The size and type of reinforcement also has a significant role in determining the mechanical and tribological properties of the composites.

There is a growing interest worldwide in manufacturing hybrid metal matrix composites [HMMCs] which possesses combined properties of its reinforcements and exhibit improved physical, mechanical and tribological properties.

Aluminium Metal Matrix Composite (AMMC) is competent material in the industrial world. Due to its excellent mechanical properties it is widely used in aerospace, automobiles, marine, etc. The aluminium matrix is getting strengthened when it is reinforced

with the hard ceramic particles such as B_4C, SiC, TiC, Al_2O_3 etc. Aluminium alloys are still the subject of intense studies, as their low density gives additional advantages in several applications. These alloys have started to replace cost iron and bronze to manufacture wear resistance parts.

2. LITERATURE SURVEY

A lot of contributions (or) studies are existing for the manufacturing of Hybrid Aluminium Metal Matrix Composites (HAMMC) by reinforcing Aluminium Metal with different combination of materials (Reinforcements). Some of them are reviewed and discussed below:

E. Subbarao, N. Ramanaiah [1] This study is aimed in evaluating the mechanical properties of aluminium metal matrix composite (AMMC). AMMCs were made, AA6061 as matrix material and B_4C as reinforcement material, through stir casting method. AMMCs with varying percentage by different wt. %, 1%,2 %, 3%, 4%,5% B_4C were fabricated. It was noticed that, mechanical properties are increase with the increase in wt. % of the reinforcement up to 4% B_4C further addition there is a diminution in both the conditions (as cast and heat treatment condition). It was also thought-out that 4% B_4C composite shows better mechanical (hardness, yield strength and tensile strength) properties and low % of elongation than all other compositions in both the conditions. Optical micrographs and SEM micrographs revealed that the B_4C particles were well distributed in the Aluminium matrix in heat treatment condition.

N. Venkat Kishore, Dr. K. Venkata Rao [2] In thist study Aluminum alloy (A356/LM25) and Boron Carbide (B_4C) were taken as matrix and reinforcement respectively. The Fabrication, mechanical and metallurgical investigation of Aluminum alloy (A356/LM25) and Boron Carbide (B_4C) composites containing the three different weight percentages 5%, 7.5% and 10% of B_4C by means of Two Step-Mixing method of Stir Casting Technique. Further it was found from the experimentation is that the developed method is quite successful to obtain uniform dispersion of reinforcement in the matrix. The results indicated that the wear rate decreases and an increasing trend of hardness and tensile strength with increase in weight percentage of B_4C have been observed. The internal structure of the composite is observed using Optical Metallurgical Microscope. It is observed that B_4C particles are dispersed uniformly in the aluminum matrix for all wt% and also Grain refinement was increased by increasing in percentage of Boron Carbide (B_4C) reinforcement in the Aluminum (LM25) Matrix.

M.D.Antony Arul Prakash, M.Arockia Jaswin [3] In this project silicon carbide and boron carbide particulate reinforced aluminium alloy matrix composites are produced by stir casting process by varying the particulate addition by weight fraction of Al (90%), SiC (5%, 6.5%, 8%) and B_4C (5%, 3.5%, 2%). Characterization study was made by SEM and optical microscopic analysis, the result predict that the dispersion of the SiC and B_4C particles are equal in all over the specimens and also an increase in the particles cluster corresponding to an increase in the processing temperatures.

Gaurav Mahajan, Nikhil Karve, Uday Patil, P. Kuppan, K. Venkatesan [4] In this paper an effort has been made to fabricate a hybrid metal matrix composite, silicon carbide and titanium diboride reinforced in Al 6061 matrix using stir casting method. Microstructure and mechanical properties such as micro hardness and wear are studied for various compositions of reinforcements, 10% SiC and 2.5%, 5% and 10% TiB□. The results indicate that the hardness value increases with the addition of the SiC and TiB□ reinforcements to matrix Al6061, while the wear resistance increases up to certain amount and reduces drastically when crossed the transition load.

A. Singh, A. S. Rana, N. Bala [5] In this study, aluminium composite with 5% reinforcement of Al_2O_3 + fly-ash was prepared using a cost effective stir casting technique. Testing of wear behavior was done on pin on disc apparatus at a normal load of 40 N and sliding velocities of 0.8 m/sec and 1 m/sec. The fabricated composites showed improvement in wear resistance over the monolithic aluminum metal.

T. Raviteja, N. Radhika, R. Raghu [6]) The present study was made to understand the fabrication and mechanical properties of Al-Si12Cu/B_4C Metal Matrix Composites. The composites were fabricated by reinforcing B_4C particles with varying wt % of 2, 4, 6, 8 and 10, using stir casting process. The microstructure was examined on the composite specimens using optical microscope to confirm the homogeneous dispersion of reinforcement particles in the matrix. Mechanical properties such as hardness and tensile strength were tested on the composite using Brinell hardness tester and computerized Universal Testing Machine respectively. The results revealed that the B_4C particles were homogeneously distributed in the composite. The hardness and tensile test results showed that, by increasing wt % of reinforcement particles in the matrix, hardness and tensile strength of the composites was improved to 6.97 % and 33 % respectively compare to base alloy.

T. Thirumalai, R. Subramanian, S. Kumaran, S. Dharmalingam, S. S. Rama Krishnan [7] Aluminum matrix composites reinforced with up to 12 wt % B_4C and 3 wt % Gr particulates are investigated in the present study. Hybrid composites exhibit better wear characteristics compared to aluminium alloy. Wear tests were carried out with loads varying from 10 to 40 N and sliding distances of 500 and 1000 m with a constant sliding speed of 1m per second. An interaction between load and sliding distance was observed in the composites which may be attributed to the presence of Gr particulates. Decrease in wear with an increase in speed and vice versa were observed with both load and sliding distance. Hardness of the composites measured using Vicker's Hardness Tester indicated that hardness increased with increasing percent of B_4C reinforcement while addition of Gr imparted the lubrication effect in the composites.

Md. Habibur Rahman, H. M. Mamun Al Rashed [8] The Purpose of this work is to study about the

microstructures, mechanical properties and wear characteristics of as cast silicon carbide (SiC) reinforced aluminum matrix composites (AMCs). AMCs of varying SiC content (0, 5, 10 and 20 wt. %) were prepared by stir casting process. Microstructures, Vickers hardness, tensile strength and wear performance of the prepared composites were analyzed. The results showed that introducing SiC reinforcements in aluminum (Al) matrix increased hardness and tensile strength and 20 wt. % SiC reinforced AMC showed maximum hardness and tensile strength. Microstructural observation revealed clustering and non-homogeneous distribution of SiC particles in the Al matrix. Porosities were observed in microstructures and increased with increasing wt. % of SiC reinforcements in AMCs. Pin-on-disc wear test indicated that reinforcing Al matrix with SiC particles increased wear resistance.

Mr. Prashant Kumar Suragimath, Dr. G. K. Purohit [9] In this study a modest attempt has been made to develop aluminium based MMCs with reinforcing material, with an objective to develop a conventional low cast method of producing MMCs and to obtain homogeneous dispersion of reinforced material. To achieve this objective stir casting technique has been adopted. Aluminium Alloy (LM6) and SiC, Fly Ash has been chosen as matrix and reinforcing material respectively. Experiment has been conducted by varying weight fraction of Fly Ash (5% and 15%) while keeping SiC constant(5%). The result shown that the increase in addition of Fly Ash increases the Tensile Strength, Impact Strength, Wear Resistance of the specimen and decreases the percentage of Elongation.The microstructure study shows fairly uniform distribution of SiC and Fly Ash in LM6 based metal matrix composite.

S. Dhinakaran, T. V. Moorthy [10] The focus of the work is on fabricating the aluminium (AA6061) matrix composites reinforced with the varied propositions of the percentage of the weight of B_4C particle of size at 220μm such as 3%, 6% and 9% by means of the stir casting method. The enhancement in the wettability of B4C particles in the matrix by adding K2TiF6 flux into the molten metal, has been significant. Besides, the microstructure and mechanical properties of the fabricated AMCs have also been analyzed. Uniform distribution of the presence of the B_4C particle in the matrix has been confirmed using the Scanning Electron Microscope (SEM) images. It has been found that the tensile strength and hardness of the fabricated AMCs increases phenomenally with the increased content of the B_4C particle.

J. David Raja Selvam, D. S. Robinson Smart, I. Dinaharan [11] This work focuses on the fabrication of AMCs reinforced with various weight percentages of SiC particulates and a constant weight percentage of Fly Ash by modified stir casting route. The wettability of SiC and Fly ash particles in the matrix was improved by adding magnesium into the melt. The microstructure and mechanical properties of the fabricated AMCs were analyzed. The optical and scanning electron micrographs revealed a homogeneous dispersion of both SiC and Fly ash particles in the aluminum matrix. The SEM micrographs revealed that the addition of Fly Ash helped to prevent SiCp dissolution and the formation of Al_4C_3. The mechanical properties like hardness and tensile strength were improved with the increase in weight percentage of SiC particulates with constant weight percentage of Fly Ash in the aluminum matrix.

S. Rama Rao, G. Padmanabhan [12] In this context aluminium alloy - boron carbide composites were fabricated by liquid metallurgy techniques with different particulate weight fraction (2.5, 5 and 7.5%). Phase identification was carried out on boron carbide by X-ray diffraction studies. Microstructure analysis was done with scanning electron microscope. Scanning electron microscopy images shows that boron carbide particles are uniformly distributed in aluminium matrix.

J. Babu Rao, D. Venkata Rao, N. R. M. R. Bhargava [13] In the present investigation, pure aluminium – 5 to 15% (by weight) fly ash composites were made by stir casting route. Phase identification and structural characterization was carried out on fly ash by X- ray diffraction studies. Scanning electron microscopy and optical microscopy was used for microstructure analysis. There was a uniform distribution of fly ash particles in the matrix phase and also existing a good bonding between matrix and fly ash.

From the literature survey it is clear that the different combination of reinforcements used for the manufacturing of Hybrid Aluminium Metal Matrix Composite's (HAMMC). Hybrid Aluminium Metal Matrix Composite's (HAMMC) can be manufactured effectively by using an appropriate manufacturing technique depending on choice of reinforcement. Aluminium alloy with reinforcement is always better than base alloy because reinforcement particle's improves the mechanical properties like tensile strength, impact strength, wear resistance, hardness and corrosion resistance etc.

2.2 Problem statement

There are numerous studies has been reported on Aluminium Metal Matrix Composite reinforced with B_4C or Fly Ash particles individually or with other combination but limited work is carried out on Aluminium reinforced with both Boron Carbide (B_4C) & Fly ash.Thus the present investigation has been focussed on utilization of waste Fly Ash and Boron Carbide (B_4C) in useful manner by dispersing it in aluminium alloy matrix to manufacture Al-B_4C-Fly Ash Hybrid Composites with different percentages of reinforcements,further the study of Wear & Microstructural behavior of these Hybrid composites are also evaluated.

3. MATERIALS & METHODS

3.1 Materials

Aluminium 7075 T651 is used as Matrix Material, Boron Carbide (B_4C) & Fly Ash powders are used as Reinforcement material.

3.2 Experimental work

3.2.1. Stir Casting

The simplest and most effective method used for the manufacturing of Hybrid Composites is the Stir Casting method. This Stir Casting technique is employed to manufacture is a Liquid state method and in this method a dispersed phase (reinforcement particles) is mixed with a molten metal by means of mechanical stirring. In this process Aluminium 7075 T651 (in proper wt %) was placed in crucible and melted at 1000□. The reinforcements Boron Carbide (B_4C) & Fly Ash of proper wt% were preheated to 500□ in an Electric furnace to remove the moisture. The preheated reinforcements were slowly added to the molten metal at 1000□ with continuous stirring by the stirrer for evenly dispersing Boron Carbide & Fly Ash particles in the molten aluminium alloy. The high temperature Hybrid Aluminium Metal Matrix Composite (HAMMC) was poured in to the mould having inside mould dimensions of 250 mm X 20 mm Diameter and left for some time to get solidified before withdrawing it from the mould. Three number of samples were manufactured having different composition (wt%) as listed in the Table 1.

Fig. 1. Stir Casting Furnace

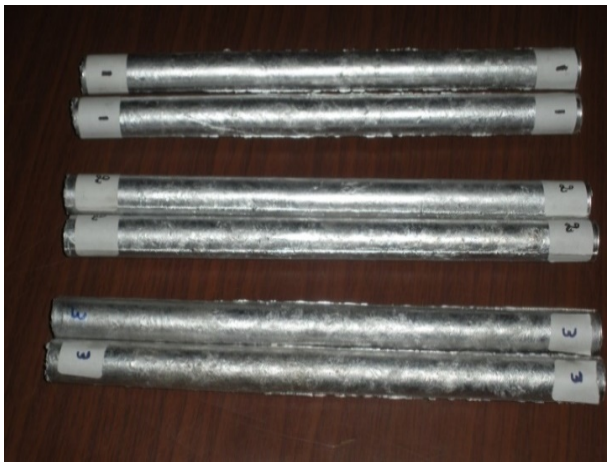

Fig. 2. HAMMC specimens after Stir Casting

Sl. No.	Materials with Compositions (% of Reinforcements)	Sample Number
1	Al + 1wt% B_4C + 9wt% Fly Ash	S1
2	Al + 2wt% B_4C + 8wt% Fly Ash	S2
3	Al + 3wt% B_4C + 7wt% Fly Ash	S3

Table 1. HAMMC samples with their compositions

3.2.2. SEM Sample Preparation

Sample preparation plays an important and vital role in getting accurate results for the microstructure analysis. To study the Microstructure of the specimens were cut and prepared as per the standard metallographic procedure. The specimen is then polished with SiC abrasive papers of various grades. To give a scratch free surface , it is finally polished by using a disc polishing machine.After that the specimens were etched using Keller's reagent (HCl + HF + HNO_3). The microstructure of etched specimens were observed using Scanning Electron Microscope (SEM).

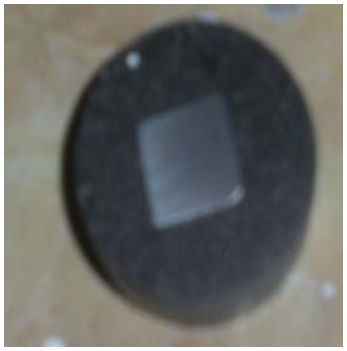

Fig. 3. Specimen for SEM Analysis

3.3 TESTING OF HYBRID ALUMINIUM METAL MATRIX COMPOSITE

The manufactured specimens were proposed to test for Waer Test & also Microstructural analysis is going to be performed.

3.3.1 Wear Testing:

The Wear Testing of the Hybrid Aluminium Metal Matrix Composites (HAMMC) has been determined by Wear Testing Machine .

Fig. 4. Wear Testing Machine

Fig. 5. Specimens before Wear Testing.

Fig. 6. Specimens after Wear Testing

4. RESULTS & DISCUSSIONS:

4.1 Wear Resistance:

The test revealed that the Abrasion loss of the Hybrid Aluminium Metal Matrix Composite (HAMMC) was decreased gradually with the increase in the wt% of Boron Carbide powder. Table 2 shows the Wear Resistance of Hybrid Aluminium Metal Matrix Composite (HAMMC) at various percentages of Reinforcements (B_4C + Fly Ash).

$$Abrasion\ Lost\ (\%) = \frac{(Final\ Weight - Initial\ Weight)}{Initial\ Weight} \times 100$$

Sample Number	Initial Weight (Gms)	Final Weight (Gms)	Abrasion Loss (Gms)	Abrasion Loss (%)
S1	5.2974	5.1208	0.1766	3.33
S2	6.1777	6.0037	0.1740	2.82
S3	5.7123	5.5354	0.1769	3.09

Table 2. Wear Resistance of HAMMC

4.2 Evolution of Microstructure

The Microstructural analysis of the specimen was carried out by using Scanning Electron Microscope (SEM). In general, SEM is used to observe the topography and morphology of a specimen. Th function of SEM is as a mapping device which probed by a beam of electron scanned across the surface.

A Scanning Electron Microscope (SEM) is a type of electron microscope that produces images of a sample by scanning it with a focused beam of electrons. The electrons interact with atoms in the sample, producing various signals that can be detected and that contain information about the samples surface topography and composition.The following figures i.e Figure 7 to Figure 21 shows the microstructures of the three samples (Sample 1, Sample 2 & Sample 3) at different magnifactions .

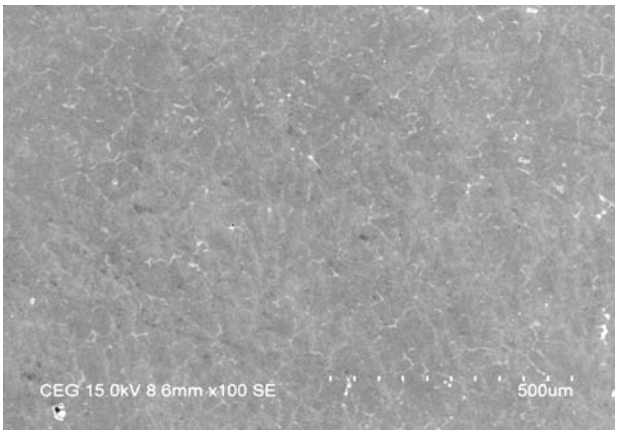

Fig. 7. Microstructure of Sample 1 at 100 X Magnification

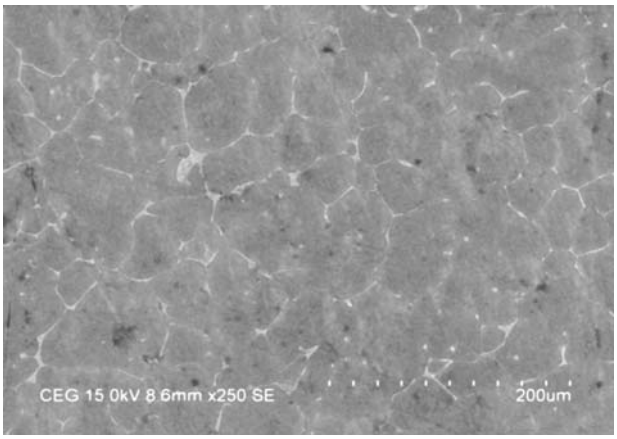

Fig. 8. Microstructure of Sample 1 at 250 X Magnification

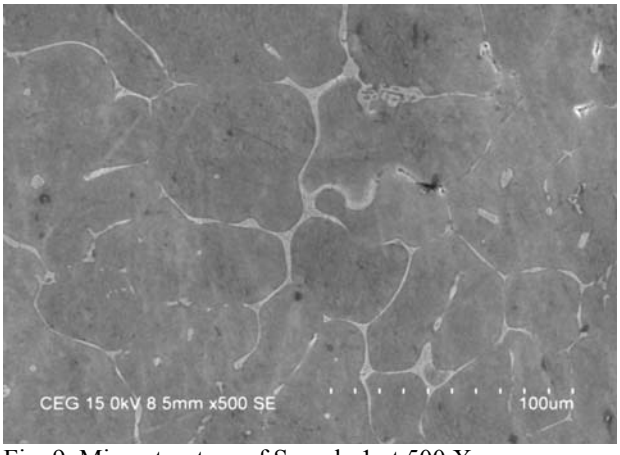

Fig. 9. Microstructure of Sample 1 at 500 X Magnification

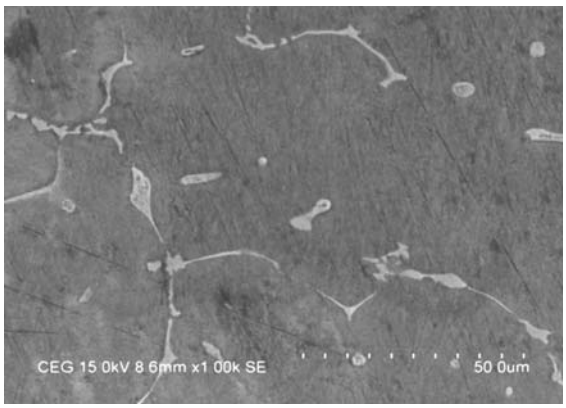

Fig. 10. Microstructure of Sample 1 at 1000 X Magnification.

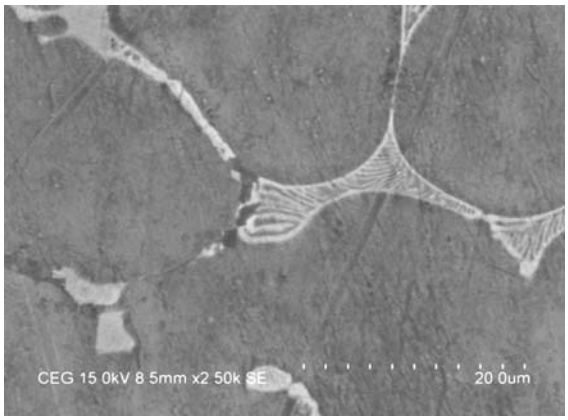

Fig. 11. Microstructure of Sample 1 at 2500 X Magnification.

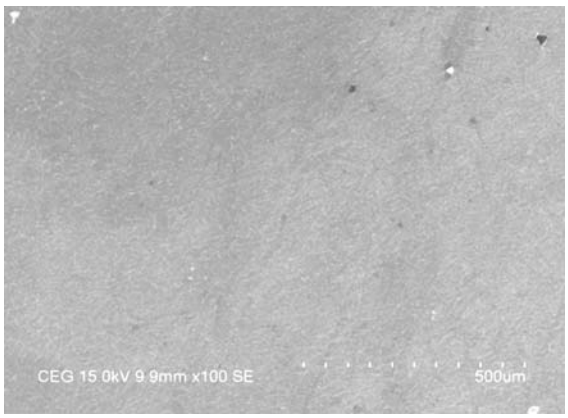

Fig. 12. Microstructure of Sample 2 at 100 X Magnification.

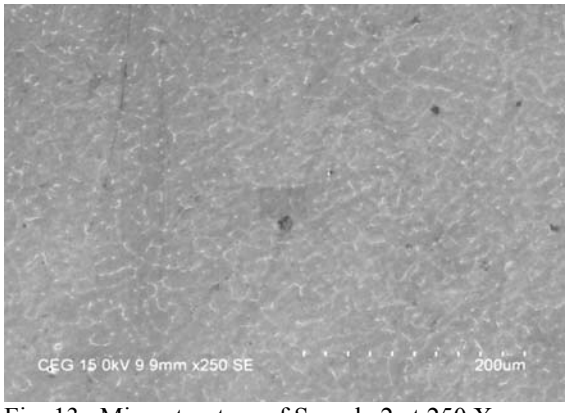

Fig. 13. Microstructure of Sample 2 at 250 X Magnification.

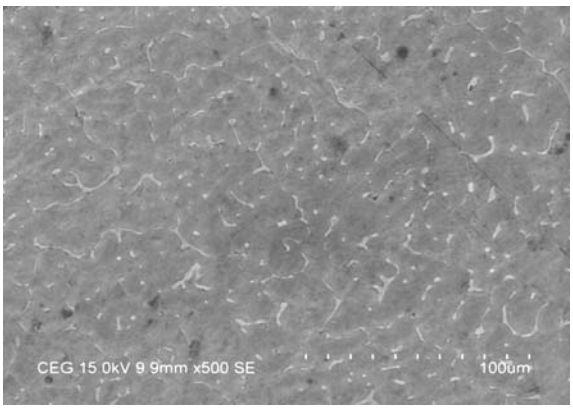

Fig. 14. Microstructure of Sample 2 at 500 X Magnification.

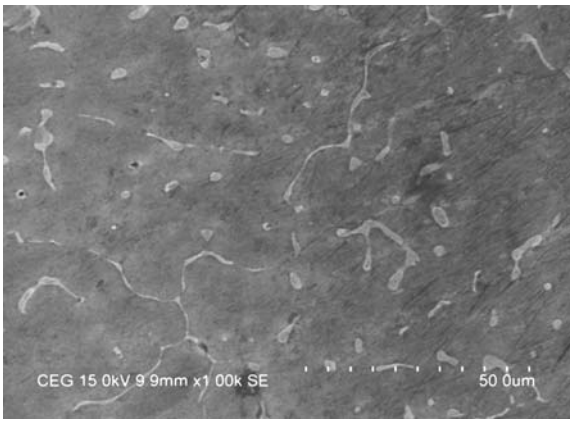

Fig. 15. Microstructure of Sample 2 at 1000 X Magnification.

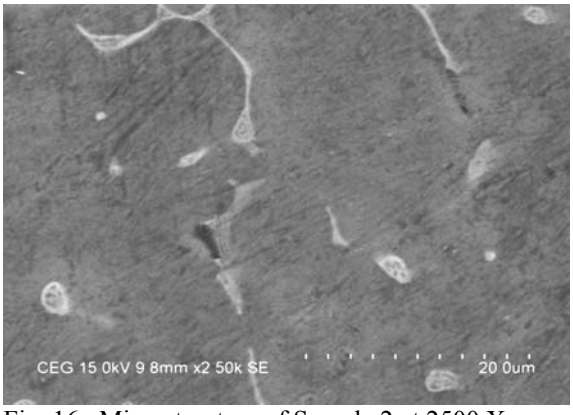

Fig. 16. Microstructure of Sample 2 at 2500 X Magnification.

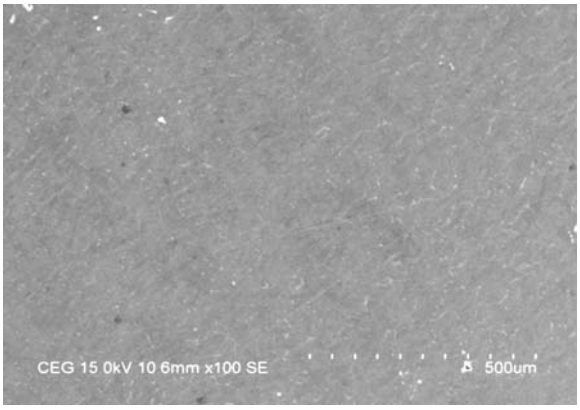

Fig. 17. Microstructure of Sample 3 at 100 X Magnification.

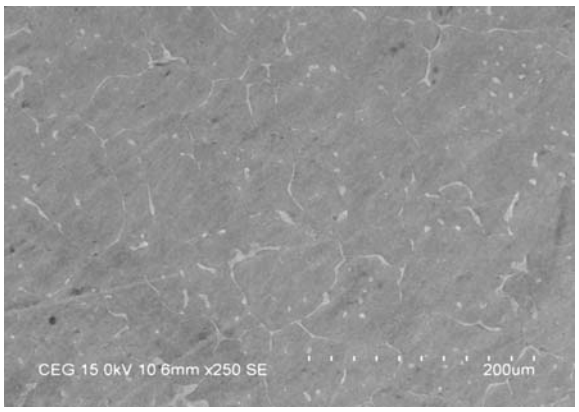

Fig. 18. Microstructure of Sample 3 at 250 X Magnification.

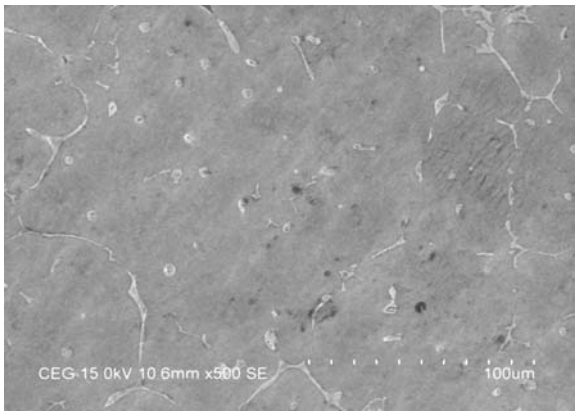

Fig. 19. Microstructure of Sample 3 at 500 X Magnification.

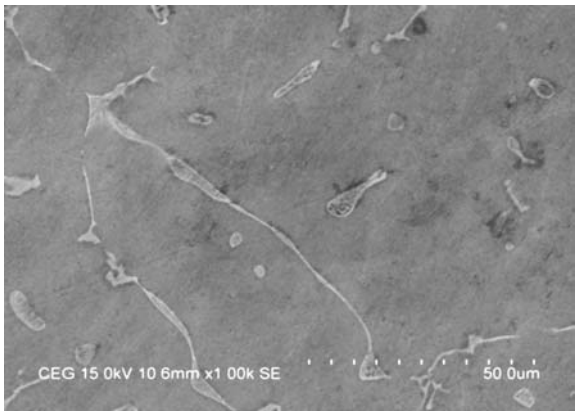

Fig. 20. Microstructure of Sample 3 at 1000 X Magnification.

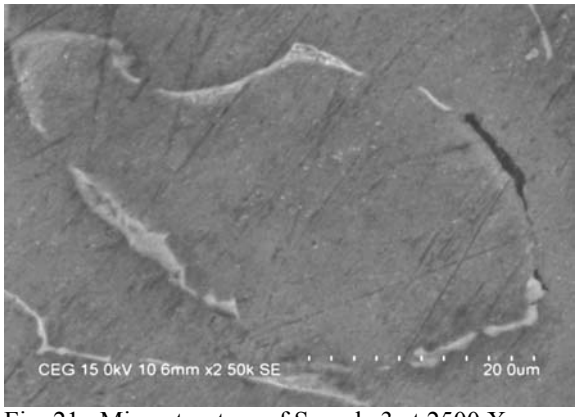

Fig. 21. Microstructure of Sample 3 at 2500 X Magnification**.**

5. CONCLUSIONS

The Hybrid Aluminium Metal Matrix Composite (HAMMC) was produced with different Wt% of Reinforcements i.e Boron Carbide (B_4C) & Fly Ash. The Wear & Microstructural Properties of the Hybrid Aluminium Metal Matrix Composite (HAMMC) were evaluated and the following conclusions are drawn from the study:

1) The Hybrid Aluminium Metal Matrix Composite (HAMMC) was successfully fabricated by Stir Casting Technique.
2) The test revealed that the Abrasion loss of the Hybrid Aluminium Metal Matrix Composite (HAMMC) was decreased gradually with the increase in the wt% of Boron Carbide powder. Also the Hybrid Aluminium Metal Matrix Composite with 2% Boron Carbide (B_4C) and 8% Fly Ash is having less Abrasion loss indicating that it posses High Wear Resistance.
3) The SEM micrographs revealed the presence of Boron Carbide & Fly Ash and also shows a homogenous distribution of Boron carbide & Fly Ash Particles in the Aluminium matrix material.

6. REFERENCES

[1] E.Subbarao and N.Ramanaiah, *Microstructure and Mechanical properties of Al-Mg-Si based metal matrix composites reinforced with B_4C particles produced through Stir Casting processes*, Journal of Production Engineering, Vol.19(1), 2016, 75 – 80.

[2] N.Venkat Kishore and Dr.K.Venkata Rao, *Mechanical properties in MMC of aluminium alloy (A356/LM25) matrix and boron carbide (B_4C) reinforcement*, International Journal of Engineering Research & Technology (IJERT), Vol.5, Issue 02, February-2016, 683-689.

[3] M.D.Antony Arul Prakash and M.Arockia Jaswin, *Microstructural analysis of aluminium hybrid metal matrix composites developed using stir casting process*, International Journal of Advances in Engineering, Vol.1(3), 2015, P.P:333-339.

[4] Gaurav Mahajan, Nikhil Karve, Uday Patil, P.Kuppan and K.Venatesan, *Analysis of microstructure, hardness and wear of Al-SiC-TiB2 hybrid metal matrix composite*, Indian Journal of Science and Technology, Vol 8(S2), January 2015, P.P: 101-105.

[5] Amardeep Singh, Ajay Singh Rana and Niraj Bala, *Study of wear behaviour of aluminium based composite fabricated by stir casting technique,* International Jounal of Mechanical Engineering and Robotics Research, Vol. 4, No.1, January 2015, 271-278.

[6] T.Raviteja, N.Radhika and R.Raghu, *Fabrication and mechanical properties of stir cast Al-Si12Cu/B4C composites*, International Journal of Research in Engineering and Technology, Volume 03, Issue 07, Jul-2014, P.P:343-346.

[7] T.Thirumalai, R.Subramanian, S.Kumaran, S.Dharmalingam and S.S.Ramakrishnan, *Production and characterization of hybrid aluminium matrix composites reinforced with boron carbide (B_4C) and graphite,* Journal of Scientific & Industrial Research, Vol.73, October 2014, P.P:667-670.

[8] Md.Habibur Rahman, H.M.Mamum Al Rashed, *Characterization of silicon carbide reinforced aluminium matrix composites*, 10th International Conference on Mechanical Engineering ICME 2013,Procedia Engineering 90(2014), P.P:103-109.

[9] Prashant Kumar Suragimath, Dr.G.Purohit, *A study on mechanical properties of aluminium alloy(LM6) reinforced with SiC and fly ash*, IOSR Journal of Mechanical and Civil Engineering, Volume 8, Issue 5, Sep-Oct 2013, P.P:13-18.

[10] S.Dhinakaran and T.V.Moorthy, *Fabrication and characteristic of boron carbide particulate reinforced aluminium metal matrix composites.*

[11] David Raja Selvam, D.S.Robinson Smart, I.Dinaharan, *Synthesis and characterization of Al6061-Fly AshP-SiCP composites by stir casting and compocasting methods*, 10th Eco-Energy and Materials Science and Engineering (EMSES2012), Energy Procedia 34 (2013), P.P:637-646.

[12] Rama Rao and G. Padmanabhan, *Fabrication and mechanical properties of aluminium-boron carbide composites*, International Journal of Materials and Biomaterials Applications 2(3), 2012,P.P:15-18

[13] J.Babu Rao, D.Venkata Rao and N.R.M.R.Bhargava, *Development of light weight ALFA composites*, International Journal of Engineering Science and Technology, Vol.2, No.11, 2010, P.P:50-59.

Authors: **Bandaru Sivakumar, P.G.Student,** Advanced Manufacturing Systems, Department of Mechanical Engineering, Sri Venkateswara College of Engineering, Tirupati, Chittoor District, Andhrapradesh, India.

Pudi Chran Theja, Assistant Professor, Department of Mechanical Engineering, Sri Venkateswara College of Engineering, Tirupati, Chittoor District, Andhrapradesh, India.

E-mail: bsivatpt@gmail.com
pcttej1@gmail.com

http://doi.org/10.24867/JPE-2017-01-093

Journal of Production Engineering

Vol.20 No.1

JPE (2017) Vol.20 (1) Original Scientific Paper

Khanna, P., Maheshwari, S.

MICROHARDNESS ANALYSIS IN MIG WELDING OF STAINLESS STEEL 409M

Received: 14 March 2017 / Accepted: 17 April 2017

Abstract: *Stainless steel 409M is a utility grade ferritic steel and was developed as a cheaper alternative to Austenitic stainless steel as it has less amounts of Ni, but still posses very good corrosion resistance, mechanical properties and weldability. In the present investigation, effect of heat input and cooling rates on the magnitude and distribution of microhardness values in different weld zones developed during the MIG welding of this material have been studied and analyzed. A weld can broadly be divided into four main zones namely; fusion zone (FZ), weld interface or fusion boundary zone (FBZ), heat affected zone (HAZ) and unaffected base metal zone. These zones experience different rates of cooling, resulting in the formation of different microstructures. Microhardness study is one of the methods of testing the quality of a weld as it enables the mechanical properties to be determined in different weld zones by corroborating the nature of microstructure constituents present therein.*

Keywords: *microhardness, fusion zone, fusion boundary zone, heat affected zone, microstructure*

Analiza mikrotvrdoće MIG zavarivanja nerđajućeg čelika 409M. *Nerđajući čelik 409M je konstrukcioni ferritni čelik i nastao je kao jeftinija alternativa austenitnnog nerđajućeg čelika, jer ima manje količine Ni, ali i dalje poseduje veoma dobru otpornost na koroziju, mehanička svojstva i zavarljivost. U ovom istraživanju je proučavan i analiziran efekat unete toplote i hlađenja na veličinu i distribuciju vrednosti mikrotvrdoće u različitim zonama šava razvijenih u MIG zavarivanju ovog materijala. Zavar se može podeliti u četiri glavne zone naime; zona fuzije zavara (FZ), interfejs ili granična zona fuzije (FBZ), zona uticaja toplote (ZUT) i zona osnovnog metala. Ove zone su pod razlicitim uticajem toplote i hlađenja, što dovodi do formiranja različitih mikrostruktura. Studija mikrotvrdoće je jedna od metoda ispitivanja kvaliteta vara jer omogućava da se mehanička svojstva utvrde u različitim zavarenim zonama potkrepljena prirodom mikrostrukture sastojaka prisutnih na njima.*

Ključne reči: *mikrotvrdoća, zona fuzija, zona granice fuzije, zona uticaja toplote, mikrostruktura*

1. INTRODUCTION

In a fusion welding process, the rate of cooling is of prime importance as it decides the kind of phase transformation that takes place at a given point. The rate of cooling further depends upon the welding process, welding procedure, weld parameters, weld metal etc. MIG welding process is capable of welding all metals for which electrode wires are available [1]. Selection of welding parameters has a significant effect on the resulting microstructures [2, 5].The different weld zones formed are shown in fig.1(a & b). The rate of cooling decreases as the distance from the weld centreline increases, which suggests schematically that different phase transformations will take place in different zones. MIG welding is a high cooling rate process where the heating and cooling of the weld and the base metal are so fast that it is not always possible to predict as to what extent a particular phase transformation has taken place [3]. The FZ is characterized by a homogeneous mixture of base and filler metal and has columnar structure. It exhibits a typical cast structure. The weld interface or FBZ is a narrow zone consisting of partially melted base metal which immediately solidified before any mixing could take place. HAZ is where the heat from the welding causes heat treatment of the parent metal. The amount of metallurgical damage is decided by the maximum temperature reached, distance from FZ, time of exposure to maximum temperature, cooling rate etc. HAZ exhibits heat treated structure involving phase transformation, recrystallization and grain growth [4]. The unaffected zone is the region where heat from welding could not bring about any phase change as the temperature here stays less than the recrystallization temperature. In order to differentiate one transformation from the other, microhardness survey of different zones of interest is carried out [6].

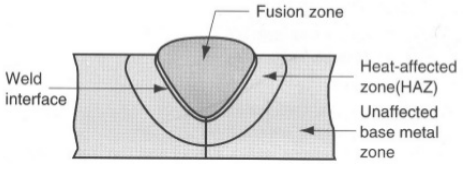

Fig. 1(a) Different weld zones

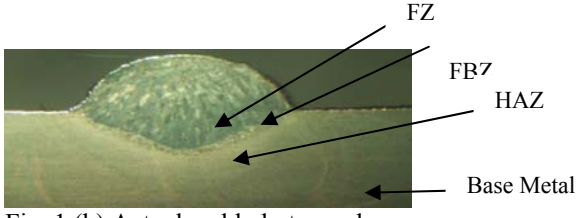

Fig. 1 (b) Actual weld photograph

2. EXPERIMENTAL INVESTIGATIONS

A detailed microhardness survey was carried out in various weld zones shown in fig.1a & 1b, to ascertain

the effects of following weld parameters on microhardness.

1. Effect of wire feed rate
2. Effect of arc voltage
3. Effect of welding speed
4. Effect of nozzle to plate distance
5. Effect of torch angle

The working limits of weld parameters are shown in table-1. The standard bead on plate technique was used to lay the weld beads on SS409M plates of 250mmx150mmx6mm size with a wire of Ø1.2mm of Stainless steel 308L. Single beads were laid lengthwise at the centre of each plate. Specimen of 25mm width each were cut from the middle of each plate and were polished as per the standard metallurgical practices and etched using a recommended etchant, a mixture of Ferric chloride, Hydrochloric acid and water in this case.

The microhardness value of the parent metal was determined (as per ASTM E834) separately and was superimposed on the graphs depicting the microhardness values fusion zone, fusion boundary zone and heat affected zone. Microhardness values of all the samples were determined by using Vickers microhardness tester of make Future Tech , model FM-700e, in two directions, one along the horizontal axis parallel and near the surface of the plate and the other along the vertical axis, starting from the centre of the weld bead towards HAZ as shown in figure 2 (a &b). The results were graphically plotted to clearly understand the effect of different weld parameters on microhadness values in various weld zones.

(a) horizontal axis

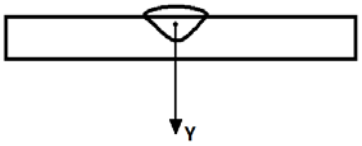

(b) vertical axis

Fig. 2. micrhardness along

Welding variables	Unit	Symbol	limits				
			-2	-1	0	1	2
Wire feed rate	m/min	I	2.8	4.8	6.8	8.8	10.8
Welding speed	cm/min	S	30	35	40	45	50
Arc voltage	volts	V	20	23	26	29	32
Nozzle to plate distance	mm	N	10	12.5	15	17.5	20
Electrode to work angle	degrees	θ	75	82.5	90	97.5	105

3. RESULTS

The results in the form of microhardness graphs are presented in figures 3-7. Each of these figures has two parts (a) and (b). Part (a) represents the microhardness values along the horizontal axis parallel and close to the workpiece surface. and part (b) shows microhardness values along the vertical axis of the weld bead. Microhardness values of the parent metal have been superimposed in each figure for comparison.

4. ANALYSIS OF RESULTS

The graphical results are analyzed to understand the effects of various welding parameters on the microhardness values in different zones as given below;

4.1 Effect of wire feed rate

The microhardness values along the horizontal andvertical axes of the weld are shown in Figure 3 (a & b). It shows that the microhardness was much higher in the fusion zone and dropped suddenly at the fusion boundary zone to nearly the same value as that of parent metal. The wire feed rate of 2.8 m/min consistently showed higher values than at 6.8 m/min and 10.8m/min in the fusion zone. The reason may be that at lower values of WFR, the cooling rate is faster.

4.2 Effect of welding speed

Figure 4 (a) and (b) shows the microhardness values along the horizontal andvertical axes of the weld respectively. Microhardness is maximum at a welding speed of 50cm/min, which is indicative of the fact that at higher welding speeds due to faster cooling rates, a hard microstructure is formed.

4.3 Effect of arc voltage

Figure 5 (a) and (b) shows the microhardness values along the horizontal and vertical axes of the weld respectively. It is evident that the microhardness is maximum at an arc voltage of 20v and minimum at 32v. The change in microhardness with voltage could be attributed to the change in arc spread with voltage.

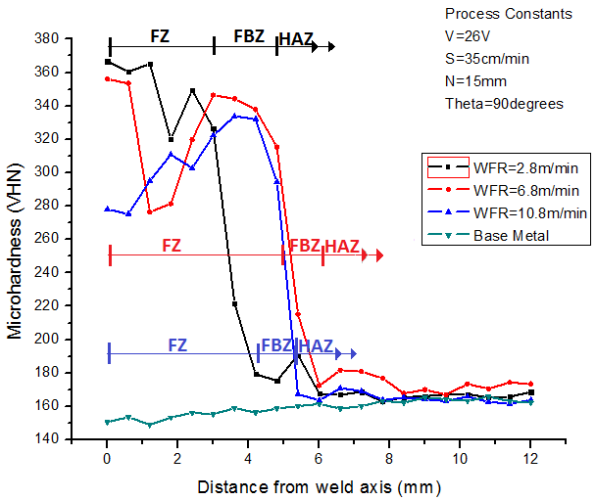

Fig. 3 (a) effect of wire feed rate on microhardness along horizontal axis

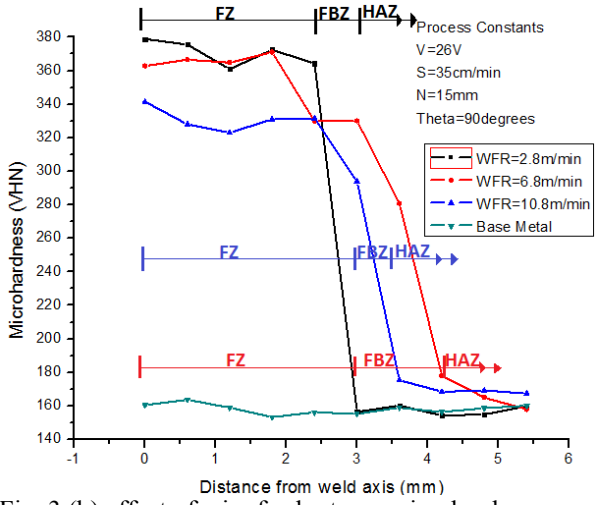

Fig. 3 (b) effect of wire feed rate on microhardness along vertical axis

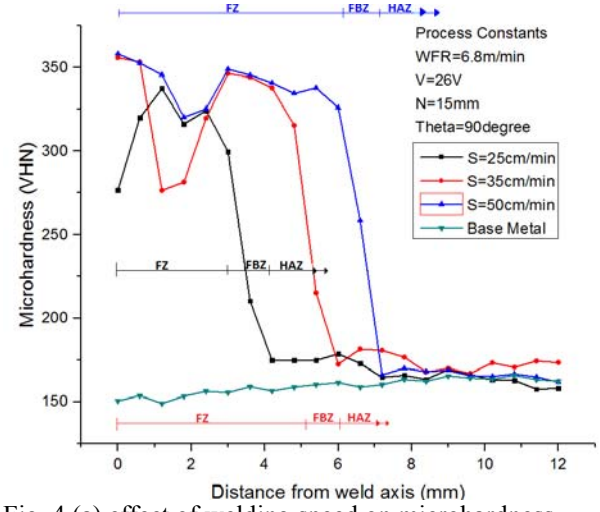

Fig. 4 (a) effect of welding speed on microhardness along horizontal axis

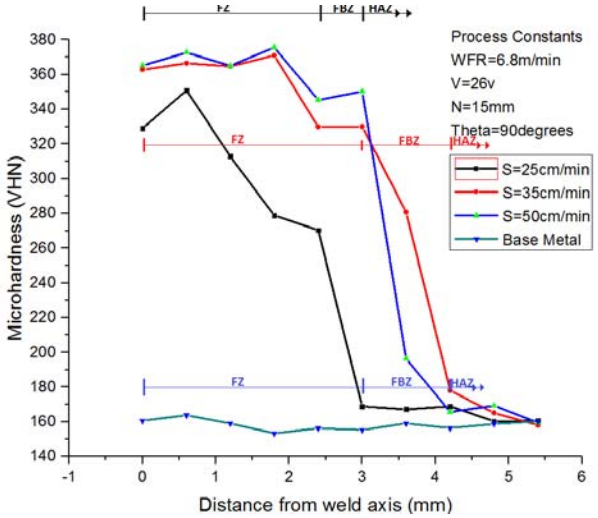

Fig. 4 (b) effect of welding speed on microhardness along vertical axis

At low voltage the average microhardness value is maximum indicating that it was the result of high cooling rate which did not give enough time for the grain growth and hence increased hardness.

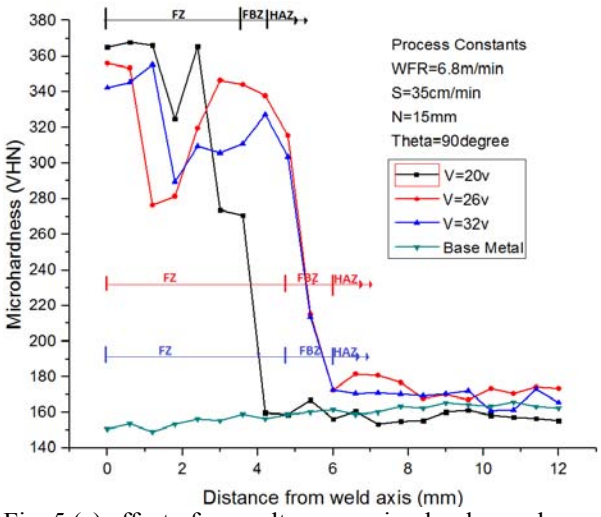

Fig. 5 (a) effect of arc voltage on microhardness along horizontal axis

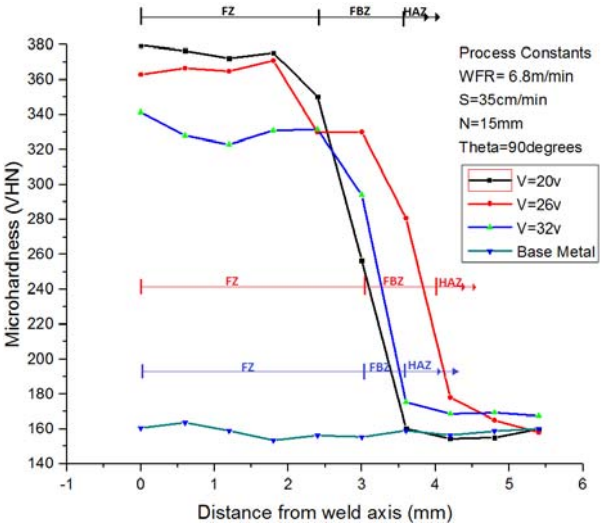

Fig. 5 (b) effect of arc voltage on microhardness along vertical axis

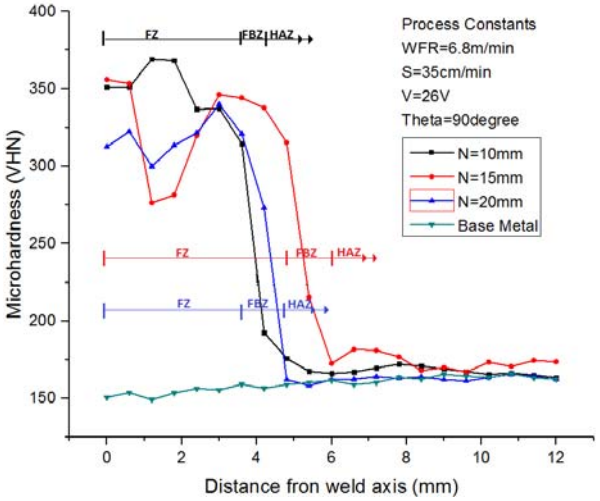

Fig. 6 (a) effect of NPD on microhardness along horizontal axis

4.4 Effect of nozzle to plate distance

The effects of change in NPD on microhardness along the vertical axis of the bead are shown in fig. 6 (b). It is evident that at lowest value of NPD the microhardness is maximum and vice-versa.

The probable reason could be that at maximum NPD the shielding gas experiences maximum spread thereby its cooling effect reduces, resulting in slow cooling rate and hence lower hardness.

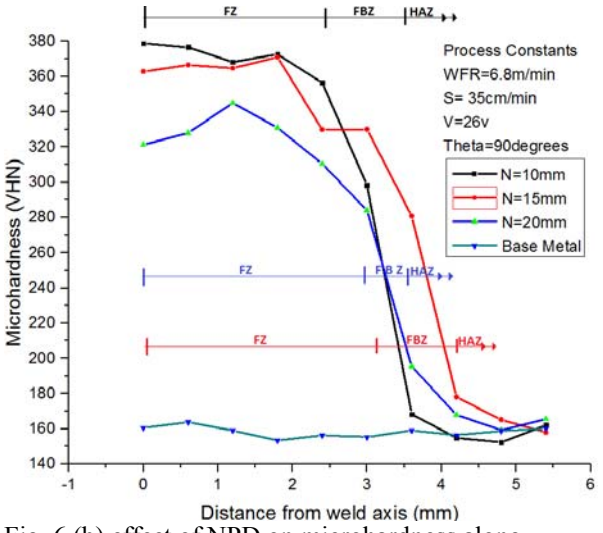

Fig. 6 (b) effect of NPD on microhardness along vertical axis

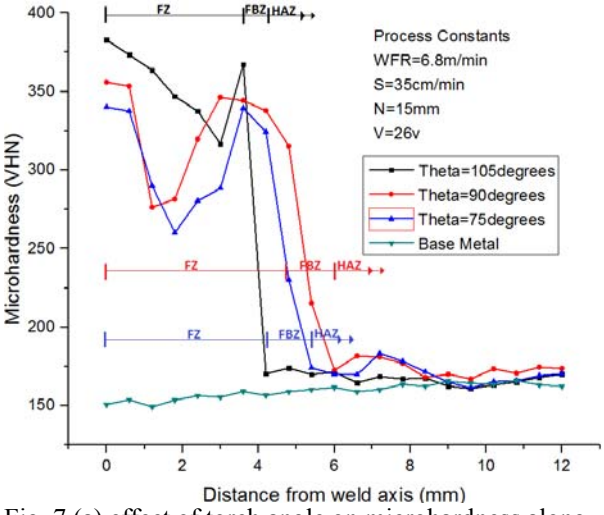

Fig. 7 (a) effect of torch angle on microhardness along horizontal axis

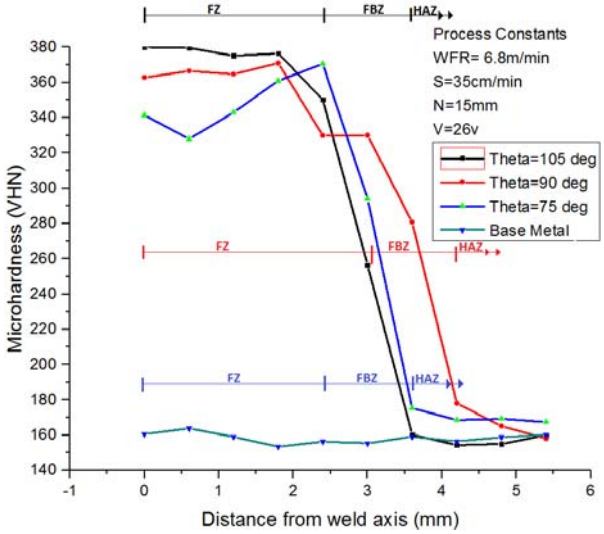

Fig. 7 (b) effect of torch angle on microhardness along vertical axis

Figure 6 (a) shows the variations in microhardness along the horizontal axis. In this case there are excessive fluctuations in microhardness values for all the NPD's. This could probably be due to the changing heat flow patterns possibly caused by changing flow patterns of the shielding gas.

4.5 Effect of torch angle

Figure 7 (a) indicates that microhardness of weld metal for torch angle of 105° i.e. forehand welding was maximum, whereas it was lowest for torch angle 75° i.e. backhand welding. The reason could be that for forehand welding the cooling rate was maximum and it was minimum for backhand welding. Figure 7 (b) also shows nearly the same trend.

5. CONCLUSIONS

The following conclusions can be drawn from the above observations

1. The heat input and cooling rate decide the kind of microstructure formed and resulting microhardness at a given point.
2. Microhardness varied with variations in weld parameters
3. Microhardness was reduced in HAZ probably due to grain growth
4. Microhardness was maximum at minimum WFR
5. Microhardness was maximum at maximum welding speed.
6. Microhardness was maximum at minimum arc voltage.
7. Microhardness was maximum at minimum NPD.
8. Microhardness was maximum at maximum torch angle.

6. REFERENCES

[1] Parmar, R. S., "Welding Processes and Technology". Khanna Publishers, 10th edition, New Delhi, 2010.

[2] Rao, C.S., Prasad, K.S and Rao, D.N., "Study on Effect of Welding Speed on Microstructure and Mechanical Properties of Pulse Current Micro Plasma Arc Welded Inconel 625 sheets". Journal of Minerals and Materials characterization and Engineering, Vol. 11, pp. 1027-1033, 2012.

[3] Pandey, S., Ph.D. Thesis on "Some Studies on MIG Welding of Aluminum and its Alloy 5083". Department of Mechanical Engineering. IIT Delhi, India, 1986.

[4] Davies, A.C., "Welding", Cambridge University Press, 10th edition, UK.

[5] Raveendra, A., Ravi Kumar, B.V.R., "Microhardness and Mechanical Properties of EN-24 Alloy Steel Weldments using Pulsed and Non Pulsed Current Gas Tungsten Arc Welding". International Journal of Innovative Research in Science, Engineering and Technology. Vol. 3, issue 10, pp 16588-16593, October-2014.

[6] Kurt, H.I., Samur, R., "Study on Microstructure, Tensile Strength and Hardness of Stainless Steel 316 Joined by TIG Welding". International Journal of Advances in Engineering, Science and Technology. Vol. 3, No.1, pp. 1-6, Feb-April 2013.

Authors: Pradeep Khanna, Associate Professor, Dr. Sachin Maheshwari, Professor, Division of Manufacturing Processes and Automation Engineering, Netaji Subhas Institute of Technology, New Delhi, India, Phone: 91-011-25000200
E-mail: 4.khanna@gmail.com
ssaacchhiinn@gmail.com

http://doi.org/10.24867/JPE-2017-01-097

Journal of Production Engineering

Vol.20 No.1

JPE (2017) Vol.20 (1) Original Scientific Paper

Singh, B.

THE CORRELATION OF WELD MICROSTRUCTURE AND PROPERTIES WITH ELEMENT TRANSFER IN SAW WELDS

Received: 07 March 2017 / Accepted: 19 April 2017

Abstract: *This study explores the effect of various elements transfer to the welds on its microstructure and properties. The fluxes were designed using RSM and were made by agglomeration technique. This study reveals that the pearlite or ferrite formation in the welds depends upon the flux constituents. The carbon, manganese, oxygen and nickel transfer have been correlated with the pearlite formation in the welds. The welds dilution also shows a significant effect on weld properties.*

Key words: *SAW, dilution, weld oxygen, pearlite, ferrite*

Korelacija mikrostrukture šava i osobine elementa u SAW varovima. *Ova studija istražuje uticaj prelaza različitih elemenata u zavaru na njihova mikro svojstava. Prelazi su dizajnirani korišćenjem RSM i rađeni su tehnikom aglomeracije. Ova studija otkriva da formacija perlita ili ferita u zavaru zavisi od fluksa sastojaka. Prelaz ugljenika, mangana, kiseonika i nikla su u korelaciji sa formiranjem perlita u zavarima. Razblaživanje zavarenih spojeva takođe pokazuje značajan efekat na svojstva zavara.*

Ključne reči: *SAW, razređivanje, kiseonik za zavarivanje, perlit, ferit*

1. INTRODUCTION

Submerged arc welding is also known as hidden arc welding was developed for making high quality butt welds in thicker plates. The arc is produced from the end of a continuous electrode which is buried under the thick layer of flux. The heat of the arc causes the melting of electrode, base plate and the adjacent flux. The lower layer of the flux is melted and reacts with the impurities and forms a slag while the upper unused layer is collected by a hopper and it is again used. It gives the double protection against the atmospheric contamination [1]. In recent years fully automatic and semiautomatic SAW equipments have resulted in an increase in welding speed and their use has made possible to obtain high quality joints. The electrodes used for SAW are either bare or copper coated to prevent them from corrosion. The coating also increases the electrical conductivity of the electrode wire. For welding of various types of steels various combinations of electrodes and fluxes are in use. Fluxes are the chemical substances that are used as a cleaning agent in welding. The SAW fluxes contain lime, silica, manganese oxide, calcium fluoride and other compounds. In SAW the weld pool is protected from the atmospheric contamination by being submerged under a blanket of granular fusible flux. In the molten state, the flux becomes conductive and provides a current path between the electrode and work piece. Fluxes can be categorized depending upon the method of manufacture, the extent to which they can affect the alloy content of the weld deposit and the effect on weld deposit properties.

The basic functions of the fluxes in SAW are to improve arc stability, to refine the weld metal and to add the alloying elements [2-3].The various ingredients of flux decides the weld composition and properties. The physical and chemical properties of flux and welding process parameters decide the transfer of various elements to the weld.

The mechanical properties of the weldments depend upon the microstructure developed during submerged arc welding [4]. The microstructure of a weld metal in turn largely depends on the heating and cooling cycle. The microstructure is also affected by the welding process, process parameters and the material to be welded. The important factors that decide the microstructure are chemical composition of the weld, heating and cooling rate and flux composition used for welding. The weld oxygen content and the shape and size of inclusions also have a definite effect on microstructure [5].

The heat input and cooling rate both have a direct effect on the microstructure of final weld metal composition [6-7]. The austenite - ferrite transformation, cooling rate and different ferrite morphologies are important considerations for improving the mechanical properties. The various microstructures formed in low carbon steel welds are grain boundary ferrite, widmanstatten ferrite, side plate ferrite and micro phases (A small amount of martensite, retained austenite or degenerated pearlite) depending on the cooling rate and composition. Dallam et al. [8] studied the microstructure of low carbon steel weld and HAZ and observed various subzone microstructures in HAZ such as spheroidized zone, partially transformed zone, grain refined zone and grain coarsened zone. The same has been verified by the various other researchers [8-10]. The weld metal microstructure is controlled mainly by cooling cycle while the metallurgical transformations in HAZ are related to both heating and cooling cycle [11-12]. The various microstructures

obtained in welds of low carbon steel are widmanstatten ferrite,acicular ferrite, pearlite, grain boundary ferrite, bannite and polygonal ferrite. Following microstructures are obtained in the weld of low carbon steels.

Weld microstructure is affected by the weld oxygen content [13-15]. For formation of acicular ferrite an optimum level of oxygen is required. The acicular ferrite is also increased with increase of Al content in the weld up to a certain limit. If it is increased beyond a certain limit the formation of acicular ferrite is reduced. Jordar et al.[16] have reported that the pro-eutectoid ferrite was obtained when the size of inclusions were lying between (0.2 - 0.7)μm, while acicular ferrite was formed when the size of the inclusions were larger.
Various contents like Calcium and Mg are insoluble in steel while Al, Mn, Si, and Ti contents are soluble in steel. These can react with the sulphur and oxygen present in the weld and may form sulphide or oxide inclusions. Sulphur may be present as an impurity in the flux or base metal and it is usually found in those inclusions which may have Mn content. In the same way Al content may be present in the flux or base plate or wire, which may change the inclusion population and finally the microstructure of the weld metal. Aluminum reacts with weld oxygen and forms aluminum oxide. This is given in equation (1).

$$2Al^{3+} + 3O^{2-} \rightarrow Al_2O_3 \quad (1)$$

These inclusions may be present in the form of alumino silicates, aluminates and mixed oxides. In the same way silicon and titanium are soluble in steel and easily reacts with oxygen in the weld to form dioxides but these oxides further reacts with oxygen and give reactive positive ions and negative ions. These cations or anions react with elements present in the weld pool. The silicon ions react with oxygen to form silicates as shown in equations (2) and (3).

$$Si^{4+} + O^{2-} \rightarrow SiO^{2+} \quad (2)$$

$$SiO_2^{2+} + 3O^{2-} \rightarrow SiO_4^{4-} \quad (3)$$

Silicon may be present in the inclusion in the form of manganese silicates, manganese alumino silcates etc. Thus sulphur and oxygen both are mainly responsible for inclusion formation. These inclusions also affect the mechanical properties.Besides the element transfer oxygen affects the volume fraction, type and size of inclusions which finally may decide the toughness and strength of the welds. The Tables 1-4 represent the design matrix, factors and their levels, wire and plate composition and welding parameters respectively.

2. EXPERIMENTAL PROCEDURE

1. Twenty fluxes were designed as per RSM by using central composite design. The designed matrix in the coded form is given in Table 1. The three factors, wire and plate composition are given in Table 2 and 3 respectively. While, the welding parameters are shown in Table 4.
2. The base fluxes CaO, SiO_2 and Al_2O_3 were selected and mixed in the ratio of 7:10:2 as per binary and ternary phase diagrams. The additives CaF_2, FeMn and NiO were added in the range of (2 − 8)%.
3. Twenty fluxes were prepared by agglomeration technique.
4. Beads on plate welds were made on 18 mm thick MS plates of the given composition. Welding parameters such as voltage, current and travel speed were kept constant. These parameters are given in Table 4.
5. In this study 10 % dilution effect of the base plate has been assumed.
6. Chemical analysis of the bead was done from the powder, extracted from the top bead with the help of a drill. The measured responses are given in Table 5.
7. The transfer of manganese was calculated by a Δ Delta quantity = Analyzed composition − Expected composition.
   The expected composition was calculated from the below given relation:

$$\frac{\text{dilution} \times \text{base plate composition} + (100 - \text{dilution}) \times \text{wire composition}}{100} \quad (4)$$

No. of Exp.	CaF_2 wt % A	FeMn wt% B	NiO wt % C
1	+1	-1	-1
2	0	+1	0
3	+1	-1	+1
4	-1	-1	-1
5	0	0	0
6	0	0	0
7	+1	+1	+1
8	0	0	0
9	0	-1	0
10	+1	0	0
11	0	0	+1
12	-1	-1	+1
13	0	0	0
14	0	0	0
15	+1	+1	-1
16	-1	0	0
17	0	0	0
18	0	0	-1
19	-1	+1	+1
20	-1	+1	-1

Table 1. Design matrix in coded form.

3. CORRELATIONS OF MICROSTRUCTURE WITH ELEMENT TRANSFER

With an increase of C, Mn and Ni contents to the welds, the pearlite percentage of the microstructure is reduced. This has been depicted in the Figures 1-3 respectively. These figures show that the element transfer has a significant effect on the microstructure of the weld. With the increase of carbon proportion, the pearlite content is reduced although it is assumed that with increase of carbon content in the weld, the pearlite content increases in carbon steels [17]. This is shown in

the Figure 1.This may be dueto very low carbon present in the welds and also dueto reduction in impact strength with increasing weld carbon. In this study it has been verified that the impact strength increases with increase of pearlite content in the welds. As with the increase of carbon content, the impact strength is reduced so, the pearlite content might also be reduced. Weld Mn content also reduces the pearlite content. This has been given in Figure 2. It may be attributed to its nature of increasing hardness and promoting ferrite formation [18]. The increase of weld Mn content increases the hardness and consequently, the reduction in impact strength [19] and [20]. So the pearlite content might also be low. The same type of variation is also observed for Ni content. This is shown in the Figure 3. Although, the impact strength of the welds increase with increase of Ni content to a certain extent but the pearlite content is reduced.The pearlite content is high in both the cases when the weld oxygen is either very low or very large.This has been depicted in Figure 4. The weld oxygen has a definite effect on microstructure of the welds [21] and [22]. The BI also affects the various elements transfer to the weld.

Factors	**Additives**	**Lower Level %**	**Middle Level %**	**High Level %**
A	CaF_2	2	5	8
B	FeMn	2	5	8
C	NiO	2	5	8

Table 2. The three factors and their levels.

Composition	Base Plate	Wire
Carbon %	.03	.11
Silicon %	.07	.09
Manganese %	.34	.45
Sulphur %	.017	.021
Phosphorus %	.022	.021
Nickel %	-	-

Table 3. The wire and plate composition

S.No.	**Voltage**	**Current**	**Travel speed**
1	30 volts	475 ampere	20 cm/minute.

Table 4. The Welding parameters

Flux NO	Weld C%	Mn %	Ni %	UTS MPa	Impact Strength	ΔMn	Weld dilution %	BI
1	0.03	0.17	0.177	270	58	-0.267	0.387	0.839
2	0.03	0.37	0.702	318	55	-0.069	0.179	0.847
3	0.04	0.23	0.544	320.2	64	-0.209	0.454	0.973
4	0.04	0.17	0.374	189.8	20	-0.269	0.366	0.710
5	0.04	0.35	0.388	300	12	-0.089	0.467	0.840
6	0.08	0.31	0.25	320	14	-0.129	0.281	0.840
7	0.04	0.38	0.477	190.7	56	-0.059	0.257	1.00
8	0.08	0.34	0.27	284.7	23	-0.099	0.555	0.840
9	0.03	0.34	0.474	280.1	60	-0.099	0.399	0.832
10	0.04	0.42	0.744	292.6	46	-0.019	0.388	0.910
11	0.04	0.15	1.33	240	12	-0.289	0.251	0.910
12	0.03	0.57	0.44	175.7	14	0.131	0.357	0.832
13	0.07	0.38	0.32	330.9	14	-0.059	0.473	0.840
14	0.04	0.39	0.32	326.5	40	-0.049	0.411	0.840
15	0.04	0.24	0.054	351	56	-0.199	0.388	0.847
16	0.04	0.25	0.344	152.3	36	-0.189	0.396	0.773
17	0.03	0.50	0.452	319.5	14	0.061	0.482	0.840
18	0.04	0.29	0.366	351	12	-0.149	0.405	0.773
19	0.04	0.33	0.502	128.8	58	-0.109	0.454	0.847
20	0.04	0.33	0.288	319.5	60	-0.109	0.566	0.714

Table 5. Measured Responses

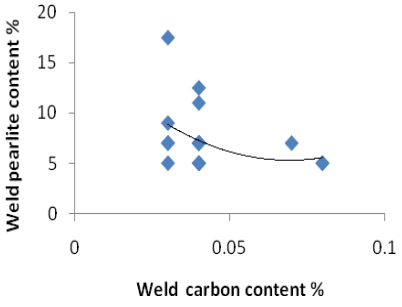

Fig. 1. Correlation of pearlite content with carbon proportion

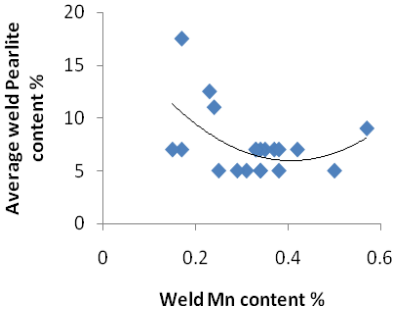

Fig. 2. Correlation of pearlite content with weld Mn content.

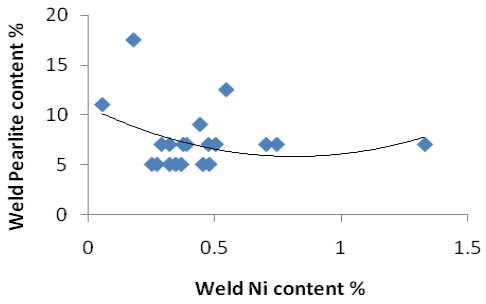

Fig. 3. Correlation of pearlite content with weld Ni proportion

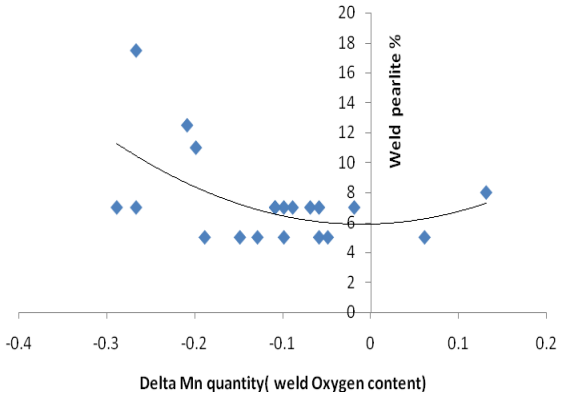

Fig. 4. Effect of weld Oxygen on pearlite content.

4. CONCLUSIONS

1. The correlation of C and Ni transfers show that the pearlite content is reduced with increase of these elements.
2. The weld pearlite after an initial decrease, it increases with increasing weld Mn comtent.
3. The pearlite content is high in either case when the weld oxygen is either very high or very low.
4. The element transfer to the weld has a definite correlation with the weld microstricture.

5. REFERENCES

[1] Hould Croft, P.T., (1989) Submerged arc welding Second Ed. Abington publishing, Cambridge, England.
[2] Linert, G., (1995) Weld. Metallurgy, American welding society, New York.
[3] Jackson, C.E., (1960) The science of arc welding part-1 Definition of arc. Welding Journal 30: 129-140.
[4] Jordar, A., Saha, S.C., Ghosh, A.K., (1991) Study of submerged arc weld metal and HAZ microstructure of plain carbon steel welding. Welding research supplement: 141-147.
[5] Jang, J.W., Shah, S., and Indacochea, J.E., (1987) Influence of SAW fluxes on low carbon steel weld microstructure. J. Materials for Energy systems, 8(4): 391-400.
[6] Easterling, K.E., (1992) Introduction to physical metallurgy of welding. Butter worth-Heinemann.
[7] Svensson, L.E., (1994) Control of microstructure and properties in steel arc welding, CRC press, Boca Raton, FL: 101-106.
[8] Dallam, C.B., Liu, S., Olson, D.L., (1985) Flux composition dependence of microstructure and toughness of submerged arc HSLA weldments. Welding journal, 64(5): 140-151.
[9] Kou, S., (1987) Welding metallurgy, Wiley International Publisher, New York: 66-75.
[10] Rasanen, E., and Tenkula, J., (1972) Phase changes in the welded joints of construction steels. Scandivian Journal of metallurgy, 1:75-80.
[11] Cornu, J., (1988) Advanced welding systems part 2. IFS Publication Ltd, London: 97-123.
[12] Dolby, R.E, (1983) Advances in welding metallurgy of steels. Metals Technology, 10(9): 349-362.
[13] Abson, D.J., Dolby, R.E., Hartn, P.H., (1978) The role of non-metallic inclusions in ferrite nucleation in carbon steel weld metals. Proc. Intl. Conf. on trends in steels and consumables for welding, London, England, The welding institute, ibid: 75-101.
[14] Abson, D.J., Dolby, R.E., (1978) Microstructural transformation in steel weld metal- A Reappraisal. Welding Institute research bulletin: 202-206.
[15] Cochrane, R.C., Kirkwood, P.R., (1978) The effect of oxygen on weld metal microstructure Trends in steel and consumables for welding. The welding Institute, London, Paper 35: 103-121.
[16] Jordar, A., Saha, S.C., Ghosh, A.K., (1991) Study of submerged arc weld metal and HAZ microstructure of plain carbon steel welding. Welding research supplement: 141-147.
[17] Heuschkel J. weld metal composition control.Welding J. 1963;48(8):323-347
[18] Gonzaga RA, Martenz L,P, Perez A , Villanueva P. Mechanical properties dependency of the pearlite content of ductile iron.Journal of Achievements in Materials and Manufacturing Engg. 2009; 33(2):150-158.
[19] Heuschekel,J. Weld metal property control. Welding J.1973; 52(1):1-20.
[20] Abson DJ, Dolby RE, Hartn PH. The role of nonmetallic inclusions in ferrite nucleation in carbon steel weldmetals. Proc. Intl. Conf .on trends in steels and consumables for welding, London, England,The welding institute, ibid, 1978; : 75-101.
[21] LIU S, Olson DL. The role of inclusions in controlling HSLA steel weld microstructure. Welding journal, 1986; 65(6):139-149.
[22] Sammy-Armstrong Atta-Aayemang. Optimization of strength and toughness on the effect of the weldable HSS used in offshore structures. Master of science thesis Lappeenavanta University of Technology 2013.

Authors: **Dr Brijpal Singh,** A.P Mech Engg. Department, Maharaja Surajmal Institute Of Technology, C-4 Janakpuri, New Delhi, India 110059
Email : brijpalsingh101@gmail.com

http://doi.org/10.24867/JPE-2017-01-101

Journal of Production Engineering

Vol.20 No.1

JPE (2017) Vol.20 (1) Original Scientific Paper

Shuaib-Babata, Y. L., Adewuyi, R.A., Aweda, J. O.

EFFECTS OF THERMAL TREATMENT PROCESSES (TTP) ON SOME OF THE MECHANICAL PROPERTIES OF WELDED 0.165% CARBON STEEL

Received: 15 March 2017 / Accepted: 19 April 2017

Abstract: *One of the major causes of structural failure in service is attributed to failure in its parts, especially at the welded joints. Engineers and other users of low carbon steel tend to find solution to this problem by considering the application of Post weld heat treatment (TTP).The Microstructure and mechanical properties of heat-treated and untreated welded low carbon steel samples were determined. Simulation of the specimens was also generated using Autodesk Inventor Simulation CFD 2015 Application Software. The CFD model (simulation) showed clearly the visual style wireframe and shaded mesh (XY, and XZ planes and the temperature profiles for different passes), which is a veritable tool to evaluate residual stress that is likely to happen in real welding process. The results also revealed that better quality mechanical behaviour of welded low carbon steel is elicited by post-weld normalizing and annealing TTP.*

Key words: *welding, simulation, failure, microstructure and thermal treatment process*

Uticaj procesa termičke obrade (TTP) na neke od mehaničkih osobina zavarenih 0,165% ugljeničnih čelika. *Jedan od glavnih uzoraka loma u strukturi konstrukcije se pripisuje otkazu njegovih delova, posebno na zavarenim spojevima. Inženjeri i drugi korisnici nisko ugljeničnih čelika teže da pronađu rešenje za ovaj problem a to je primena termičke obrade posle zavarivanje (TTP). Mikrostruktura i mehaničke osobine termički obrađenih i netretiranih zavarenih uzoraka čelika sa niskim sadržajem ugljenika su ovde pripremljeni. Za simulaciju uzoraka korišćena je simulacija izrađena u softveru Autodesk CFD 2015. CFD model (simulacije) je pokazao vizuelno jasnu konstrukciju rama i mreže u (XY i XZ ravni i profil temperature za različite preseke), što je pravi instrument za određivanje zaostalih napona kao u stvarnom procesu zavarivanja. Rezultati su takođe otkrili da je bolji kvalitet u pogledu mehaničkog ponašanja zavarenih nisko ugljeničnih čelika postignut posle normalizacije i žarenja TTP zavara.*

Ključne reči: *zavarivanje, simulacija, otkaz, mikrostruktura i proces termičke obrade*

1. INTRODUCTION

Welding process is highly significant in production of tools, equipment and in other structural developments. Currently, the process is used for fabrication and construction of a variety of structures such as buildings, bridges, ships, offshore structures, boilers, storage tanks, pressure vessels, pipelines, automobiles and rolling stock [1]. As a result of the quest for materials that can perform such task at optimum efficiency, Metallurgist, Designers and Engineers have been forced to look into the ways of developing materials that will be able to suite specific engineering applications [2].

In welding, pieces to be joined (*the work pieces*) are melted at the joining interface and usually a filler material is added to form a pool of molten material (*the weld pool*) that solidifies to become a strong joint. The weld metal and the base metal close to the fusion zone are subjected to cyclic thermal loads during the welding process [3]. To certain degree, the materials in the fusion zone do undergo plastic deformation during the process. This may lead to work hardening at the zone, and formation of residual stress may also occur. Dean *et al.* is also of the opinion that welding residual stress may also occur in Heat affected zone (HAZ), which may accelerate corrosion attack and cracking propagation [3]. Poor or incorrect welding procedure may also produce imperfections, stress corrosion cracking, fatigue failure, or brittle failure that may eventually lead to premature failure at the welded joint while in service.

One of the major causes of structural failure in service is attributed to failure in its parts, especially at the welded joints. This phenomenon is peculiar to the components made with low carbon steel (NST 44-2). High residual stress and distortion in materials that are attributed to welding process cannot be neglected as contributing factors to structural failure due to welded joint failure. Common leading structural failures are classified into four [4], in which defective materials which occur during manufacturing process is one of them. Inferior constructional material is also identified by Bright Hub Engineering [5] as part of the causes of structural failure.

Heat treatment is the term used to alter or improve some properties of materials by heating to certain temperature, holding at that temperature and cool appropriately to ambient temperature [6]. The treatment is an easiest process of improving material properties. It is an important operation in the final fabrication process of many engineering components [7]. Post weld heat treatment (TTP), is a procedure that is used to influence the structure and the properties obtained in

the weld zone and in the heat affected zone (HAZ) [8]. Effective post weld heat treatment has been a the primary means by which welded zone, heat affected zone properties and minimum potential for hydrogen induced cracking are corrected [9]. Only by heat treatment is it possible to impart high mechanical properties on steel parts and tools for sophisticated applications [10]. Among other factors that influence the need for TTP are dimensions, joint design, welding parameters and the likely mechanism of failure [11]. Hard microstructure of the Heat affected zone (HAZ), which is also another known factor responsible for the property deterioration of weld and cold cracking susceptibility are preventable by pre and post weld heat treatment [12]. This was concluded while searching the methods for predicting maximum hardness of Heat Affected Zone and selecting necessary preheat temperatures for steel welding [13]. Due to failure at welded joints, Engineers and other users of low carbon steel tends to find solution to this problem, hence the application of Post weld heat treatment (TTP) is considered.

Defectiveness or inferiority of a material, either in raw or as result of fabrication process, nor through thermal treatment could be known through better understanding of the material's properties**.** More so, the effective usage of materials or effectiveness of any materials process can be realized only when an engineer fully understands the various properties of materials. This can be obtained through mechanical testing. It is also necessary to note that in multi-pass welding, the welded materials' properties at the fusion zone and Heat affected zone (HAZ), such as yield strength and hardness depend on the welding process [3]. Therefore, there would be need for better understanding of the real situation of the welded joints as result of welding processes and pre/post thermal treatment through knowledge of the materials' properties, which is the basis of this study. Mechanical tests such as tensile test, hardness test and microstructure observation would reveal improved properties of the materials that could reduce failure at Welded joints.

2. MATERIALS AND METHODS

A Commercial steel of 14 mm thickness was obtained for this study, being a material universally used by local fabricators and Engineers.

2.1 Chemical Composition of the Test Specimens

The chemical composition of the sample was obtained using an Optical Emission Spectrometer (OES), MODEL JEOL *JEM*2100, for proper classification of the steel.

2.2 Preparation of the Test Specimens

The low carbon steel was cut into 40 pieces with dimension 100 mm by 50 mm by 14mm and welded into 20 pieces with dimension 100 mm by 100 mm by 14 mm shown in Plates 1. For ease thermocouple placement on samples, 5.0 mm diameter hole was drilled and taped close to the upper edge of each of the samples, prior to welding operation, as shown in Plates 1. The thermocouple was used to measure temperature during welding process. Edge preparation was done for each pair of the specimens by chamfering one of the 100mm by 14mm faces of all the pieces to get Double-V where the pairs were welded (Double-V-butt welded joint).The joint configuration considered for this type of design was Double-V-butt joint, achievement of the required static strength is a primary criterion in the selection of joint design. The two pieces to be joined (*the workpieces*) were melted at the joining interface (Double-V-butt joint) by the use of filler material (Olikon type of Electrode ø8mm (E6013) (G_{10}) added. The welding at assumed speed 15mm/s selected to form pool of molten material (*the weld pool*) at one pass on each side that solidifies to become a strong joint.

(a)

(b)

Plate 1. Welded specimens (a) before thermal treatment (b) after thermal treatment

2.3 Simulation of the Test Specimens

An Autodesk Inventor Professional Modeling Software was used to generate the 3D drawing (model) shown in Figure 1. Autodesk Inventor Simulation CFD 2015 Application Software was also used to show the heat distribution across the weld bead, Planes YZ, XZ and XY (shown in Figure 2), fully described in Shuaib-Babata & Adewuyi earlier study [14].

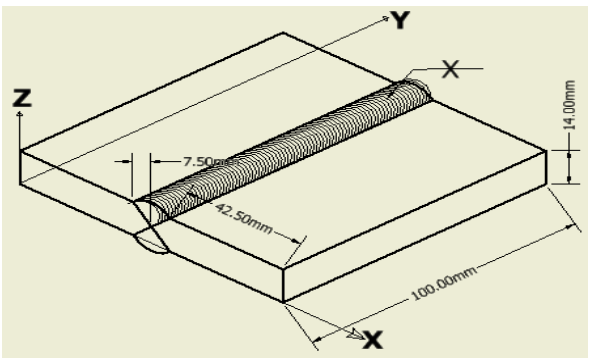

(a)

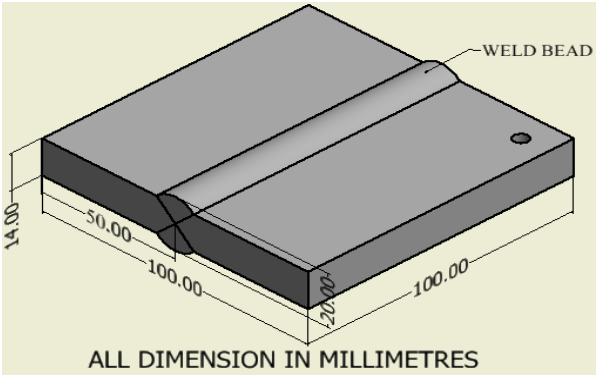

(b)

Fig. 1. 3-D Model of the Test Specimen Generated from Autodesk Inventor Professional Modeling Software,(a) Double-V-butt welded joint and (b) 5.0mm hole drilled and taped respectively.

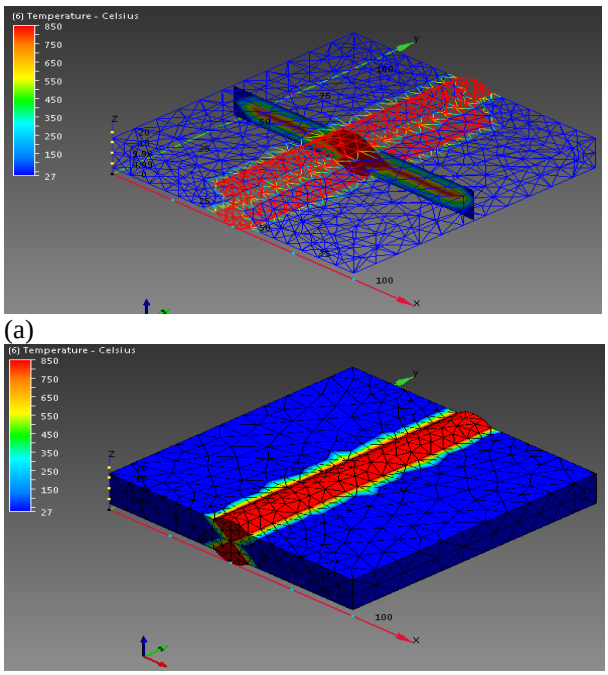

(a)

(b)

Fig. 2. Simulated Model of low carbon steel showing Haet Affected Zone and welded zone on the three Planes (YZ, XZ, XY) Using; Autodesk Inventor Simulation CFD 2015 Application Software; (a) Visual style –Wire frame and (b) Visual style –Shaded mesh.

2.3 Thermal Treatment and Quenching

Sequel to thermal treatment, Thermocouple of K-Type (Plat-inum Rhodium) (-30 to +13700C) were placed on each of the holes drilled on upper edge of the welded specimen, connected to the temperature controller to read the core temperature of the specimen while inside the furnace, as shown in Plates 1above.

A set of five standard specimens was annealed by heating to a temperature of 920°C in a furnace and cooled in the furnace environment to room temperature. The next set of five specimens were normalized by heating to a temperature of 920°C and held for about 20 minutes and allowed to cool naturally in air. A set of two standard specimens at a time was heated to temperature of 920°C and was allowed to homogenize at that temperature for 20 minutes and this was repeated for four different periods. After 20 minutes, the specimen was taken out of the furnace and directly quenched in different media (Tap Water, Palm oil, Quartz 5000 Total Engine oil and Groundnut oil) maintained at room temperature in the quenching tank. After thirty minute the specimen was taken out of the quenching tank and cleaned properly. The remaining two as-weld (untreated) specimens served as control.

2.4. Mechanical tests

2.4.1 Hardness test

Prior to the test, the specimens were grounded and polished. The hardness values of the specimens were obtained using software driven Optical Microscopy Machine by means of Brinell hardness tester in accordance with BS 240: 1986 and ASTM E10-15a standards [15, 16]. The hardness was measured across the radial distance at 5 equal intervals on each specimen. The test was carried out five times and the average corresponding hardness values versus specimens obtained were documented graphically.

2.4.2 Impact test

The specimens were subjected to impact test on an Izod V-Notch impact testing machine shown in Plate 2. The specimens were prepared and notch at reference point and clamped at pendulum swinging axis waiting for external force. The pendulum of the machine was allowed to swing freely through a known angle, some energy was used to break the specimen, and the energy was recorded directly on the scale attached to the machine. The corresponding impact values versus specimens were plotted.

Plate 2. Izod Impact Machine

2.4.3 Fatigue Test:

Fatigue test was carried on all the samples using an Avery Denison Fatigue Tester shown in Plate 3. The corresponding values for each specimen were obtained and documented. The machine consist of an electric motor capable of running at 1,000 rev/min, a large bearing whose purpose is to relieve the motor of the large bending moment which was applied to the specimen, collected and held the specimen and a rotating level arm, subjected to download force, in order to place specimen in a state of bending. The specimen was clamped into the machine, and loaded before switching on the machine.

Plate 3. Avery Denison Fatigue Machine Tensometer.

2.4.4 Tensile test

The tensile specimens (heat treated and non-heat treated) were prepared as shown in Figure 3 and individually subjected to tensile forces on Computerized Universal Testing Machine (UTS), a Testometric Materials product (shown in Plate 4 below). The values of the tensile stress, tensile strain and energy (toughness) at yield, peak, and fracture for each specimen were obtained and documented from the system.

The results of the specimen's elemental chemical composition and that of standard low carbon steel obtained in a technical literature are presented in Table 1.

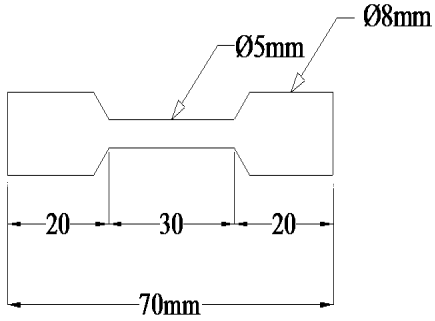

Fig. 3. Tensile Test Specimen

Plate 4.Computerized Universal Testing Machine(UTS)

2.5 Microstructural Analysis

The specimens were mounted in hot phenolic powder and were ground on a water lubricated hand grinding set-up of abrasive papers, from the coarsest to the finest grit sizes. Polishing was carried out on a rotating disc of a synthetic velvet polishing cloth impregnated with micron alumna paste. Final polishing was carried out with diamond paste. The specimens were then etched with standard 2% nital so as to reveal the ferrite grain boundaries. The optical microscopic examinations were carried out on a metallurgical microscope with magnification 40*16 (shown in Plate 5). Low carbon steel has several structures such as ferrite, pearlite, and martensite depending on how the carbon is distributed in the material. Differences in microstructure are important because they can help to determine if a metal has been subjected to corrosive chemicals, is softer or harder at the surface, has been deformed, was welded properly, or has been over-heated.

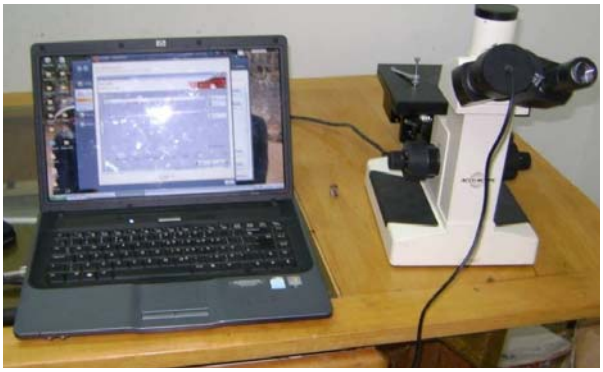

Plate 5. Microscope with Cam for microstructural analysis.

3. RESULTS AND DISCUSSION

3.1 Chemical composition

Grade	Colour code	% Weight Carbon	% Weight Silicon	% Weight Manganese
NST 44-2 [2]	Yellow	0.135 - 0.330	0.180 - 0.280	0.40 - 0.600
NST 44-2	Yellow	0.165	0.190	0.500

Table 1. Chemical composition of low carbon steel sample as obtained using optical emission spectrometer.

The result revealed that the specimen possessed 0.165% of carbon, 0.19% of Silicon and 0.50% Manganese. The elemental composition of the specimen fell within the standard values for low carbon steel as shown in Table 1.

3.2 Simulated Result of Heat Affected Zone on the three Planes (YZ, XZ, XY) using Autodesk Inventor Simulation CFD 2015 Application Software.

The thermal simulation of heat affected zone and welded pool on low carbon steel showing the three Planes (YZ, XZ, XY) using Autodesk Inventor Simulation Computational fluid dynamics (CFD) 2015 Application Software in Figure 1b above helps to understand how the temperature distribution changes with time. This sort of information is useful for assessing thermal stresses which may lead to failure.

A heat-affected zone (HAZ) is the portion of the base metal that was not melted during brazing and cutting/welding process, but whose microstructure and

mechanical properties were altered by the heat generated. This alteration can be detrimental, causing stresses that reduce the strength of the base metal, leading to catastrophic failures. The HAZ occurs inside the base metal and cannot be seen. The HAZ may need to be partially or completely removed (by grinding or some other process like heat treatment) before the metal part can be used.

The simulated results are also shown in Figures 4a, 4b and 4c for YZ-Plane heat affected zone across the welded area, XZ-plane heat affected zone along the welded area and XY-plane heat affected zone on the welded area respectively. These figures are the same but show different views / planes of the graphical result of the simulation.

YZ-Plane Heat Affected Zone across the Welded area

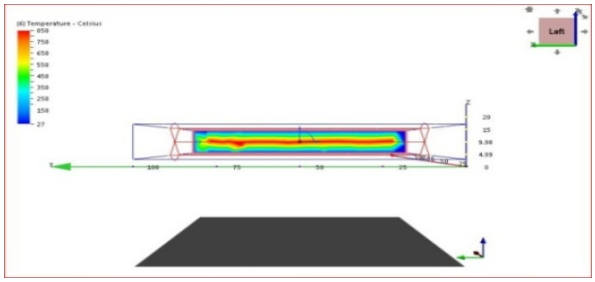

(i)

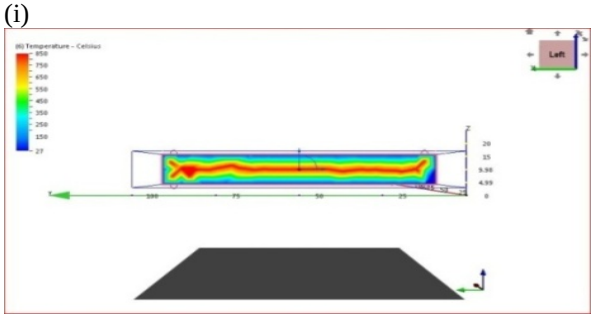

(ii)

Fig. 4a. Heat Affected Zone across the Welded area (i) YZ-Plane 61.00, 66.3, 7.00, (ii) YZ-Plane 10.6, 66.3,7.00.

Figures 4a (i) and (ii) indicate Heat Affected Zone on different coordinate points determined from the base metal to the weld metal viewed from YZ-plane (100 x 14 mm). The microstructure of the center of heat-affected zone (Reddish area) is completely different from the heat-affected zone (Yellowish, Greenish and Bluish area) to the edges of the plate. The effect of Heat Affected Zone decreases to the edges of the plate, Reddish area was greatly affected.

XZ-Plane Heat Affected Zone along the Welded Area

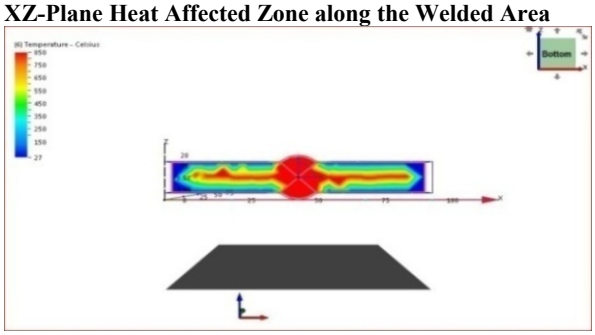

(i)

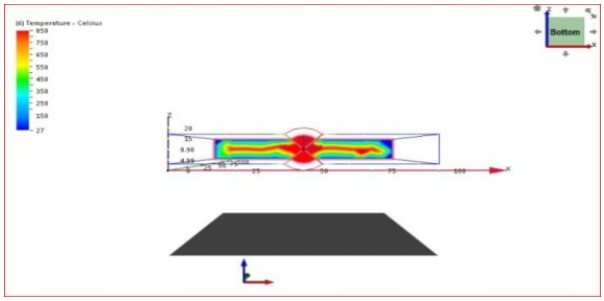

(ii)

Fig. 4b. Heat Affected Zone along the Welded Area (i) XZ-Plane 61.00, 66.3, 7.00 (ii) XZ-Plane 10.6, 66.3,7.00.

Figures 4b (i) and (ii) indicate Heat Affected Zone on different coordinate points determined from the base metal to the weld metal viewed from XZ-plane (100 x 14 mm). The microstructure of the center of weld zone (Reddish area) is also completely different from the heat-affected zone (Reddish, Yellowish, Greenish and Bluish area) to the edges of the plate.The effect of the heat affected zone as shown in XZ plane view also decreases towards the edges of the plate.

XY-Plane Heat Affected Zone on the Welded area

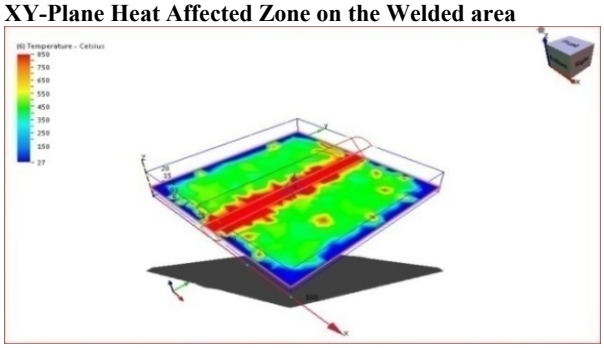

(i)

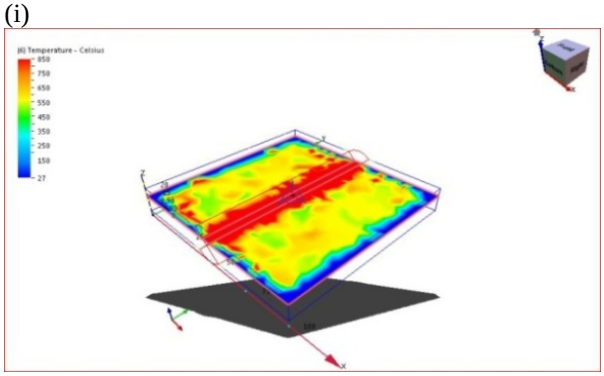

(ii)

Fig. 4c. Heat Affected Zone on the Welded area (i)XY-Plane 61.00, 66.3, 7.00 (ii) XY-Plane 10.6, 66.3,7.00.

Figures 4c (i) and (ii) indicate Heat Affected Zone on different coordinate points determined from the base metal to the weld metal viewed from XY-plane (100 x 100 mm). The microstructure of the center of weld zone (Reddish area) is completely different from the heat-affected zone (Reddish, Yellowish, Greenish and Bluish area). The effect of Heat Affected Zone decreases towards the edges of the plate.

Generally, the heat affected zone decreases as the colour of the affected area changes from Reddish-Yellowish-Greenish-Bluish area. That is, the heat affected zones concentrate more at the centre and decreases towards the edges of the plate. Hard microstructure of the Heat affected zone, (HAZ) is said to be responsible for the property deterioration of weld and cold cracking susceptibility and these are preventable by pre and post weld heat treatment [17].

The first and second passes profiles from CFD model are clearly shown in figures 5 and 6.

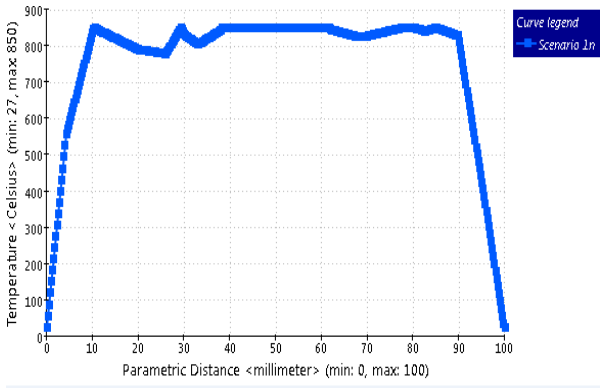

Fig. 5. Temperature Profile from CFD Model for the first pass

The welding temperature profiles from CFD model enhance better understanding of the temperature profile during welding process, which may assist to proffer solution to structural failure that may arise in the welded joints as result of welding residual stress. The temperature profile model as shown Figures 5 and 6 is a veritable tool to evaluate the welding residual stress that is likely to occur in practice (real welding process). According to Dean, *et al.*[3], a good prediction and efficient evaluation of welding residual stress are necessary, since welding residual stress depends on welding process parameters like heat input, number of weld pass, among others. These parameters are clearly revealed through the simulation (Figures 4 – 6). The welding temperature profiles will assist both Engineers and Fabricators to put in place necessary measures required to afford over-heating, structural defects that may result from the welding process and other forms of structural failures.

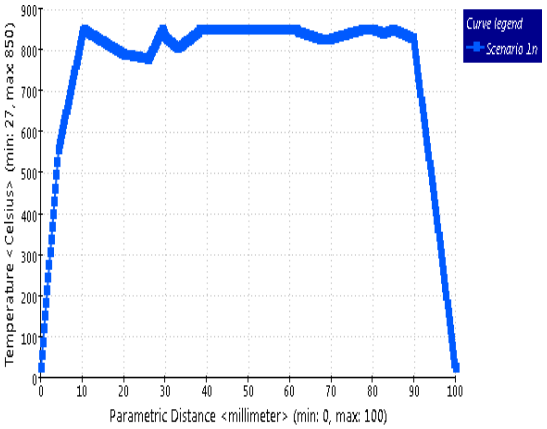

Fig. 6. Temperature Profile from CFDModel for the second pass

MECHANICAL TESTS:

(I) Tensile Properties

Some of the results obtained from the tensile test are presented in Table 2. The tensile behaviours of the tested materials under tensile are also graphically presented using the stress-strain curves in Figure 7.

Specimens	Stress at yield (MPa)	Stress at peak (MPa)	Extension at yield (mm)	Energy at yield (J)
Untreated welded steel (UN)	847.26	965.12	14.8	202.5
Annealed welded steel (AN)	283.49	669.80	17.3	215.8
Normalized welded steel (N)	272.55	714.06	15.4	231.3
Quenched-hardened with water welded steel (QHW)	669.80	755.52	14.0	170.3
Quenched-hardened with palm oil welded steel (QHP)	714.06	847.26	12.2	15.9
Quenched-hardened with total oil quartz 5000 welded steel (QHT	755.52	919.16	13.7	14.7
Quenched-hardened with ground nut oil welded steel (QHG)	283.75	898.16	13.4	13.7

Table 2. Tensile properties of post weld heat-treated and untreated specimens

In Figure 7 below, variations of Tensile Stress (MPa) against Tensile Strain (mm/mm) for different conditions of quenching media are shown. The curve (Figure 7) reveals the structural loadability (loading bearing capability) of each of the tested materials, which is one of the most important material properties [18]. Three different regions (Elastic, Non-uniform plastic and Necking regions) with each region showing the uniqueness of the engineering materials behaviour are depicted in the result graphically. In multi-pass welds, weld metal in different locations experiences different thermal cycle, restraint conditions and strain-hardening magnitude in each location. The difference in their locations is said to be responsible for the variation in the experiences [19].

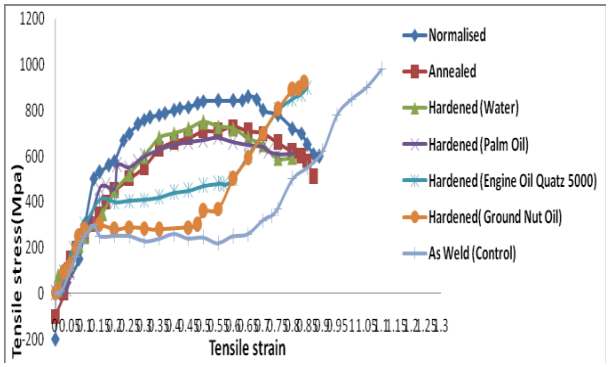

Fig. 7. Stress/Strain curves for thermal treated samples (quenched-hardened) and untreated sample of welded 0.165% low carbon steel

All mechanical properties of low carbon steels are significant when considering its ability to resist mechanical forces / loads. But in this study, the yield properties of the welded steel will be the main basis of the results' discussion due to its significant. Yield stress is the stress which produces a small amount of permanent deformation [20], which is mostly used for design in engineering practice. For a component to support a force successfully in service, high yield strength value is required, since it must not deform plastically while in use. Hence, yield strength is an important value use engineering structural design, since it is the amount of a stress at which plastic deformation is noticeable and significant [21]. The yield strength of the weld metal has a significant effect on the final hoop stress in the weld zone and its vicinity [19].

The studied steel recorded yield stress in descending order of untreated specimen (847.26 MPa), quench-hardened specimen with total quartz 5000 (755.52 MPa), quench-hardened specimen with palm oil (714.06 MPa), quench-hardened specimen with water (669.80 MPa), quench-hardened specimen with groundnut oil (283.75 MPa), annealed (283.49 MPa), and normalized (272.55 MPa). This shows that all PWHT processes reduced the ability of the steel resist deformation as results of force applied, since yield stress increases as the amount of stress a metal can support without deforming increases [22]. The analysis of the experimental results revealed that the thermal treatment processes reduced the stress of the low carbon steel at yield point. Thus, any accumulated gas in resulted blow-hole as result of welding process and stresses in the steel material during welding process were reduced significantly. Though yield strength is unimportant for a ductile material selection and application, because too much plastic deformation takes place before it is reached [21].

The noticeable differences in the yield strength of the tested steel can be attributed to the difference in the process of heat treatment. Differences in yield strength arise from different heat treatment processes rather than composition of the material [21].

The stress of welded steel at peak (Ultimate tensile strength) also decreased in order of untreated specimen (965.12 MPa), quench-hardened specimen with total oil quartz 5000 (919.16 MPa), quench-hardened specimen with groundnut oil (898.16 MPa), quench-hardened specimen with palm oil (847.26 MPa), quench-hardened specimen with water (755.5 MPa), normalized (714.06 MPa) and lastly annealed (669.86 MPa). These are the maximum amounts of stresses that the tested samples can support before they deform totally. At peak, the ultimate tensile strength of the welded steel was reduced as result of PWHT.

The extension of the steel samples at yield is the extent of their being plastically deformed at the yield point without failure. The result (Table 2) showed that the PWHT processes affected the values of the steels' ductility. The ductility of the specimens were in descending order of normalized (15.4 mm), annealed (17.3 mm), untreated specimen (14.8 mm), quench-hardened specimen with water (14.0 mm), quench-hardened specimen with total oil quartz 5000 (13.7 mm), quench-hardened specimen with groundnut oil (13.4 mm), and quench-hardened specimen with palm oil (12.2 mm). The level of safety in using the steel in service is also revealed. Ductile material will deform and also increase in its strength through work hardening, once the load on one of the parts increases over the yield stress [23]. Thus, the component will not fail catastrophically and abruptly like that of material with very low ductility.

The absorb shocking load (toughness) ability of the studied steel at yield is also expressed with the energy values at yield in descending order of normalized (231.3 J), annealed (215.8 J), untreated specimen (202.5J), quench-hardened specimen with water (170.3 J), quench-hardened specimen with palm oil (15.9 J), quench-hardened specimen with total quartz 5000 (14.7 J) and quench-hardened specimen with groundnut oil (13.7 J). The result shows the ability of the tested materials to absorb energy and plastically deform without fracturing.

(II)Hardness properties

The hardness of the test-pieces was tested at welded pool and HAZ. The variations of hardness values at welded pool and heat affected zone (HAZ) for welded specimens are shown in Figure 8.

At welded pool zone, the average hardness values of all heat-treated specimens were lower than that of untreated specimen. The steel hardness value at the region was in descending order of Untreated (106.86 BHN), Quenched-hardened with total engine oil (100.77 BHN), Quenched-hardened with ground nut oil (99.87 BHN), Quenched-hardened with palm oil 89.7 BHN), Quenched-hardened with water (84.06 BHN), Normalized (69.84 BHN) and Annealed (62.11 BHN). This shows that normalizing and annealing post-weld heat treatments resulted into lower strengths of the low carbon steel at heat affected zone and at the welded pool region. Normally, the decrease in hardness value of the heat-treated specimens when compared with that of untreated specimen was expected for normalizing and annealing thermal treatment processes.

Meanwhile at the heat affected zone (HAZ), the quench- hardened specimens (martensite) had average hardness values of 133.73 BHN, 125.64 BHN, 123.99 BHN and 88.13 BHN for Quatz 5000 Engine oil, Ground nut oil, Water and Palm oil media

respectively. Untreated specimen had 88.13 BHN average hardness value at heat affected zone. This signifies that quench-hardening improved the strength of low carbon steel at heat affected zone.

Hardness and tensile strength are indicators of a metal's resistance to plastic deformation [23].

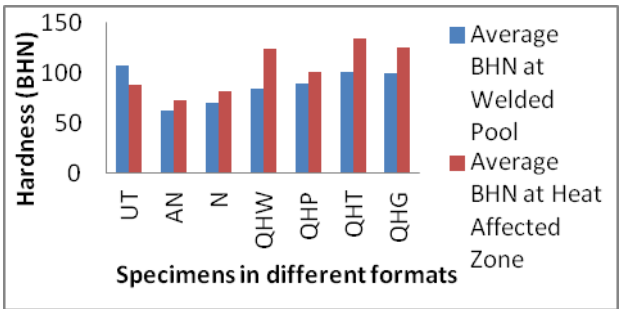

Fig. 8. The average Brinell hardness of the welded steel in different formats at both welded pool and heat affected zone..

Impact Test

Figure shows variations of impact values at heat affected zone (HAZ) for welded specimens.These results indicated the impact values for heat affected zone (HAZ) for all the specimens. The annealed specimens had the highest impact average value of 45.5 J, followed by normalized specimens with average value of 42.96 J; while the quenched-hardened specimens (quenched in different media) had the lowest average values of 35.8, 36.65, 37.75, 39.1 J as shown in Figure 7. Meanwhile, untreated welded specimens had average value of 41.55 J. The results show that annealed and normalised as thermal treatment processes improved the ability of the steel to absorb shock before fracture. This is an indication that untreated welded specimens (at the welded zone) exhibited a poor toughness compared to annealed and normalized specimens. But as the TTP duration time is increased, the toughness level of the HAZ region of welded specimens also increased.

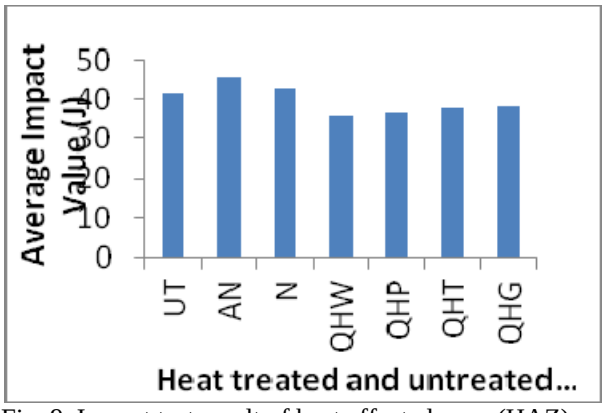

Fig. 9. Impact test result of heat affected zone (HAZ)

Fatigue Test

Fatigue testing was to ascertain the actual load the heat treated low carbon steel could withstand before failure in service. Upon the application of bending load the fatigue strength of each sample conditions for 0.165% carbon steel are as shown in Figure 8. The average number of cycles obtained for each material condition could be deduced in the Figure. The fatigue strength of untreated welded samples declined to 284 MPa from 2840 MPa resulting into failure at the 5th cycle. When compared with the heat-treated samples, higher fatigue strength of 386 MPa was achieved with the normalized samples at 5.8 cycles, followed by annealed samples that exhibited fatigue strength value of 273.8 MPa at 6.6 cycles. It was also noted that the average highest number of cycles (13.9) was obtained with untreated welded samples. Meanwhile, the quench-hardened (Water) samples gave the least number of cycles (1.8). All the samples exhibited considerable amount of deformation within relatively number of cycle. The result therefore showed that for the four material conditions (annealing, normalizing, quenching and non- heat treated), the failure mechanism was by low-cycle fatigue.

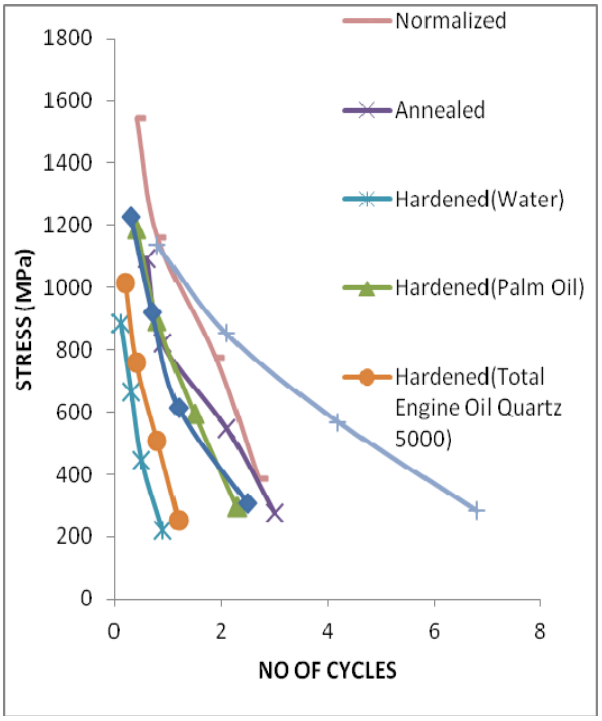

Fig. 10. Stress against number of Cycles for TTP Low Carbon Steel Specimens

Microstructural analysis

The microstructures of untreated welded (As-received weld) specimen and Post weld heat treated specimens were presented in Plates 6 to 12. Microstructure of the samples varied from one another. According to TTP [21], "hardening and tempering heat-treating process for AISI 4140 will give rise to microstructural change in the steel".

The microstructure of the untreated welded carbon steel sample revealed ferrite in the grain boundaries of the acicular pearlite grains. This can be described as having a ferrite-austenite duplex phase (Plates 6). Annealing (a post weld heat treatment process) affected the spatial distribution of ferrite at the grain boundaries. Due to oxidation at the metal surface during PWHT, scales were formed as observed to be present in ferrite in Plates 7. Normalizing PWHT gave a uniform large grained structure of ferrite and pearlite with fine

grained (Plates 8). Through quench-hardening PWHT processes in various selected media (Water, Palm oil, Engine oil quatz 5000 and Groundnut oil), the presence of scales was revealed and more widely distributed on the metal surface and highly dispersed ferrite (Plates 9 to Plates 12).

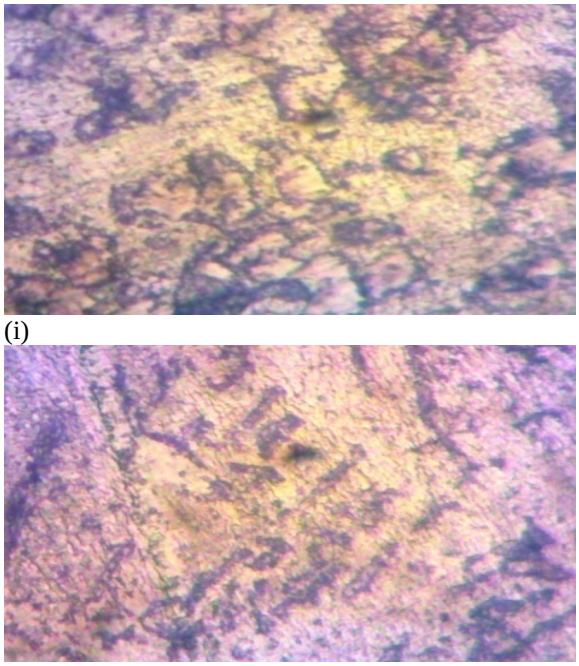

(i)

(ii)

Plate 6. Microstructural of Untreated (As-weld) specimens, (i) Welded pool, (ii) HAZ. 40 x 16

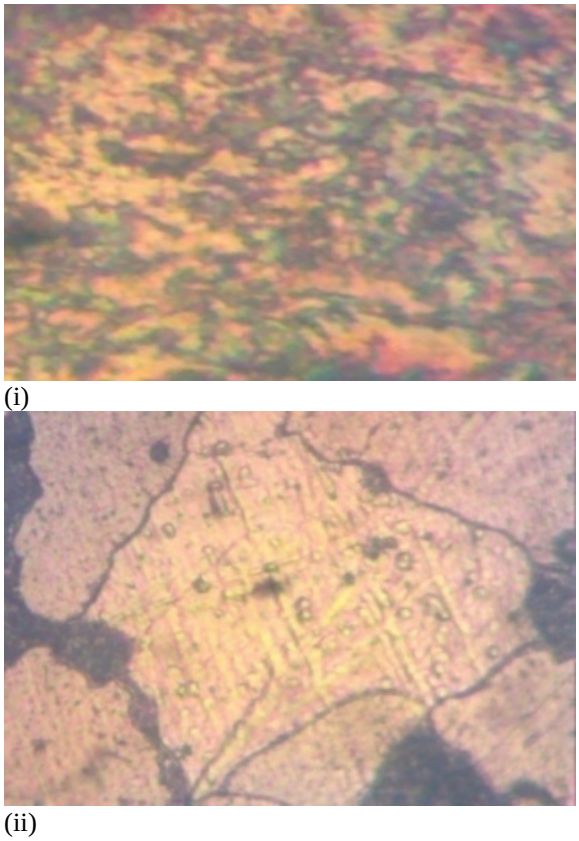

(i)

(ii)

Plate 7. Microstructural of annealed specimens, (i) Welded pool, (ii) HAZ. 40x16

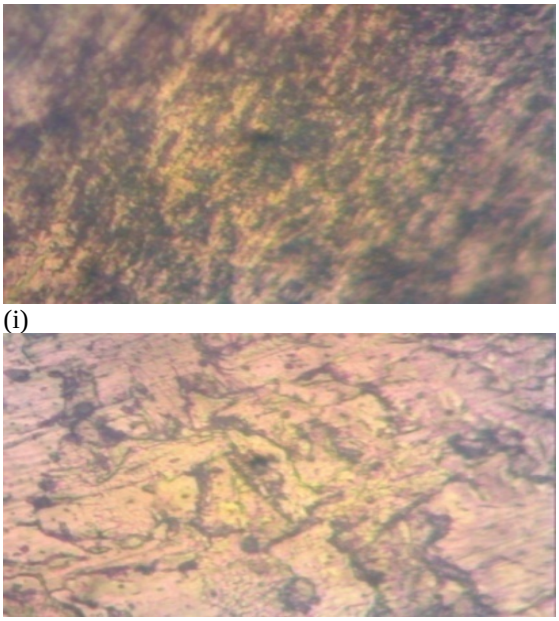

(i)

(ii)

Plate 8. Microstructural of normalized specimens, (i) Welded pool, (ii) HAZ. 40x16

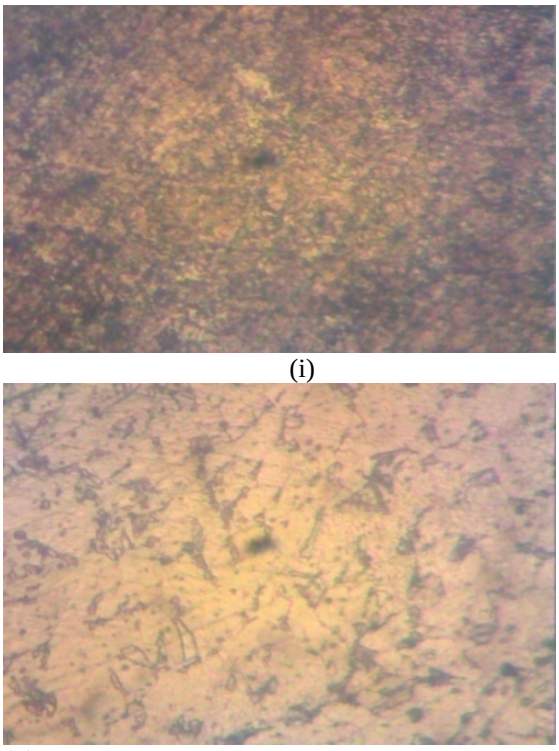

(i)

(ii)

Plate 9. Microstructural of Water quenched specimens, (i) Welded pool, (ii) HAZ. 40x16

(i)

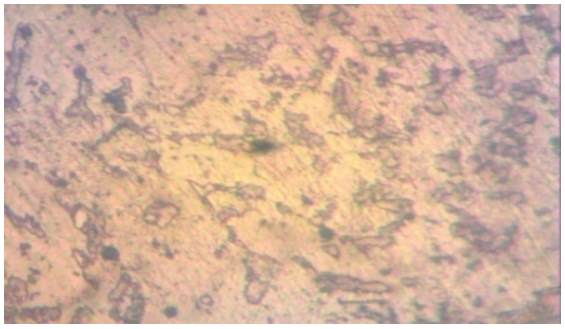

(ii)

Plate 10. Microstructural of Palm oil quenched specimens, (i) Welded pool, (ii) HAZ. 40x16

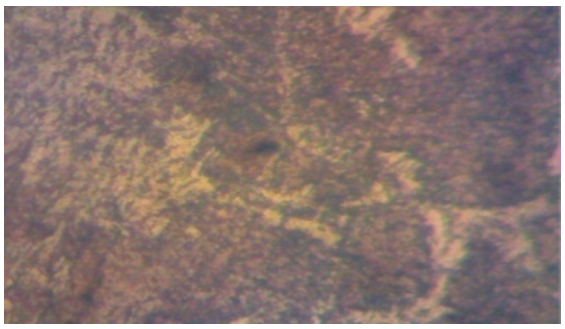

(i)

(ii)

Plate 11. Microstructural of Quartz 5000 Total Engine oil quenched specimens, (i) Welded pool, (ii) HAZ. 40x16

The observed variations in the microstructure and mechanical properties of the samples can be attributed the differences in heat treating parameters, majorly mode of cooling after heat treatment. Quenching media is an important parameter in heat treatment that affects the microstructure, grain size and eventually the mechanical parts of the steel [23].

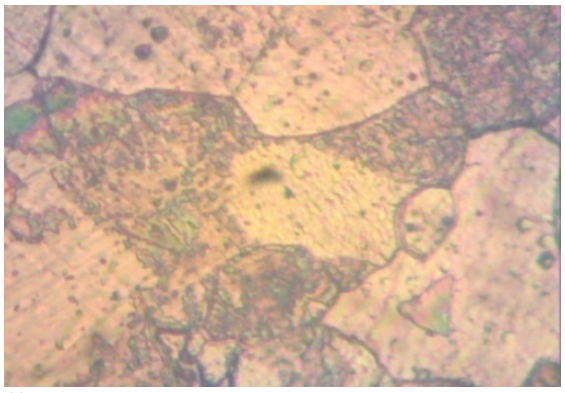

(i)

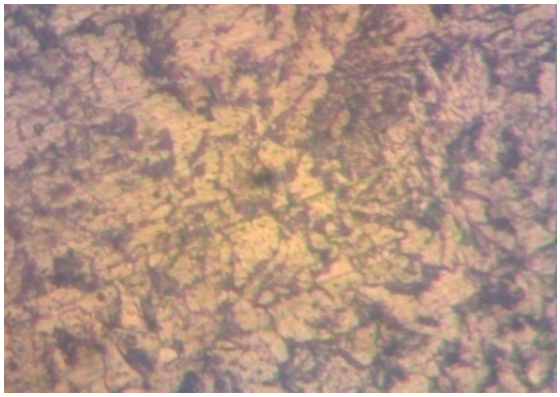

(ii)

Plate 12. Microstructural of Ground nut oil quenched specimens, (i) Welded pool (ii) HAZ. 40x16

Differential microstructures resulted from the different heat treating parameters used by the heat treatment providers also led to difference in yield strength [23]. The heat treating parameters include austenitizing temperature, soaking time, quenching media and tempering temperature and time.

4. CONCLUSION

From the study the following conclusions were derived:

(i). The CFD model revealed real welding conditions temperature profiles and microstructure showing XY, YZ and ZX planes of the welded steel. This enhances better understanding of the real welding conditions that may assist to proffer solution to likely structural failure that may arise in the welding joints as result of welding residual stress

(ii) The PWHT processes reduced the stress of the low carbon steel at yield point.

(iii) Annealing and normalising as PWHT processes enhanced the steels' ductility and the toughness, while quench-hardening processes reduced the properties

(iv) At the heat affected zone and welded pool, annealing and normalising PWHT processes reduced the hardness of the steel, which implies that the steels' strengths at the points were enhanced. Though, quench-hardened was found to improve the steels' hardness at HAZ. Meanwhile, all PWHT processes reduced the steels' hardness at the welded pool.

(v) The failure mechanism in the steel by fatigue was by low-cycle fatigue.

(vi) Butt-welded annealed and normalized low carbon steel specimens tend to be more resilient to failures at welded joints. This is because of their higher tensile stress at yield, tensile strain at yield, load at yield and Energy at break; and lower hardness value at welded zone and at the HAZ. Hence, TTP techniques significantly improves the mechanical property of butt-welded annealed, normalized low carbon steel. (vii) Better quality mechanical behaviour of welded low carbon steel is elicited by post-weld normalizing and annealing TTP.

5. REFERENCES

[1] Ejilah, R. I., Onuh, E.I., and Datau, S.: *A Study of the effect of post weld heat treatment (ttp) on the torsional behavoir of low carbon steel*, NIMechE 22nd International conference, pp.13, 2009.

[2] Oloabi, A.G. and Hashmi, M. S. J.: *The effect of post weld teat treatment on mechanical properties and residual stresses mapping in welded structural steel*, Journal of Material Processing Technology, Vol.55,issue 2, pp.117-122,1995.

[3] Dean, D. and Hidekazu, M.: *Numerical simulation of temperature field and residual stress in multi-passwelds in stainless steel pipe and comparison with experimental measurement*. Computational Material Science, Vol. 37, pp 269-277, 2006.

[4] Atlas: *Common culprits – 4 factors leading to structural failure*. Atlas Foundation Co. Retrieved from www.atlasfoundations.com/common-culprits-4factors-leading-structural-failure/, accessed October 18, 2016.

[5] Bright Hub Engineering: Structural Failure. Retrieved from www.brighthubengineering.com/building-design/52749-structuralfailure/, accessed October 18, 2016.

[6] Merchant, S. Y.: *A review of effect of welding and post weld heat treatment on microstructure and mechanical properties of grade 91 steel*, International Journal of Research in Engineering and Technology, Vol.04, March, pp 574-580, 2015.

[7] Daramola, O. O., Adewuyi, B. O. and Oladele, I. O. (2010): *Effects of Heat Treatment on the Mechanical Properties of Rolled Medium Carbon Steel*,Journal of Minerals & Materials Characterization & Engineering, Vol. 9, No.8, pp.693-708, 2010.

[8] Chen L.: *Effect of TTP temperature on mechanical properties of High-Cr ferritic heat-resistant steel weld metal*. Welding in the World, Vol.56, pp 1-2, January-February, 2012.

[9] Davies A.C., (1996): Welding, New york, 10th Edition,Cambridge University Pres, pp.343-377.

[10] The New International Webster's Comprehensive Dictionary of the English Language, (2010) : Deluxe Encyclopedic Edition, Typhoon Media Corporation, USA, pp.583.

[11] Senthilkumar, T. and Ajiboye, T.K. (2012): Effect of heat treatment processes on the mechanical properties of medium carbon steel, Journal of Minerals and Materials Characterization and Engineering 11(2) pp. 143-52.

[12] Devinder,P.S., Mithlesh,S. and Jaspal,S.G., (2013): Effect of Post Weld Heat Treatment on the Impact Toughness and Microstructural Property of P-91 Steel Weldment, Vol. 3, Issue 2, International Journal of Research in Mechanical Engineering & Technology, pp 216-219. http://www.ijrmet.com/vol32/devinder.pdf

[13] Joseph, O. O. and Alo, F. I.: *An Assessment of the Microstructure and Mechanical Propertiesof 0.26% Low Carbon Steel under Different Cooling Media: Analysis by one-way ANOVA*, Industrial Engineering Letters,Vol.4,No.7, pp 39-43, 2014.

[14] Shuaib-Babata, Y. L. and Adewuyi, R. A.: *Simulation of Heat Affected Zone (HAZ) in Multi-Pass Welds in Low Carbon Steel*. Book of Proceedings of the 15th Annual International Nigerian Materials Congress (NIMACON), pp 642-647, 2016.

[15] BS 240: *Method for Brinell test and for verification of Brinell hardness machine*. British standards Institution, 1986

[16] ASTM E10-15a: *Standard test method of Brinell hardness of metallic materials*. ASTM International, West Conshohocken, PA, 2015.

[17] Shuaib-Babata & Adewuyi:.*Effects of Thermal Treatment Processes (TTP) on the Tensile Properties of 0.165% Carbon Steel*. FUOYE Journal of Engineering and Technology, Volume 1, Issue 1, pp 15-19, 2016b.

[18] Rime: Stress-Strain curve. Retrieved from: http://www.rime.de/en/101/stress-strain-curve/. Accessed March 8, 2017.

[19] Deng, D., Murakawa, H. and Liang, W.: *Numerical and experimentation investigations on welding residuals stress in multi-passwelds butt-welded austenitic stainless steel pipe*. Computational Material Science, Vol. 42, pp 234-244. 2008, Available online at www.sciencedirect.com

[20] Dieter, G. E. (1988). Mechanical Metallurgy, SI Metric Edition, McGraw-Hill Book Company (UK) Ltd, London.

[21] TPP (2017). Yield strength and heat treatment, Available from http://www.tppinfo.com/defect_analysis/yield_strength.html

[22] Industrial Metallurgists (2017). The difference between strength and toughness. http://www.imetllc.com/training-article/strength-toughness, 27/2/2017

[23] Quora (2017). Why is ductility important in some metals? https://www.quora.com/Why-is-ductility-important-in-some-metals

Authors: **Senior Lecturer, Dr. Yusuf Lanre Shuaib-Babata**, Department of Materials and Metallurgical Engineering, University of Ilorin, Ilorin, Nigeria. +2348033945977

Senior Engineer, M.Eng, R.Eng,Reuben Adebare Adewuyi, Olusegun Obasanjo Centre for Engineering Innovation, The Federal Polytechnic, Ado-Ekiti, Nigeria. +2348038458613

Associate Professor, Dr. Jacob O. Aweda Department of Mechanical Engineering, University of Ilorin, Ilorin, Nigeria.

E-Mail: sylbabata@gmail.com/shuaib-babata.yl@unilorin.edu.ng
reuben1178@yahoo.com

http://doi.org/10.24867/JPE-2017-01-112

Journal of Production Engineering

Vol.20 No.1

JPE (2017) Vol.20 (1) Preliminary Note

Mohapatra, C. R.

A STUDY ON NATURAL CONVECTION HEAT TRANSFER IN COMPLEX BOUNDARIES

Received: 23 February 2017 / Accepted: 01 April 2017

Abstract: *In the present work a computer code has been developed for heat transfer problems. SIMPLE algorithm based on finite volume method has been used. Deferred QUICK scheme have been implemented for all calculations. To solve momentum, pressure correction and energy equations, a solver (Line-by-Line solver) is used. This code is used for natural convection problems for Ra = 10^3, 10^4, 10^5, 10^6 and Pr = 0.71. The results were compared with the benchmark solution of de Vahl Davis, Markatos and Perikleous and Hadjisophocleous et al. for Ra = 10^3; 10^4; 10^5, 10^6 and Pr = 0.71. Very good agreements were obtained except for the x and y location of the maximum u and v velocity to the mid-plane.*

Key words: *rayleigh number, finite volume method, benchmark solutions, complex boundaries*

Studija o prirodnoj konvekciji toplote u složenim granicama. *U ovom radu kompjuterski kod je razvijen za probleme prenosa toplote. Korišćen je jednostavan algoritam na osnovu metoda konačnih zapremina. Odložena brza šema je primenjena za sve kalkulacije. Da bi se rešio impuls, korekcija pritiska i jednačine energije, primenjeno je rešenje (red-po-red). Ovaj kod se koristi za probleme sa prirodnim konvekcionim za Ra = 103, 104, 105, 106 i PR = 0.71. Rezultati su poređeni sa referentnim rastvorom de Vahl Davis [4], Markatos i Perikleous [7] i Hadjisophocleous et al. [8] za Ra = 103; 104; 105, 106 i Pr = 0,71. Dobijeno je vrlo dobri slaganje, osim za x i y lokacije maksimalne u i v brzine do sredine ravni.*

Ključne reči: *Raileigh broj, metoda konačnih zapremina, referentna rješenja, složene granice*

1. INTRODUCTION

Natural convection flows are driven by the density difference that can arise in a fluid, with these density differences causing a buoyancy force which drives the flow. The density difference can be caused by temperature gradients in the fluid. Natural convection has many practical applications. It is important in the fields of cooling of micro-electric devices, nuclear reactors, electronic equipment, solar collectors, ventilations of rooms, atmospheric study etc. Patankar and Spalding [1] proposed SIMPLE(Semi-Implicit Method for Pressure-Linked Equation) algorithm method that became very popular for solving fluid flow problems. Ghia et al. [2] solved lid driven cavity flow using finite difference vortices-stream function method. Day to day natural convection heat transfer in complex boundaries are getting importance in engineering fields and many researchers have been focused to make a study in this area [3, 4]. Van Doormal and Raithby [5] proposed a popular version like SIMPLE that helped to increase the convergent rate. Their version is better known as the SIMPLEC algorithm where C refers to the word consistent. Maliska and Raithby [6] developed a method known as finite volume method for solving fluid flow problems using non-orthogonal grids and SIMPLEC algorithm. A good number of research has been carried out on natural convection in enclosures as it is a topic of considerable engineering importance. [4, 5, 7]. Hadjisophocleous et al. [7] used non-orthogonal boundary fitted coordinate system to solve the natural convection of a square cavity problem and compared the results with that of de Vahl Davis [4] and Markatos and Perikleous [8]. Thompson et al.[9] used the coordinate transformation technique to solve the problems over complex geometry.

2. GOVERNING EQUATIONS

Governing equations for two dimensional laminar, no viscous, incompressible, steady flows with Boussinesq approximation in dimensionless form can be written as follows

Continuity equation:

$$\frac{\partial U}{\partial X}+\frac{\partial V}{\partial Y}=0 \tag{1}$$

X-Momentum equation:

$$\frac{\partial (U)^2}{\partial X}+\frac{\partial (UV)}{\partial Y}=-\frac{\partial P}{\partial X}+\Pr(\frac{\partial^2 U}{\partial X^2}+\frac{\partial^2 U}{\partial Y^2})+Ra\,\Pr\,T\cos\phi \tag{2}$$

Y- Momentum equation:

$$\frac{\partial (UV)}{\partial X}+\frac{\partial (V^2)}{\partial Y}=-\frac{\partial P}{\partial Y}+\Pr\left(\frac{\partial^2 V}{\partial X^2}+\frac{\partial^2 V}{\partial Y^2}\right)+Ra\,\Pr\,T\sin\phi \tag{3}$$

Energy equation:

$$\frac{\partial (UT)}{\partial X}+\frac{\partial (VT)}{\partial Y}=\frac{\partial^2 T}{\partial X^2}+\frac{\partial^2 T}{\partial Y^2} \tag{4}$$

Where,

$$X=\frac{x}{H},Y=\frac{y}{H},U=\frac{uH}{\alpha},V=\frac{vH}{\alpha},P=\frac{pH^2}{\rho\alpha^2},$$

$$T=\frac{T'-T_c}{T_h-T_c},\Pr=\frac{\upsilon}{\alpha},Ra=\frac{g\beta H^3(T_h-T_c)}{\alpha\upsilon}$$

x and y are the distances, u and v are the velocity components measured along the horizontal and vertical directions, H is the side of the cavity, p is the pressure and ρ is the density, T_h and T_c are the temperatures at hot and cold walls, β is the volume of coefficient of expansion,α is the thermal diffusivity and υ is the kinematic viscosity.

3. BOUNDARY CONDITIONS

The figure 1 shows the boundary conditions of the natural convection in a two dimensional square cavity whose top and bottom walls are adiabatic and side walls are isothermal.

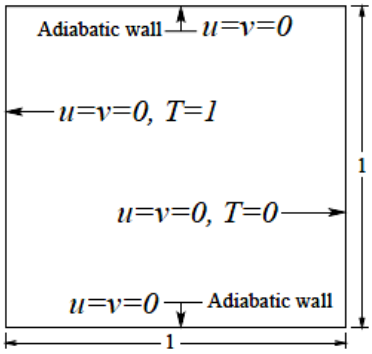

Fig. 1. Geometry and boundary conditions of the problem

4. NUSSELT NUMBER CALCULATION

In the present work, the Nusselt number is used to calculate the rate of heat transfer by convection. This can be possible by knowing the heat transfer rate by convection in an enclosure and temperature distribution in the fluid. Mathematically, it can be written as:

$$Nu = \frac{hl}{k} = \frac{\partial T}{\partial \eta} \tag{5}$$

Where $\frac{\partial}{\partial \eta}$ is the dimensionless derivative along the direction of the outward drawn normal to that surface and is expressed in terms of the η, ξ independent variables. For different walls, the local Nusselt numbers can be expressed as follows

Top wall $$Nu = \frac{1}{J\sqrt{\gamma}}\left(\gamma T_\eta - \beta T_\xi\right) \tag{6}$$

Right wall $$Nu = \frac{1}{J\sqrt{\alpha}}\left(\gamma T_\xi - \beta T_\eta\right) \tag{7}$$

Bottom wall $$Nu = \frac{1}{J\sqrt{\gamma}}\left(\gamma T_\eta - \beta T_\xi\right) \tag{8}$$

Left wall $$Nu = \frac{1}{J\sqrt{\alpha}}\left(\gamma T_\xi - \beta T_\eta\right) \tag{9}$$

5. RESULTS AND DISCUSSIONS

In this study, an air filled (Pr = 0.71) enclosure with 61 ×61 grid points and Rayleigh numbers between 10^3 to 10^6 have been considered for all calculations. An advanced algorithm (SIMPLE) with a solver (Lin-by-Line) has been used for numerical predictions. To solve energy equation followed by momentum equations, an iterative procedure is continued until convergence is achieved. The results obtained from the present work shown in Table 1 are compared with the results of de Vahl davis [4], Markatos and Perikleous [8] and Hadjisophocleous et al. [7]. The results are in very good agreement with the benchmark solution, at lower Rayleigh numbers. At higher Rayleigh numbers more points are needed close to the vertical walls for an accurate evaluation of the wall temperature gradient [4].

[a] Ra= 10^3

Observation	m	n	o	p	100×(p-m)/p
u_{max}	3.65	3.54	3.54	3.66	0.30
y	0.81	0.83	0.81	0.72	-
v_{max}	3.70	3.59	3.59	3.70	0.24
x	0.18	0.19	0.19	0.26	-
Nu	1.12	1.11	1.14	1.10	-1.18
Nu_{max}	1.50	1.50	1.54	1.49	-0.94
y	0.09	0.08	0.14	0.13	-
Nu_{min}	0.69	0.72	0.73	0.67	-3.28
y	1.000	0.992	0.991	0.991	-

[b] Ra = 10^4

Observation	m	n	o	p	100×(p-m)/p
u_{max}	16.18	16.18	16.00	16.29	0.700
y	0.82	0.83	0.81	0.74	-
v_{max}	19.62	19.44	18.89	19.74	0.64
x	0.12	0.11	0.10	0.19	-
Nu	2.24	2.20	2.29	2.22	-0.90
Nu_{max}	3.53	3.48	3.84	3.51	-0.66
y	0.14	0.14	0.14	0.16	-
Nu_{min}	0.59	0.64	0.67	0.57	-2.99
y	1.000	0.992	0.991	0.991	-

[c] Ra = 10^5

Observation	m	n	o	p	100×(p-m)/p
u_{max}	34.73	35.73	37.14	34.99	0.63
y	0.86	0.86	0.86	0.78	-
v_{max}	68.59	69.08	68.91	68.79	0.29
x	0.067	0.067	0.061	0.125	-
Nu	4.52	4.43	4.96	4.48	-0.78
Nu_{max}	7.12	7.63	8.93	7.58	6.13
y	0.081	0.082	0.080	0.091	-
Nu_{min}	0.73	0.82	1.01	0.70	-3.99
y	1.00	0.99	1.00	0.99	-

[d] Ra = 10^6

Observation	m	n	o	p	100×(p-m)/p
u_{max}	64.63	68.81	66.42	64.99	0.554
y	0.85	0.87	0.90	0.77	-
v_{max}	217.40	221.80	226.40	221.27	1.749
x	0.038	0.037	0.021	0.075	-
Nu	8.80	8.75	10.39	8.91	1.27
Nu_{max}	17.92	17.87	21.41	20.04	10.58
y	0.038	0.037	0.030	0.025	-
Nu_{min}	0.99	1.23	1.58	0.92	-7.97
y	1.00	0.99	1.00	0.99	-

m-solution of de Vahl Davis [4]; n- solution of Markatos and Perikleous [8]; o- solution of Hadjisophocleous et al [7]; p- present solution on 61×61 grid.

Table 1. Comparison of solutions for natural convection in an enclosed cavity

Fig. 2 shows the *u* velocity profile along the vertical centerline of the cavity and *v* velocity profile along the horizontal centerline. Very good agreements were obtained except for the x and y location of the maximum u and v velocity to the mid-plane. With increase of Ra, the intensity of convection increased. Small values of the Rayleigh number corresponded to low convective heat transport i.e., the case of pure conduction. Fig. 3(a) shows the streamlines of a single vortex with circular shape and in Fig. 3(b) isotherms are parallel to the heated walls, indicating that most of the heat transfer is by heat conduction (Ra=10^3). Fig .4(a) shows the central streamline is distorted into an elliptic shape and in Fig. 4(b), the effect of convection is more pronounced in the isotherms (Ra=10^4). As the Rayleigh number increases, the central streamline is further elongated and two secondary vortices appear inside it shown in Fig. 5(a). At Ra = 10^6, it is found that the secondary vortices move closer towards the walls and a third vortex appears in the centre of the section, again rotating clockwise as shown in Fig. 6(a). As the fluid moves near the walls, the heat transfer is mostly by convection. The flow of all cases is rotationally symmetric about the center of the cavity.

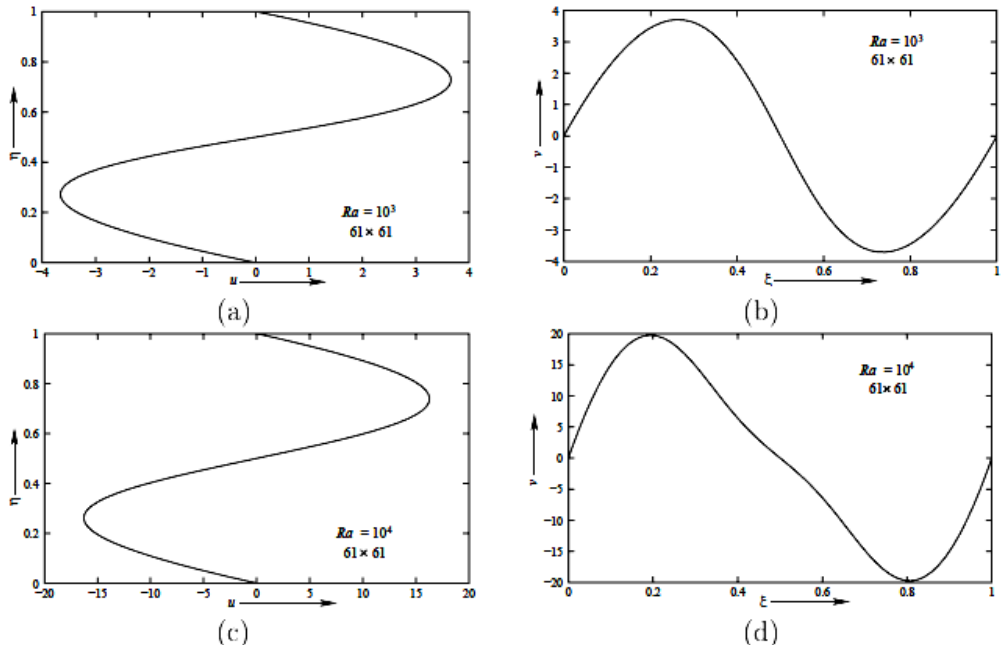

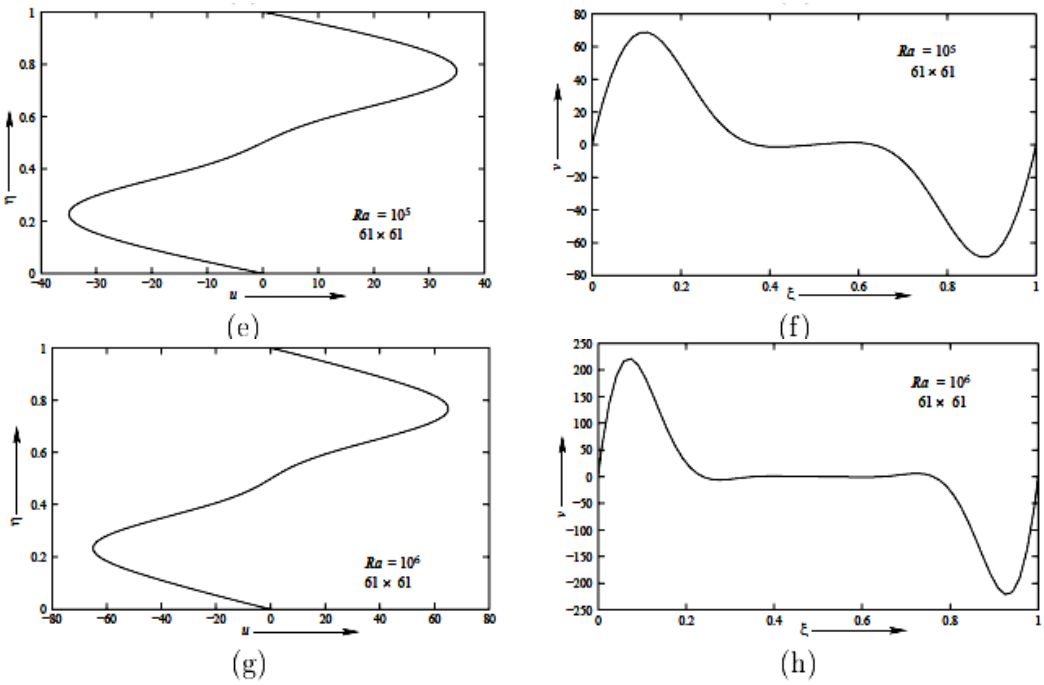

u- Velocity along vertical centerline *v*- Velocity along horizontal centerline

Fig. 2. *u* and *v* velocity plot for Ra = 10^3, Ra = 10^4, Ra = 10^5 and Ra = 10^6

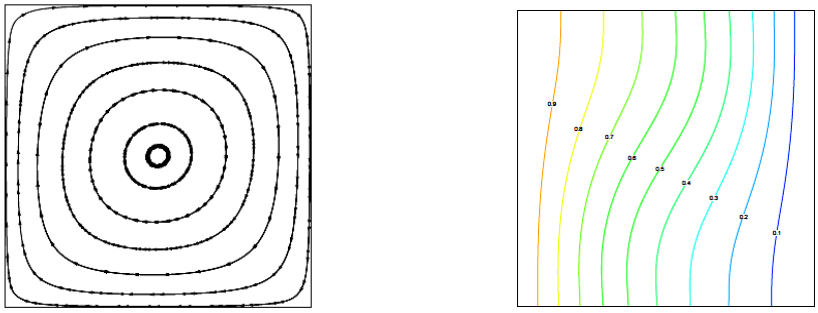

(a) (b)

Fig. 3. Ra = 10^3 (a) Streamline (b) T contour

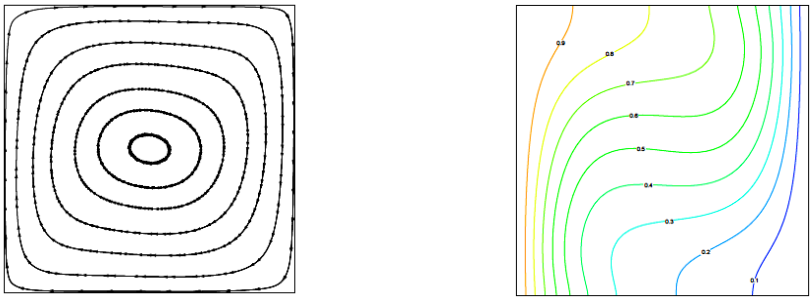

(a) (b)

Fig. 4. Ra = 10^4 (a) Streamline (b) T contour

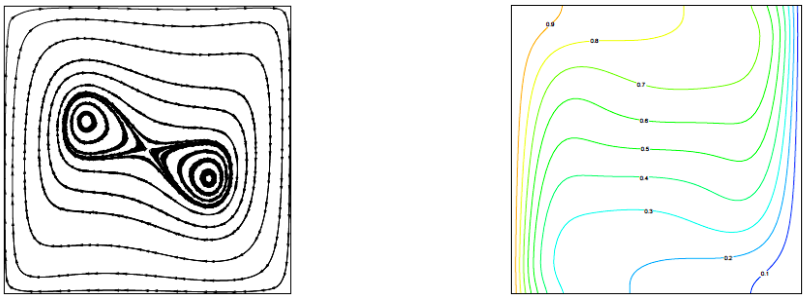

(a) (b)

Fig. 5. Ra = 10^5 (a) Streamline (b) T contour

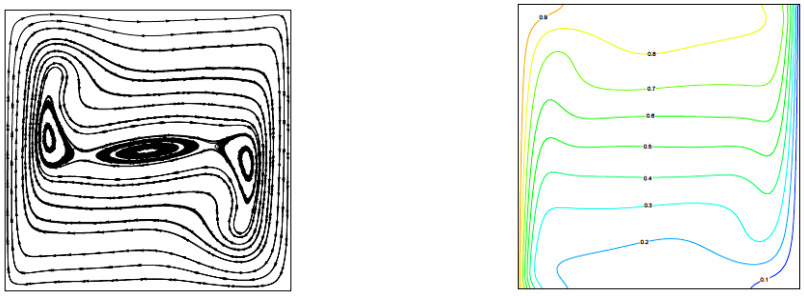

(a) (b)

Fig. 6. Ra = 10^6 (a) Streamline (b) T contour

6. CONCLUSION

The problem of natural convection of an incompressible, Boussinesq fluid within a rectangular cavity with differentially heated walls (de Vahl Davis [4] problem) was investigated numerically. The computation had been done using complex geometry formulation in non-orthogonal grids. The convergence problem for higher Rayleigh numbers had been experienced. This problem was overcome using small value of pseudo-time step. The results were compared with the benchmark solution of de Vahl Davis [4], Markatos and Perikleous [8] and Hadjisophocleous et al. [7] for Ra = 10^3; 10^4; 10^5, 10^6 and Pr = 0.71. Very good agreements were obtained except for the x and y location of the maximum u and v velocity to the midplane. With increase of Ra, the intensity of convection increased. Small values of the Rayleigh number corresponded to low convective heat transport i.e., the case of pure conduction.

Nomenclature:

Ra	Rayleigh Number
Pr	Prandtl Number
Nu	Nusselt Number
Nu_{max}	Maximum value of local Nusselt number on the boundary at $x = 0$
Nu_{min}	Minimum value of local Nusselt number on the boundary at $x = 0$
J	Jacobian
u, v	Dimensionless velocity components in x and y directions
u_{max}	Maximum horizontal velocity on the vertical mid-plane of the cavity
v_{max}	Maximum horizontal velocity on the vertical mid-plane of the cavity
k	Thermal conductivity
h	Convective heat transfer coefficient
β	Volumetric expansion coefficients
α	Thermal diffusivity
υ	Kinematic viscosity
η, ξ	Dimensionless curvilinear coordinates
SIMPLE	Semi-Implicit Method for Pressure-Linked Equation
SIMPLEC	Semi-Implicit Method for Pressure-Linked Equation Consistent
QUICK	Quadratic Upstream Interpolation for Convective Kinematics

7. REFERENCES

[1] S. V. Patankar and D. Spalding, "A Calculation of Time Dependent V Incompressible with Free Surface," *International Journal of Heat and Mass Transfer*, vol. 15, 1972, pp. 1787-1806.

[2] U. Ghia, K. N. Ghia and C. T. Shin, "High-Re Solutions for Incompressible Flow Using the Navier-Stokes Equations and a Multigrid Method," *Journal of Computational Physics*, vol. 48, 1982, pp. 387-411.

[3] de Vahl Davis, G., and Jones, I. P., "Natural Convection in a Square Cavity-A Comparison Exercise," *International Journal of Numerical Methods in Fluids*, Vol. 3, 1983, pp. 227-248.

[4] de Vahl Davis, G., Natural Convection of Air in a Square Cavity: A Benchmark Numerical Solution," *International Journal of Numerical Methods in Fluids*, Vol. 3, 1983, pp. 249-264.

[5] J. P. Van Doormall and G. D. Raithby, "Enhancements of the Simple Method for Predicting Incompressible Fluid Flows," *Numerical Heat Transfer*, vol. 7, 1984, pp 147-163.

[6] C. R. Maliska and G. D. Raithby, "A Method for Computing Three Dimensional Flows Using Non-Orthogonal Boundary-Fitted Co-Ordinates," *International Journal for Numerical Methods in Fluids*, vol. 4, 1984, pp. 519-537.

[7] Hadjisophocleous, G. V., Sousa, A. C. M., and Venart, J. E. S., "Prediction of Transient Natural Convection in Enclosures of Arbitrary Geometry using a Non-orthogonal Numerical Model," *Numerical Heat Transfer*, Vol. 13, 1988, pp 373-392.

[8] Markatos, N. C., and Perikleous, K. A., " Laminar and Turbulent Natural Convection in an Enclosed Cavity," *International Journal of Heat & Mass Transfer*, Vol. 27, No. 5, 1984, pp. 755-772.

[9] J. F. Thompson, Z. U. A. Warsi and C. W. Mastin, "*Numerical Grid Generation*," North Holland,1985.

Author: **Ramesh Chandra Mohapatra Reader**, Mechanical Department, Department of Mechanical Engineering, Government College of Engineering, Keonjhar, Odisha, India, Phone No. 9438551072
E- mail: rameshmohapatra75@gmail.com

http://doi.org/10.24867/JPE-2017-01-117

Journal of Production Engineering

Vol.20 No.1

JPE (2017) Vol.20 (1) Preliminary Note

Babič, M.

NEW METHOD FOR IMAGE ANALYSIS USING METHOD OF ESTIMATING FRACTAL DIMENSION OF 3D SPACE

Received: 07 April 2017 / Accepted: 19 May 2017

Abstract: *In Mechanical Engineering we have many problems. Which materials use to build complex structure. How can we analyze materials? Have we good methods? How we prepare materials to have a long time a life. In this article we present a new method for image analysis using method of estimating fractal dimension of 3D space for robot laser hardened specimens. We analyze SEM picture of microstructure of robot laser hardened specimens with mathematical method. In this open problem we use graph theory and fractal geometry. We use methods of intelligent systems to make prediction in Mechanical Engineering. In imaging science, image processing is processing of images using mathematical operations by using any form of signal processing for which the input is an image, such as a photograph or video frame; the output of image processing may be either an image or a set of characteristics or parameters related to the image. Losely related to image processing are computer graphics and computer vision. In computer graphics, images are manually made from physical models of objects, environments, and lighting, instead of being acquired (via imaging devices such as cameras) from natural scenes, as in most animated movies.*

Key words: *image processing, intelligent system, fractal dimension, graph theory*

Novi metod za analizu slike primenom metode procene fraktalne dimenzije u 3D prostoru. *U mašinstva imamo mnogo problema. Koje materijale koristiti za izgradnju složene strukture. Kako možemo analizirati materijale? Da li su dobre metode? Kako ćemo pripremiti materijale da se dugo vremena koriste. U ovom članku ćemo predstaviti novu metodu za analizu slike metodom procene fraktalne dimenzije 3D prostora pomoću robota za lasersko stvrdnjavanje uzoraka. Analiza SEM slike mikrostrukture stvrdnutih uzoraka pomoću lasera je pomoću matematičke metode. U ovom otvorenom problemu koristena je teoriju grafova i Fraktala geometrija. Korisćena je metoda inteligentnih sistema za predviđanje u mašinstvu. U nauci o slikama, obrada slike je obrada pomoću matematičke operacije koristeći bilo koji oblik obrade signala za koje je ulaz slika, kao što su fotografije ili video okviri; izlaz obrade slike može biti ili slika ili skup karakteristika ili parametara vezanih za slike. U blagoj vezi sa obradom slike su kompjuterske grafike i kompjuterska vizija. Kod kompjuterske grafike, slike su ručno izrađene od fizičkih modela objekata, okruženja, i osvetljenja, umesto da se stiče (preko uređaja za snimanje, kao što su kamere) od prirodnih scena, kao i u većini animiranih filmova.*

Ključne reči: *obrada slike, inteligentni sistem, fraktalna dimenzija, teorija grafova*

1. INTRODUCTION

Image processing [1] is a method to convert an image into digital form and perform some operations on it, in order to get an enhanced image or to extract some useful information from it. It is a type of signal dispensation in which input is image, like video frame or photograph and output may be image or characteristics associated with that image. Usually Image Processing system includes treating images as two dimensional signals while applying already set signal processing methods to them. It is among rapidly growing technologies today, with its applications in various aspects of a business. Image Processing forms core research area within engineering and computer science disciplines too. Image processing is a method to perform some operations on an image, in order to get an enhanced image or to extract some useful information from it. It is a type of signal processing in which input is an image and output may be image or characteristics/features associated with that image. Nowadays, image processing is among rapidly growing technologies. It forms core research area within engineering and computer science disciplines too. Image processing basically includes the following three steps: Importing the image via image acquisition tools; Analysing and manipulating the image; Output in which result can be altered image or report that is based on image analysis. There are two types of methods used for image processing namely, analogue and digital image processing. Analogue image processing can be used for the hard copies like printouts and photographs. Image analysts use various fundamentals of interpretation while using these visual techniques. Digital image processing techniques help in manipulation of the digital images by using computers. The three general phases that all types of data have to undergo while using digital technique are pre-processing, enhancement, and display, information extraction. In this lecture we will talk about a few fundamental definitions such as image, digital image, and digital image processing. Different sources of digital images will be discussed and examples for each source will be provided. The

continuum from image processing to computer vision will be covered in this lecture. Finally we will talk about new methot of image calculate with fractal dimension in 3D space with different types of image application in mechanical engineering, especialy in laser technology in hardening. Digital Processing techniques help in manipulation of the digital images by using computers. As raw data from imaging sensors from satellite platform contains deficiencies. To get over such flaws and to get originality of information, it has to undergo various phases of processing. The three general phases that all types of data have to undergo while using digital technique are Pre- processing, enhancement and display, information extraction.Fractals [2] is a new branch of mathematics and art. Perhaps this is the reason why most people recognize fractals only as pretty pictures useful as backgrounds on the computer screen or original postcard patterns.Process of robot laser hardening is presented in many articles [3-5]. Laser hardening offers customers an excellent alternative to induction and flame hardening. With laser precision and robot control, laser hardening can be applied to complex surfaces while achieving repeatable hardness and case depth. The aim of this study is to present a new method of image processing and it's aplication in calculate volume of 3D space with analize SEM images of robot laser hardened specimens using method of estimating calculating fractal dimansion of 3D objects.

2. MATERIAL PREPARATION AND EXPERIMENTAL METHOD

Firstly, we hardened tool steel with a robot laser cell. We changed two parameters, speed v∈[2, 5] mm/s and temperature T ∈ [1000, 1400] °C. Detailed characterization of their microstructure before and after surface modifications was conducted using a field emission scanning electron microscope (SEM), JEOL JSM-7600F. Also the SEM pictures were converted into binary images, from which we calculated the fractal dimension and into 3D graph, from which we calculate volume. For each *(x,y,z)* we use only *z* coordinate. Coordinate z have maximal value 255. Also, we calculate volume of robot laser hardened specimens with (1)

$$V = \frac{Z_1+Z_2+\ldots+Z_{n4}}{n} \qquad (1)$$

for all *n*.

A random process is statistically evaluated using Hurst parameter *H* or by determining the distribution function. Hurst parameter *H* as self-similarity criteria can not be accurately calculated, but it can be only estimated. We use new method for calculating fractal dimension for 3D object [6]. For analyze results, we use one method of intelligent system, Genetic programming [7], neural network [8] and multiple regression [9]. In genetic programming we evolve a population of computer programs. That is, generation by generation, GP stochastically transforms populations of programs into new, hopefully better, populations of programs. GP, like nature, is a random process, and it can never guarantee results. In GP, programs are usually expressed as syntax trees rather than as lines of code. There are many problems where solutions cannot be directly cast as computerprograms. For example, in many design problems the solution is an artifact of some type: a bridge, a circuit, an antenna, a lens, etc. GP has been applied to problems of this kind by using a trick: the primitive set is set up so that the evolved programs construct solutions to the problem. This is analogous to the process by which an egg grows into a chicken.Genetic Algorithms are numerical optimization algorithms inspired by both natural selection and natural genetics (David 2001). It is a probabilistic search algorithm that iteratively transforms a set (called a population) of mathematical objects (typically fixed-length binary character strings), each with an associated fitness value, into a new population of offspring objects using the Darwinian principle of natural selection and using operations that are patterned after naturally occurring genetic operations, such as crossover (sexual recombination) and mutation (John 2007).

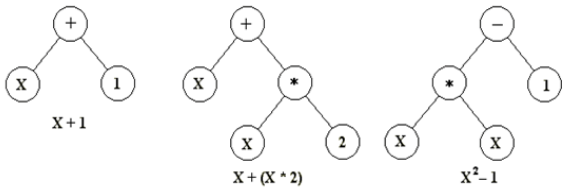

Fig. 1 - Model of genetic programming

Computer scientists have long been inspired by the human brain. In 1943, Warren S. McCulloch, a neuroscientist, and Walter Pitts, a logician, developed the first conceptual model of an artificial neural network [10]. In their paper, "A logical calculus of the ideas imminent in nervous activity," they describe the concept of a neuron, a single cell living in a network of cells that receives inputs, processes those inputs, and generates an output. Their work, and the work of many scientists and researchers that followed, was not meant to accurately describe how the biological brain works. Rather, an artificial neural network (which we will now simply refer to as a "neural network") was designed as a computational model based on the brain to solve certain kinds of problems. It's probably pretty obvious to you that there are problems that are incredibly simple for a computer to solve, but difficult for you. Take the square root of 964,324, for example. A quick line of code produces the value 982, a number Processing computed in less than a millisecond. There are, on the other hand, problems that are incredibly simple for you or me to solve, but not so easy for a computer. Show any toddler a picture of a kitten or puppy and they'll be able to tell you very quickly which one is which. Say hello and shake my hand one morning and you should be able to pick me out of a crowd of people the next day. But need a machine to perform one of these tasks? Scientists have already spent entire careers researching and implementing complex solutions. The most common application of neural networks in computing today is to perform one of these "easy-for-a-human, difficult-for-a-machine" tasks, often referred to as pattern recognition.

Applications range from optical character recognition (turning printed or handwritten scans into digital text) to facial recognition. We don't have the time or need to use some of these more elaborate artificial intelligence algorithms here, but if you are interested in researching neural networks, I'd recommend the books Artificial Intelligence: A Modern Approach by Stuart J. Russell and Peter Norvig and AI for Game Developers by David M. Bourg and Glenn Seemann.

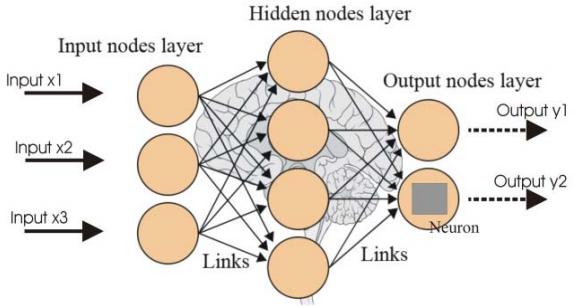

Fig. 2 - Model of neural network

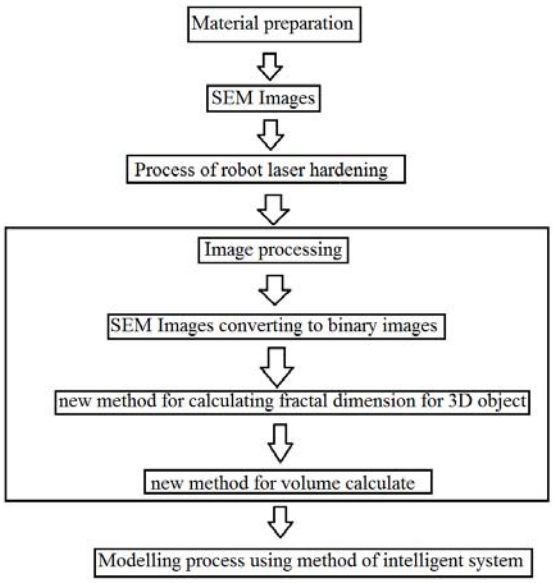

Fig. 3 - Model of intelligent system

Multiple linear regression analysis is used to examine the relationship between two or more independent variables and one dependent variable. The independent variables can be measured at any level (i.e., nominal, ordinal, interval, or ratio). However, nominal or ordinal-level IVs that have more than two values or categories (e.g., race) must be recoded prior to conducting the analysis because linear regression procedures can only handle interval or ratio-level IVs, and nominal or ordinal-level IVs with a maximum of two values (i.e., dichotomous). If there are k predictor variables, then the regression equation model is

$$Y = \beta_0 + X_1\beta_1 + \cdots + X_n\beta_n$$

The x_1, x_2, ..., x_k represent the k predictor variables. Those parameters are the same as before, β_0 is the y-intercept or constant, β_1 is the coefficient on the first predictor variable, β_2 is the coefficient on the second predictor variable, and so on. ε is the error term or the residual that can't be explained by the model. Those parameters are estimated by b_0, b_1, b_2, ..., b_n.

This gives us a regression equation used for prediction of

$$Y = \beta_0 + X_1\beta_1 + \cdots + X_n\beta_n$$

Basically, everything we did with simple linear regression will just be extended to involve k predictor variables instead of just one.

3. RESULTS AND DISCUSSION

In Table 1, the parameters which impact on SEM image of hardened materials. We mark specimens from P1 to P21. Parameter X_1 presents the parameter of temperature in degree of Celsius [C], X_2 presents the speed of hardening [mm/s], X_3 presents fractal dimension in 3D space and X_4 presents basic volume of laser-hardened robot specimens in 3D space. The last parameter Y is the measured volume of laser-hardened robot specimens. Table 2 presents experimental and prediction data regarding the volume of laser hardened robot specimens. In Table 2 present symbol S name of specimens, E experimental data, NM1 prediction with neural network with 30% learn set, NN2 prediction with neural network with 50% learn set, NN3 prediction with neural network with method one live out, R prediction with regression, GP prediction with genetic programming. In Table 1, we can see that specimen P16 has the largest volume; 77,7. The measured and predicted volume of robot laser hardened specimens is shown in the graph in Fig. 4. The genetic programming model is presented under Table 2. Under model of genetic programming is presented model of regression. The genetic programming model presents a 20,79% deviation from the measured data, which is less than the regression model, which presents a 35,11% deviation. The best neural network NN3 present 31,48% deviation from the measured data.

S	X_1	X_2	X_3	X_4	Y
P1	1000,0	2,0	2,304	8,3	28,0
P2	1000,0	3,0	2,264	8,3	20,6
P3	1000,0	4,0	2,258	8,3	25,4
P4	1000,0	5,0	2,341	8,3	22,5
P5	1400,0	2,0	2,222	8,3	22,9
P6	1400,0	3,0	2,388	8,3	19,3
P7	1400,0	4,0	2,25	8,3	13,2
P8	1400,0	5,0	2,286	8,3	21,0
P9	1000,0	2,0	2,178	28,0	24,0
P10	1000,0	3,0	2,183	20,6	27,5
P11	1000,0	4,0	2,408	25,4	28,7
P12	1000,0	5,0	2,210	22,5	23,7
P13	1400,0	2,0	2,257	22,9	26,3
P14	1400,0	3,0	2,265	19,3	22,1
P15	1400,0	4,0	2,433	132	20,3
P16	1400,0	5,0	2,289	21,0	77,7
P17	800,0	0,0	2,232	8,3	15,3
P18	1400,0	0,0	2,235	8,3	31,8
P19	2000,0	0,0	2,261	8,3	36,9
P20	950,0	0,0	2,282	8,3	70,8
P21	850,0	0,0	2,319	8,3	43,9

Table 1. Parameters of images of hardened specimens

S	E	NN1	NN2	NN3	R	GP
P1	28	28,3	28,33	27,77	26,6	21,29
P2	20	19,8	19,92	21,47	23,4	19,84
P3	25	25,4	25,27	24,79	21,2	21,87
P4	22	22,7	23,12	22,63	21,5	22,86
P5	22	22,7	22,80	22,71	28,3	21,57
P6	19	19,1	19,06	19,43	30,8	21,04
P7	13	14,6	14,70	12,72	25,0	13,47
P8	21	20,1	20,01	20,86	23,9	22,71
P9	24	5,57	24,07	24,09	32,8	24,42
P10	27	6,48	27,51	27,65	27,2	22,86
P11	28	6,85	28,73	28,62	33,8	28,49
P12	23	10,8	30,84	80,26	24,8	28,06
P13	26	8,71	49,43	24,72	36,4	26,38
P14	22	7,08	42,85	23,50	32,8	25,51
P15	20	10,6	18,83	20,21	32,5	20,20
P16	77	6,59	35,92	77,47	30,2	30,94
P17	15	48,1	49,92	15,22	26,7	13,72
P18	31	41,2	30,49	31,81	32,7	30,94
P19	36	30,6	17,95	36,79	39,4	36,90
P20	70	46,0	48,08	70,76	29,5	34,35
P21	43	44,2	56,22	43,85	29,6	43,98

Table 2: Experimental and prediction data

A statistically significant relationship was found between volume, the parameters of the robot laser cell and image analysis with new method of fractal geometry calculate for object in 3D space. In addition, image analysis of SEM images of robot laser hardened specimens is an interesting approach. Specimen P16 has the most volume after robot laser hardening, that is 77,7%. Parameter X3 (fractal dimension) has most impact on Regression model. Parameter X4 (base volume) has most impact on genetic programing. We use method of intelligent systems; genetic programming, neural network and multiple regression to predict volume of robot laser hardened specimens. We show that the genetic programming give us the best predicted results. The neural network model is better than the regression model.

Model of regression

$$Y = 47{,}35891887 + 0{,}0098937467 \times X_1 - 2{,}03904329 \times X_2 + 27{,}81672014 \times X_3 + 0{,}0491686011 \times X_4$$

Model of genetic programming

$$Y = 0{,}0162358 \times \left(-5{,}51153 + X_1 + 6 \times X_4 - \frac{X_1}{\frac{-2 \times X_1}{X_4} + X_4} - \frac{X_1}{\frac{-5 \times X_1}{2 \times X_4} + X_4} - \frac{2 \times (-11{,}0231 + X_1)}{-0{,}181438 + 2 \times X_4} - \frac{2 \times (-5{,}51153 + X_1)}{-0{,}181438 \times X_1 + 2 \times X_4} - \frac{-16{,}5346 + X_1 + 3 \times X_4 - \frac{X_1 + X_2}{X_2} + \frac{X_1}{X_4}}{X_2} - \frac{2 \times (-5{,}51153 + 1{,}18144 \times X_1 + X_4)}{2 \times X_4 - 0{,}181438 \times (X_1 + X_4 - 11{,}0231)} - \frac{-11{,}0231 + X_1 - \frac{X_1}{X_2} - \frac{2 \times X_1}{X_4} - 4 \times X_4 - \frac{X_1 + X_3 + X_4}{X_2}}{X_2} - \frac{X_1}{-5{,}51153 + X_2 + 4 \times X_4 - \frac{-0{,}818562 \times X_1 + X_4}{X_2} + \frac{X_1 + \frac{-5{,}51153 + 0{,}818562 \times X_1 + X_4}{X_2}}{X_4}} \right)$$

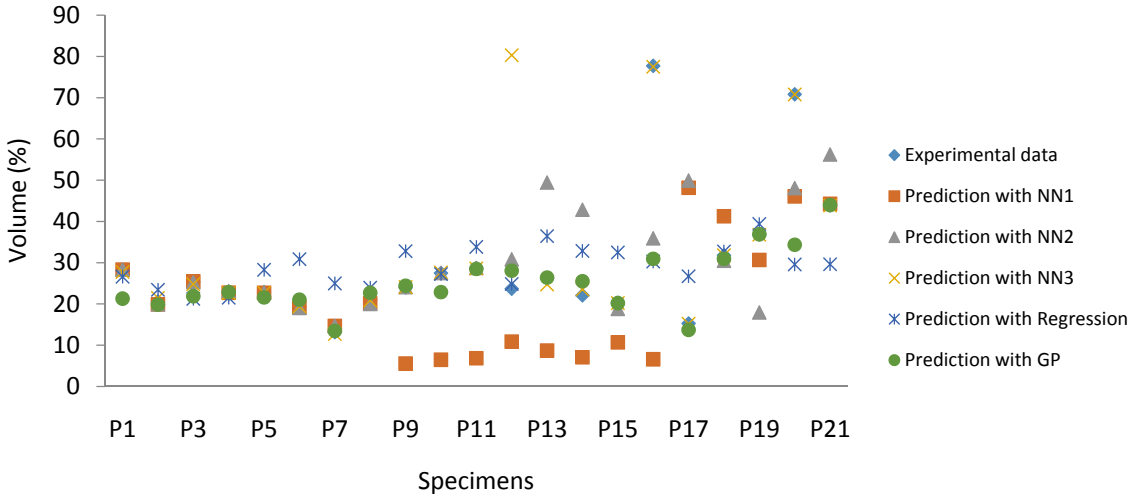

Fig. 4. The measured and predicted volume of robot laser hardened specimens

4. CONCLUSIONS

In this article we present a new method for image analysis of robot laser hardened materials, which have many applications in Mechanical Engineering, like in construction of bridges, railways, skyscrapers. The SEM pictures were converted into 3D graph, from which we calculate volume. The paper presents the use of method of intelligent system namely genetic programming, neural network and multiple regression to predict volume of hardened specimens. We use method for describe complexity, estimating fractal dimension in 3D space. In the future, we want to explore new method for image processing in 3D space as a function of the parameters of a robot cell for laser hardening for pinned robot laser hardening: laser parameters such as power, energy density, focal distance, energy density in the focus, focal position, the shape of the laser flash, flash frequency, temperature and speed of hardening. We are interested in new method for image processing in SEM pictures of:

- Two-beam laser robot hardening (where the laser beam is divided into two parts) specimens
- Areas of overlap (where the laser beam covers the already hardened area) specimens
- Robot laser hardening at different angles (where the angles change depending on the *x*- and *y*-axes) specimens.

5. References

[1] Rafael C. Gonzalez; Richard E. Woods (2008). Digital Image Processing. Prentice Hall. pp. 1–3. ISBN 978-0-13-168728-8.

[2] Mandelbrot, B. B. The fractal geometry of nature. New York: W. H. Freeman, 1982:93.

[3] J. Grum, P. Žerovnik, R. Šturm: Measurement and Analysis of Residual Stresses after Laser Hardening and Laser Surface Melt Hardening on Flat Specimens; Proceedings of the Conference "Quenching ’96", Ohio, Cleveland, 1996.

[4] BABIČ, Matej, MILFELNER, Matjaž, BELIČ, Igor, KOKOL, Peter. Problems associated with a robot laser cell used for hardening = Problematika robotskega laserskega kaljenja. Materiali in tehnologije, ISSN 1580-2949. [Tiskana izd.], jan.-feb. 2013, letn. 47, št. 1, str. 37-41.

[5] BABIČ, Matej, BALIČ, Jože, MILFELNER, Matjaž, BELIČ, Igor, KOKOL, Peter, ZORMAN, Milan, PANJAN, Peter. Robot laser hardening and the problem of overlapping laser beam. Advances in production engineering & management, ISSN 1854-6250, 2013, vol. 8, no. 1, str. 25-32.

[6] BABIČ, Matej, KOKOL, Peter, GUID, Nikola, PANJAN, Peter. A new method for estimating the Hurst exponent H for 3D objects. Materiali in tehnologije, ISSN 1580-2949, 2014, letn. 48, št. 2, str. 203-208. http://mit.imt.si/Revija/.

[7] Koza, John (1992). Genetic Programming: On the Programming of Computers by Means of Natural Selection. Cambridge, MA: MIT Press. ISBN 978-0262111706.

[8] Graves, Alex; and Schmidhuber, Jürgen; Offline Handwriting Recognition with Multidimensional Recurrent Neural Networks, in Bengio, Yoshua; Schuurmans, Dale; Lafferty, John; Williams, Chris K. I.; and Culotta, Aron (eds.), Advances in Neural Information Processing Systems 22 (NIPS'22), December 7th–10th, 2009, Vancouver, BC, Neural Information Processing Systems (NIPS) Foundation, 2009, pp. 545–552.

[9] Box, G. E. P. (1954). "Some Theorems on Quadratic Forms Applied in the Study of Analysis of Variance Problems, I. Effect of Inequality of Variance in the One-Way Classification". The Annals of Mathematical Statistics 25 (2): 290. doi:10.1214/aoms/1177728786.

[10] Daniel Shiffman. The Nature of Code. http://dep.fie.umich.mx/~garibaldi/data/uploads/graficacion/nature_of_code-005_shiffman_12.4.12.pdf

Author: **Dr. Matej Babič, Bs. M.**
Jožef Stefan Institute, Ljubljana, Slovenia
E-mail: babicster@gmail.com

http://doi.org/10.24867/JPE-2017-01-122

Journal of Production Engineering

Vol.20 No.1

JPE (2017) Vol.20 (1) Preliminary Note

Jindal, U., Jain, S., Piyush, Khanna, P.

MATHEMATICAL ANALYSIS OF VIBRATORY BOWL FEEDER FOR CLIP SHAPED COMPONENTS

Received: 15 March 2017 / Accepted: 16 April 2017

Abstract: *In the present scenario, to meet the increasing demand of the consumers, the industries are adopting more and more automation to save time and money. Automation not only reduces human effort but also improves the quality of product and efficiency of production which is the need of the hour. Feeders play a major role in automation that helps to deliver the components in the desired orientation discretely. Present work aims at mathematical analysis of a vibratory bowl feeder for feeding clip shaped components. The path of the feeder was modified and the principle of center of gravity was used to feed the clips in desired orientation. A process model was formulated on the basis of Analysis of Variance (ANOVA) using Design-Expert Statistical Package.Interaction among the factors was studied and a full 2^3 factorial experimental approach was adopted.*

Key words: *ANOVA, factorial experimental approach*

Matematička analiza posude vibracionog snabdevača za komponente oblika spajalice. *U prikazanom scenariju, da se zadovolji sve veća potražnja potrošača, industrija usvajaja sve više automatizacije da bi uštedili vreme i novac. Automatizacija ne samo da smanjuje ljudski napor, ali i poboljšava kvalitet proizvoda i efikasnost proizvodnje gledano na nivou od sat vremena. Hranilice igraju glavnu ulogu u automatizaciji koje pomažu da se komponente isporuče sa željenom orijentacijom diskretno. Ovaj rad ima za cilj da uz pomoću matematičke analize prikaže vibracije posude hranilice za komponente u obliku spajalice. Put hranilice je modifikovan i princip centra gravitacije se koristi za hranjenje spajalica u željenoj orijentaciji. Model procesa je formulisan na osnovu analize varijanse (ANOVA) upotrebom Dizajn-Ekpert statističkog paketa. Interakcija među faktorima je analizirana i puni 2^3 faktorijalni eksperimentalni dizajn je usvojen.*

Ključne reči: *ANOVA, faktorni eksperimentalni pristup*

1. INTRODUCTION

What are feeders?

Feeders form a critical part of automated assembly lines. Assembly processes demand the presence of components in desired amount and orientation. Feeders serve this purpose by feeding discrete parts to assembly cells on the production line from bulk and disoriented supplies [1].

Need for optimization

Part feeders are critical for automated assembly lines. Ad-hoc setting of parameters results in either starvation or saturation, where too less or too many parts are delivered to the work cells respectively [2]. Hence, optimization of feeders is a cause of concern. This project aims at mathematical analysis of a vibratory bowl feeder. Different input parameters were carefully chosen to establish the relationship between the system inputs and outputs.

2. EXPERIMENTAL SETUP

The existing path was modified to take care of the orientation of the clips. Centre of mass of the clips was used to sort the disoriented ones [3].

A cardboard setup consisting of a cut mark (as shown in figure 1) of the shape of the clip was designed with calculated cuts so as to sort the disoriented clips. Cardboard material was chosen so as to minimize the effect of vibrations that could fail the setup.

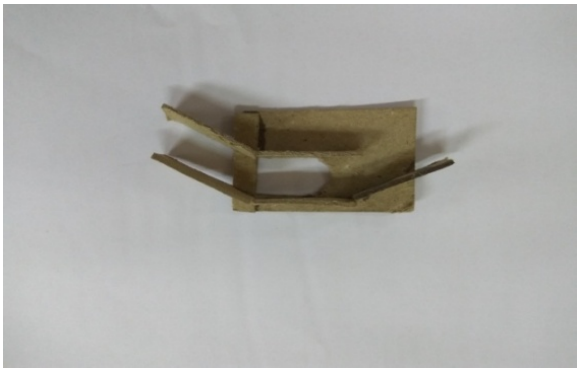

Fig. 1. Setup for feeding clip shaped components

Guiding paths were designed upto the cut mark and further beyond it in a proper manner to avoid jamming of the clips.

Further a simple chute was constructed to allow the clips to feed one at a time. Width of the chute was slightly greater than the width of the clips (as shown in figure 2).

2.1 Factors affecting the feed rate

1. Frequency of Operation – 55Hz – 75Hz
2. Part Population – 25 – 100

3. Length of Clips – 28mm - 50mm

Fig. 2. Vibratory bowl feeder with modified path

2.2 Factorial approach

The aim of the experiment was to establish a statistical model to predict the output feed rate and its successful
optimization using 2^k factorial design. The three factors chosen for experiment are the controllable variables which play a key role in the process characterization. These factors are varied within a controllable range purely on the experimental basis and feasibility [4].

Since there are three factors to be considered namely frequency of operation, part length and part population, the experiment design is called a 2^3 full factorial design which required eight test runs, each with combinations of the three factors across two levels of each. Therefore, twenty four observations were taken in all to employ full factorial design as shown inTable1and Table2.

S No	Part Length	Frequency	Part Population	Feed rate
1	-1	1	-1	31
2	1	-1	-1	17
3	-1	1	1	51
4	1	1	-1	33
5	1	1	1	50
6	-1	-1	1	26
7	-1	-1	-1	15
8	1	-1	1	30

Table 1. Range of parameters

S No.	Parameter	Low Level (-1)	High Level (+1)
1	Part Length (mm)	28	50
2	Frequency (Hz)	55	75
3	Part Population	25	100

Table 2. Range of Parameters in Actual Values

3. ANALYSIS OF EFFECTS OF FACTORS ON FEED RATE

3.1 Cube Plot

The cube plot for feed rate shows the average feed rates at the critical points which are those points where the parameters have their limiting values [5]. The vertices of the cube depict the maximum value of each of the parameters. Feed rate corresponding to any other combination of parameters lies within the cube as plotted in figure 3.

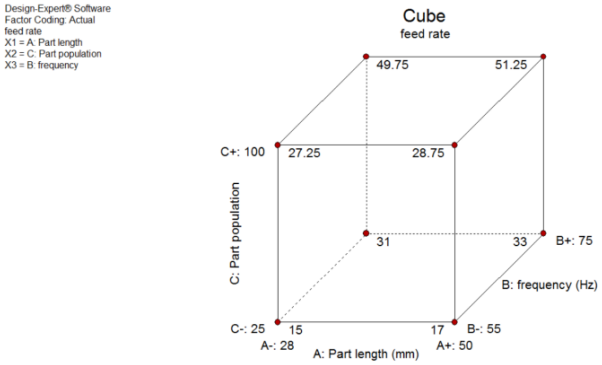

Fig. 3. Cube Plot (fitted means) for Feed rate

3.2 One factor plots

One factor plots are plotted as a simple two dimensional graph between two factors. The independent parameter is taken on the x-axis while the dependent one on the y-axis.

Here the dependent parameter is the feed rate while the independent parameters are part population, part length and frequency of operation. The one factor graphs can be used to compare the relative strength of the effects across factors.

In the one-factor plots, only the first and the last readings are plotted and these are connected by a simple line as shown in figure 4, 5 and 6.

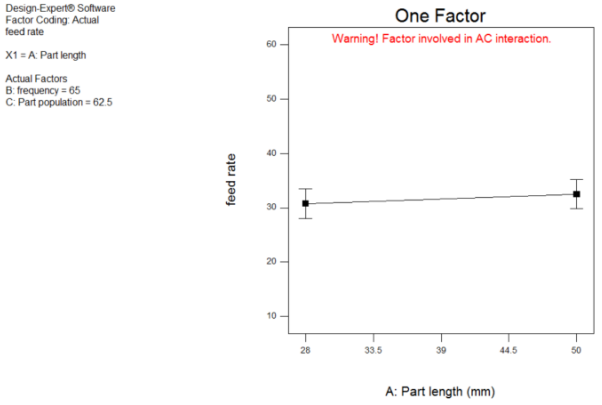

Fig. 4. Main Effects Plot (feed rate vs part length)

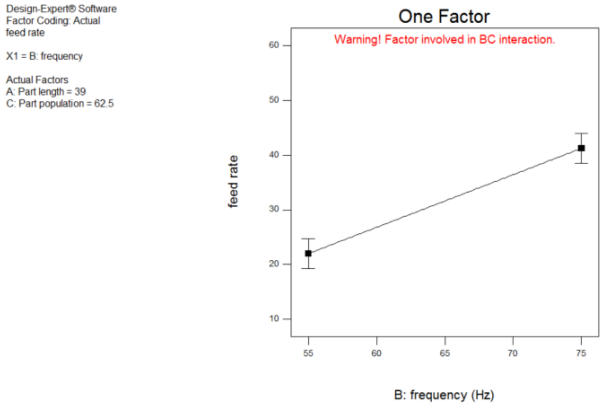

Fig. 5. Main Effects Plot (feed rate vs frequency)

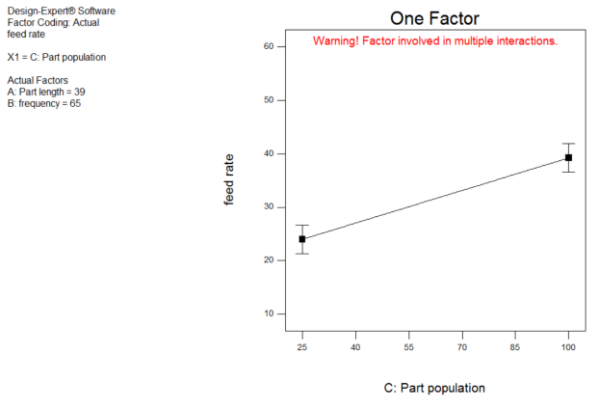

Fig. 6. Main Effects Plot (feed rate vs part population)

3.3 Interaction plots

Figures 7 and 8 depict a plot of average output for each level of two factors with the level of third and fourth factor held constant. These plots are used to interpret interaction between the process parameters. When the response at a factor level depends upon the levels of other factors, interaction is present. These interactions can either magnify or diminish the main effects of the parameters,hence, their evaluationis extremely important.

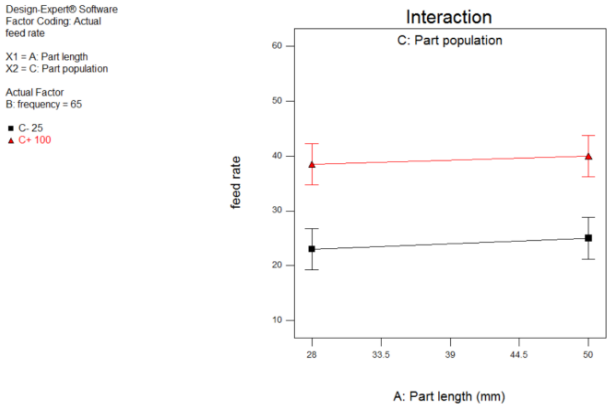

Fig. 7. Interaction Plot (part length & Part population)

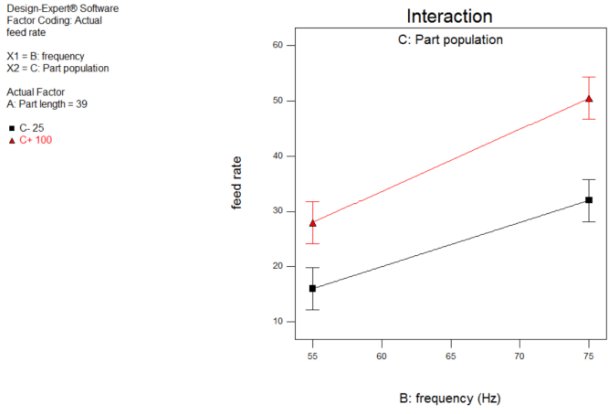

Fig. 8. Interaction Plot (frequency & Part population)

The interaction plots are useful in judging the interaction between various parameters by looking at the parallelism of the lines. Higher the degree of parallelism, lesser is the extent of interaction between them.

Only the interaction plot of *Part population and frequency* depict synergic interaction. Although the lines on the plot do not cross each other but lack of their parallelism depicts significant interaction. While the interaction of part length and part population shows parallelism but they do intersect outside the graph, hence, this confirms negligible interaction between the two. Interaction plot of part length and frequency was not generated because combination of these two factors had no effect on response (as shown in figure 9).

3.4 Final Equation in Terms of Actual Factors:

Feed rate = -29.88258 + (0.098485 * Part length) + (0.69167 * frequency) – (0.066515 * Part Population) – (3.03030E-004 * Part length * Part Population) + (4.33333E-003 * frequency * Part Population)

The equation in terms of actual factors can be used to make predictions about the response for given levels of each factor. Here, the levels should be specified in the original units for each factor. This equation should not be used to determine the relative impact of each factor because the coefficients are scaled to accommodate the units of each factor and the intercept is not at the center of the design space.

4. SIGNIFICANCE OF VARIOUS PARAMETERS

The Pareto Chart and the Half Normal Plot of the parameters determine the absolute importance and relative importance with respect to other parameters and draws a reference line on the chart, any effect that extends beyond this reference line is considered to be significant [4]. The effect of frequency (B) has the highest standardized effect on the feed rate followed by part population (C), BC, part length (A) and so on as depicted in figure 9 and 10.

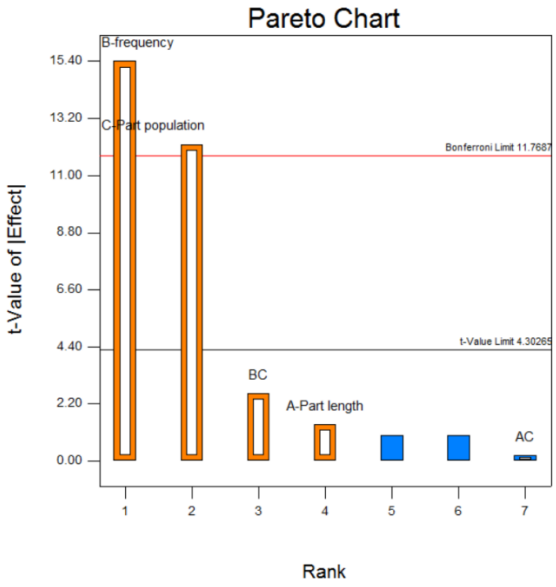

Fig. 9. Pareto Chart of the Standardized Effects

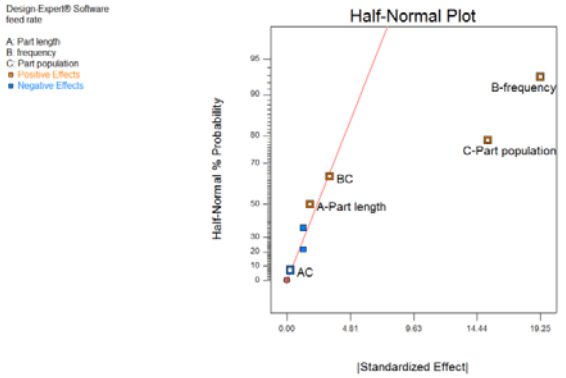

Fig. 10. Half normal Plot

The F Value for a term is the test for comparing the variance associated with that term with the residual variance. It is the Mean Square for the term divided by the Mean Square for the Residual. P value is the probability value that is associated with the F Value for this term. It is the probability of getting an F Value of this size if the term did not have an effect on the response.The calculated F-value and P-value are shown in Table 3. The Model F-value of 78.95 implies that there is a chance that such a large "Model F-value" could occur due to noise.

Source	Sum of Squares	DF	Mean Square	F Value	p-value Prob> F
Model	1233.63	5	246.72	78.95	0.0126
A-Part length	*2.49*	*1*	*2.49*	*0.80*	*0.4666*
B-frequency	*101.31*	*1*	*101.31*	*32.42*	*0.0295*
C-Part population	*0.89*	*1*	*0.89*	*0.29*	*0.6467*
AC	*0.13*	*1*	*0.13*	*0.04*	*0.86*
BC	*21.13*	*1*	*21.13*	*6.76*	*0.1215*
Residual	6.25	2	3.12		
Cor Total	1239.88	7			

Table 3. Analysis of Variance

The terms that have a probability value less than 0.05 are significant. A probability value greater than 0.10 indicate the model terms are not significant. In this case, B (frequency) is the significant model term, while all others are insignificant.

Std. Dev.	1.77	R-Squared	0.995
Mean	31.6	Adj R-Squared	0.9824
C.V. %	5.59	Pred R-Squared	0.9193
PRESS	100	Adeq Precision	23.678
-2 Log Likelihood	20.73	BIC	33.2
		AICc	116.73

Table 4. Diagnostics case statics

R square measures the proportion of total variability explained by the model. From Table 4, the value of R squared is 0.995. A potential problem with this statistic is that it always increases as factors are added to the model even if these factors are insignificant. So the adjusted R squared was calculated to be 0.9824.

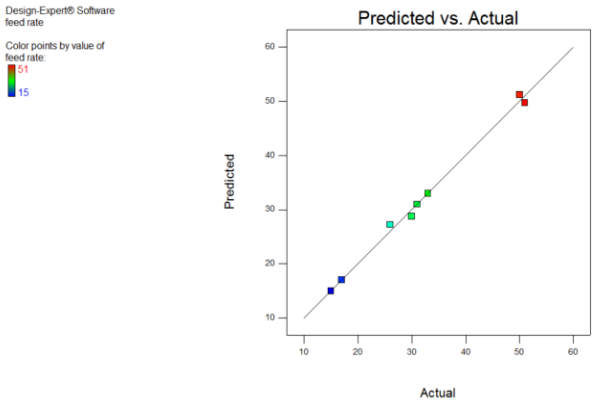

Fig. 11. Predicted vs Actual value Plot

The "Predicted R-Squared" of 0.9193 is in reasonable agreement with the "Adj R-Squared" of 0.9824. "Adeq Precision" measures the signal to noise ratio. A ratio greater than 4 is desirable. Hence a ratio of 23.678 indicates an adequate signal. This model can be used to navigate the design space. The Diagnostics Case Statistics compares the actual and predicted values and obtains the residual as shown in figure 11 and 12.

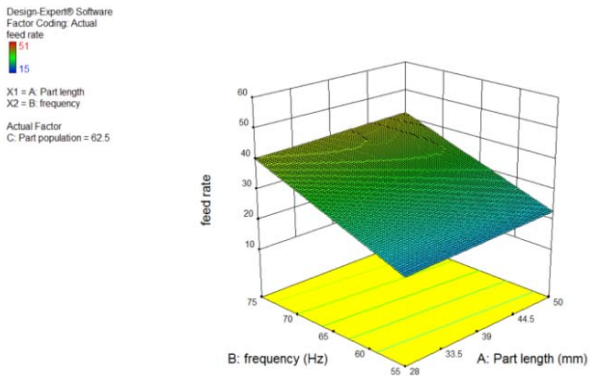

Fig. 12. Surface Plot

5. OPTIMIZATION OF FEED RATE

Beginning of the optimization procedure starts from picking several starting points from which the optimal factor is searched. There are two types of solutions for the search:

Local solution: There is a local solution for each starting point. These solutions are the combination of parameters beginning from a particular starting point.

Global solution: The global solution is the best of all the local solutions. The global solution is obtained by combining the parameters in such a way, that

desired response is obtained. For each of the local solution, predicted value of the response is calculated.

Desirability is rated on a scale of 0 to 1 and 1 being the most desirable solution.

Solutions found for the constraints in Table 5 are shown in Table 6.

A total of 79 solutions were obtained, out of which 10 most desirable solutions are tabulated below.

Name	Goal	Lower Limit	Upper Limit	Lower Weight	Upper Weight	Importance
A: Part Length	Is in range	28	50	1	1	3
B: Frequency	Is in range	55	75	1	1	3
C: Part Population	Is in range	25	100	1	1	3

Table 5. Constraints

Number	Part Length	Frequency	Part Population	Feed Rate	Desirability	
1	49.996	74.953	99.745	51.134	1	Selected
2	47.661	74.991	99.988	51.078	1	
3	48.131	74.971	99.831	51.048	1	
4	49.946	74.95	99.333	51.028	1	
5	47.535	74.964	99.981	51.037	1	
6	48.497	74.997	99.477	51.017	1	
7	47.056	74.984	99.893	51.005	1	
8	48.945	74.999	99.783	51.124	1	
9	49.101	74.992	99.564	51.074	1	
10	49.441	74.917	99.536	51.005	1	

Table 6. Solutions

Factor	Coefficient Estimate	DF	Standard Error	95% CI Low	95% CI High	VIF
Intercept	-29.88	1	9.08	-68.93	9.17	
A-Part Length	0.098	1	0.11	-0.38	0.57	3.78
B-Frequency	0.69	1	0.12	0.17	1.21	3.78
C-Part Population	-0.067	1	0.12	-0.60	0.47	55.8
AC	-3.03E-04	1	1.52E-03	6.82E-03	6.22E-03	16.4
BC	4.33E-03	1	1.67E-03	2.84E-03	0.012	46

Table 7. Formulation of Mathematical Relation

6. CONCLUSION

Optimization of feed rate of the Vibratory Bowl Feeder has been done using an authentic statistical model based on full factorial experiment design. This model can be used to explain 91% of variability in new data. Frequency and part population are found to be the most significant parameters followed by the interaction of these two parameters taken together and part length was found to be least significant.

7. REFERENCES

[1] Groover M.P., *Automation, Production Systems, and Computer-Integrated Manufacturing*, Second Edition, Prentice Hall of India Pvt. Ltd., New Del

[2] Hesse S., "*Rationalisation of small workpiece feeding*", Festo AG & Co., 2000

[3] Ujjwal Jindal, Shrey Jain, Piyush, Pradeep Khanna, *Graphical Analysis of a Vibratory Bowl Feeder for Clip shaped Components*, IJISET - International Journal of Innovative Science, Engineering & Technology, Vol. 4 Issue 2, February 2017

[4] Astha Kukreja, Pankaj Chopra, Akshay Aggarwal, Pradeep Khanna, "*Statistical Modeling Approach for Optimization of a Stationary Hook Hopper*", 2nd International Conference on Mechanical, Industrial, and Manufacturing Technologies (MIMT 2011), pp.V1-594-598

[5] Tanushi Pandey, Vishesh Garg, Sheetal Bhagat, Pradeep Khanna, *Mathematical Analysis of Vibratary Bowl Feeder*, International Journal of Latest Trends in Engineering and Technology (IJLTET)

Authors: **Ujjwal Jindal**, **U.G. Student**, **Shrey Jain**, **U.G. Student**, **Piyush**, **U.G. Student**, **Pradeep Khanna**, **Associate Professor**, Department of Manufacturing Processes and Automation Engineering, Netaji Subhas Institute of Technology, Delhi, India.
E-mail: shreyjain1@gmail.com

http://doi.org/10.24867/JPE-2017-01-127

Journal of Production Engineering

Vol.20 No.1

JPE (2017) Vol.20 (1) Preliminary Note

Agboola, O. O., Ikubanni, P. P.

APPLICATION OF STATISTICAL QUALITY CONTROL (SQC) IN THE CALIBRATION OF OIL STORAGE TANKS

Received: 22 April 2017 / Accepted: 05 May 2017

Abstract: *Calibration of storage tanks is an exact means of determining the accurate capacity of storage tanks at a given incremental level. When calibrating a certain number of oil storage tanks having the same dimensions, it is assumed that if the specified tank dimensions are within the statistical control limits, a calibration chart generated for one tank can be used for the other tanks. This study used X-bar and R-control chart to investigate the stability of the tank calibration process for some fabricated oil storage tanks. The method of control chart was used to check if the process is under control or not. The variables of the calibration process are Circumference of each course shell, Height of each course shell and Elevations for the bottom profile. Results revealed that the calibration process was statistically stable and under control with no special or assignable cause of variation. Process capability conducted also showed that the calibrated tanks met the pre-set limits.*

Key words: *Calibration, Process capability, Quality Control, Storage tanks, X-bar & R-Chart*

Primena statističke kontrole kvaliteta (SQC) u kalibraciji uljnih rezervoara. *Kalibracija rezervoara je egzaktna metoda utvrđivanja tačnog kapacitet rezervoara pri datom inkrementalnom nivou. Kada se kalibriše određeni broj rezervoara nafte koji imaju iste dimenzije, pretpostavlja se da ako su dimenzije navedenog rezervoara u granicama statističkih odstupanja, grafikon kalibracija generisana za jedan rezervoar može se koristiti i za druge rezervoare. Ova studija koristi X-bar i R-kontrolne karte za ispitivanje stabilnosti procesa kalibracije rezervoara za neke gotove rezervoare za skladištenje nafte. Metod kontrolne karte je korišćen da se proveri da li je proces pod kontrolom ili ne. Promenljive procesa kalibracije su obim svakog predmeta ljuske, visina svakog kursa ljuske i profil uzvišenja danca. Rezultati ukazuju da je proces kalibracije bio statistički stabiln i pod kontrolom bez posebnih uzroka varijacija. Sprovedeni proces je takođe pokazao da su kalibrisani rezervoari bili u unapred utvrđeneim granicama.*

Ključne reči: *kalibracija, proces sposobnosti, kontrole kvaliteta, rezervoari, X-bar & R- karte*

1. INTRODUCTION

Calibration of storage tanks is an exact means of determining the accurate capacity of storage tanks at a given incremental level [1]. It is essential to accurately determine the quantity of product going in and coming out of the storage tanks for proper inventory control. Crude oil and its refined products are precious fluids owing to their market value and therefore cannot be sold above the expected measured quantity to the customers and also cannot be bought below the expected quantity from the suppliers. Various geometrical methods of tank calibration such as Manual Strapping Method (MSM), Optical Reference Line Method (ORLM), Optical Triangulation Method (OTM), and Electro-Optical Distance Ranging Method (EODRM) had been identified and discussed by [2] and [3].

In Nigeria, the most applicable geometrical method that is prevalently used for storage tank calibration is Manual Strapping Method [3]. The required field data that must be accurately determined while using MSM are Circumference of each Course Shell, Height of Each Course, and Elevations for the Bottom geometry/profile [4] [5]. Experimental research is considered necessary for a group of storage tanks (uniform dimensions) fabricated by the same company but for different clients. This is to see if the aforementioned required field data (Circumference, Height, Elevations of bottom) are within the statistical control limit in order to check whether the calibration chart generated for one of the tanks in the group can be used for the others. Though X-bar and R-chart and X-bar and S-chart are variable charts for sub-group; however, X-bar and R-chart was chosen as the most preferred Statistical Quality Control Chart (SQCC) for this study because data sub-group was less than eight (8) and also because only few works had been done using it. Tank calibration process involves adequate planning and scheduling as proper scheduling saves time and minimizes cost [6]. Hence, each of the above identified variable data are properly scheduled to obtain optimal output. The quality control analysis of any product is determined by its conformity with the standard set dimensions [7]. Statistical quality control uses different dimensions to evaluate the quality of products. The said dimensions could be conformance to the set limits, maintainability, serveability, availability and durability [8]. [9] improved on the works of [10] and [11] by going beyond the design and application of Cumulative Sum (Cum-Sum) control chart but stated when to use it with much emphasis on practical problems as regards to monitoring changes in the parameters. [12] applied X-bar and S charts to investigate process stability in Electric Wire Industry and was able to show that that the production process was in statistical process control with respect to the diameter and electrical resistance of the without any

assignable cause of variation.

[13] used statistical calculations to eliminate quality problems such as undesirable tolerance limits and out of circularity of spheroidal cast iron parts during machining. X-bar and R control charts was constructed based on the data obtained from this manufacturing to detect and eliminate assignable causes, so that the machine capability (Cp) and the process capability (Cpk) can be ascertained. In order to compare design tolerance on working drawings and attained tolerances on work pieces after machining five mass production lines were set up in a medium sized company. The results obtained from five X–R control charts and the data gathered from all production lines were processed and evaluated. At this stage of the study, it was observed that some parts were oval and out of tolerance limits, machines and processes were insufficient and production was unstable. Through follow up studies on machine data, some assignable causes for faulty work pieces were discovered, and ovalness and out of tolerance limits errors were corrected. Their findings showed that in small or medium sized companies, statistical quality control can be useful component of production provided that sufficient finance and qualified personal are used.

Pattern recognition techniques have been widely applied to identify unnatural patterns in control charts [14]. [14] presented a control chart pattern recognition system using a statistical correlation coefficient method. Most of them are capable of recognizing a single unnatural pattern for different abnormal types. However, before an unnatural pattern occurs, a change point from normal to abnormal may appear at any point in control charts for most practical cases. Moreover, concurrent patterns where two unnatural patterns simultaneously exist may also occur in a control chart pattern recognition system. They concluded by confirming that statistical correlation coefficient approach is a simple mechanism for recognizing these unnatural control chart patterns with good performance. Cumulative Sum (CUSUM) chart, one of the Statistical Process Control (SPC) techniques, is a powerful tool in monitoring emissions data so that abnormal changes can be detected in a timely manner, using process capability indices to evaluate environmental performance in terms of the risk of non-compliance situations arising [15]. It explores how process capability indices have the potential to be useful as a risk management tool for practitioners and to help regulators execute and prioritize their enforcement efforts. [16] used X-bar and R Control chart in manufacturing industry to enhance productivity while minimizing defective products, thereby solving rejection problem. They used Apurvi Industries in India as a case study, out of control process was detected by X-bar and R chart and the root cause analysis was performed on the defective KSB Pumps.

One of the Calibration Companies in Nigeria, Concise Engineering & Technical Services Limited who has calibrated more than 90% of the tank fabricated by DeltaWeld Engineering Limited was consulted to get some of the field data. In 2015, DeltaWeld was awarded a contract of fabricating 15Nos Oil storage tanks by Alluvial Oil in its new depot. Calibration of the said tanks was subsequently given to Concise Engineering. The method of calibration employed by Concise Engineering was MSM which involves accurate measurement of circumference by winding a strapping tape round each course shell. Pocket tape was used to determine the height of each course while the Leveling instrument was used to obtain the Elevations for the bottom profile. The measured field data for each fabricated tank was collected and checked if they are within the statistical control limit using X-bar and R control chart. Available data revealed that each tank has five (5) course shells with an average capacity of 1,500,000 litres. Hence, the work aimed at using the X-bar and R-chart in determining the stability and capability of calibration process for same set of oil tanks.

2. MATERIAL AND METHOD

Related data needed for the calibration were obtained directly from the field engineer. The data include: 1.) Circumference of each course, 2.) Height of Course Shells, and 3.) Elevations of the Bottom profile. Plate thicknesses for each course shell were not considered because they were all new tanks. Each of the above-mentioned data was analyzed using Minitab 17. X-bar charts were first drawn followed by R-charts but the analysis for the stability of tank calibration process started from R-chart using “Run rules”. If the R-charts indicate that the calibration process is stable, we then proceed to X-bar charts to further confirm the process stability. If both conditions for stability were met, then the next step was to check if the calibrated tanks were within the predefined specifications/limits. The predefined limits for the Circumference, Height of Course Shell and Elevations of the Bottom profile are ±30mm, ±20mm and ±10mm respectively. It is not only enough to confirm the stability of the calibration process but there is also need to find out if the products (fabricated tanks) were within the specified limit. Process Capability was employed to check if the products are within the preset limits.

Strapping tape (Figure 1) was used for measuring the circumference of each course shell by winding it firmly round the tank shell. Pocket tape (Figure 2) and leveling instrument (Figure 3) were used to measure the Course shell height and elevation for bottom profile respectively.

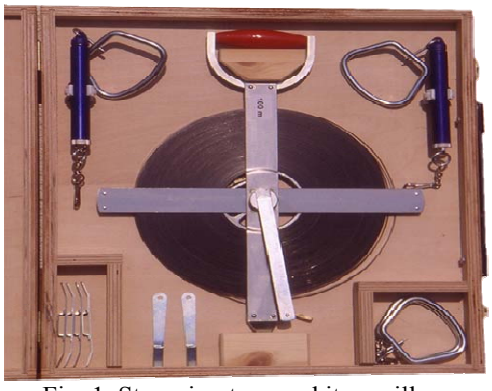

Fig. 1. Strapping tape and its ancillary

Fig. 2. Pocket tape

Fig. 3. Leveling instrument

2.1 X-bar and R-Control Charts

X-bar and R-Control Charts is one of the Statistical Process Control (SPC) methods used for monitoring and improving a company's quality and productivity. X-bar chart is used to monitor the average value of a process over time. For each subgroup, the x-bar value is plotted. The upper and lower control limits define the range of inherent variation in the subgroup means when the process is in control.

R-Chart on the other hand is a control chart that is used to monitor process variation when the variable of interest is a quantitative measure. These charts give deviations from desired limits within the quality process and, in effect, allow the company to make necessary adjustments to improve quality.

The following are the steps for constructing X-bar and R-charts.

i. Collection and entering of the data into sub-group

ii. Determination of the Average $\overline{X}$ of each sub-group;

$$\overline{X} = \frac{X_1 + X_2 + X_3 \ldots\ldots X_n}{n} \quad (1)$$

iii. Calculate the grand mean $\overline{\overline{X}}$ of the sub-group's average. The grand mean of the subgroup's average becomes the centerline for the upper plot.

$$\overline{\overline{X}} = \frac{\overline{X}_1 + \overline{X}_2 + \overline{X}_3 \ldots\ldots \overline{X}_n}{n} \quad (2)$$

iv. Determine the Range R of each sub-group by subtracting lowest value from the highest value in the sub-group. Range = Highest-Lowest (3)

v. Calculate average of subgroup Ranges

$$\overline{R} = \frac{R_1 + R_2 + R_3 \ldots\ldots R_n}{k} \quad (4)$$

vi. Determine the Upper Control Limit UCL and Lower Control Limit LCL for sub-group averages.

For X-bar chart:

$$UCL_{\overline{X}} = \overline{\overline{X}} + A_2\overline{R} \quad (5)$$

$$LCL_{\overline{X}} = \overline{\overline{X}} - A_2\overline{R} \quad (6)$$

For R-chart:

$$UCL_{\overline{R}} = D_4\overline{R} \quad (7)$$

$$LCL_{\overline{R}} = D_3\overline{R} \quad (8)$$

3. RESULTS AND DISCUSSION

3.1 Results

The measured field data as entered into sub-group, the mean as well as the range for the Circumference of Course shells, Height of Course shells and Elevations for Bottom Profile were presented in Table 1, Table 2 and Table 3 respectively.

Tank	C_1	C_2	C_3	C_4	C_5	Average	Range
1	56050	56046	56061	56063	56055	56055	17
2	56055	56062	56071	56063	56064	56063	16
3	56061	56058	56056	56056	56051	56056.4	10
4	56065	56063	56064	56066	56058	56063.2	8
5	56058	56062	56062	56065	56050	56059.4	15
6	56063	56064	56064	56061	56053	56061	11
7	56061	56058	56056	56050	56046	56054.2	15
8	56065	56063	56064	56070	56058	56064	12
9	56061	56063	56055	56072	56063	56062.8	17
10	56069	56063	56064	56056	56056	56061.6	13
11	56064	56072	56063	56062	56062	56064.6	10
12	56061	56071	56056	56066	56065	56063.8	15
13	56063	56058	56063	56064	56050	56059.6	14
14	56060	56061	56061	56053	56050	56057	11
15	56053	56050	56058	56062	56062	56057	12

Table 1. Samples Circumference of Course Shells

Using equation 3 through equation 8, the following information were obtained from Table 1 which were used to construct X-bar and R-chart in Figure 4.

Grand mean $\overline{\overline{X}}$ = 56060.17, Average Range $\overline{R}$ =13.07, $UCL_{\overline{X}}$ = 56067.71, $LCL_{\overline{X}}$ = 56052.64, $UCL_{\overline{R}}$ =27.63, $LCL_{\overline{R}}$ = 0

Tank	H_1	H_2	H_3	H_4	H_5	Average	Range
1	1200	1211	1209	1207	1207	1206.8	11
2	1202	1200	1208	1215	1212	1207.4	15
3	1195	1199	1203	1205	1204	1201.2	10
4	1207	1201	1198	1199	1201	1201.2	9
5	1210	1205	1206	1208	1202	1206.2	8
6	1206	1200	1201	1198	1195	1200	11
7	1205	1200	1195	1192	1207	1199.8	15
8	1204	1201	1193	1198	1205	1200.2	12
9	1205	1200	1203	1199	1196	1200.6	9
10	1197	1201	1206	1210	1209	1204.6	13
11	1198	1199	1208	1200	1201	1201.2	10
12	1203	1201	1193	1205	1204	1201.2	12
13	1205	1206	1208	1205	1200	1204.8	8
14	1207	1207	1193	1199	1203	1201.8	14
15	1209	1207	1193	1198	1205	1202.4	16

Table 2. Samples Height of Course Shells

Using equation 3 through equation 8, the following information were obtained from Table 2 which were used to construct X-bar and R-chart in Figure 5.

Grand mean $\overline{\overline{X}}$ = 1202.63, Average Range $\overline{R}$ =11.53, $UCL_{\overline{X}}$ = 1209.28, $LCL_{\overline{X}}$ = 1195.97, $UCL_{\overline{R}}$ =24.39, $LCL_{\overline{R}}$ = 0

Using equation 3 through equation 8, the following information were obtained from Table 3 which were used to construct X-bar and R-chart in Figure 6.

Grand mean $\overline{\overline{X}}$ = 117.2, Average Range $\overline{R}$ =4.067, $UCL_{\overline{X}}$ = 119.546, $LCL_{\overline{X}}$ = 114.854, $UCL_{\overline{R}}$ =8.54, $LCL_{\overline{R}}$ = 0

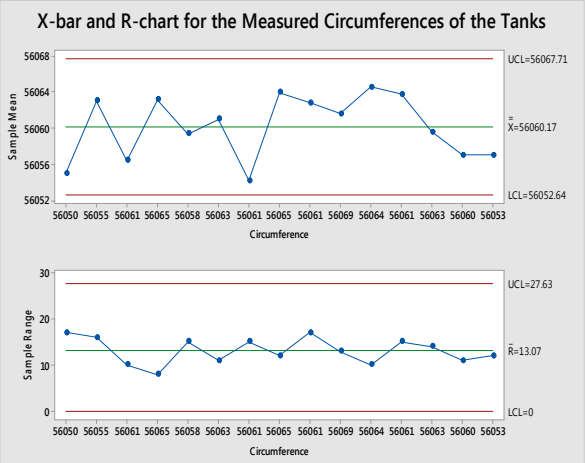

Fig. 4. X-bar and R-chart for the Samples Circumference

Tank	E_1	E_2	E_3	E_4	E_5	Average	Range
1	119	118	116	117	115	117	4
2	120	119	115	116	117	117.4	5
3	116	118	119	116	115	116.8	4
4	120	119	118	116	117	118	4
5	116	116	115	117	116	116	2
6	118	118	117	115	116	116.8	3
7	118	117	119	117	116	117.4	3
8	115	117	118	119	120	117.8	5
9	119	117	118	116	115	117	4
10	118	116	120	119	115	117.6	5
11	114	117	116	118	115	116	4
12	117	119	120	118	116	118	4
13	115	117	119	120	118	117.8	5
14	115	117	116	119	117	116.8	4
15	115	120	118	116	119	117.6	5

Table 3. Samples Elevation for the Bottom Profile

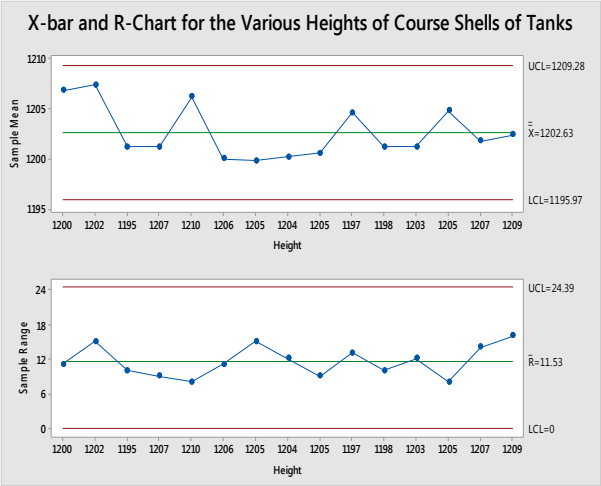

Fig. 5. X-bar and R-chart for the Various Height of the Course Shells

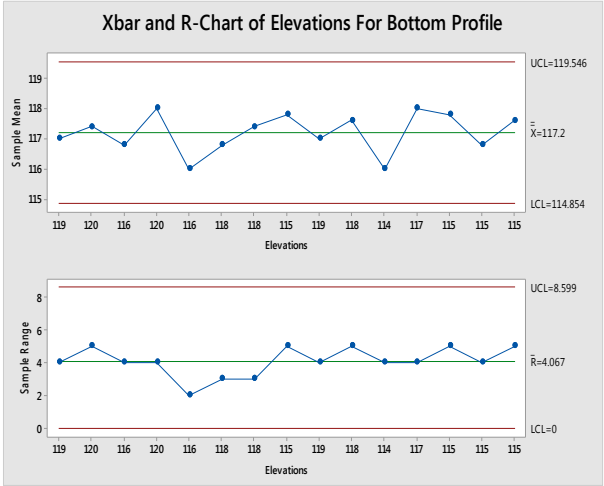

Fig. 6. X-bar and R-chart of Elevations for Bottom Profile

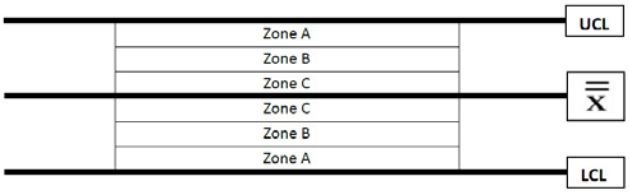

Fig. 7. Analysis of X-bar and R-control chart

3.2 Discussion

To check if the calibration process is in control or not, "Run rules" were applied, first to the R-chart and then to the X-Bar chart by dividing the distance between centerline CL ($\overline{\overline{X}}$ *or* $\overline{R}$) and Upper Control Limit UCL into three zones A(3σ), B(2σ) and C(σ). The same procedure was applied for the distance between the centerline CL and Lower Control Limit LCL as shown in Figure 7.

Analysis of control charts in Figure 4, 5 and 6 revealed the following: 1.) that there is no point outside the LCL and UCL, 2.) that there are no 2 out of 3 subsequent points in Zone A, 3.) that there are no 4 out of 5 subsequent points in Zone B or beyond, 4.) that there are no 8 or more points lying on one side of the center line, 5.) that there are no 6 or more subsequent points increasing or decreasing steadily. Control charts in Figure 4, 5 and 6 fulfilled all the conditions set out in Run rules and thereby confirmed that the process is stable (under control) with no assignable cause of variation.

Confirming that a process is stable is not enough; rather, it is expedient to check if calibration variables are within the pre-set limits/specifications. This was the reason for performing Process capability analysis on the obtained field data. The Process capability analysis for the measured Circumference, Height and Elevations were as shown in Figures 8, 9 and 10. Since all the Overall Capability indicators Pp, PPL, PPU, Ppk and Cpm as well as the Potential Capability (within) indicators C_P, C_{PL}, C_{PU} and C_{PK} were greater than one, and that implied that the process is capable of giving measurements (products) within the pre-set limits. Also, closer look at the process capability charts (Figures 8 – 10) revealed that the Normal distribution curves fell between Lower Specified Limit (LSL) and Upper Specified Limit (USL) which further confirmed the capability of the process.

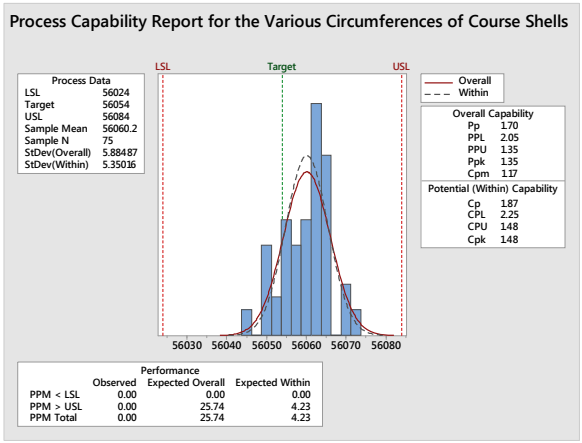

Fig. 8. Process capability analysis for the various Circumferences of Course Shells

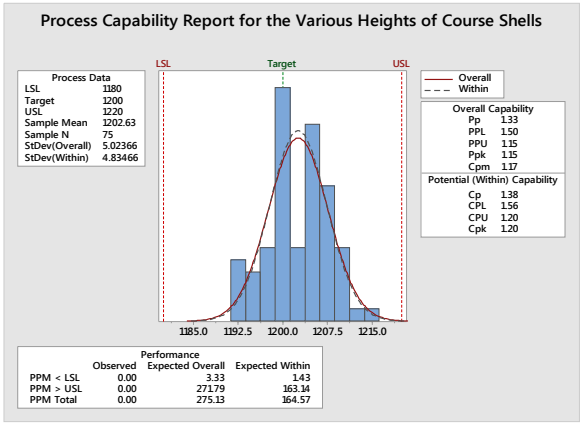

Fig. 9. Process capability analysis for the various Heights of the Course Shells

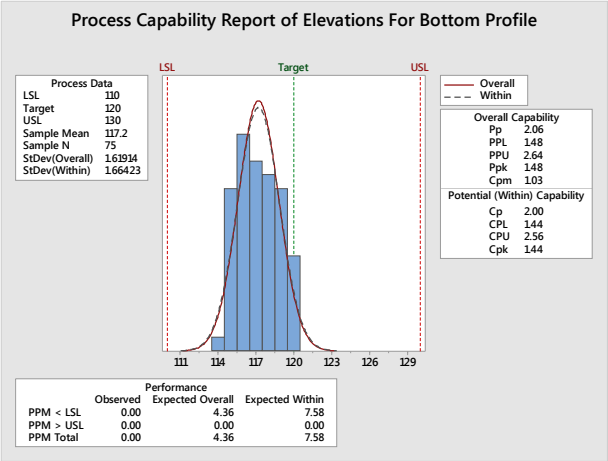

Fig. 10. Process capability analysis for the Elevations for the Bottom Profile

4. CONCLUSION

Having successfully applied X-bar and R-control chart to the calibration of storage tanks manufactured by Deltaweld Engineering Limited in Nigeria, it has been observed that there is no assignable (special) cause of variation in the measured field data which could have resulted in sudden sharp change in the calibration chart. Since the calibration process for this group of tanks had been confirmed to be stable with high process capability index. It can be concluded that a calibration chart generated for one tank can be used for other tanks. Using one chart generated for one tank for the other ones will not only save cost but also reduce the time of generating tank calibration chart.

5. REFERENCES

[1] ISO 7507: *Petroleum and Liquid Petroleum Products–Calibration of Vertical Cylindrical Tanks*, ISO copyright office, Geneva, 2002.

[2] Savaraman, S.: *Vertical cylindrical storage tank calibration technologies and application*, In-Proceedings of API Conference & Expo, Singapore, March 2012.

[3] Agboola, O.O., Ikubanni, P. P., Ibikunle, R. A., Adediran, A.A., Ogunsemi B. T.: *Generation of Calibration Charts for Horizontal Petroleum Storage Tanks Using Microsoft Excel*, MAPAN-Journal of Metrology Society of India, In press.

[4] Nosach, V., Belyave, B.: *The calibration of large vertical cylindrical tank by a geometrical method*, Journal of Measurement Techniques, Volume 45, pp 11, 2002.

[5] Makushkin, S. G., Kuzmin, S. A., Kalashnik, G.G.: *Tank Deformation and Accuracy in Measuring Oil Product Mass*, Chemical and Petroleum Engineering, Volume 37, pp. 278, 2001.

[6] Agboola, O. O., Kareem, B., Akinnuli, B. O.: *Development of a diagnostic schedule for a defective LC-195V5 CNC milling machine using PERT*, Leonardo Electronic Journal of Practices and Technologies, Volume 28, pp. 107-118, 2016.

[7] Montgomery, D.C.: *Introduction to Statistical Quality Control,* John Wiley and Sons, Inc., 6th Edition, USA, 2009.

[8] Steiner, S.H.: *Grouped Data Exponentially weighted Moving Average Control Chart*, Journal of the Royal Statistical Society, Series C, Volume 47, No. 2, pp. 203-261, 1998.

[9] Ott, E.R., Schilling, E.G., Neubauer, D.V.: *Process Quality Control Troubleshooting and Interpretation of Data*, ASQ Quality Press, USA, 2005.

[10] Page, E.S.: *Cumulative Sum Chart*, Technometrics, Volume 3, No. 1, pp. 1-9, 1961.

[11] Woodall, W., Adam, B.: *Quality Engineering*, Volume 5, No. 4, pp. 559-570, 1993.

[12] Ogedengbe, T. I., Apalowo R. K., Akinde A. B.: *Application of Statistical Quality Control for Investigating Process Stability and Control in an Electric Wire Industry*, International Journal of Science and Technology, Volume 5, Number 3, pp. 81-87, 2016.

[13] Ali, R. M., Abdulkadir, G.: *Statistical process control in machining: A case study for machine tool capability and process capability*, Materials and Design, Volume 27, pp. 364–372, 2006.

[14] Jenn-Hwai, Y., Miin-Shen Y.: *A control chart pattern recognition system using statistical correlation coefficient method*, Computers & Industrial Engineering, Volume 48, pp. 205–221, 2005.

[15] Charles, J. C., Jeh-Nan, P.: *Evaluating environmental performance using process control techniques*, European Journal of Operational Research, Volume 139, pp. 68–83, 2002.

[16] Kapil, B., Amit P., Diptesh P.: *Implementation of Statistical Quality Control (S.Q.C.) in Welded Stainless Steel Pipe Manufacturing Industry*, International Journal of Research in Engineering and Technology, Volume 03, Issue 09, pp. 270-273, 2014.

Authors: **Engr. Agboola Oluwole Olayinka[1], Engr. Ikubanni Pelumi Peter[1]**

[1]Landmark University Omu Aran, PMB 1001, Omu Aran, Kwara State, Nigeria.

+2348035411976, +2347065993936

E-mail: agboola.olayinka@lmu.edu.ng

ikubanni.peter@lmu.edu.ng

http://doi.org/10.24867/JPE-2017-01-133

Journal of Production Engineering

Vol.20 No.1

JPE (2017) Vol.20 (1) Preliminary Note

Stanojković, J., Radovanović, M.

SELECTION OF SOLID CARBIDE END MILL FOR MACHINING ALUMINUM 6082-T6 USING CRITIC AND TOPSIS METHODS

Received: 30 March 2017 / Accepted: 20 April 2017

Abstract: *The selection of the best end mill is a complex task because there are many alternatives and criteria to be taken into consideration when making decisions. In this paper, the selection of solid carbide end mill for machining Al 6082-T6 is presented using TOPSIS multi-criteria decision making method, where the objective weights are determined by CRITIC method. Based on the four criteria (number of end mill teeth, cutting speed, feed per tooth and the price) a selection of the most appropriate alternative of the six, i.e. from different manufacturers of cutting tools (Seco, YCT and Iscar).*

Key words: *multi-criteria decision, TOPSIS, CRITIC.*

Izbor glodala od tvrdog metala za obradu aluminijuma 6082-T6 primenom CRITIC i TOPSIS metode. *Izbor optimalnog reznog alata predstavlja problem usled postojanja velikog broja alternativa i kriterijuma koje treba uzeti u obzir prilikom donošenja odluke. U radu je predstavljen izbor vretenastog glodala za obradu legure aluminijuma 6082-T6 primenom TOPSIS metode višekriterijumskog odlučivanja, pri čemu je za izbor težinskih koeficijenata primenjena CRITIC metoda. Na osnovu četiri kriterijuma (broj zuba glodala, brzina rezanja, korak i cena) izvršen je izbor najboje altenative od šest, tj. od šest vretenastih glodala različitih proizvođača reznih alata (Seco, Young cutting tools i Iscar).*

Ključne reči: *višekriterijumsko odlučivanje, TOPSIS, CRITIC.*

1. INTRODUCTION

Multiple-criteria decision making is one of the most used methods of decision making theory. Multi-criteria decision making method is a set of mathematical methods and tools for solving real problems in different areas where there are many alternatives and criteria, i.e. objectives.

The procedure of decision making consists of the following steps: identifying the problem, gathering relevant information, identifying the alternatives and criteria, selecting among the alternatives. The process is very simple when it comes to making a decision, taking into account one criterion. In this case, the selection of an alternative is made based on the evaluation of alternative priorities. In the case where there are more criteria, it is necessary to define the objective weights for each criterion, and the importance of each criterion relative to other criteria. Objective weights are usually numbers that are subjectively selected, then for each criterion, it is determined whether it is necessary to choose an alternative so that the criterion is the maximum or minimum [1].

Today there are many numbers of multi-criteria decision making methods. In this paper, to solve the problem of selecting a solid carbide end mill for machining Al 6082-T6 the CRITIC method is used for determining the objective weights and the TOPSIS method for determining the best alternative based on defined criteria and methods.

2. CRITIC METHOD

The conflict between the various criteria is one of the main problems in multi-criteria decision making. Problem solving requires the use of complex procedures for the selection of a preferred variant or determining the order of the variables.

CRITIC (Criteria Importance Through Intercriteria Correlation) is a method for determining the value of objective weights. This method belongs to the class of correlation methods and is based on the analytical examination of the decision making matrix. This method involves determining the intensity of contrast and conflict [2].

Before using the CRITIC method for determining the objective weights it is necessary to define alternatives and the criteria based on which the selection of solid carbide end mill for machining alloy 6082-T6 will be made.

Alternatives		Criteria			
Solid carbide end mills		C1	C2	C3	C4
		z_n	V_c m/min	f_z mm/tooth	price euro
		max	max	max	min
A_1	JS412 (SECO)	2	285	0.15	95
A_2	E5E49 (YCT)	3	210	0.096	100
A_3	JS413 (SECO)	3	275	0.15	105
A_4	ECA-B-3 (ISCAR)	3	234	0.05	138
A_5	EC-E-4L (ISCAR)	4	320	0.13	158
A_6	JS554 (SECO)	4	300	0.09	128

Table 1. Criteria and alternatives

Six alternatives are presented in Table 1 (end mills of different manufacturers), while the criteria are: the number of end mill teeth, cutting speed, feed per tooth and price. The goal is to select an end mill with the maximum number of teeth, cutting speed and feed per tooth and the minimum price.

Determining the objective weights using the CRITIC method is performed by applying the six steps [2, 3].

Step 1: Determining the elements of normalized decision matrix using the equation (1).

$$r_{ij} = \frac{x_{ij} - x_j}{x_j^{\max} - x_j^{\min}} \qquad (1)$$

Where: $x_j^{\max} = \max(x_{ij}, i = 1,...,m)$ and $x_j^{\min} = \min(x_{ij}, i = 1,...,m)$.

Based on the equation (1) normalized decision making matrix is presented in Table 2. Value r_{ij} shows how an alternative is close to the ideal value $x_j^{\max}$ and how far it is from the anti-ideal values. The normalized matrix does not take into account the type of criteria (maximum or minimum).

Step 2: Based on the value r_{ij} it is possible to form a vector of criteria, each vector has a standard deviation σ_j, using the equation (2), that represents the degree of deviation of alternatives for the given criterion, Table 2.

$$\sigma_j = \sqrt{\frac{1}{n}\left(\sum_{i=1}^{m} r_{ij} - \bar{r}\right)^2} \qquad (2)$$

Where: n is a number of elements and $\bar{r}$ is an arithmetic mean.

	C_1	C_2	C_3	C_4
A_1	0	0.682	1	0
A_2	0.5	0	0.46	0.079
A_3	0.5	0.591	1	0.159
A_4	0.5	0.218	0	0.683
A_5	1	1	0.8	1
A_6	1	0.818	0.4	0.524
σ_j	0.37638	0.37580	0.39471	0.39401

Table 2. Normalized decision making matrix

Step 3: Determining a matrix $n \times n$ with elements R_{ij}, which represent linear correlation coefficients r_j, r_k, and n represents a number of alternatives, using the equation (3). In the case of a large discrepancy between the values of attributes for criteria j i k, it is the lower value of the coefficient R_{ij}, Table 3 [3, 4].

$$R_{ij} = \frac{n\sum r_j r_k - \sum r_j \sum r_k}{\sqrt{n\sum r_j^2 - \left(\sum r_j\right)^2} \cdot \sqrt{n\sum r_k^2 - \left(\sum r_k\right)^2}} \qquad (3)$$

	C_1	C_2	C_3	C_4
C_1	1	0.413229	-0.27597	0.752851
C_2	0.413229	1	0.514659	0.436627
C_3	-0.27597	0.811717	1	-0.36844
C_4	0.752851	0.436376	-0.36844	1

Table 3. The coefficients of linear correlation

Step 4: Determining the rates of the conflict criteria using the equation (4), Table 4 [5].

Criteria	C_1	C_2	C_3	C_4
C_1	0	0.586771	1.275973	0.247149
C_2	0.586771	0	0.485341	0.563373
C_3	1.275973	0.188283	0	1.368443
C_4	0.247149	0.563624	1.368443	0

Table 4. The rates of conflict criteria

Step 5: Determining the quantity of the information in relation to each criterion using the equation (5), Table 5.

$$C_j = \sigma_j \sum_{k=1}^{n} \left(1 - R_{jk}\right) \qquad (5)$$

Criteria	C_1	C_2	C_3	C_4
C_1	0	0.586771	1.275973	0.247149
C_2	0.586771	0	0.485341	0.563373
C_3	1.275973	0.188283	0	1.368443
C_4	0.247149	0.563624	1.368443	0

Table 5. Thequantity of information in relation to each criterion

The quantity of information in relation to each criterion for the given example is: C_j=(0.794135, 0.503079, 1.235362, 0.85855).

Step 6: Determining the objective weight coefficients by normalizing the value C_j using the equation 6, Table 6 [2, 3].

$$w_j = \frac{C_j}{\sum_{j=1}^{n} C_j} \qquad (6)$$

C_j	0.794135	0.503079	1.235362	0.85855
w_j	0.23418	0.148352	0.364293	0.253176

Table 6. Objective weight coefficients

The objective weights of the criteria for selection of solid carbide end mills are: w_j=(0.23418, 0.148352, 0.364293, 0.253176).

3. TOPSIS METHOD

TOPSIS (Technique for Order Preference by Similarity to Ideal Solution) is a method based on the concepts that the chosen alternative should have the shortest distance from the ideal (positive) solution and the farthest distance from the anti-ideal (negative) solution [6].TOPSIS approach was developed by Hwang (1981). TOPSIS method is shown in Fig. 1, which represents the spatial distribution of alternative defined for two maximum criteria (C_1, C_2). In the figure it can be observed that the alternative A1 although closer to the ideal solution (A+) in comparison with alternative A_2, is at the same time closer to the anti-ideal solution (A-) in comparison with alternative A_2.

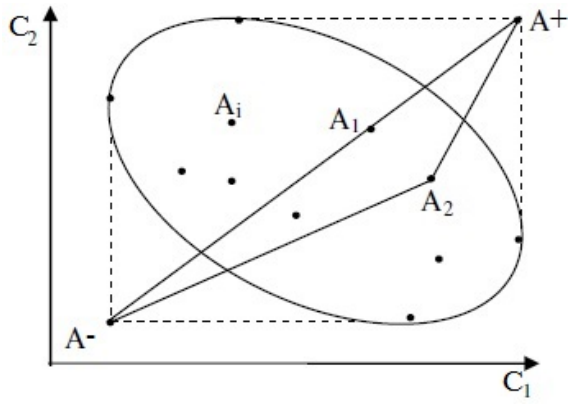

Fig. 1. TOPSIS method

TOPSIS method is performed by applying the nine steps [2, 3, 4]

Step 1: Determining the objective, alternatives and criteria.

The objective is to evaluate the six alternatives (solid carbide end mills from different manufacturers of cutting tools for machining aluminum alloy 6082-T4) based on the four criteria (number of teeth, cutting speed, feed per tooth and price) from which one criterion is minimized, in this case the price of the slolic carbide end mill.

Step 2: Based on the given values the decision matrix X (7) is defined [6]:

$$X = [x_{ij}] = \begin{vmatrix} x_{11} & x_{12} & \cdots & x_{1n} \\ x_{21} & x_{22} & \cdots & x_{2n} \\ \vdots & \vdots & \vdots & \vdots \\ x_{m1} & x_{m2} & \cdots & x_{mn} \end{vmatrix} \qquad (7)$$

Based on the values of the Table 1, decision matrix (8) for selection of solid carbide end mills is given:

$$X = [x_{ij}] = \begin{vmatrix} 2 & 285 & 0.15 & 95 \\ 3 & 210 & 0.096 & 100 \\ 3 & 275 & 0.15 & 105 \\ 3 & 234 & 0.05 & 138 \\ 4 & 320 & 0.13 & 158 \\ 4 & 300 & 0.09 & 128 \end{vmatrix} \qquad (8)$$

Step 3: Normalization of the decision matrix, Table 7, is calculated by equation (9) [7, 8]:

$$r_{ij} = \frac{x_{ij}}{\sqrt{\sum_{n=1}^{m} x_{ij}^2}} \qquad (9)$$

A_1	0.251976	0.42575	0.524732	0.315892
A_2	0.377964	0.31371	0.335829	0.332518
A_3	0.377964	0.410811	0.524732	0.349144
A_4	0.377964	0.349563	0.174911	0.458875
A_5	0.503953	0.478035	0.454768	0.525378
A_6	0.503953	0.448158	0.314839	0.425623

Table 7. Normalized the decision matrix

Step 4: Determining the values of the objective weight coefficients with the following equation (10) [2, 3]:

$$\sum_{j}^{n} w_j = 1 \qquad (10)$$

Critic method is used for determining the objective weight coefficients w_j=(0.23418, 0.148352, 0.364293, 0.253176).

Step 5: Determining the weighted decision making matrix represents the multiplication of elements of a column of the normalized matrix with appropriate objective weight coefficients by using the equation (11) [7]:

$$v_{ij} = r_{ij} \cdot w_j \qquad (11)$$

Weight normalized decision making matrix for the selection of solid carbide end mills is shown in Table 8:

A_1	0.059008	0.063161	0.191156	0.079976
A_2	0.088512	0.046539	0.12234	0.084185
A_3	0.088512	0.060945	0.191156	0.088395
A_4	0.088512	0.051858	0.063719	0.116176
A_5	0.118016	0.070917	0.165669	0.133013
A_6	0.118016	0.066485	0.114694	0.107757

Table 8. Weight normalized decision making matrix

Step *6*: Identifying the positive and negative ideal solution based on the equations (12) and (13) [8]:

$$V^+ = \{\max(v_{ij}), j \in J, \min(v_{ij}), j \in J', i = 1,...,m\} = \{V_1^+, V_2^+, ..., V_n^+\} \qquad (12)$$

$$V^- = \{\min(v_{ij}), j \in J, \max(v_{ij}), j \in J', i = 1,...,m\} = \{V_1^-, V_2^-, ..., V_n^-\} \qquad (13)$$

With the maximum criteria it has the highest value of the attribute, while with the minimum criteria it has the lowest value of the attribute. Positive and negative solution values of the attribute relative to each criterion are given in Table 9.

V_{C1}^+=0.118016	V_{C1}^-=0.059008
V_{C2}^+=0.070917	V_{C2}^-=0.046539
V_{C3}^+=0.191156	V_{C3}^-=0.063719
V_{C4}^+=0.079976	V_{C4}^-=0.133013

Table 9. Positive and negative solution

Step 7: Calculating the separation distance of each competitive alternative from the positive and negative solution based on the equations (14) and (15) [8, 9]:

$$S_i^+ = \sqrt{\sum_{j=1}^{n} \left(v_{ij} - V_j^+\right)^2} \qquad (14)$$

$$S_i^- = \sqrt{\sum_{j=1}^{n} \left(v_{ij} - V_j^-\right)^2} \qquad (15)$$

Separation distance of each competitive alternative from the positive and negative solution for selection of solid carbide end mills are given in Table 10.

S_{A1}^{+}=0.059515	S_{A1}-=0.13903
S_{A2}^{+}=0.078855	S_{A2}-=0.081799
S_{A3}^{+}=0.032262	S_{A3}-=0.138957
S_{A4}^{+}=0.137056	S_{A4}-=0.034384
S_{A5}^{+}=0.058843	S_{A5}-=0.120291
S_{A6}^{+}=0.081474	S_{A6}-=0.084357

Table 10. Distance of each competitive alternative from the positive and negative solution

Step 8: Measuring the relative closeness of each location of the ideal solution P_i, Table 11. For each competitive alternative the relative closeness of the potential location with respect to the ideal solution is calculated by equation (16) [8]:

$$P_i = \frac{S_i^-}{S_i^+ + S_i^-} \qquad (9)$$

Alternative	P_i
A_1	0.700243
A_2	0.509161
A_3	0.811577
A_4	0.20056
A_5	0.671514
A_6	0.508693

Table 11. Relative closeness of each location of the ideal solution

Step 9: According to the value of P_i the order of the alternatives is A3-A1-A5-A2-A6-A4, which means that in the first place it is an alternative A3, i.e. JS413 solid carbide end mill by Seco.

4. CONCLUSION

There is a large number of methods for implementing multi-criteria decision making analysis. For the selection of solid carbide end mills for machining aluminum alloy 6082-T6 TOPSIS method was used for ranking alternatives based on the criteria. To determine the objective weight coefficients CRITIC method was used. Based on the four criteria (number of teeth cutters, cutting speed, feed per tooth and price) the first choice is solid carbide end mill JS413 (Seco), thenJS412 (Seco), EC-E-4L (Iscar), E5E49 (Young Cutting Ttools), JS554 (Seco) and finally ECA-B-3 (Iscar).

5. REFERENCES

[1] Hwang, C. L. & Yoon, K..: *Multiple-criteria decision making: Methods and Applications*, A state of art survey. New York. Springer-Verlag, 1981.

[2] Madić, M., Nedić, B., Radovanović, M.: *Business and Engineering Decision Making by by using Multi-Criteria Decision Making Methods*, University of Kragujevac, 2015.

[3] Madić, M, Radovanović, M.: *Ranking of some most commonly used nontraditional machining process using ROV and CRITIC methods*, U.P.B. Sci. Bull., Series D, Vol. 77, No. 2, p.p. 193-204, 2015.

[4] Milić, M., Župac, G.: *An objective approach to determining the weight criteria*, Original Bulletin, Vol. 29, No. 2, p.p. 39-56. 2012.

[5] Diakoulaki, D., Mavrotas, G. Papayannakis, L.: *Determining objective weights in multiple criteria problems: The critic method* Computers and Operations Research, Vol. 22, No. 7, p.p. 763-770, 1995.

[6] Srikrishna, S., Sreenivasulu, A., Vani, S.: *A New Car Selection in the Market using TOPSIS Technique*, International Journal of Engineering Research and General Science, Vol. 2, No. 4, p.p. 177-181, 2014.

[7] Naga, A. Phaneendra, A, Diwakar Reddy, V., Srikrishn, S.: *TOPSIS Based Approach for Selection of Third Party Reverse Logistics Service Provider: A Case Study of Mobile Phone Industry*, Imperial Journal of Interdisciplinary Research (IJIR) , Vol. 2, No. 4, p.p. 177-181, 2016.

[8] Balli, S. Korukoglu, S.: *Operating System Selection Using Fuzzy AHP and TOPSIS Methods*, Mathematical and Computational Applications, Vol. 14, No. 2, p.p. 119-130, 2009.

[9] Malaki, A., Owens, G., Bruce, D.: *Combining AHP and TOPSIS Approaches to Support Site Selection for Lead Pollution Study*, 2nd International Conference on Environmental and Agriculture Engineering, Vol. 37, p. p. 1-7, 2012.

ACKNOWLEDGEMENT

The paper is a part of the research done within the project TR35034. The authors would like to thank to the Ministry of Education and Science, Republic of Serbia

Authors: **Jelena Stanojković, PhD student, Prof. Dr. Miroslav Radovanović**, University of Niš, Faculty of Mechanical Engineering in Niš, Aleksandra Medvedeva 14, 18 000 Niš, Serbia, Phone: +381 18 500-687, Fax: +381 18 588-244;
E-mail: jstanojkovic@masfak.ni.ac.rs
mirado@masfak.ni.ac.rs

http://doi.org/10.24867/JPE-2017-01-137

Journal of Production Engineering

Vol.20 No.1

JPE (2017) Vol.20 (1) Preliminary Note

Kovács, Gy.

GLOBAL PRODUCTION TENDENCIES – LEAN MANUFACTURING PHILOSOPHY

Received: 17 April 2017 / Accepted: 20 May 2017

Abstract: *The growing market globalization, global competition, and complex products results in application of new production processes and methods. Optimization of supply chains results new concepts of value chains. In a competitive market the manufacturing companies have to produce cost effective products which can be realized by minimized production cost and higher effectiveness. These goals can be achieved by the application of Lean manufacturing philosophy. There are lots of Lean methods and tools which can result the improvement of the production line performance. The paper shows global production tendencies, novel supply chain paradigms and summarizes the advantages of application of Lean philosophy.*

Key words: *Lean production, value adding activity, waste, efficiency improvement*

Globalna proizvodna tendencija - filozofija LEAN proizvodnje. *Sve veća globalizacija tržišta, globalna konkurencija, i kompleksni proizvodi rezultatiraju u primeni novih proizvodnih procesa i metoda. Optimizacija lanaca snabdevanja rezultat je novog koncepta lanaca vrijednosti. U konkurentnom tržištu proizvodne kompanije moraju da proizvode isplative proizvode koji se mogu realizovati uz minimalnei troškove proizvodnje i povećanje efektivnosti. Ovi ciljevi se mogu postići primenom Lean proizvodne filozofije. Postoji mnogo Lean metoda i alata koji mogu biti rezultat poboljšanje performansi proizvodne linije. Ovaj rad pokazuje globalne proizvodne tendencije, nove lance nabavke paradigme i rezimira prednosti primene Lean filozofije.*

Ključne reči: *Lean proizvodnja, aktivnost dodate vrednost, otpad, poboljšanje efikasnosti*

1. INTRODUCTION

Changing market environment, market globalization, increasing global competition and fluctuating customer demands require efficient operation of production and logistical processes where the enterprises have to focus on cost reduction and productivity. These global tendencies and novel supply chain conceptions (Lean-, Agile-, Leagile Supply Chains) are introduces in this study.

This research study is very important and actual, because the cost reduction and the improvement of productivity are very important goals of all of manufacturing companies.

Lean manufacturing is a performance-based process used in more and more manufacturing companies to increase competitive advantage in the global market. Nowadays this philosophy is applied in many sectors including automotive, electronics, etc. in order to optimize productivity and costs.

In the study the essence, properties and tools of the Lean philosophy is introduced. Lean manufacturing focuses on cost reduction by eliminating non-value added activities. Originating from the Toyota Production System, many of the tools and methods of Lean manufacturing have been widely used in manufacturing.

2. GLOBAL PRODUCTION AND LOGISTICAL TENDENCIES

Fast changing market environment and fluctuating customer demands require efficient operation of production and logistical processes.

The following short description of the global production and logistic tendencies focuses on the changes in the main processes and activities, and reasons behind them.

2.1 Changes in the customers' demands and product characteristics

Due to the more unique and rapidly changing customer demands nowadays many industrial sector has completely different strategies than few decades or even few years before. The traditional mass production is replaced by the production of unique products in case of several industries, the variation of finished products that can be chosen by the consumers is almost infinite, and the costumer can freely determine the properties and components of the ordered finished products. For instance in case of a vehicle the finished product variations can reach up to 1000 (a combination of colours, types of engines, other components etc.). At the same time the acceptable delivery time has decreased while the demand for quality has increased. Typically the production of products with shorter lifecycle but more complexity requires novel, more flexible production technologies and logistic processes, and their sales need new business approaches.

2.2 Changes in production philosophies and production processes

The traditional mass production is replaced by unique production (or smaller batches), or from the

philosophical point of view the "**Push**" approach (make to stock) is replaced by "**Pull**" approach (make to order) [1].

In case of Push production planning is based on forecasted data (not actual customer demand), so that the result is high amount of products, including unsalable stocks. On the contrary, the uniqueness of production with Pull philosophy lies in the fact, that production starts only when an actual customer demand appears (with detailed specification), which starts procurement and manufacturing processes.

Based on the fundamental differences between the two approaches it is clear the unlike push approach the pull approach results in the realization of the following logistical goals: 1.) shorter lead time; 2.) production is scheduled based on the customer's demands; 3.) only small amount of stock is realized before (raw materials), during (semi-finished products) and after (finished product stock) the production process; 4.) flexible reaction to the changing customer demands; 5.) dedication to continuous improvement; 6.) smaller place for production; 7.) higher utilization of human resources and equipment; 8.) higher productivity, etc.

The **Lean production philosophy utilizes the advantages of Pull philosophy**, and it is spreading throughout the many sectors, both at production and service companies in automotive industry, electronic industry, offices and health industry as well.

2.3 Trends in the formation of supply chains

The rapidly changing market environment and global competition resulted in more complex networks of supply chains. The value chains are globalized, the cooperation between members became more dynamic. The key of success for chains is to understand the customers' demands, and to fulfil it with the highest quality, and at the same time to adapt to the expected changes of market demands.

The competitiveness of each chain originates from the utilization of and synergy between the partners. Although on the global market the supply chains compete as well to fulfil the customer demands with high quality products. Customers choose also between the supply chains by buying a finished product.

Novel supply chain conceptions (Lean-, Agile- and Leagile supply chains) are introduced besides the traditional ones in order to retain the competitiveness of the company [2,3,4,5].

- **Lean Supply Chain**

The main goal of the application of „Lean Supply Chains" is to minimize losses in the whole supply chain, by eliminating non value-adding activities, and to improve the processes continuously. These goals are supported by several Lean strategies, such as shortening waiting times and set-up times etc. This results in the realization of production smaller in volume, but more economical and flexible.

This strategy can be applied mostly in case of products with relatively longer lifetime (more than 1-2 years), and the members of the chain work in traditional networked organizational form.

- **Agile Supply Chain**

Agile Supply Chain is an other new concept in the formation of supply chains, which are already applied in many sectors. Agility refers to the connection between the finished-product producing company and the customers' market, in other words how fast can the supply chain respond to the customers' demands. The competitiveness and profit of Agile Supply Chain origins from the fast respond of the supply chain to the new challenges of the market.

The produced goods are more custom designed, more unique, produces in smaller quantities, shorter lead time and with reduced cost. This strategy can be applied mostly in case of innovative products with relatively shorter lifetime (maximum 1 year).

- **Leagile Supply Chain**

Leagile is a combination of the Lean and the Agile paradigms. Lean supply chain can not quick respond to changing customer demands, thus Leagile supply chain which combine the advantages of Lean production and Agile manufacturing has been used in manufacturing industries.

3. LEAN PRODUCTION PHILOSOPHY

Lean thinking focuses on value-added flow and the efficiency of the overall system. The goal is to keep product flowing and add value as much as possible. The focus is on the overall system and synchronizing operations.

Lean manufacturing is a performance-based process used in manufacturing organizations and service sector to increase competitive advantage in an increasingly global market.

Nowadays this philosophy (originating from the Toyota Production System) is applied in many sectors including automotive, electronics, white goods, and consumer products manufacturing, etc.

The focus of the approach is on cost reduction by eliminating non-value added activities [6.].

In today's increasingly global marketplace, many manufacturers are adopting Lean manufacturing practices in order to optimize quality and costs, thereby gaining a competitive advantage.

Advantages of Lean manufacturing [7.]**:** 1.) production lead times are short; 2.) imbalances in operation timing (bottlenecks) are apparent – improvement can focus on bottlenecks; 3.) defects are immediately apparent and the underlying cause can be quickly determined; 4.) constant motivation for improvement – problems have immediate production impact; 5.) operations can quickly shift to a new product (e.g., A to B) without interrupting the flow, each operation makes just what is needed when it is needed; 6.) inventory holding costs are minimized, etc.

3.1 Lean principles

The challenge to organizations utilizing Lean manufacturing is to create a culture that will create and sustain long-term commitment from top management through the entire workforce. There are many literatures in topic of Lean production principles and

application of it [8,9,10].

Lean manufacturing techniques are based on the application of five principles to guide management's actions toward success:

1. Value: The foundation for the value stream that defines what the customer is willing to pay for.

2. The Value Stream: The mapping and identifying of all the specific actions required to eliminate the non-value added activities from design concept to customer usage.

3. Flow: The elimination of all process stoppages to make the value stream "flow" without interruptions.

4. Pull: The ability to streamline products and processes from concept through customer usage.

5. Perfection: The ability to advocate doing things right the first time through the application of continuous improvement efforts.

All of processes can be categorized into three groups [11]**:**

- **value added activities** (e.g. manufacturing, assembly, …),
- **required but non-value added activities** (e.g. exchange of die),
- **wastes** are "any element that does not add value, or that the customer is not prepared to pay for" (e.g. over-production, transportation, …).

The results of the Lean approach are illustrated in Fig. 1. In case of Lean manufacturing the ratio of the value adding and non-value adding activities will be improved compared to traditional manufacturing by elimination of wastes in processes.

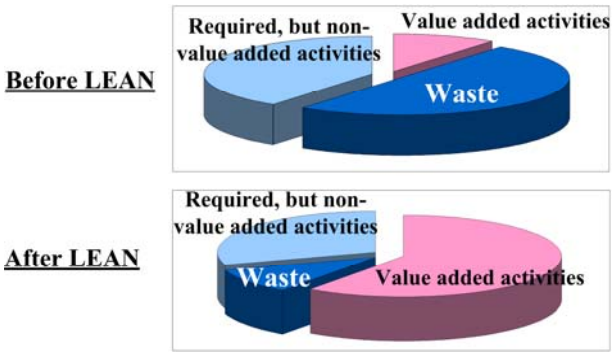

Fig. 1. Traditional manufacturing vs. Lean manufacturing

3.2 Lean wastes

Seven types of wastes [12] can be identified in processes (Fig. 2.).

1. Over production – Producing more final products than is needed or before it is needed for the customer is a fundamental waste in Lean manufacturing.

2. Waiting – Worker or machine is waiting for material or information. Material waiting is not material flowing through value-added operations.

3. Motion – Any unnecessary motion that does not add value to the product is waste.

4. Transportation – Moving material does not enhance the value of the product to the customer.

5. Inventories – Material sits taking up space, costing money, and potentially being damaged. Due to stocks problems are not visible.

6. Over- processing – Extra processing not essential to value-added from the customer point of view is waste.

7. Producing defective products – Defective products impede material flow and lead to wasteful handling, time, and effort.

8. Other additional wastes – Underutilized worker creativity and resource, application of non adequate equipments and systems, wasted energy and water, damage of environment.

Fig. 2. Seven types of wastes

These wastes are readily apparent in every manufacturing facility in the business world. Companies who identify, manage, and minimize these wastes are able to succeed the best in the very competitive marketplace.

A central element of the Lean philosophy is the systematic elimination of unneeded resources, or waste.

The basics of Lean manufacturing employ continuous improvement processes to focus on the elimination of waste or non-value added steps within an organization and production.

4. MAIN TOOLS AND TECHNICS OF LEAN MANUFACTURING

Lean tools and techniques focus on certain aspects and areas of the manufacturing process in order to help reduce costs and improve efficiencies of the processes at the company.

The main tools and techniques of Lean manufacturing [6,10,13,14] are for example Value Stream Mapping, JIT, One-piece flow, Takt–time analysis, Heijunka, Single Minute Exchange of Dies (SMED), Jidoka, Pull system, Kanban, Supermarket, Kaizen, Standardised processes, 5S, Total Productive Maintenance (TPM), 6σ, Cell design and layout for flow (Cellular production, U-shaped cells), Work group team error proofing, Zero defects (ZD), Station and operation process control, Error proofing (poke-yoke), Balanced flow-, Synchronous flow, Mixed flow lines, etc.

The application of Lean production philosophy can result the improvement of the following Key Performance Indicators (KPI): shorter lead times, shorter set up times, smaller stocks, increase of free production area, increased quality of products, general increase of the efficiency of production, increase of productivity.

The Lean manufacturing and a Lean enterprise mean that the company is focused on supplying exactly

what the customer wants, in the form they want it in, free of defects, at the exact time that they want it, with minimal waste in the process.

5. CONCLUSION

Globalization, changing economic environment and customers' demands and the ever increasing competition in the market results in application of new manufacturing technologies, methods. The paper showed these global production tendencies.

Novel supply chain concepts are formed besides the traditional ones in order to retain the competitiveness of the supply chains and the supply chain members. In this study these supply chain conceptions (Lean-, Agile-, Leagile Supply Chains) were introduced.

In a competitive market the manufacturing companies have to produce cost effective products which can be realized by minimized production cost and higher effectiveness. Recently more and more companies apply the Lean production philosophy which focuses on cost reduction and productivity improvement by eliminating non-value added activities.

In this study the author defined the essence and characteristics of the Lean philosophy and emphasized the importance of application of Lean manufacturing, techniques and tools. Nowadays this philosophy is applied in many sectors including automotive, electronics, etc. in order to optimize productivity and costs.

Based on the above mentioned facts, it was confirmed that the Lean manufacturing philosophy is an effective tool for production process improvement.

6. REFERENCES

[1] Kovács, Gy.: *Lean production philosophy*, textbook, (in Hungarian), University of Miskolc, Institute of Logistics, 2014.

[2] Vonderembse, M. A. et al.: *Designing supply chains: Towards theory development,* International Journal of Production Economics, 100, p.p. 223-238, 2006.

[3] Naylor, J. B., Naim, M. M., Berry D.: *Leagility: Integrating the lean and agile manufacturing paradigms in the total supply chain*, International Journal of Production Economics, 62, p.p. 107-118, 1999.

[4] Schönsleben, P.: *With agility and adequate partnership strategies towards effective logistics networks*, Computers in Industry, 42 (1), p.p.: 33-42, 2000.

[5] Agarwal, A., Shankar, R., Tiwari M. K.: *Modeling the metrics of lean, agile and leagile supply chain: An ANP-based approach*, European Journal of Operational Research - Production, Manufacturing and Logistics, 173, p.p.: 211-225, 2006.

[6] Womack, J. P., Jones, D. T., Roos, D.: *The Machine that Changed the World: The Story of Lean Production*, Harper Collins Publishers, New York, 1990.

[7] Kovács, Gy.: *Productivity improvement by lean manufacturing philosophy,* Advanced Logistic Systems: Theory and Practice, 6 (1), p.p. 9-16, 2012.

[8] Fawaz, A. A., Jayant, R.: *Analyzing the benefits of lean manufacturing and value stream mapping via simulation: A process sector case study,* International Journal of Production Economics, 107, p.p. 223-236, 2007.

[9] Fullerton, R. R., McWatters, C. S., Fawson, C.: *An examination of the relation ships between JIT and financial performance*, Journal of Operations Management, 21 (4), p.p. 383-404, 2003.

[10] Womack, J. P., Jones, D. T.: *Lean Thinking: Banish Waste and Create Wealth in Your Corporation,* Simon & Schuster, New York, 1996.

[11] Liker, J. K., Lamb, T.: *Lean manufacturing principles guide DRAFT,* Version 0.5, University of Michigan, 2000.

[12] McLachlin, R.: *Management in initiatives and just-in-time manufacturing*, Journal of Operations Management, 15 (4), p.p. 271-292, 1997.

[13] Holweg, M.: *The genealogy of lean production,* Journal of Operations Management, 25 (2), p.p. 420-437, 2007.

[14] Senderská, K., Lešková, A., Mareš, A.: *Design characteristics of manual assembly workstation system in the lean production system*, Jurnal of Production Engineering, 16 (1), p.p. 87-92, 2013.

ACKNOWLEDGEMENT

This project has received funding from the European Union's Horizon 2020 research and innovation programme under grant agreement No 691942".

Author: **György Kovács PhD, Assoc. Professor**, University of Miskolc, Faculty of Mechanical Engineering and Informatics, Institute of Logistics, Miskolc-Egyetemváros, Miskolc, Hungary
E-mail: altkovac@uni-miskolc.hu

http://doi.org/10.24867/JPE-2017-01-141

Journal of Production Engineering

Vol.20 No.1

JPE (2017) Vol.20 (1) Preliminary Note

Mácsay, V., Bányai T.

TOYOTA PRODUCTION SYSTEM IN MILKRUN BASED IN-PLANT SUPPLY

Received: 15 March 2017 / Accepted: 13 April 2017

Abstract: *The optimization of manufacturing related logistic systems and processes is a key factor of the economical operation. The Toyota Production System (TPS), as precursor of the lean philosophy, is a well known tool to support the operation of manufacturing processes. However TPS includes the logistic processes of supply chain, but a wide range of TPS applications can be found in in-plant supply, especially in the field of automotive industry. After a careful literature review, the authors describe the impact of TPS on milkrun based in-plant supply. Next, a general milkrun morphology is presented, by the aid of which it is possible to describe typical in-plant supply processes. An evaluation method is also described to analyse the cost efficiency of the typical supply methods.*
Key words: *inventory, logistics, manufacturing, milkrun, supply*

Toyota proizvodni sistem Milkrun baziran na snabdevanju fabrike. *Optimizacija proizvodnih logističkih sistema i procesa je ključni faktor ekonomskog poslovanja. Proizvodni sistem Tojota (TPS), kao preteča lean filozofije, je dobro poznat alat za podršku rada proizvodnih procesa. Međutim TPS uključuje logističke procese lanca snabdevanja, ali širok spektar TPS aplikacije može se naći u ponudi snabdevanja fabrike, posebno u oblasti automobilske industrije. Nakon pažljivog pregleda literature, autori opisuju uticaj TPS na Milkrun sistem baziranih ponuda snabdevanja fabrike. Sledeće, opšta Milkrun morfologija je predstavljena, pomoću koje se može opisati tipičn proces snabdevanja fabrike. Takođe je opisan metod evaluacije za analiziu efikasnost troškova tipične metode za snabdevanje.*
Ključne reči: *inventar, logistika, proizvodnja, milkrun, snabdevanje*

1. INTRODUCTION

Logistics can be divided into four main parts: purchasing, production, distribution and recycling. Production logistics is placed in the middle of the supply chain, so the characteristics of suppliers and customers has an impact on the efficiency of the production related logistic processes. The purposes of production logistics are the followings: (1) increased utilization of manufacturing and logistic resources; (2) decreased lead-time of products and losts; (3) decreased inventory in the manufacturing process; (4) decreased costs; (5) increased flexibility of the manufacturing and related logistic process; (6) increased transparency to support lean philosophy based solutions; (7) increased quality of products; (8) integration of the production logistics into the enterprise resource planning (ERP) system.

The material supply of machines in a manufacturing system can be realised in many ways. In the last few years, the milkrun-based in-plant supply is widely spread, especially in the field of the automotive industry. Milkrun supply makes it possible to fed manufacturing and assembly workstations keeping on the 7R rule: the right product, in the right quantity and condition, from the right place, at the right time, to the right place, for the right costs.

Where did the idea of milkrun come from? As it can be deducible from its name, the milkrun idea had been gained from an old version of milk delivery. The milkman distributed the full bottles and collected the empty bottles. If you left him two empty bottles in front of the door then he put two full bottles of milk instead of them. After it the milkman returned with the empties back to the starting point where bottles had been refilled.

This method spread more and more between international companies as both the delivery to customers and the return are making value. The fierce competition between companies claim to eliminate the non-value added activities. What does bottle symbolise? It symbolises the empties. The companies have to pay a large amount of environmental product fee for packaging, so they try to use more reusable packagings. When the customer own the empties, the truck takes the pallets, boxes, containers to the supplier company where they are loaded with the requested quantity of the product. When the truck goes back to the customer, they discharge the empties and the process starts from the beginning again. The design and operation of milkrun based in-plant supply include a wide range of problems: location of stores, supermarkets and machines; routing of milkruns; scheduling; assignment of machines, products, milkruns and operators; inventory optimisation, queuing problems.To our best knowledge, the design of milkrun based in-plant supply of manufacturing plants has not been considered in the current literature.

The main contribution of this work include: (1) the description of the impact of TPS on milkrun based in-plant supply including 5S (seiri, seiton, seiso, seiketsu, shitsuke), kaizen and 3MU (muda, mura, muri); (2) the morphology of milkrun based in-plant supply including the sources, milkruns, machines and strategies; (3) the

description of typical milkrun based supply solutions; (4) an evaluation method to analyse the supply solutions from the point of view costs, efficiency, performance and reliability.

2. LITERATURE REVIEW

This section reviews relevant literature related to TPS and milkrun based supply. Due to the large amount of researches on these fields, the most relevant scientific results have to be summarized before to elaborate impacts, morphology and typical models.

There are integrated approaches of TPS to include the rules or principles underlying TPS strategies [1]. These works are focusing on the fact, that few companies are able to apply TPS strategies successfully. However TPS is widely used in the field of automotive industry, but there are successful applications in other fields, like services [2]. The milkrun based supply is a common in-plant supply strategy in the field of automotive industry and assembly companies, where vehicles circulate between component sources (warehouses or storages) and production or assembly plants according to the supply strategy based on just-in-sequence philosophy [3].

The design of milkrun based in-plant supply includes a huge number of optimisation problems: facility location of supermarkets or pick-up stations; routing [4] of external or internal milkrun vehicles; scheduling. However analytical and heuristic methods are suitable to solve design and control problems of milkrun based in-plant supply, but in many cases simulation based optimisation is the best tool to find optimal solutions of the problems related to milkrun operation [5]. The in-plant supply problems can be defined as NP-hard problems and most of them can be solved with different metaheuristics, like genetic algorithms, evolution strategies, ant colony optimisation, firefly algorithm, cuckoo search, harmony search, etc [6].

The most important tasks of manufacturing and assembly companies are the followings: manage their external and internal supply chain efficiently, increase profit and improve the quality and efficiency of delivery and in-plant supply through production strategies like JIT and JIS. The milkrun concept is the best tool to support JIS in-plant supply, including the following advantages: increased efficiency of material handling processes (storage, transportation, loading, unloading, packaging), up-to-date identification solutions, demand-based feeding process of production and assembly stations, decreased in-process inventory.

The just-in-sequence supply based on milkrun vehicles can be divided into two main streams. The first stream is represented by static assignment and route design while the second stream can be described as dynamic, flexible process including realtime milkrun routing and scheduling [7, 8].

The milkrun based in-plant supply has a wide range of object included in the supply process, like warehouses, supermarkets, production stations, in-process storages, empty bin storages [9]. The operation strategy of the different milkrun solutions depends on the structure. The different strategies for handling delivery peaks can be evaluated with respect to operation costs (including technical and human resources), lead time, inventory in warehouses and in-process storages and service level [10].

The aim of this paper is to investigate the impact of TPS on the performance of milkrun based in-plant supply. The contribution of this paper to the literature is twofold: description of a morphology including structural and process-oriented parameters; development of an evaluation method to analyse the different supply methods.

This paper is organized as follows. Section 2 presents a literature review, which systematically summarizes the research background of milkrun based supply. Section 3 describes the impacts of TPS on milkrun based supply. Section 4 presents the morphology of possible milkrun based in-plant supply solutions including technological and logistic resources. Section 5 demonstrates the most important in-plant supply processes and strategies. For our study, in Section 6 we focus on an evaluation method to analyse the performance of different solutions. Conclusions and future research directions are discussed in Section 7.

3. TPS IMPACT ON MILKRUN BASED SUPPLY

Pull-system, kanban-system and just-in-time can be implemented perfectly through the milkrun concept. When the stock of the users is below the required level, they send a truck with the necessary amount of empties in it.

The milkrun concept can use not only the delivery between companies and customers but also in the in-plant supply. You can attach any number of wagon to a milkrun so it is easy to change the capacity. Its other advantage is that different kind of boxes, pallets and so one can be transported by it. They supply not only the manufacturing cells but also collect the empty packagings from them.

So the milkrun can increase the rate of value add activities in the in-plant supply chain. The introduction of milkrun can help to improve the processes of the Present State Value Stream Map and to reach the Future State Value Stream Map. Now, see how to milkrun can implement the 5S-Method:

- Seiri (Sorting): The milkrun is able to take the necessary components to the manufacturing cells, and to collect the redundant materials, boxes and other packagings.
- Seiton (Setting in order): The milkrun is able to supply more manufacturing cells in one round and to do it in the most satisfactory order. We can determine the place of the different components and packaging on the vehicles too.
- Seiso (Shining): Wagons can be unplugged and replaced, so they can be cleaned easily. Beside of it, the milkrun helps to keep the tidiness of manufacturing cells, as it collects the redundant materials and transport them to an empty bin storage.
- Seiketsu (Standardizing) Standards can be

introduced for the supply method, the schedule and the route of the milkrun can be standardised in the case of static operation strategies.

- Shitsuke (Sustaining) The established standards have to be sustained and taught.

The kaizen philosophy in the milkrun includes the following aspects:

- Shortening: You can supply more cells with a milkrun than with a forklift or with a pump truck.
- Linking and simplifying processes: You can take different kind of components, packaging and waste on one milkrun.
- Flexibility: You can change flexibly the order of cells supplying. You can't do it with a conveyor.

However beside its positives the milkrun concept can be the source of wastes too.

The 3 MU in the milkrun includes the following aspects:

- Muda consists of The Seven Wastes: transport, inventory, motion, waiting, overproduction, over-processing, defects. Most of them can appear in the milkrun method, for example, we take too much or too little component to the cells, we delay, we have to take back materials to the warehouse because of a sudden SMED, etc.
- Mura is The Waste of Unevenness: The cells need very different and fluctuant component quantities and the milkrun can't cope with it.
- Muri is The Waste of Overburden: For example the milkrun have to supply too many cells and the delays cause the shortages of components in the cells.

Ideally, the milkrun would be able to supply the cells according to a defined schedule. It can be able to take the components in the manufacturing cells just in time.

Implementation of it needs a huge amount of information, for example:

- How many units of components have been placed in a cell?
- How many parts are in a unit?
- How many parts need for example for an hour?

Product ID	Number of boxes	Pcs/bin	Total amount	Speed of through-put	Required upload rate	Speed of through-put of bins
1	3	45	75	20 pcs/hours	3,75 hours	2,25
2	4	32	128	20 pcs/hours	6,4 hours	1,6
3	1	4000	4000	80 pcs/hours	50 hours	50
4	1	4000	4000	20 pcs/hours	200 hours	200
5	3	100	300	40 pcs/hours	7,5 hours	2,5
6	12	12	144	20 pcs/hours	7,2 hours	0,6
7	6	12	72	60 pcs/hours	1,2 hours	0,2

Table 1. Dataset for a case study of milk-run based supply of manufacturing machines

As we can see from the table, it is sufficient to recharge the 1), 2), and 5) components in every 4,5 hours. In that case, we have still one box for emergency. If we have only 8 or 9 units from the 6) component in the cells it will be fit to this time too.

The introduction of the milkrun concept is a very good idea, but we can reach the highest possible efficiency only if we do the necessary analysis and calculations. We have to know for example which the best route is, or which the best upload rate is. We have to make standards and instructions. One milkrun can supply either 10 or 20 manufacturing cells, so the coordination is a very complicated task. We need a large amount of information and data to be able to set up an efficient system. The cells usually have a different upload rate; they can make different products by different operations.

We have to assess the following: the route of the milkrun operator, the most effective direction of the route, the best order of supplying. We have to take into consideration the period required for the supplying, collecting the left-over components and waste of packagings from the cells. We have to find a balance between the frequency of upload and the number of milkrun operators.

The efficiency of the milkrun is influenced significantly by the method of order picking in the warehouse. It can be solved in one or two steps. When we fulfil it in one step the milkrun operator is the order picker too. The operator collects the required components in the warehouse and then takes them to the manufacturing cells. In the two steps version, we distribute the two activities between two operators, one prepares the orders in the warehouse and the other takes it to the cell. We have to take into consideration the most practical rate of order pickers and milkrun operators. Depending on the specifics of the company the ratio of order pickers to milkrun operators can be other than 1:1, for example, it can be 2:3 or 1:2. In the two steps version coordination of the work is very important to avoid waiting time.

We can use different methods in the supply too, for example, supply according to a fix schedule. Maybe we will take into consideration the number of empty boxes and other empties in the cells when we make the next component order.

The aim is to implement the just-in-time strategy and to reduce the component stocks in the cells. When the assembly workers have only the necessary components in the cells, it makes their work easier as they have more place and it increases the transparency of processes. According to it, the milkruns have to take a small amount of components to the manufacturing cells and they have to take them frequently. It is important to remove from the cells the unnecessary materials, packagings and the defect parts or products.

We have to investigate why they have remained in the cells so far.

It is essential too that we have the proper shape and size shelves, supermarkets and so one in the cells. The wrong layout can cause difficulties both to the milkrun operators and to the assembly workers. When we create a storage facility, it can be useful to implement the First in First out method.

In order to make rules and standards in the component supply chain sometimes we have to change the quantity of the components in the cells and we have to create new storage facilities or we have to remove old ones. Ideally, the rate of uploads is the submultiple of the shift and it counts with the breaks too.

When all the mentioned conditions are right we still have problems which have to solve. These are the following:

- The assembly workers work slower than they should work and because of its components pile up.
- The assembly workers work quicker than they should work and because of its components run out in the cells.
- The manufacturing cell have to change from a product to another one and because of it the milkrun operator has to remove the previous component and then take the new component to the cell.

In order to solve the first problem, we have to keep in the manufacturing cells more smaller units instead of few bigger units. In that case, we are able to upload the required quantity of components. We can keep the superfluous component on the wagon so in the end of the shift, we will see how many components remain. We can investigate what the cause of it, maybe the assembly workers are overburdened and we have to change the rate of upload.

The other solution is to upload the cells according to the empty boxes and other empties.

As in the pull-system, we need to produce only a certain number of end product we don't have to make more. This kind of waiting of the assembly workers don't cause waste, but if it is a usual problem and we need more capacity somewhere else we can change the rate of upload.

Unfortunately, the milkrun can't cope with the third problem. The milkrun supplies the cells according to a schedule and the urgent cases disturb this process. We have to separate the scheduled processes from the urgent cases as we separate the public transport from the ambulance.

It can be a good solution if we use forklifts or pump truck for emergency situations.

4. MORPHOLOGY OF MILKRUN SUPPLY

It is possible to define different parameters and characteristics, by the aid of which it is possible to build a general model structure of milkrun based supply [11]. The below-described general model represents the morphology of the milkrun based component supply of an assembly plant. The component sources of assembly stations (sinks) can be automated or manual warehouses, supermarkets or machines in manufacturing plants. The handling units of products are either boxes (bins) or pallets, but it is also possible to use mixed handling units, especially in the case of a wide range of macrogeometry of components. The number of milkruns depends on the required component supply performance. If the required performance is variable, the number of milkruns is flexible; in other cases the number of milkruns can be fixed. One of the most important characteristics of the supply is the operation strategy. There are different types of operation strategies; the most widely used strategies are the on-demand strategy and the fixed schedule strategy. If the source of components is placed in warehouses, it is possible to split the tasks of milkrun supply and define two stages: the first stage is the internal milkrun which perform the picking process in the warehouse; the second stage is the external milkrun, which performs the feeding of assembly stations. The milkrun operators can perform a wide range of operation tasks, like loading at sources, unloading at sinks, opening loading units and boxes at assembly stations, loading goods return, final products, empty bins or wrapping at assembly stations. The integration of empty bin handling depends on the operation strategy; a wide range of milkrun based supply the empty bin handling is not integrated into the milkrun process. From the point of view warehouse management, we can also define some important parameters: check-in and check-out location of components. Route planning is a very important part of the design of material handling systems. In the case of milkrun supply routes can be fixed, mixed stationary or dynamical. The assignment of milkruns to assembly stations, warehouses, components or operators is also an important characteristics of milkrun supply.

Product source	automated warehouse	manual warehouse	manufacturing machines	manufacturing supermarkets	mixed
Handling unit	bins or boxes		pallets		mixed
No. of milkruns	fixed		flexible		
Operation strategy	on-demand (kanban)		fixed schedule		mixed
Milkrun levels	integrated milkrun		splitted milkrun		mixed
Tasks of milkrun operators	loading at sources	unloading at sinks	opening bins at sinks	loading at sinks	mixed
Empty bin handling	integrated to warehouse		integrated to other location		not integrated
Check-in	at sources		at sinks		both
Check-out	at sources		at sinks		both
Goods return process	integrated		not integrated		
Route	fixed	mixed stationary	dinamical		mixed
Assignment	fixed		flexible		

Table 2. Morphology of milkrun based supply of assembly stations

5. MILKRUN BASED SUPPLY STRATEGIES

Within the frame of this chapter, the authors describe four different milkrun based supply. These scenarios represent the most widely spread solution in the field of assembly plant supply.

Scenario one is based on an external milkrun. The source of components is an automated warehouse, where the required components are collected and placed on a pick-up area. In this case, there are no internal milkruns in the warehouse. The milkrun feeds the assembly stations and the external bin storage with empty bins from assembly stations. In this scenario, the check-out process is located at the exit of the warehouse.

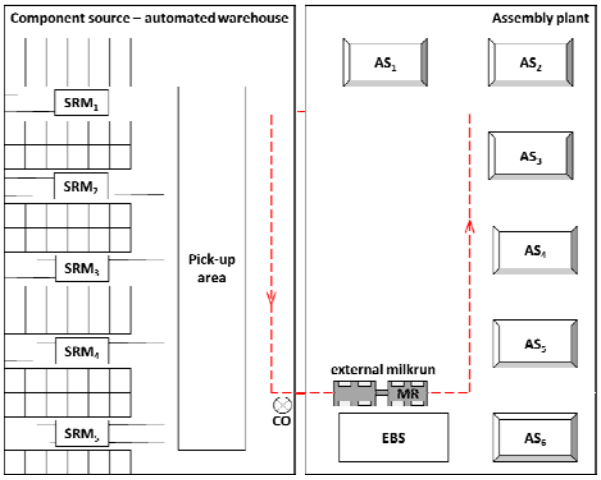

Fig. 1. Scenario1 with external milkrun

In the case of scenario two the collection of required components and the supply of assembly stations is based on an integrated milkrun. The operator is responsible for the whole material supply process from picking through supply to the handling of empty bins and pallets. In this case, the components are checked out at the assembly stations.

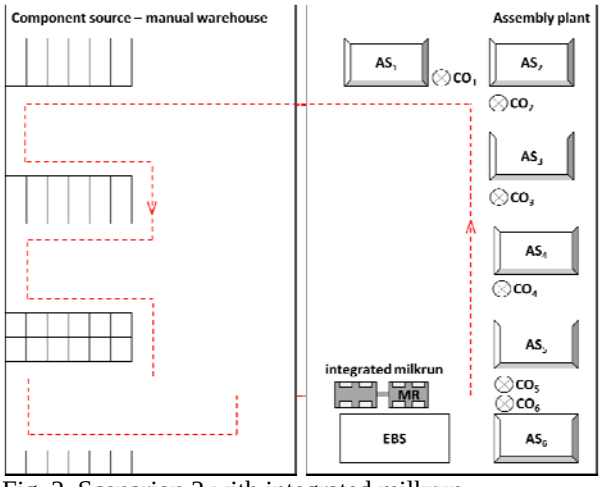

Fig. 2. Scenarion 2 with integrated milkrun

In the case of scenario three, the collection and supply process is divided into two rounds: internal and external milkruns. In this case, components are checked out at the pick-up area, where the external milkrun operator changes vehicles. The divided milkruns make it possible to decrease the cycle time of milkruns, but more operator is required. An additional design aspect is to match the cycle time of collection process with the cycle time of the external milkrun.

Scenario four represents a complex source of required components. Components can be collected both warehouses and manufacturing plants. In general cases, the pick-up location of required components is the output supermarket of the manufacturing plant. In special cases, components can be collected from manufacturing machines, but in this case, the collection route and the cycle time of collection process is greatly increased. The check-out of required components is located in two different places; warehouse for stored components and manufacturing plant for produced components. The handling of empty bins or pallets are not integrated into the milkrun routes, therefore an additional vehicle (e.g. forklift) is required for this material handling task.

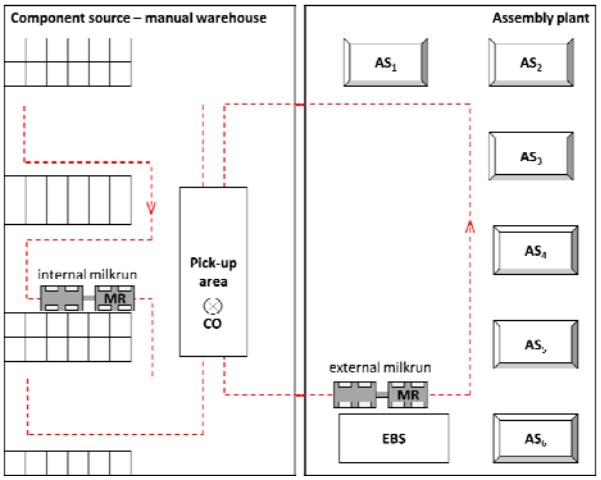

Fig. 3. Scenario 3 with two-level milkrun

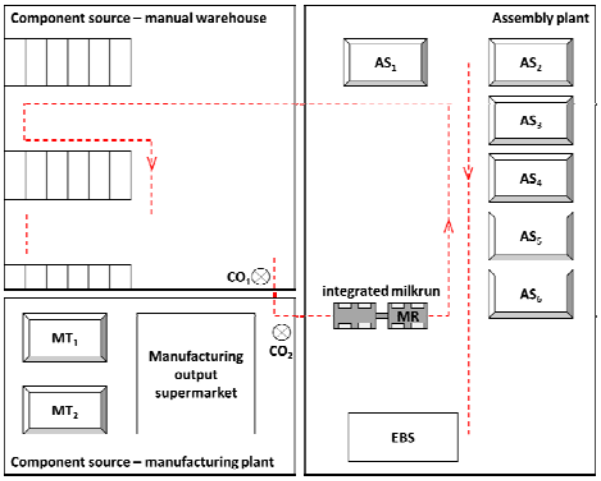

Fig. 4. Scenario 4 with integrated milkrun

6. EVALUATION MODEL

Within the frame of this chapter, the general aspects of an evaluation method are described, by the aid of which it is possible to analyse the different solutions of milkrun based component supply of assembly plants.

It is possible to evaluate the milkrun supply from

the point of view time, cost, efficiency and performance. The below-described method is focusing on time-based evaluation. As Table 3 shows, we can define different processes of the milkrun supply.

Operation		S1	S2	S3	S4
collection	t_c	+	++	++	+++
pick-up	t_{pu}	+			
check-out	t_{co}	+	+++	+	+
running time of milkrun	t_{rm}	+	++	+	+++
unloading of components	t_{uc}	+	+	+	+
opening bins	t_{ob}	+	+	+	+
loading empty bins	t_{leb}	+	+	+	
unloading empty bins	t_{ueb}	+	+	+	
loading goods return	t_{lr}	+	+	+	+
unloading goods return	t_{ur}	+	++		++
empty bin handling vehicle	t_{ev}				+

Table 3. Time span components of milkruns (number of + means small, medium or large time span)

Depending on the schedule of the different operations, it is possible to calculate the cycle time of the milkrun and evaluate each solution.

In the case of overlapped operations, the cycle time can be decreased. However this solution can ensure higher efficiency and performance, but the costs of overlapped operations, like two level milkrun and collection in automated warehouses, increase the costs caused by increased number of required operators or expensive technology.

Depending on the required upload rate by each assembly station and the speed of throughput of components and bins the cycle time and the related costs can be calculated.

7. CONCLUSIONS

As a very delicious and complicated food which preparation needs a lot of experience and attention, the milkrun method requires a very good planning and implementation to be well-organised and efficient.

Of course, this requires a lot of experience, calculations and tests. The human factor is also an important part of the process as we need operators who understand, support and follow the rules and standards.

In conclusion, the milkrun method can be a practical part of the TPS as it can implement the pull-system, the 5S, the continuous material flow and the kaizen principles. To continuous improvement, we have to examine emerging problems, find the cause and the solution of them.

8. REFERENCES

[1] Jayaram, J., Das, A., Nicolae, M.: *Looking beyond the obvious: Unraveling the Toyota production system*. International Journal of Production Economics, 128(1) pp.280-291. 2010

[2] Stapleton, B. F., Hendricks, J., Hagan, P., Del Beccaro, M.: *Modifying the Toyota Production System for Continuous Performance Improvement in an Academic Children's Hospital*. Pediatric Clinics of North America, 56(4) pp.799-813. 2009

[3] Kovács, A.: *Optimizing the storage assignment in a warehouse served by milkrun logistics*. International Journal of Production Economics, 133(1) pp. 312-318. 2011

[4] Gyulai, D., Pfeiffer, A., Sobottka, T., Váncza, J.: *Milkrun Vehicle Routing Approach for Shop-floor Logistics*. Procedia CIRP, 7 pp. 127-132. 2013

[5] Wiegel, F., Immler, S., Knobloch, D., Abele, E.: *Simulation-based optimization of internal Milkruns: Development of a simulation model for planning and optimizing the provision of material*. Productivity Management 18(1) pp. 51-54, 2013

[6] Jafari-Eskandari, M., Sadjadi, S.J., Jabalameli, M.S., Bozorgi-Amiri, A.: *A robust optimization approach for the milk run problem (an auto industrysupply chain case study)*. International Conference on Computers and Industrial Engineering, pp. 1076-1081, 2009

[7] Kitamura, T., Okamoto, K.: *Automated route planning for milk-run transport logistics using model checking*. Proceedings of the 2012 3rd International Conference on Networking and Computing, pp. 240-246, 2012

[8] Satoh, I.: *A formal approach for milk-run transport logistics*. IEICE Transactions on Fundamentals of Electronics, Communications and Computer Sciences pp. 3261-3268, 2008

[9] Vieira, A., Dias, L.S., Pereira, G.B., Oliveira, J.A., Carvalho, M.S., Martins, P.: *Automatic simulation models generation of warehouses with milk runs and pickers*. Proceedings of the 28th European Modeling and Simulation Symposium, pp. 231-241, 2016

[10] Klenk, E., Galka, S., Giinthner, W.A.: *Operating strategies for in-plant milk-run systems*. 15th IFAC Symposium on Information Control Problems in Manufacturing. pp 1882-1887, 2015

[11] Klenk, E., Galka, S., Günthner, W. A.: *Analysis of parameters influencing in-plant milk run design for production supply*, Proceedings of the International Material Handling Research Colloquium, pp. 25-28, 2012

ACKNOWLEDGEMENTS

The described research was carried out as part of the EFOP-3.6.1-16-00011 "Younger and Renewing University – Innovative Knowledge City – institutional development of the University of Miskolc aiming at intelligent specialization" project implemented in the framework of the Szechenyi 2020 program. The realization of this project is supported by the European Union, co-financed by the European Social Fund.

Authors: **Vivien Mácsay BSc, Tamás Bányai PhD, Assoc. Professor,** University of Miskolc, Faculty of Mechanical Engineering and Informatics, Institute for Logistics, Miskolc-Egyetemváros, 3515, Hungary, Phone.: +36 46 565-111, Fax: +36 46 565-111.
E-mail: alttamas@uni-miskolc.hu
vivienmacsay@gmail.com

Journal of Production Engineering

PUBLICATION ETHICS AND PUBLICATION MALPRACTICE STATEMENT

The statement is based on the worldwide recognized Elsevier's Publishing ethics resource kit (http://www.elsevier.com/ethics/toolkit) and on the Committee on Publication Ethics (COPE) Code of Conduct (http://publicationethics.org/resources/guidelines). Full detailed guidelines of international standards for authors and editors can be found here: http://publicationethics.org/international-standards-editors-and-authors.

1. Authors' duties

Reporting standards. Authors of original research reports should present an accurate account of the work performed as well as an argumentatively coherent discussion of its significance. Underlying data should be represented accurately in the paper. A paper should contain sufficient detail to permit others to judge the academic and scientific merits of the work. Fraudulent or knowingly inaccurate statements constitute unethical behaviour and are unacceptable.

Data access and retention. Authors may be asked to provide the raw data in connection with a paper for editorial review, and should be prepared to provide public access to such data, if practicable, and should in any event be prepared to retain such data for a reasonable time after publication.

Originality and plagiarism. The authors should ensure that they have written entirely original works, and if the authors have used the work and/or words of others that this has been appropriately cited or quoted. Plagiarism takes many forms, from 'passing off' another's paper as the author's own paper, to copying or paraphrasing substantial parts of another's paper (without attribution), to claiming results from research conducted by others. Plagiarism in all its forms constitutes unethical publishing behaviour and is unacceptable.

Multiple, redundant or concurrent publication. An author should not in general publish manuscripts describing essentially the same research in more than one journal or primary publication. Submitting the same manuscript to more than one journal concurrently constitutes unethical publishing behaviour and is unacceptable. In general, an author should not submit for consideration in another journal a previously published paper.

Acknowledgement of sources. Proper acknowledgment of the work of others must always be given. Authors should cite publications that have been influential in determining the nature of the reported work. Information obtained privately, as in conversation, correspondence, or discussion with third parties, must not be used or reported without explicit, written permission from the source.

Authorship of the paper. Authorship should be limited to those who have made a significant contribution to the conception, design, execution, or interpretation of the reported study. All those who have made significant contributions should be listed as co-authors. Where there are others who have participated in certain substantive aspects of the research project, they should be acknowledged or listed as contributors. The corresponding author should ensure that all appropriate co-authors and no inappropriate co-authors are included on the paper, and that all co-authors have seen and approved the final version of the paper and have agreed to its submission for publication.

Disclosure and conflicts of interest. All authors should disclose in their manuscript any financial or other substantive conflict of interest that might be construed to influence the results or interpretation of their manuscript. All sources of financial support for the project should be disclosed.

Fundamental errors in published works. When an author discovers a significant error or inaccuracy in his/her own published work, it is the author's obligation to promptly notify the journal editor or publisher and cooperate with the editor to retract or correct the paper.

2. Editors' duties

Publication decisions. The editors of a peer-reviewed journal are responsible for deciding which of the articles submitted to the journal should be published. The editors may be guided by the policies of the journal's editorial

board and constrained by such legal requirements as shall then be in force regarding libel, copyright infringement and plagiarism. The editors may confer with other editors or reviewers in making this decision.

Fair play. An editor should evaluate manuscripts for their intellectual content without regard to race, gender, sexual orientation, religious belief, ethnic origin, citizenship or political philosophy of the authors.

Confidentiality. The editors and any editorial staff must not disclose any information about a submitted manuscript to anyone other than the corresponding author, reviewers, potential reviewers, other editorial advisers, and the publisher, as appropriate.

Disclosure and conflicts of interest. Unpublished materials disclosed in a submitted manuscript must not be used in an editor's own research without the expressed written consent of the author. Privileged information or ideas obtained through peer review must be kept confidential and not used for personal advantage.

3. Reviewers' duties

Contribution to editorial decisions. Peer review assists the editors in making editorial decisions and through the editorial communications with the author may also assist the author in improving the paper.

Promptness. Referees who feel unqualified to review the research reported in a manuscript or knows that a prompt review will be impossible, should notify the editor and excuse themselves from the review process.

Confidentiality. Any manuscripts received for review must be treated as confidential documents. They must not be shown to or discussed with others except as authorized by the editors.

Ethics. Reviews should be written respectfully. Personal criticism of the author is inappropriate. Referees should express their views clearly with supporting arguments. Sweeping general remarks that disfavour the author's paper is unacceptable and such remarks needs to be backed up with clear arguments and concrete references to the content of the paper reviewed.

Acknowledgement of sources. Reviewers should identify relevant published work that has not been cited by the authors. Any statement that an observation, derivation, or argument had been previously reported should be accompanied by the relevant citation. A reviewer should also call to the editors' attention any substantial similarity or overlap between the manuscript under consideration and any other published paper of which they have personal knowledge.

Disclosure and conflict of interest. Unpublished materials disclosed in a submitted manuscript must not be used in a reviewer's own research without the express written consent of the author. Privileged information or ideas obtained through peer review must be kept confidential and not used for personal advantage. Reviewers should not consider manuscripts in which they have conflicts of interest.

INSTRUCTIONS FOR CONTRIBUTORS

No. of pages:	4 DIN A4 pages
Margins:	left: 2,5 cm
	right: 2 cm
	top: 2 cm
	bottom: 2 cm
Font:	Times New Roman
Title:	Bold 12, capitals
Abstract:	Italic 10
Headings:	Bold 10, capitals
Subheadings:	Bold 10, small letters
Text:	Regular 10
Columns:	Equal column width with 0,7 cm spacing
Spacing:	Single line spacing
Formulae:	Centered and numerated from 1 in ascending order. Equations must be typed in Equation Editor, with following settings: Style>Math – Times New Roman Size>Full 12pt, Subscript/Superscript 7pt, Symbol 18 pt
Figures:	High quality, numerated from 1 in ascending order (e.g.: Fig.1, Fig. 2 etc.); Figures and tables can spread over both two columns, please avoid photographs and color prints
Tables:	Numerated from 1 in ascending order (e.g..: Tab. 1, Tab. 2, etc.)
References:	Numerated from [1] in ascending order; cited papers should be marked by the number from the reference list (e.g. [1], [2, 3] ...)
Submission:	**Papers prepared in MS Word format should be e-mailed to: pkovac@uns.ac.rs, savkovic@uns.ac.rs**
Notice:	**Papers are to be printed in Journal of Production Engineering** Sample paper with detailed instructions can be found at: **http://www.jpe.ftn.uns.ac.rs/**

FOR MORE INFORMATION, PLEASE CONTACT:

Prof. Pavel Kovač, PhD, MEng.
Assist. Prof. Borislav Savković, PhD, MEng.
FACULTY OF TECHNICAL SCIENCES
Department for Production Engineering
Trg Dositeja Obradovica 6
21000 Novi Sad
Serbia

Tel.: (+381 21) 485 23 24; 485 23 20 ; 450 366;
Fax: (+381 21) 454 495
E-mail: pkovac@uns.ac.rs, savkovic@uns.ac.rs
http://www.jpe.ftn.uns.ac.rs/